Design and Testing of a Permeable Reactive Barrier System for Treatment of Sulphate Rich Waters at the Former Steep Rock Iron Mine, Atikokan, Ontario.

By

Bret B. Timmis

A thesis submitted in partial fulfillment of
the degree of Master of Science

Department of Geology
Lakehead University

ABSTRACT

Acid mine drainage (AMD) is one of the greatest challenges facing the mining industry globally. Methods for addressing this issue have been widely studied; however, few studies have addressed sites with a less common water quality problem resulting from AMD: neutral pH, metal-poor, and sulphate-rich water. The Steep Rock Iron Mine site in Atikokan, Ontario is utilized as a case study where AMD-affected waters have acidity neutralized by carbonate rocks, and metals precipitate out of solution as the pH rises. This process alleviates major environmental hazards associated with acidic waters and toxic metal concentrations; however, sulphate is not removed and presents toxic conditions for aquatic fauna. These sites are also a risk to human health, and can potentially contaminate drinking water supplies. Funding for the remediation of abandoned mine sites is limited, and innovative solutions utilizing passive treatment mechanisms are needed in order to deliver efficient and effective remediation. The goals of this project were: 1) to assess the capability of a permeable reactive barrier (PRB) system to remediate sulphate-rich, pH neutral, metal-poor water, 2) to assess nutrient balance within the system to ensure the availability of nutrients is not a rate-limiting factor for sulphate reduction, and 3) to improve reactive substrate selection procedures by determining which assessment tools are most useful in selecting substrates effective at stimulating sulphate reducing bacteria (SRB).

Candidate reactive substrates including cow, horse, poultry, rabbit, and sheep manures, as well as leaf compost and hay, were assessed according to their concentrations of vital nutrients for SRB, including carbon, nitrogen, and phosphorous. Additionally, their relative degradability was tested via a procedure known as easily available substances (EAS). This testing determined how readily a given substrate could be broken down by bacteria, as well as the change in concentration of desired nutrients in the substrate before and after EAS testing, which gives an

indication as to the availability of those specific nutrients. Plant and manure substrates were tested, with one of each type used in each reactive mixture. Based on this testing, poultry and sheep manures were selected as the most likely manure substrates to provide effective nutrition for SRB. In contrast, there was no significant difference found between hay and leaf compost. Poultry consistently performed the best in each test, with a C:N ratio of 11, a C:N:P ratio of 1772:160:1, and an EAS mass loss of 71%.

Eight flow-through reactors were constructed and operated for a period of 23 weeks. Six of these reactors contained organic materials to stimulate SRB, while two were controls. Of the six reactors using organic materials, three mixtures were used, each containing a different combination of the four substrates. One control reactor assessed the impact of zero-valent iron which was also added to all of the organic reactors, while an additional control simulated the natural environment and contained only creek sediment and silica sand. Reactors 3 and 7 were the most effective at sustaining high rates of sulphate removal, with >80% sulphate removal maintained for the first 14 weeks. These reactors utilized a mixture of poultry manure and hay, validating the measures which indicated poultry manure as the most effective manure-based substrate. However, poultry manure was also used in reactors 1 and 5 in combination with leaf compost, and were not as effective for sulphate removal. These results indicate that hay was a more effective substrate than leaf compost. Comparing this finding against the original substrate testing presents two differences between hay and leaf compost; the C:N:P ratio and the availability of phosphorus in EAS testing both had stronger results for hay. This result indicates that phosphorus is a critical nutrient for SRB, and that tests considering phosphorus should be an integral part of reactive substrate selection procedures in systems attempting to stimulate SRB. The control reactors found that the addition of only zero valent iron did not have a significant impact on sulphate removal, as performance in this reactor was similar to the natural aquifer

conditions control reactor. Eh/pH conditions supported the activity of SRB; but did not support the stability of sulphide produced by SRB, and it is unclear of SRB were in fact active within the flow-through reactors.

Significantly reduced sulphate concentrations in reactor effluent initially appeared to indicate the sulphate reduction was occurred as intended. However, in post-experiment analysis there was no evidence of iron sulphide formation that would confirm sulphide production by SRB, and Eh/pH conditions were not supportive of sulphide stability. Furthermore, saturation index calculations using PHREEQC determined that iron sulphides were highly under saturated in effluent waters. In contrast, sulphate minerals including barite, gypsum, and jarosite were slightly oversaturated, and present a viable sink for the sulphate removed from solution. Following experiment completion it was found that the reactors with the greatest sulphate removal also had the most significant declines in nutrient concentration, with 52-64% C, 45-58% N, and 24-62% P losses in reactors 3 and 7. This is strong evidence of a bacterially driven process for sulphate mineral precipitation. The reduced availability of these nutrients may have played a role in the decline of sulphate removal over time.

ACKNOWLEDGMENTS

I sincerely express my gratitude to Dr. Andrew Conly for his assistance, support, and guidance throughout all phases of this project. Thanks are also due to Lindsay Moore and Greg Paju for their assistance in material collection, as well as their support and encouragement over the course of this project. I would also like to thank the staff of the Lakehead University Environmental Laboratory (LUEL) and the Lakehead University Instrumentation Laboratory (LUIL) for their excellent work processing many samples, and also for their enthusiastic support whenever I needed advice or had questions about procedures. Finally, many thanks are due to my friends and family who have always supported and encouraged me throughout this process.

TABLE OF CONTENTS

LIST OF FIGURES

LIST OF TABLES

Chapter 1: Introduction

1.1 Acid Mine Drainage and Pit Lakes

Acid mine drainage (AMD) is one of the most prevalent and costly issues facing the mining industry today. AMD is produced when sulphide bearing rocks are exposed to oxygen and precipitation, causing chemical reactions that produce water containing elevated metal concentrations, high acidity, and sulphate (Akcil and Koldas, 2006). Such waters are highly damaging to local watersheds and ecosystems, and can cause acute or chronic health impacts for organisms in contact with these waters. This process occurs naturally in the environment, and is not normally an issue, except when anthropogenic mining activities result in massive amounts of fresh material being exposed at the surface in a short period of time. In nature, this process would normally occur over thousands or millions of years, resulting in only weak concentrations of these contaminants which could be easily accepted into the local watersheds without harm. Commonly AMD occurs due to the disposal of tailings or waste rock from a mine site which contains sulphide minerals, with the most common source being pyrite (Johnson and Hallberg, 2005; Lindsay et al., 2009). Pyrite, with the chemical composition FeS_2, reacts with oxygen and water, producing Fe^{2+}, SO_4^{2-} and H^+ as shown in equation 1 (Benner et al., 1997). The Fe^{2+} can further be oxidized to Fe^{3+}, which can oxidize more pyrite and continue the process as shown in equation 2 (Akcil and Koldas, 2006). The Fe^{3+} can take the place of oxygen in the first equation, to continue the process, as seen in equation 3.

(1) $2FeS_2(s) + 7O_2(g) + 2H_2O(l) \rightarrow 2Fe_2{+}(aq) + 4SO_4^{2-}(aq) + 4H^+(aq)$.

(2) $4Fe^{2+}(aq) + O_2(g) + 4H^+(aq) \rightarrow 4Fe^{3+}(aq) + 2H_2O(l)$.

(3) $FeS_2(s) + 14Fe^{3+}(aq) + 8H_2O(l) \rightarrow 15Fe^{2+}(aq) + 2SO_4^{2-}(aq) + 16H^+(aq)$.

Methods of remediating sites and watersheds impacted by AMD have been extensively studied; e.g. Hoffert (1947), Olem and Unz (1980), Gazea et al. (1996), Benner et al. (1997),

Johnson and Hallberg (2005), and Akcil and Koldas (2006). These studies typically focus on treating acidity and metals, with sulphate removal as an afterthought. However, some sites are faced with a less typical water quality concern due to AMD, where high sulphate concentrations are the primary concern, such as at the former Steep Rock Iron Mines, near Atikokan, Ontario (Fig. 1.1).

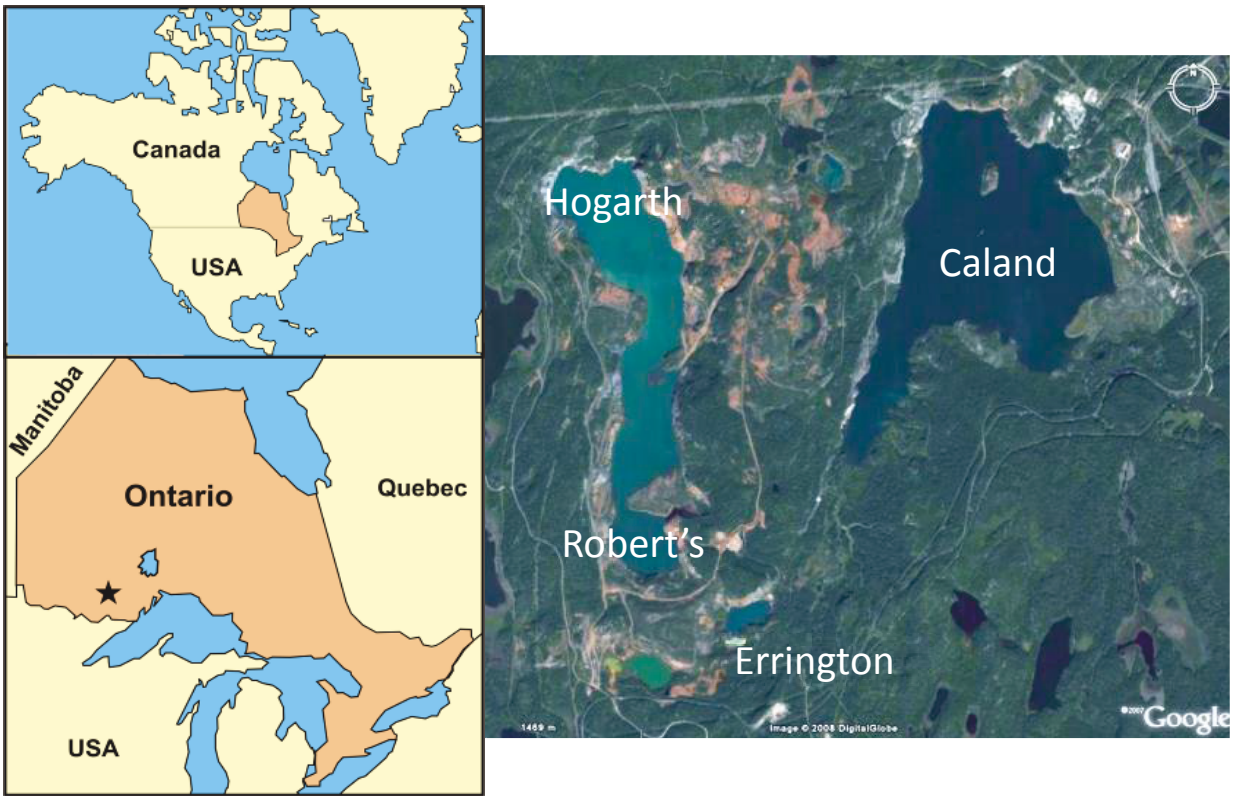

Figure 1.1: Google Earth image of Steep Rock mine site, maps to left indicate location with North America and Ontario (provided courtesy by A. Conly). Named water bodies are flooded mine pits.

1.2 Issues of Pit Lakes

The formation of pit lakes occurs due to the closure of an open pit mine and the consequent cessation of dewatering activities. Groundwater inflow, overland flow, and precipitation will result in a rebound of the water level over time until equilibrium with the water table or evaporation is reached, or water is able to exit the top of the pit via surface flow. Outflow of pit waters via groundwater or surface water flow can present a significant risk to adjacent ecosystems and drinking water supplies if toxic levels of contaminants are present. Pit

lakes exhibit unique hydrologic behaviour due to their high depth to surface area ratio, which often produces significant thermal and chemical stratification within the water column (Castro and Moore, 2000). Water chemistry is dependent upon the interaction with groundwater, wall rocks, precipitation, evaporative effects, biological processes, and interaction with mine waste materials (Eary, 1999). At some sites carbonate wall rocks may be present to buffer the solution, acting as a natural remediative tool. If sufficient organic material is present, the lower portion of the water column, or hypolimnion, will likely become anoxic (Castro and Moore, 2000). The activity of anaerobic microorganisms in these anoxic environments may be able to assist in the remediation of water quality as sulphate reducing bacteria (SRB) can consume organic matter and sulphate, converting the sulphate to sulphide, which can precipitate as metal sulphides if sufficient divalent metals are available (Castro and Moore, 2000). Seasonal overturns of the water column can cause changes in the water composition, and re-introduce dissolved oxygen to the lower levels of the pit (Mikkelsen, 2012). A thorough understanding of the hydrodynamics of a given pit lake is crucial to effective management of water quality.

1.3 Steep Rock Site Conditions

The site is located approximately 5 km north of Atikokan, Ontario, and 180 km west-northwest of Thunder Bay, Ontario. Geologically, the site is located within the south-central portion of the Wabigoon subprovince in the Superior province, just north of the contact with the Quetico subprovince (Kusky and Huddleston, 1999). The presence of iron at Steep Rock Lake has been known since 1891 (Taylor, 1978). The deposit was situated beneath Steep Rock Lake and this challenge prevented exploitation of the resource. During World War II the demand for iron for the war effort grew enormously, and available resources were not capable of providing sufficient iron to keep up with the demand. In 1938, the Steep Rock deposit was considered to be the richest undeveloped iron ore deposit in North America. As such, accelerated development of

the site was authorized under the War Measures Act (Sowa, 2002). Mine development required the diversion of the Seine River, which flowed through the lake, draining the middle and east arms of Steep Rock Lake, and the removal of approximately 15 million m^3 of lake bottom silt and clay (Sowa, 2002). At the time this was considered one of the largest engineering projects ever undertaken in Canada. The west arm of Steep Rock Lake was eventually closed from the Seine River system in order for it to be used as a settling basin. This resulted in reducing the depth of the lake from 60 m to an average depth of 3 m due to the deposition of nearly 90 million m^3 of dredged clayey silt from the areas to be mined (Sowa, 2002). In 1944, mining commenced at Errington Pit, before subsequent pits were developed at Hogarth, Roberts and finally Caland. Mining activities ceased in 1979 (Mikkelsen, 2012), and in 1988 the lands were officially returned to the province. At the time, environmental regulations did not legally require the company to undertake extensive remediation work, and as such minimal environmental cleanup was completed. The site was largely abandoned following this time, and the pits began filling with water once there were no efforts to prevent this.

At this site, AMD is generated by the oxidation of pyritic tailings and waste rock disposal sites within the former mine property. At the present time, all water within the site flows to the large open pits remaining from mining operations, which have partially filled to form lakes. AMD has severely impacted water bodies throughout the site, with several locations containing high concentrations of metals, very low pH, and high sulphate concentrations (Macdonald, 2005; Vancook, 2005; Perusse, 2009). Once the AMD contaminated water flows to the pit lakes, the pH is neutralized due to the presence of carbonate wall rocks (Conly et al., 2007). These carbonate rocks are present in the Mosher Carbonate formation, one unit among the several sedimentary units comprising the Steep Rock Group (Kusky and Huddleston, 1999). The carbonate minerals are exposed in the pit walls, and act as a buffer to the acidic solution, causing

the pH to rise, and metals to precipitate out of solution (Godwin, 2009). High sulphate remains a problem however; with concentrations present in some of the pits which are toxic to aquatic life (Goold, 2008; Godwin, 2009). This situation of sulphate being the primary contaminant of concern due to AMD is much less common than typical AMD waters, and consequently is much less investigated. At the present time, there is no direct outflow from the lakes, and the lake levels continue to rise. Eventually the lake water will rise to such a level that the pit lakes merge, and eventually water must flow off-site. The ultimate lake level is shown in Figure 1.2.

Figure 1.2: Google Earth image with outline of the eventual lake level of the merged Steep Rock Lake (provided courtesy Dr. A. Conly).

The eventual outflow from the lake presents a serious risk to nearby watersheds and ecosystems, which would be irreparably harmed by an influx of the sulphate rich water. In addition, the higher lake level will not have the commonly expected impact in pit lakes of preventing further oxidation of sulphide minerals, due to the shallow areas between the merged pit lakes. This creates a unique situation for pit lakes, the presence of a littoral zone. The existence of a littoral zone will permit long term interaction of shallow oxygenated waters with

waste rock materials, thus enabling continued production of acid-, sulphate-, and metal-rich waters. Consequently, a suitable treatment method is required in order to improve the water quality prior to release into external watersheds. This situation of a site where AMD is being generated, yet the pH and metals are mitigated by the presence of carbonate is much less common than the traditional AMD site issues. Consequently, little research has been conducted into the remediation of sites with this particular situation; however, it is an important environmental problem requiring innovative solutions. Most research into this area has focussed primarily upon the removal of dissolved metals and pH neutralization. The Steep Rock site will be utilized as a case study in this research; however, the results are applicable to other sites that are characterized by near neutral pH, low concentrations of dissolved metals, yet high concentrations of dissolved sulphate. Examples include Carlin-type Au deposits in which significant volumes of carbonate minerals are often able neutralize most generated acidity (Shevenell et al., 1999).

1.4 AMD Treatment Methods

The treatment and prevention of AMD has been increasingly noted as an important facet of mine planning. In the past, environmental regulations were much less strict, and mines were permitted to release AMD to local environments with minimal treatment or concern regarding environmental impacts (Hoffert, 1947). Following major environmental disasters, such as Kam Kotia (Ontario), Britannia Beach (British Columbia), Berkeley (Montana), and more recently, Mount Polley (British Columbia), the devastating environmental impacts of AMD release became realized. In various regions legislation was introduced (e.g., 1992 and 1996 revisions to the Ontario Mining Act), to require mining companies to put in place extensive programs to mitigate the release of environmental contaminants (such as AMD) and ensure detailed closure and rehabilitation plans were developed. Significant initiatives and organizations such as the

Mining Environment Neutral Drainage (MEND) program and the International Network for Acid Prevention (INAP) have worked with industry to achieve improved environmental outcomes for a sustainable mining industry. Traditionally, AMD treatment has focussed upon the chemical treatment of metals and acidity. Liming has been a technique used extensively to combat the problem. In this technique, lime (CaO or CaOH) is applied directly to contaminated waters, waste rock, tailings piles, or mixed into a slurry of effluent (Johnson and Hallberg, 2005). This results in a neutralization of acidity, which further causes the precipitation of metals from solution. The relatively lower cost and simplicity of this technique has resulted in widespread use. However, lime treatment causes the formation of large volumes of metal-rich sludge which needs to be removed and treated (Johnson and Hallberg, 2005). Although lime is the most commonly used material to treat acidity, other materials used include ammonia, fly ash, calcium carbonate, sodium carbonate, sodium hydroxide, and kraft mill waste (lime mud residue) e.g., Catalan and Kumari (2005), Johnson and Hallberg (2005), and Wang et al. (2006). These materials can be applied directly to contaminated waters, or used as a reactive material in a treatment system, such as a constructed wetland, bioreactor, or permeable reactive barrier (PRB) (see section 1.6 for discussion on PRBs). A variety of chemical treatment plants are also available for high-level treatment and removal of contaminants, although these can have high capital and operational costs (Egiebor and Oni, 2007). Active treatment methods can be labour intensive, and have high capital and operational costs associated with them, and as such there has been extensive research into alternative measures (e.g., Gazea et al., 1996, Ziemkiewicz et al., 2003, Johnson and Hallberg, 2005).

Passive treatment systems such as sulphate reducing bioreactors, anoxic limestone drains, successive alkalinity producing systems, and engineered wetlands have been utilized increasingly in recent years to treat AMD as a lower cost treatment method. Passive treatment requires an

initial capital investment; however, aside from water quality monitoring, the ongoing operational costs are greatly reduced as these systems are designed to use natural processes and the pre-existing hydraulic gradient (Johnson and Hallberg, 2005). These systems are particularly attractive for implementation at remote abandoned mine sites which may not have access to electricity. The downside is that these systems are less controlled, and they may not be able to achieve as high contaminant removal rates as industrial scale treatment plants, and their performance may degrade over time. Anoxic limestone drains (ALDs) are one example of a passive treatment system. In an ALD, contaminated water flows through a bed of limestone gravel, and alkalinity is generated through reactions with the carbonate minerals. This treatment has lower costs than some alternative methods; however, longevity is a problem. Over time, the limestone gravel becomes coated, or "armoured" with metal hydroxide precipitates and performance declines (Johnson and Hallberg, 2005). Another passive treatment method is stimulation of biological processes which can assist in the remediation efforts. These processes may assist in the removal of metals, generation of alkalinity, and the reduction of sulphate. An example is the growth of SRB which can reduce sulphate, generate alkalinity, and subsequent reactions assist in metals removal (see section 1.7 for discussion on SRB). The specific treatment system in which the SRB are used can vary significantly, including constructed wetlands, bioreactors, and permeable reactive barriers. Variations on models for bioreactors and permeable reactive barriers include successive alkalinity producing systems (SAPS; Kepler and McCleary, 1994) and reducing and alkalinity producing systems (RAPS; Younger et al., 2003). In constructed wetlands, a complex group of different processes can occur, with multiple biological processes, as well as bioaccumulation of metals, adsorption, ion exchange, and precipitation reactions possible (Egiebor and Oni, 2007). Commonly, one or more techniques may be utilized in order to achieve the optimal results for AMD treatment, such as a PRB which then flows into a

constructed wetland, or a PRB which combines both passive chemical (e.g., lime) and biological (e.g., SRB) processes. Because the characteristics of AMD are highly site specific, a detailed analysis of the site conditions and water quality must be undertaken to understand the necessary remediative measures for a given site.

1.5 Scope of Present Study

In this study a passive treatment system was designed, constructed, and tested as a concept for the treatment of pit waters at the Steep Rock site. Laboratory testing simulated a PRB designed to stimulate SRB activity by the addition of organic matter. In these experiments, stock water collected from Hogarth pit at the Steep Rock site was pumped into the flow-through reactors, where biological and chemical reactions were expected to result in decreased sulphate concentrations in effluent water. The use of different reactive mixtures assessed the capability of different substrates to stimulate SRB, and also allow for assessment of the effectiveness of the substrate selection process in order to improve procedures for reactive material selection in PRBs using SRB.

This study involved three phases in order to: 1) determine the optimal PRB design, mixture substrates, and proportions; 2) conduct the flow-through reactor experiments; and 3) to understand the processes which occurred in the experiments and assess the effectiveness of the reactive mixture selection procedure. Phase one focussed on the design of the flow-through reactor setup and characterization of the candidate organic substrates to determine which materials are used in the reactor experiments. This characterization also allowed for the stoichiometric determination of the organic carbon requirement, such that the appropriate mass of substrate would be utilized. Phase two included the construction and operation of the flow-through experiments, including weekly collection of effluent water samples and direct measurement of Eh (oxidation-reduction potential) to measure the performance of each reactor

over time. The final phase involved the deconstruction of the experiments and sampling and analysis of post-experiment materials in order to determine the processes which occurred inside the flow-through reactors. Additionally, a major focus was assessing the change in nutrient concentrations in order to determine if sufficient nutrients were available to SRB, as well as determine the effectiveness of the substrate selection procedure.

1.6 Permeable Reactive Barriers

One example of a passive water remediation technology is permeable reactive barriers (PRBs). PRBs have been used to treat a wide variety of water contaminants at many different types of industrial sites, including sites experiencing AMD (e.g., U.S. E.P.A., 1998, Blowes et al., 2000, Scherer et al., 2000). A PRB is constructed as a trench below grade within the aquifer, and is filled with reactive material (Fig. 1.3). This trench will intercept contaminated groundwater flowing under natural hydraulic gradient, and the materials within will cause or promote chemical or biological reactions with the contaminant (U.S. E.P.A., 1998). These reactions result in precipitation, adsorption, reduction, oxidation, or otherwise convert the contaminant to a safer or less mobile form (Scherer et al., 2000). Specific materials will be selected based upon the conditions present at a given site, and the particular contaminants desired for removal. In the case of PRBs designed to treat AMD, the intent is to stimulate the activity of SRB, which will remove sulphate and dissolved metals from solution. For sites in which the influent waters are highly acidic, alkaline materials will be needed in order to raise the pH of the solution in order to provide a hospitable environment for SRB.

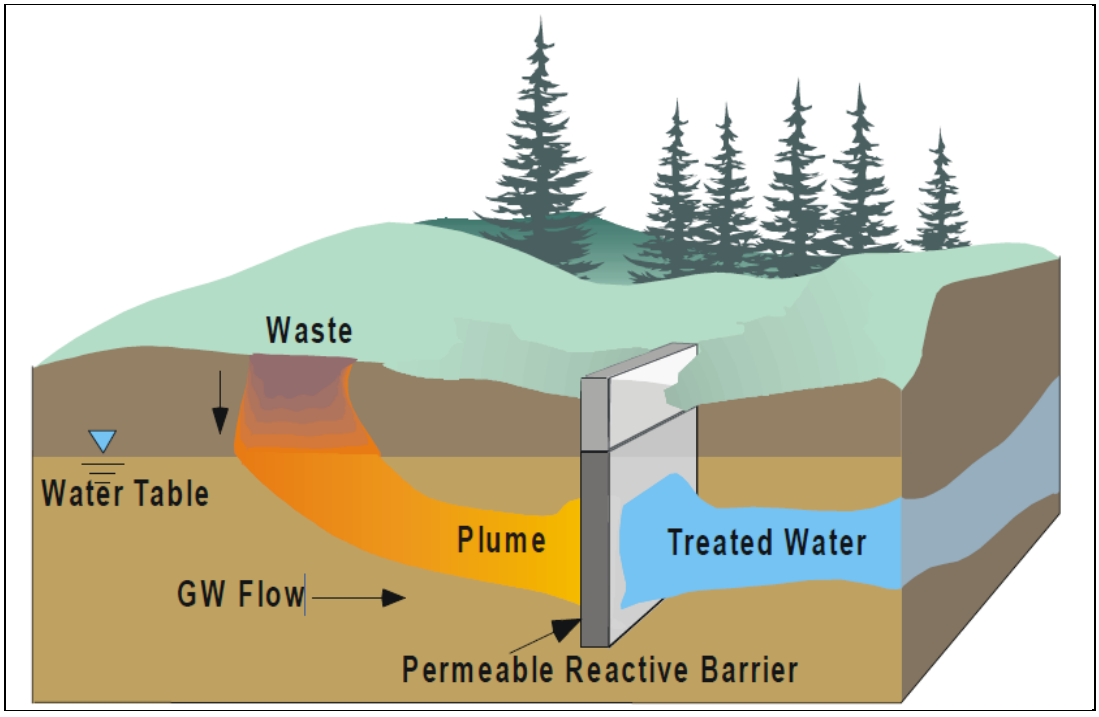

Figure 1.3: Cross-sectional view of a permeable reactive barrier (from U.S. E.P.A., 1998).

While PRBs have been utilized worldwide for a wide variety of contaminants, their use in AMD remediation has been more limited. While many lab-scale studies have been conducted (e.g., Harris and Ragusa, 2001; Gibert et al., 2004; Neculita et al., 2007; Wu et al., 2010; Song et al., 2012); only five field sites worldwide are reported in scientific literature to have installed a full-scale PRB using natural organic materials for the treatment of AMD or acid rock drainage (ARD). This does not represent a lack of viability of the concept, but rather the lack of maturity of the technology. The first site known to have installed a PRB to treat AMD is the Nickel Rim Mine site, near Sudbury, Ontario, where sulphate removal rates ranged from 25-78% (Benner et al., 1997). However, sulphate removal declined by 30% after three years (Benner et al., 2002), and longer term data has not been published. The second site was an ore storage facility in Vancouver, British Columbia, where unprocessed ore was stored on the ground surface, and serious ARD issues were present on the site due to oxidation of the minerals present (Ludwig et al., 2002). A high rate of metals removal was observed; however, sulphate was not included in

the contaminants monitored among published documents, despite likely being a significant environmental contaminant at this site.

The third site to install a PRB for AMD treatment was the Shilbottle Mine in Northumberland, UK (Jarvis et al., 2006). AMD from coal spoil heaps was treated and averaged 40% sulphate removal over a two year monitoring period. The fourth site to install a PRB for AMD treatment was the Aznalcollar Mine in Spain, where the failure of tailings pond retention dam resulted in the release of approximately 4 million m^3 of AMD (Gibert et al., 2011). Serious design flaws and construction failures resulted in a failure to fully capture the contaminant plume, and a reduced ability to effectively treat contaminated water which did flow through the PRB. Sulphate removal rates ranged from 0 to 40%, and the barrier was unsuccessful in achieving some of the project goals (Gibert et al., 2011). This project is a significant demonstration of the importance of careful planning, site characterization, and appropriate construction techniques in PRB design and construction. Finally, the fifth PRB constructed to treat similar conditions was a fertilizer plant in South Carolina, USA. The plant utilized pyrite in its production processes, and improper disposal of this material produced ARD (Ludwig et al., 2009). High rates of sulphate removal ranging from 66-99% were achieved. This study is unusual for PRBs treating acid rock drainage in that zero-valent iron (ZVI) was used as a reactive material. This was done in order to assist in the removal of arsenic; however, it may also have improved sulphate reduction as well, as sulphate can corrode ZVI in the following reaction (Blowes et al., 2000; Philips et al., 2000):

$$4Fe^0 + SO_4^{2-} + 9H^+ \rightarrow 4Fe^{2+} + HS^- + 4H_2O$$

This reaction produces both hydrogen sulphide and ferrous iron, which can then react to form an insoluble iron sulphide, such as mackinawite (FeS), or pyrite (FeS_2). The same result is

achieved through the biological reduction of sulphate by SRB, and the combined effects of chemical and biological sulphate reduction may account for the high sulphate removal.

There are a variety of factors which must be taken into account in PRB design and construction which can impact performance. First among these is the selection of materials which will encourage and support the desired chemical or biological processes. Various water quality parameters besides those desired for treatment may impact these processes and therefore must be accounted for. Another very important consideration is the hydrogeology of the site and how the natural flow will interact with the PRB. A PRB must be designed to fully intercept the plume of contaminated water, and thus must have sufficient depth and width, and align perpendicular to the actual direction of flow (U.S. E.P.A., 1998). Furthermore, the PRB should have a hydraulic conductivity higher than that of the surrounding aquifer, such that even if there is porosity loss due to degradation of PRB materials, the hydraulic conductivity is not reduced below that of the surrounding materials. If the hydraulic conductivity were to fall below that of the surrounding aquifer, it is possible that water may divert around the PRB, resulting in a failure to capture the entire contaminant plume (U.S. E.P.A., 1998). In both lab-scale and field-scale PRBs, one of the most commonly noted problems is porosity loss, and consequently it is important to include sufficient non-reactive matrix support material which will maintain porosity within the barrier (Blowes et al., 2000).

The development of preferential flow paths can also become a problem over time due to changes in PRB porosity, or the failure in initial construction to ensure a homogenous distribution of materials (Benner et al., 1997). Preferential flow paths can result in greatly reduced residence time, and the materials in a certain area being overexposed, while reactive materials in another area are not being utilized. This can result in a substantial reduction in PRB performance and longevity (Blowes et al., 2000). As flow paths and porosity greatly influence

the residence time; the desired residence time must be determined prior to construction of a PRB since the flow rate of groundwater cannot be controlled. If the groundwater flows through the barrier too quickly, resulting in a short residence time, there may be insufficient time for the desired reactions to occur, or occur to their full extent. An overly long residence time is also impractical due to construction cost considerations. Careful planning and attention during both design and construction phases can reduce the risk of these problems, and help to ensure the PRB is able to perform at a high level, and over a long period of time.

1.7 Sulphate Reducing Bacteria

Sulphate reducing bacteria have been increasingly utilized as a remediation tool for sulphate and/or metal-rich water, and for the treatment of acid mine drainage (Neculita et al., 2007). This is due to their unique ability to reduce sulphate, generate alkalinity, and produce sulphide which reacts with dissolved metals to form insoluble metal sulphides. In addition, the natural, passive, and self-sustaining operation of SRB can result in a significantly lower cost remediation program (Lindsay et al., 2009). Sulphate reducing bacteria are strictly anaerobic, which also makes them perfectly suited for use in a permeable reactive barrier which creates an anoxic environment. Sulphate reducing bacteria use organic carbon as an electron donor and dissolved sulphate as an electron acceptor; according to the following reaction (Waybrant et al., 1998; Cocos et al., 2002; Neculita et al., 2007):

$$2CH_2O_{(s)} + SO_4^{2-}{}_{(aq)} \rightarrow H_2S_{(aq)} + 2HCO_3^{-}{}_{(aq)}$$

CH_2O represents a simple organic carbon molecule; the actual form of the organic carbon available will depend upon the specific organic substrates, biodegradation processes, and the specific types of bacteria responsible for biodegradation. The reaction produces hydrogen sulphide as well as bicarbonate. Hydrogen sulphide can be a significant pollutant on its own, and also has the potential to be oxidized back to sulphate if not removed (Johnson, 2003). Commonly

in PRB systems designed to treat AMD, the water is metal-rich and the hydrogen sulphide will react with dissolved divalent metals, producing metal sulphide precipitates, thus removing the undesirable contaminant from the water. This is achieved by the following reaction, in which Me^{2+} represents a divalent metal ion (Blowes et al., 2000; Neculita et al., 2007; Sheoran et al., 2010):

$$Me^{2+}_{(aq)} + H_2S_{(aq)} \rightarrow MeS_{(s)} + 2H^{+}_{(aq)}$$

In Hogarth Pit at Steep Rock, the water is metal-poor and thus there are potentially insufficient metals available to react with dissolved sulphide. To remedy this problem, zero-valent iron is used as an additional reactant to supply Fe^{2+} to the solution and allow iron to be available to react with sulphide. This reaction yields an additional benefit of providing H_2, which some species of SRB can utilize as an alternative electron donor. Iron is supplied via the following reaction (Kumar et al., 2013):

$$Fe^{0}_{(s)} + 2H_2O_{(l)} \rightarrow Fe^{2+}_{(aq)} + 2OH^{-}_{(aq)} + H_{2(g)}.$$

In order to maximize the growth and activity of SRB, a number of environmental conditions must be optimized. Firstly, SRB are strictly anaerobic, and thus precautions must be taken to ensure oxygen infiltration into the PRB does not occur beyond levels naturally dissolved in groundwater. Reducing conditions are required, with a redox potential (Eh) lower than -100 mV considered optimal for SRB activity (Postgate, 1984). The pH of the water is an important parameter, with a pH in the range 5-8 being ideal for SRB activity (Willow and Cohen, 2003), although some strains of SRB can operate effectively outside of this range. This is an important factor to consider in the treatment of AMD, which is commonly very acidic and will require treatment to raise the pH prior to SRB treatment. Temperature also impacts SRB activity, and various strains have been reported to be able to function from -5°C to +75°C (Postgate, 1984). Lab and field scale testing has demonstrated that cold temperatures may cause a significantly

longer acclimation period, but once the population has been established and active, winter temperatures do not have a significant impact on sulphate reduction rates (Fortin et al., 2000; Zaluski et al., 2003; Tsukamoto et al., 2004). This balance in rates may also be accomplished by an increased population of SRB offsetting lower reduction rates during the winter, and lower winter flow rates also mitigate reduced SRB activity.

The selection of optimal organic carbon sources is important to ensure the highest possible rates of sulphate reduction, as organic carbon as the electron donor is often the rate limiting factor in sulphate reduction in sulphate rich water (Gibert et al., 2004). The ideal organic carbon sources are simple compounds which can be utilized directly by the SRB, such as lactate, which is considered the most effective organic carbon source (Nagpal et al., 2000). Other simple compounds such as methanol, ethanol, pyruvate, glucose, sucrose, and acetate are also highly effective sources for some strains of SRB (Dvorak et al., 1992; Tsukamoto et al., 2004; Neculita et al., 2007). Because the design from this study was intended to be able to be up-scaled to a field-scale PRB, it was necessary to use organic carbon sources which are available at low cost, in large volumes, and do not require ongoing replenishment or external storage. Such sources typically include animal manure, plant waste, sewage sludge, municipal compost, and spent mushroom compost (Neculita et al., 2007). Previous studies on PRBs and bioreactors utilizing SRB to treat mine waters have found that utilizing two different organic substrates significantly improved performance (Waybrant et al., 1998; Cocos et al., 2002; Neculita et al., 2007). This is attributed to differences in degradation rates, as well as potentially providing a better nutrient balance. To maximize this benefit, one manure and one plant based substrate was used in each reaction cell in this study in order to provide a balance in degradation rates. The manure degrades more quickly, providing nutrition to the bacteria at the start of the experiment, while the plant material degrades more slowly, providing progressive nutrition over the course of the experiment

(Neculita et al., 2007). The organic substrates will be degraded from complex organic compounds by fermenting and cellulolytic bacteria into simpler molecules which can be used by SRB.

The specific combinations of manure and plant materials were selected based upon the chemical composition of the candidate substrates. A variety of parameters have been utilized in past studies for the selection of organic carbon sources, although none have proven to be a definitive guide to resultant sulphate reduction rates, and there is considerable disagreement among authors as to which parameters are most useful (Prasad et al., 1999; Neculita et al., 2007). For this study, nutrient balance was the primary focus for selection between the candidate materials, as this is a critical requirement for biodegradation of organic materials and the metabolism of SRB (Waybrant et al., 1998; Prasad et al., 1999; Zagury et al., 2006). The primary consideration is C:N ratio, in which a 10:1 ratio is considered desirable for the biodegradation of complex organic carbon sources (Reinertson et al., 1984; Bechard et al., 1994; Prasad et al., 1999; Zagury et al., 2006). Additional sources have also quoted a C:N:P ratio of 110:7:1 as optimal for the growth of SRB (Kuyucak and St-Germain, 1994; Cocos et al., 2002).

1.8 Previous PRB Studies at Steep Rock

The issue of AMD treatment has a long and varied history, with most programs focussing on chemical treatment methods, with a bias towards acidity neutralization and metals removal. In recent years, studies have increasingly looked towards passive treatment systems utilizing biological treatment methods, with PRBs as a common approach (Blowes et al., 2000). Still, little attention has been given to sites such as the Steep Rock site where sulphate-rich waters are the primary concern. The design of a treatment system for the water conditions present at Steep Rock was first investigated in 2011 by S. J. Shankie as part of an M.Sc. thesis completed at Lakehead University. The study utilized batch reactor and flow through reactor experiments to

test reactive mixtures for their capacity to remove sulphate from water sampled from the Hogarth pit lake within the Steep Rock site. Experiments were set up to simulate PRB conditions in bench-scale testing. Organic matter was utilized to stimulate the activity of SRB in order to promote sulphate reduction to sulphide. The batch reactor tests were able to achieve up to 99% sulphate removal, using horse manure and wood chips as the organic matter source. Flow-through reactor experiments, which more closely replicate PRB conditions, were able to achieve average sulphate removal in the range of 39-49% over the course of the 20 week experiment, depending on the exact mixture and structure of the reactive column. Performance of the flow-through declined over time, with sulphate removal in the range of 25-40% at the end of the experiment.

A variety of factors have been identified as possible limitations in the performance of these flow through reactors. In the study, Shankie (2011) concluded that the availability of divalent metals, such as Fe^{2+}, was a possible limiting factor in sulphide precipitation, and thus sulphate removal. Residence time was another factor identified that could be a negative influence on performance. Shankie (2011) identified a loss of permeability in the flow through reactors over time, which limited flow, and may have caused preferential flow channeling. Such behaviour would result in certain areas of the reactor becoming nutrient depleted, while other areas with constrained permeability having available nutrients, but the water is prevented from interacting with these areas. This loss of permeability can be caused by a combination of the breakdown of organic matter, precipitates formed over the course of the experiment, and gravity induced compaction in the vertically oriented reactors. Carbonate rock was used as one of the components in the reactive mixture, which is common in PRBs treating acidic waters. However, the waters in this situation are near neutral and thus do not require neutralization; consequently, a less degradable matrix support material might be more desirable.

1.9 Format of Thesis

This thesis consists of two sections: Part One: Material Testing and Characterization, which discusses the process of analyzing and characterizing the candidate organic substrates in order to design the most effective possible reactive mixture for the stimulation of SRB; and Part Two: Flow-Through Reactor Experiments, which details the design, operation, and assessment of the flow-through reactor experiments. Part two combines the second and third phases of this research project as described in section 1.5. A combined Summary and Conclusions follows in Chapter 8.

Part 1: Material Testing and Characterization

Chapter 2: Analytical Methods for Material Testing

2.1 ICP-AES Analysis

Cow, poultry, and sheep manures, and hay were provided courtesy of Sleepy G Farms, Pass Lake, Ontario. Horse manure was provided courtesy Cryderman Quarter Horses, Murillo, Ontario. Rabbit manure and leaves were provided courtesy A. Conly. All samples were analyzed at least once, with triplicates run for hay and rabbit manure in each assessment in order to confirm homogeneity of organic materials. To characterize the organic materials, an acid digestion method modified from Hseu (2004) and Peters (2003) was followed. In this procedure, finely milled samples were dried in an oven at 65°C for 48 hours, after which time 0.75 g of each sample was added to the digestion tube and 10 ml of concentrated HNO_3 was added without heating. After one hour the solutions were heated to 95°C and allowed to digest for 8 hours, with repeated additions of HNO_3 to prevent drying. After this period, samples were removed from heat and 3 ml of 30% H_2O_2 was added in 0.5 ml increments. Once the reaction had ceased, samples were returned to heat and allowed to digest at 95°C for one hour. After cooling, samples were then filtered using Whatman #42 filter paper, diluted to 100 ml in a volumetric flask, and shaken thoroughly to ensure a homogeneous solution. The solutions were transferred to centrifuge tubes, and submitted to the Lakehead University Instrument Lab (LUIL) for ICP-AES analysis to determine the elemental concentrations in the digests (See appendix A for list of elements assessed).

Digestion of the inorganic creek sediment followed United States Environmental Protection Agency (EPA) method 3050B (1996). Samples were finely milled and oven dried at 65°C for 48 hours. One gram of each sample was added to the digestion tube, 10 ml concentrated HNO_3 was added, and the tube was swirled to create a slurry. The solution was heated to 95°C for 10 minutes, after which time 5 ml of additional HNO_3 was added. If brown fumes appeared,

the addition of HNO_3 was repeated until brown fumes were no longer produced. The digestion was allowed to proceed for two hours, or until the solution volume decreased to 5 ml. The samples were removed from heat and allowed to cool, after which 2 ml of DI water and 3 ml of 30% H_2O_2 were added (H_2O_2 added as single drops to prevent overly vigorous reaction). The samples were returned to heat at 95°C, and allowed to digest until effervescence ceased. At this point H_2O_2 was added in 1 ml aliquots until minimal effervescence occurred (a maximum of 10 ml H_2O_2 could be added). The solution was allowed to digest for two hours, or until it was reduced to 5 ml. At this point, 10 ml of concentrated HCl was added, and allowed to digest at 95°C for 15 minutes. After cooling, samples were then filtered using Whatman #42 filter paper, diluted to 100 ml, and shaken thoroughly to ensure a homogeneous solution. The solutions were transferred to centrifuge tubes, and submitted to the Lakehead University Instrument Lab (LUIL) for ICP-AES analysis to determine the elemental concentrations in the digests.

2.2 Easily Available Substances (EAS) Analysis

In order to assess the potential for biodegradability of the candidate organic substrates, a testing procedure known as Easily Available Substances (EAS) was utilized (Prasad et al., 1999; Gibert et al., 2004). The EAS fraction is ‘‘the organic portion of a substrate that can be readily used by the microorganisms”. The test was conducted following the procedure described by Prasad et al. (1999) and Zagury et al. (2006). Samples were oven dried at 60°C for 24 hours. Two grams of material (measured to nearest 0.001 g) was transferred to a digestion tube, and then soaked with acetone, agitated, and allowed to soak for 5 minutes. This material was poured out and collected using a funnel and filter paper, and dried overnight. The dried material was transferred to a digestion tube, and digested in 5% HCl at 95°C for 1 hour, adding HCl as necessary to prevent drying. The material was poured out and collected using a funnel and filter paper, and residual material was dried for 48 hours. The final mass was measured, and the

difference between the initial mass and final mass represents the lost EAS fraction. This material was then collected for acid digestion and C/N/S analysis in order to determine what chemical fractions were contained within the EAS fraction.

2.3 CNS Analysis

Carbon-nitrogen-sulphur (CNS) combustion analysis was used to determine the carbon, nitrogen and sulphur contents of the candidate organic substrates. Sample preparation for this analysis required milling samples to a powder, or in the case of hay, cutting the material to the finest degree possible. Samples for both raw substrate and EAS treated substrates were submitted to the Lakehead University Instrument Laboratory (LUIL) and analyzed using CHNS Elementar Vario EL analyzer in order to determine changes in composition following removal of the EAS fraction. Samples were loaded into tin boats and then combusted through an automated process at 1150°C. The combustion process results in gasification of the sample. These gases are reduced to N_2, CO_2, and SO_2, and carried in a helium gas stream. CO_2 and SO_2 are adsorbed while passing through the adsorption columns, while N_2 is allowed to reach the detector. Following detection of the N_2 peak, the CO_2 column is heated to release CO_2 and is detected. Finally the SO_2 column is heated and SO_2 is released and detected. A connected computer calculates the elemental concentration from the detector signal and sample weight based upon stored calibration curves (Elementar Vario EL cube technical brochure, undated).

Chapter 3: Material Testing Results

3.1 ICP-AES and Easily Available Substances Analysis

The complete results for ICP-AES and EAS analyses of candidate reactive materials are provided in Appendix A. The primary parameter of interest from the acid digestions is phosphorus (Fig. 3.1). Phosphorus is an important nutrient for bacterial metabolism, and has been reported to promote optimal levels of sulphate reducing bacteria activity when combined with carbon and nitrogen in a 110:7:1 (C:N:P) ratio (Kuyucak and St-Germain, 1994; Cocos et al., 2002).

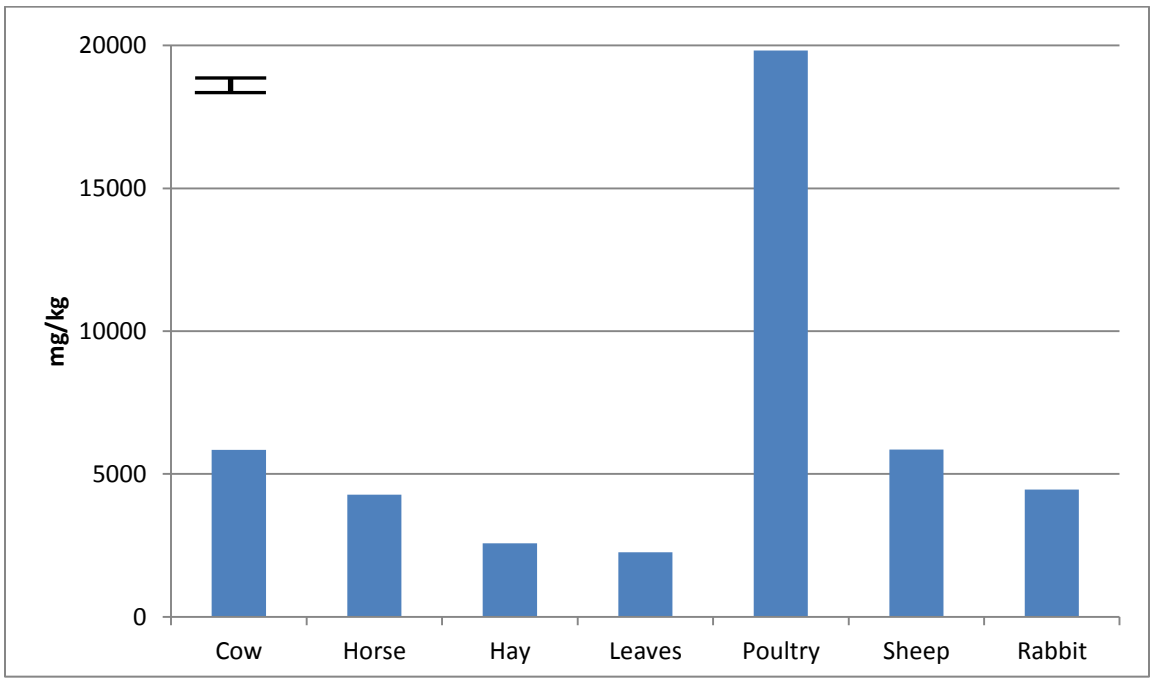

Figure 3.1: Phosphorus concentrations in untreated substrates as determined by ICP-AES. Error bar in top left illustrates a 3σ error.

Poultry manure has the highest phosphorus content at 19,825 mg/kg, with plant based substrates, hay and leaves, having the lowest phosphorus content, with 2570 mg/kg and 2264 mg/kg, respectively. The remaining substrates have somewhat higher phosphorus, with sheep at 5853 mg/kg, cow at 5847 mg/kg, rabbit at 4453 mg/kg, and horse at 4276 mg/kg. All substrates had a significantly reduced phosphorus content following EAS treatment (Fig. 3.2). The general

proportions between the different substrates remained similar, with poultry having the highest concentration at 1497 mg/kg, and rabbit the lowest at 367 mg/kg.

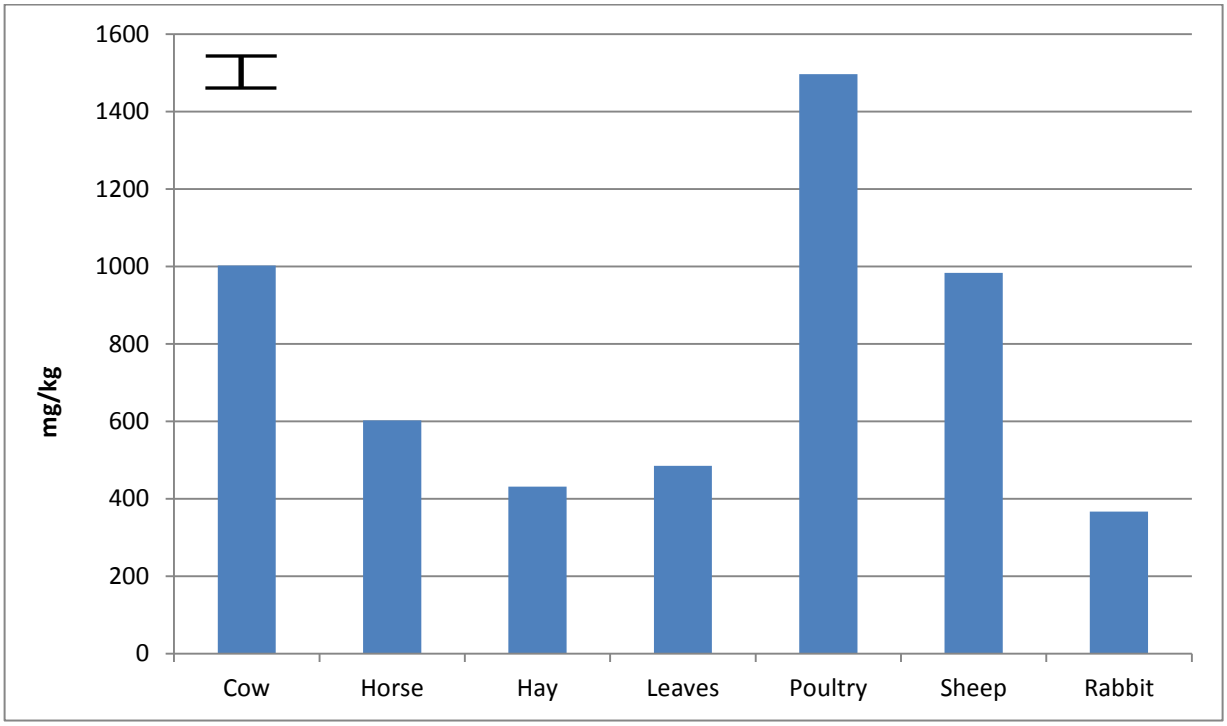

Figure 3.2: Phosphorus concentrations in EAS treated substrates as determined by ICP-AES. Error bar in top left illustrates a 3σ error.

While phosphorus was the primary constituent of interest, as it was needed in order to determine the reactive media used and the required proportions, the full array of elements available for detection by ICP-AES was also tested. The results for aluminum, iron, magnesium, sodium, and sulphur are presented in Figure 3.3, while calcium and potassium are presented in Figure 3.4. Horse manure contains elevated values for aluminum, iron, and magnesium, while poultry manure has elevated amounts of magnesium, sodium, sulphur, calcium, and potassium present relative to the other substrates tested. Hay generally has lower detected values for most parameters, with the exception of potassium, for which it has a higher than average concentration. Cow, leaf, sheep, and rabbit manure generally had unremarkable results compared to the other substrates.

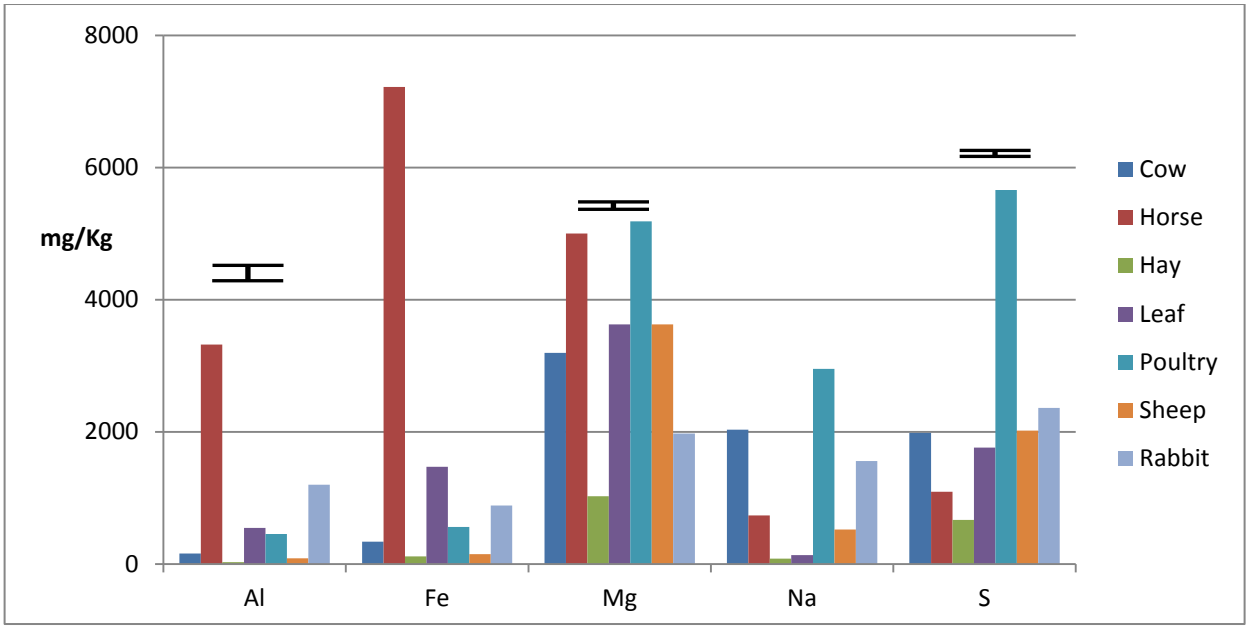

Figure 3.3: ICP-AES determined concentrations of aluminum, iron, magnesium, sodium and sulphur in raw substrates. Error bars illustrate a 3σ error. Error less than symbol size for Fe and Na.

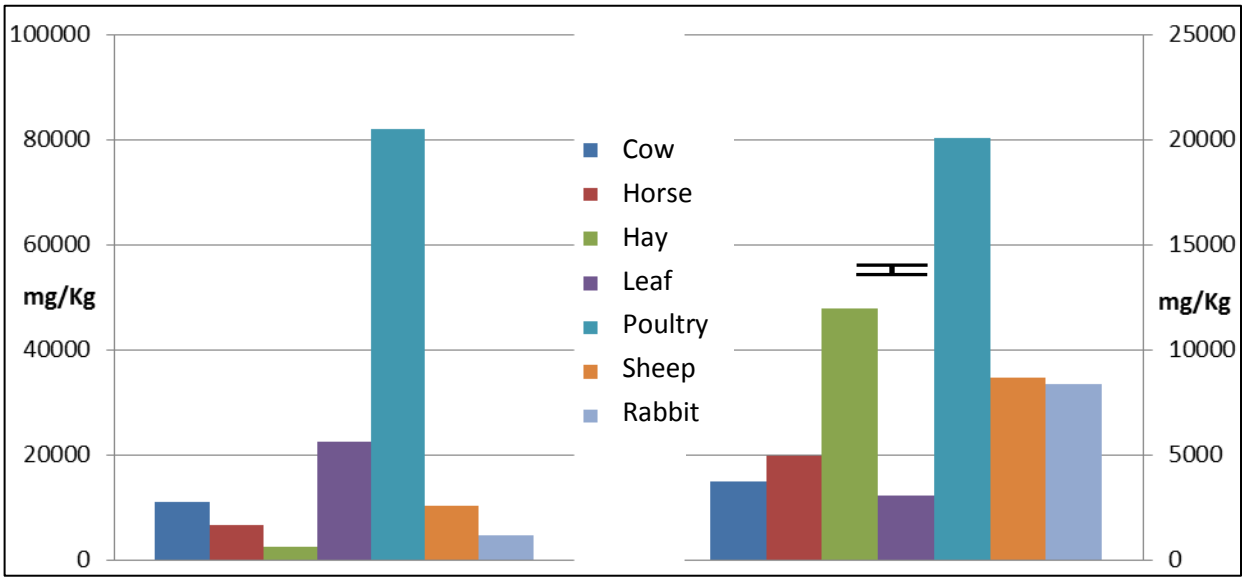

Figure 3.4: ICP-AES determined concentrations of calcium (left) and potassium (right) in raw substrates. Error bars illustrate a 3σ error. Error less than symbol size for calcium.

Two sets of EAS testing were conducted, and the averaged results are shown in Figure 3.5. These results indicate that poultry manure is by far the most readily degraded substance, with an average mass loss of 70.5%. The two plant materials performed similarly to each other, with leaves losing 36.6% of the sample mass, while hay lost 35.5%. Rabbit and sheep manure

underwent moderate mass losses of 32.6% and 28.9%, respectively. Finally, horse and cow manure proved less readily degradable, losing 21.2% and 21.1%, respectively.

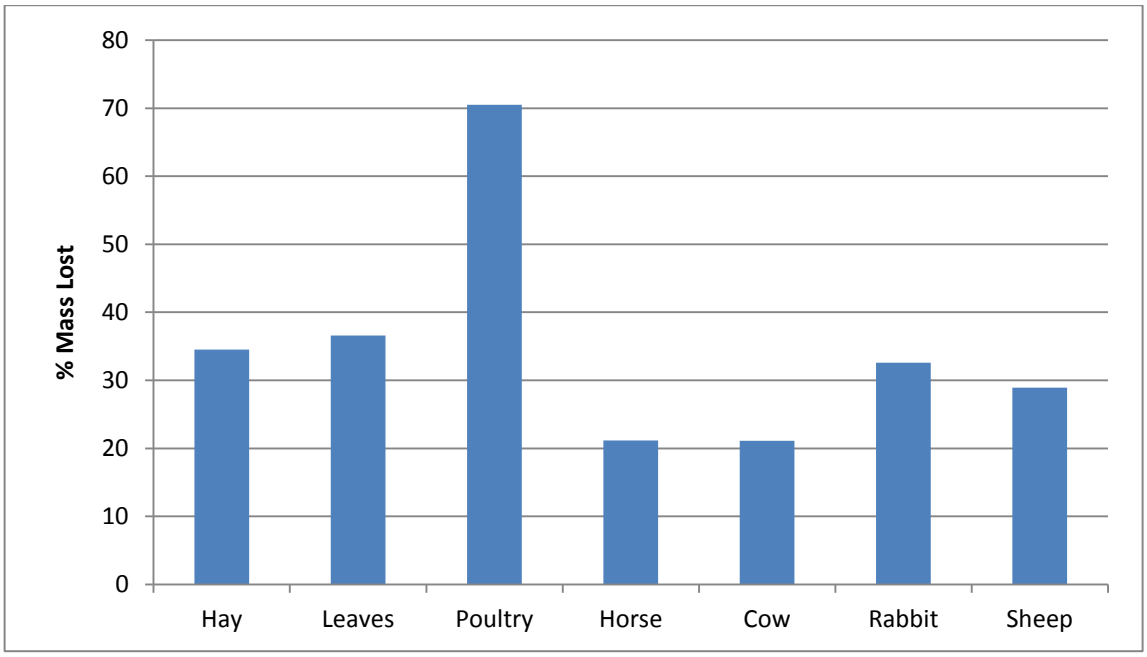

Figure 3.5: Mass losses of organic substrates resulting from Easily Available Substances analysis.

3.2 Carbon-Nitrogen-Sulphur

Each of the candidate substrates was subjected to CNS combustion analysis to determine the proportion of carbon, nitrogen, and sulphur present. Carbon and nitrogen are critical parameters for determining the C:N ratio, an important tool for final substrate selection. In addition, the carbon content is needed to determine the final mass of substrate to use, based upon organic carbon nutrition requirements for sulphate reducing bacteria. In order to assess the availability of this carbon, the CNS combustion analysis was completed on untreated substrates as well as on EAS residue. These results are presented in Figure 3.6, with full results given in Appendix A. In EAS residues, the proportion of carbon rose in cow, hay, leaves, poultry and sheep; meaning that non-carbon bearing fractions were proportionally more degraded by the EAS test. Horse and rabbit manure did not exhibit significant changes, and thus the carbon fraction was degraded in a proportionate manner.

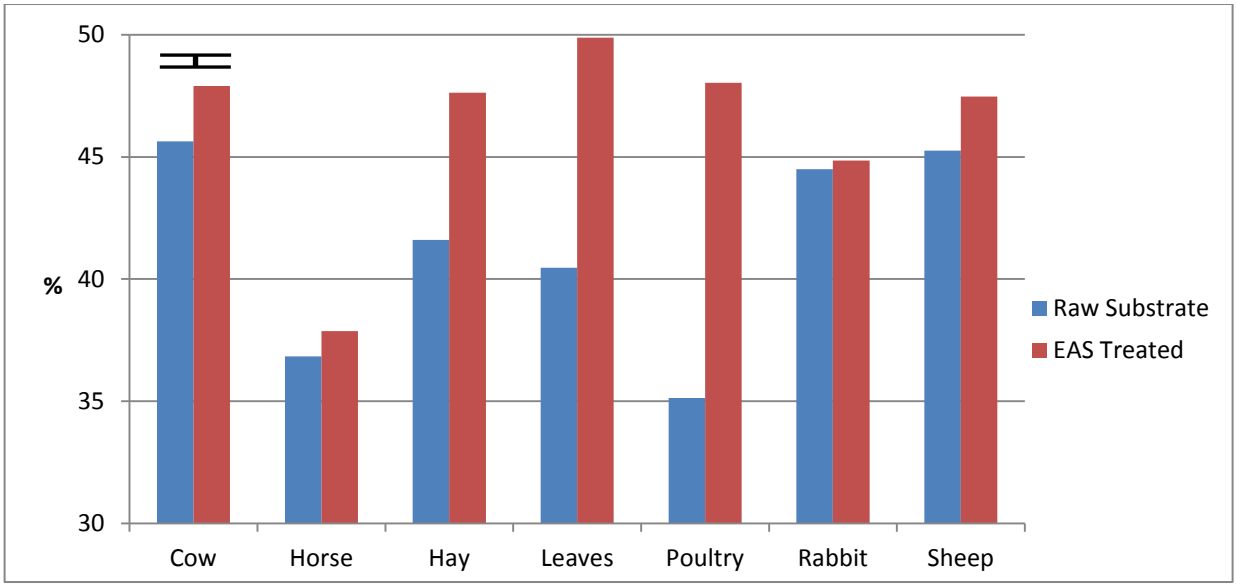

Figure 3.6: Carbon content by mass in raw substrates and EAS residues. Error bar in top left illustrates a 3σ error.

Nitrogen comprises a significantly smaller mass fraction of the substrates, ranging from 1% in hay to 3.2% in poultry (Fig. 3.7). Horse, cow, sheep, rabbit, and leaves are comprised of 1.3%, 1.7%, 1.9%, 1.9%, and 2.2% nitrogen, respectively. These proportions rose in cow, hay, and leaves for EAS residues, indicating that the nitrogen fraction is proportionately less degraded, while poultry has less nitrogen, meaning that the nitrogen fraction was more degraded. Horse, rabbit, and sheep manures are not significantly different following EAS testing.

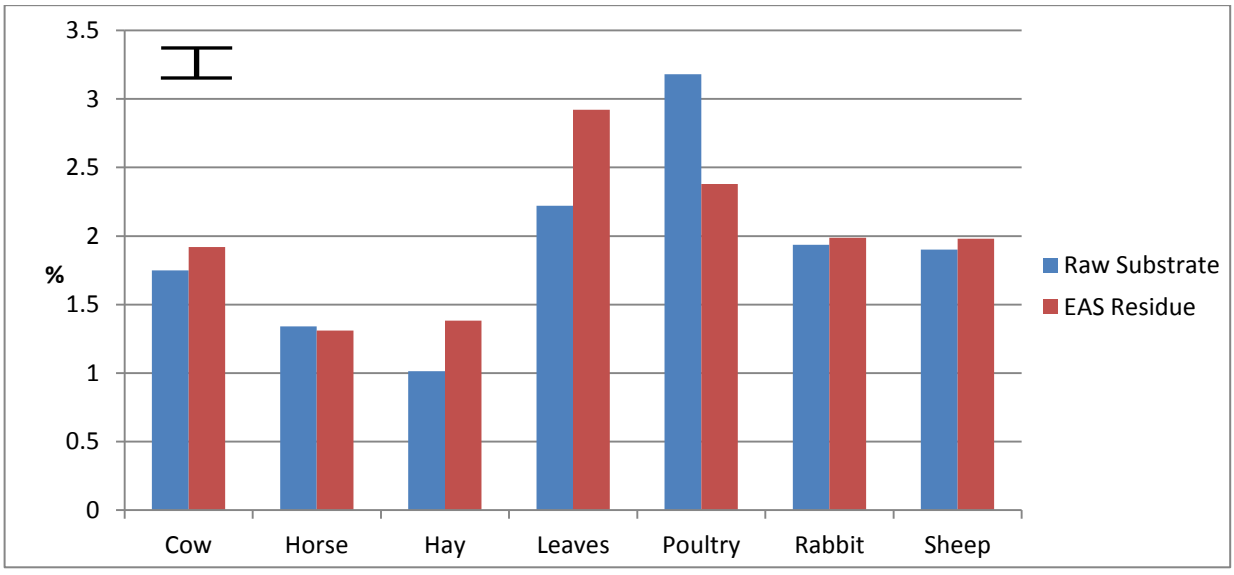

Figure 3.7: Nitrogen content by mass in raw substrates and EAS residues. Error bar in top left illustrates a 3σ error.

Sulphur comprises less than 1% of the substrate by mass in all raw substrates and EAS residues (Fig. 3.8). In raw substrates, the lowest concentration was found in hay, at 0.06%, while poultry was by far the richest in sulphur; containing 0.55% sulphur by mass. Horse, leaves, sheep, cow, and rabbit are comprised of 0.14%, 0.14%, 0.20%, 0.22%, and 0.24% sulphur, respectively. With respect to the other substrates, these proportions are similar following EAS testing. The slight increase in sulphur content in all EAS residues suggests that the sulphur fractions are consistently less degradable than other fractions comprising the organic substrates.

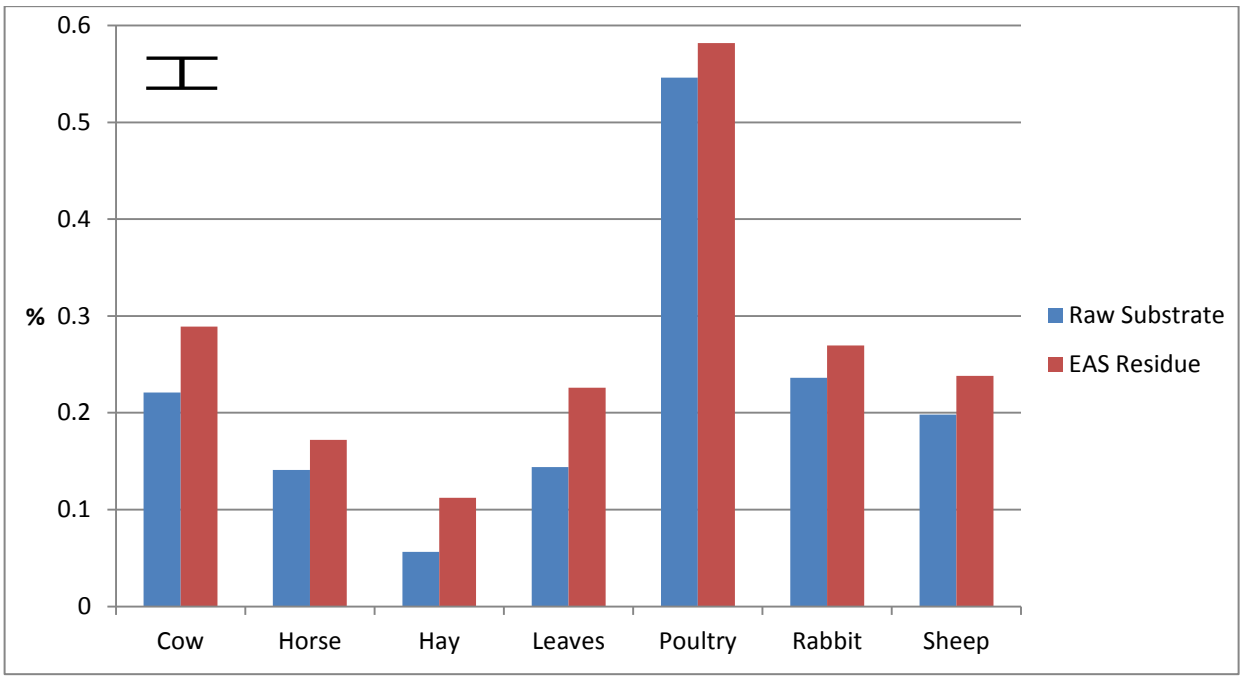

Figure 3.8: Sulphur content by mass in raw substrates and EAS residues. Error bar in top left illustrates a 3σ error.

Chapter 4: Implications for Reactive Media Design

4.1 Reactive Media Performance Considerations

Phosphorus is an important nutrient for bacterial metabolism, and has been reported to promote optimal levels of sulphate reducing bacteria activity when combined with carbon and nitrogen in a 110:7:1 (C:N:P) ratio (Kuyucak and St-Germain, 1994; Cocos et al., 2002). The results for other parameters determined by acid digestion (Section 3.1) are not critical in determining the ideal composition of the reactive mixtures. Figure 4.1 shows the phosphorous-normalized abundances of carbon and nitrogen (phosphorus assigned a value of one), and allows for comparison against the desired C:N:P ratio of 110:7:1.

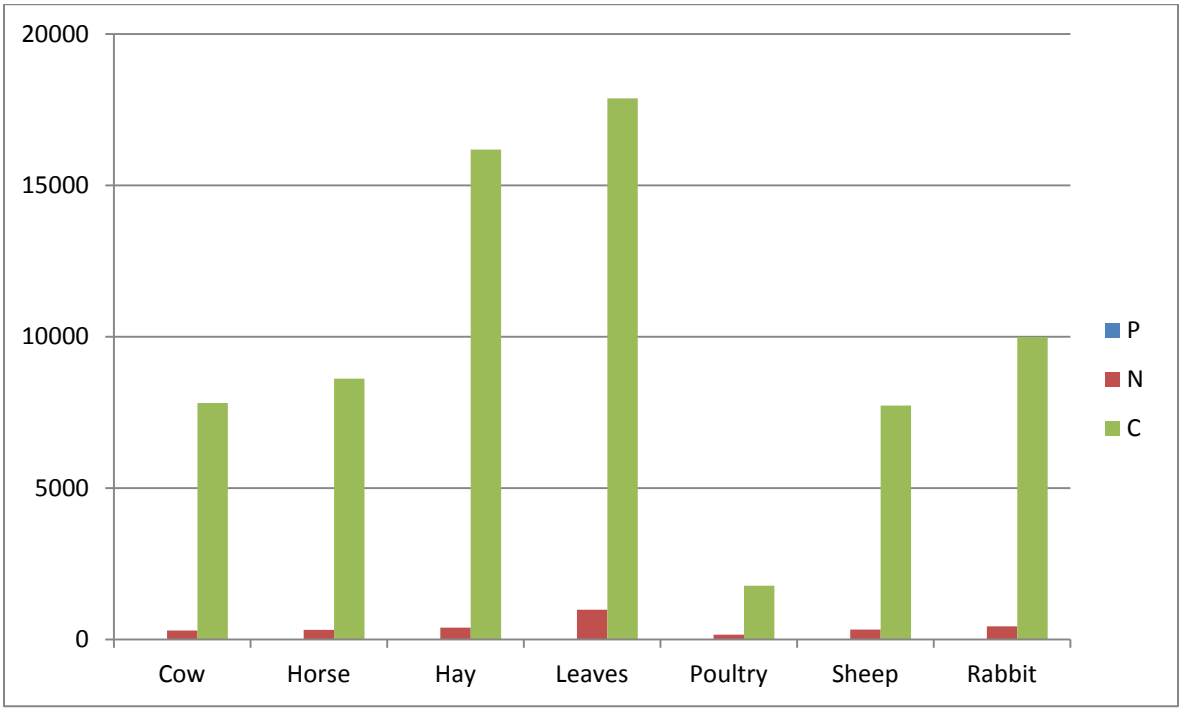

Figure 4.1: Normalized C, N, P content, with P assigned a value of 1. Combined ICP and CNS data.

These results show that phosphorus concentrations are too low to reach this ratio in any of the substrates tested. Due to the relatively higher phosphorus and lower carbon contents in poultry manure, the ratio for poultry of 1772:160:1 was the closest, while sheep manure had the next best result, with a ratio of 7730:325:1. Due to the low phosphorus content in the plant-based

substrates, both hay and leaves have C:P ratios in excess of 15000:1. The change in phosphorus content from raw samples to EAS treated samples was also assessed, in order to determine the relative availability of phosphorus in each substrate (Fig. 4.2). All substrates exceeded a 78% EAS loss, while poultry and rabbit manure exceeded 90% and phosphorus in leaf compost was the least mobile, at 79%. These results reinforce poultry manure as being the best source for phosphorus as it achieved the lowest C:N:P ratio and highest EAS mass loss.

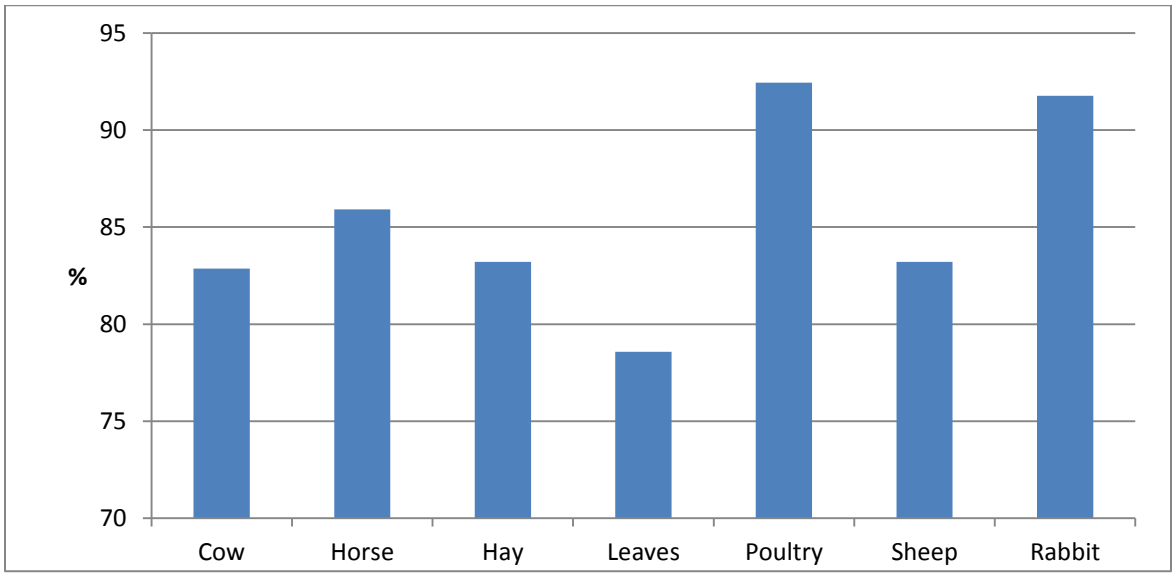

Figure 4.2: Phosphorus loss following EAS testing.

EAS testing seeks to assess the potential for biodegradation in natural environments by a chemical treatment which can simulate the bioavailability of compounds in the organic materials in a short term test. According to Prasad et al. (1999) and Gibert et al. (2004), the EAS fraction is ‘‘the organic portion of a substrate that can be readily used by the microorganisms”. The value of the EAS test is twofold: 1) this testing will help to ascertain which materials have greater biodegradability, and thus are more efficient substrates; and, 2) the values determined can be used as a guideline in determining the final masses of substrate required to sustain SRB activity over the life of the system. Based on this test alone; poultry, rabbit, and sheep would be manure candidates for further consideration, while both hay and leaves are worth further consideration as

the plant based substrate given that the results have not provided significant differentiation (Fig 4.3). The limited mass lost (~20%) by horse and cow manure suggests that these substrates would be less readily degraded, and would therefore provide less nutrients to sulphate reducing bacteria.

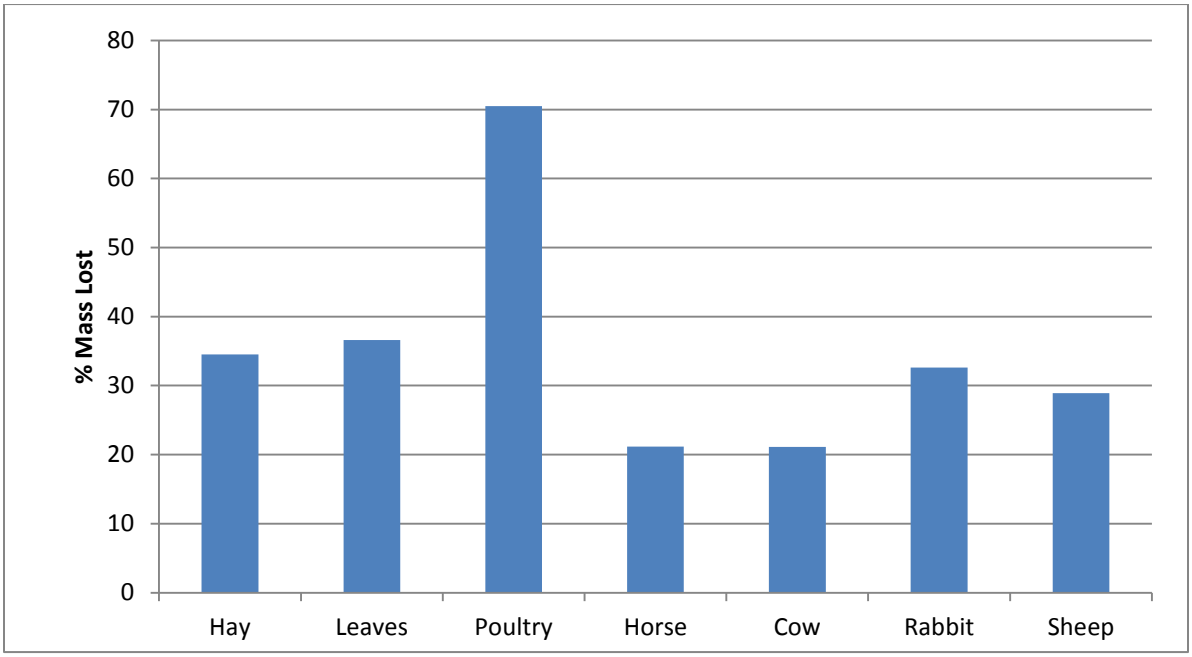

Figure 4.3: EAS determined mass losses of organic substrates.

Carbon and nitrogen are required for microbial nutrition, assisting both with biodegradation as well as sulphate reduction. A C:N ratio near 10 is generally considered ideal for the stimulation of microbial activity and biological degradation of complex substrates (Reinertson et al., 1984; Bechard et al., 1994; Prasad et al., 1999; Zagury et al., 2006). The exact value of 10 is not critical; however, it acts as helpful guide for comparing potential substrates. Carbon-nitrogen determinations were conducted on raw samples and the residues from EAS testing. By analyzing the residue from EAS analysis, it was possible to determine which fractions are more readily degradable. The C:N ratio for each substrate is presented in Figure 4.4. Poultry manure is the closest to achieving the desired ratio, with a C:N ratio of 11, while leaves and hay are less effective with a C:N ratio of 18 and 41, respectively.

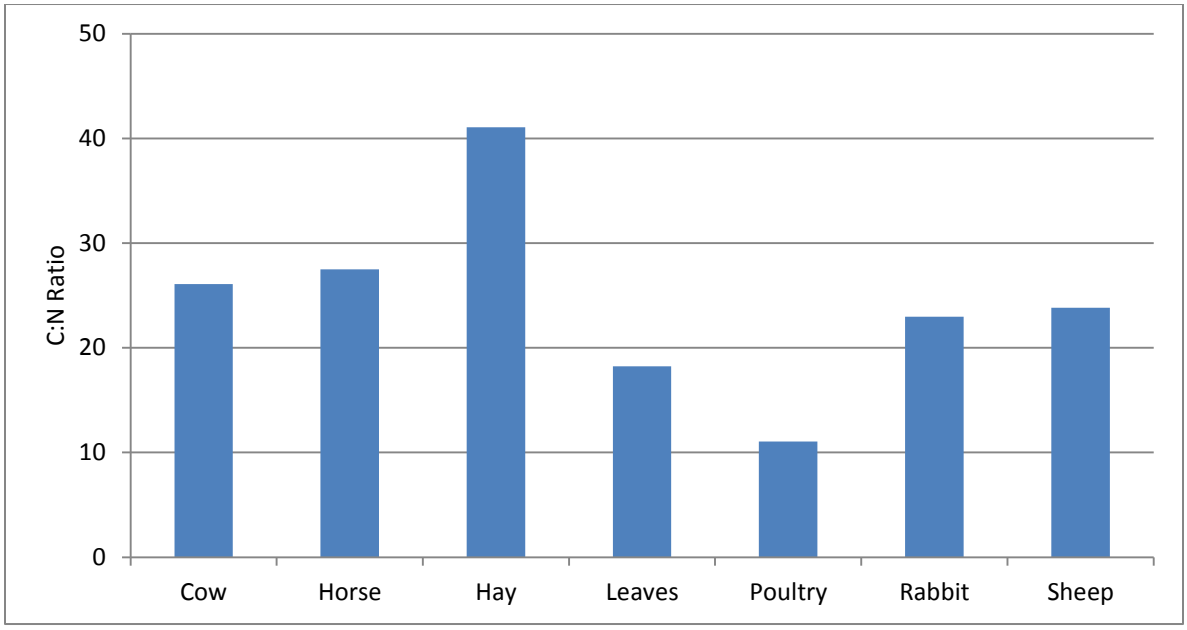

Figure 4.4: Carbon to nitrogen ratio of organic substrates.

CNS analysis of the residues from EAS testing can be used to assess the degree of degradation of organic substrates. The change in nitrogen and carbon values after EAS testing is given in Figure 4.5. For some substrates, such as horse and rabbit manure there is only a minor change in the proportions of nitrogen and carbon following EAS testing. However, others, such as hay and leaves underwent a significant (15-37%) increase in carbon and nitrogen content, meaning that fractions with low nitrogen and carbon content were preferentially removed, resulting in a higher concentration of nitrogen and carbon in the remaining substrate. This is a potential negative for nutrient supply, as the mass lost in EAS testing is not nitrogen- or carbon-rich. Cow and sheep manure both have small (4-10%) increases in carbon and nitrogen content. Finally, poultry manure is unusual in that nitrogen content declined significantly, while carbon content increased significantly. This indicates that the material lost from poultry manure in EAS testing is nitrogen-rich and carbon-poor, and consequently would have a very low C:N ratio. However, in a mixed substrate situation, this might help to balance out the higher C:N ratio compounds released by hay or leaves.

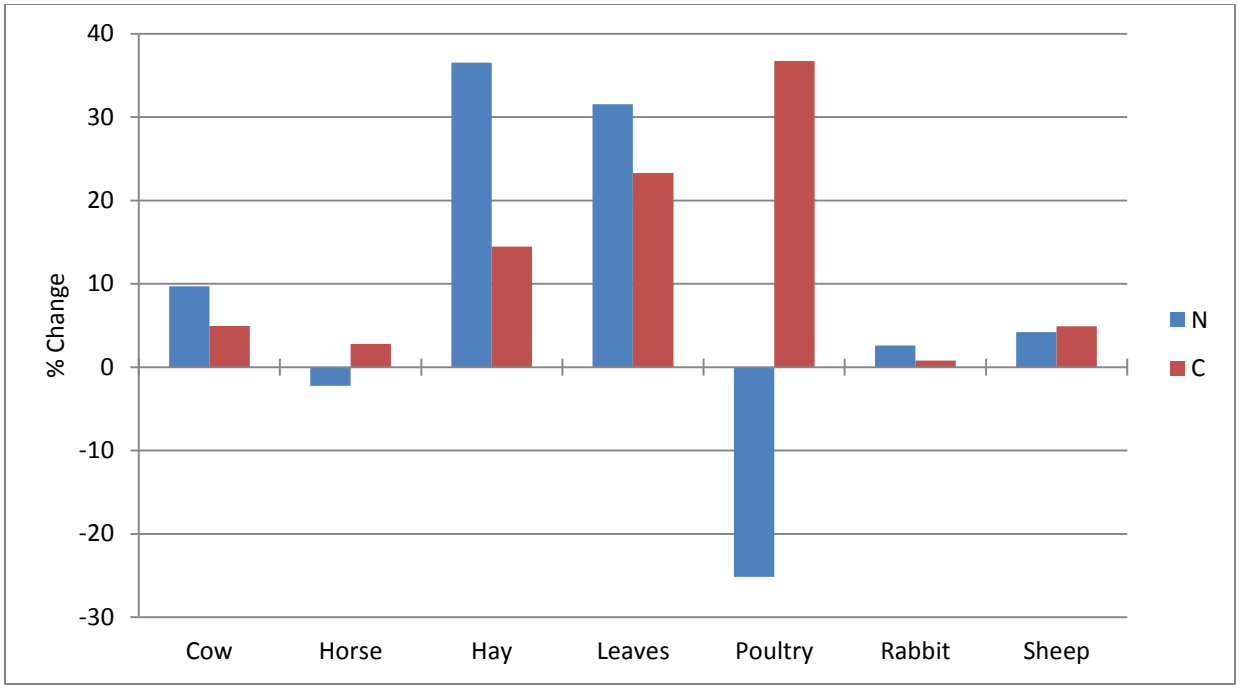

Figure 4.5: Percentage change in nitrogen and carbon after EAS testing.

Tables 4.1 and 4.2 summarize the results from the acid digestions, EAS, and CNS analyses. In each reactor one manure substrate and one cellulosic substrate were used, and thus the two types of substrates are ranked separately. The score reflects the sum of ratings on each test, and thus a low score reflects good performance. ICP-AES results from digestions determined that poultry manure has by far the highest phosphorus content, as well as the best C:N:P ratio. Hay and leaves have lower phosphorus content than the manure substrates, with hay having a slightly better C:N:P ratio than leaves. EAS testing determined that the most readily degradable manure is poultry, while hay and leaves performed similarly, although leaves are slightly more degradable. CNS testing demonstrated that poultry yields the best C:N ratio for manures, although the EAS residue indicated that the degraded fraction would have a very low C:N ratio. This low C:N ratio in poultry manure would be mitigated in a mixed substrate situation, where cellulosic substrates have a higher than desired C:N ratio. Leaves produced a better C:N ratio than hay, and their degradability is similar.

Poultry manure consistently met the desired criteria in each substrate analysis, while sheep and rabbit manure were second and third, respectively. Based on this information, poultry and sheep manures were selected as the manure substrates for the flow-through reactor experiments. The two plant based substrates achieved similar results to each other, with the notable exception of C:N ratio, in which leaves produced a more desirable result. Based on this result, leaves were used in two of the three reactive mixtures, while hay was used in one.

Table 4.1: Relative performance ranking of each manure substrate.

	Phosphorus	EAS	CNS	Score
Cow	3	5	4	12
Horse	4	4	5	13
Poultry	1	1	1	3
Rabbit	5	2	2	9
Sheep	2	3	3	8

Table 4.2: Relative performance ranking of each cellulosic substrate.

	Phosphorus	EAS	CNS	Score
Hay	1	2	2	5
Leaves	2	1	1	4

4.2 Reactive Media Selection for Flow-Through Reactor Experiments

In order to determine the required mass of each substrate to be used in the reactor experiments, calculations were made based on the stoichiometric carbon requirement for operation of the flow through reactor over a period of six months at a flow rate of 0.1 mL/min (see Appendix B for details of these calculations). These calculations yield a theoretical mass of 5.14 g of carbon per reactor as being required to remove all sulphate from solution, assuming an influent concentration of 1585 mg/L SO_4^{2-}. In order to calculate the actual mass of substrate required, the hypothetical mass is corrected for the percentage of carbon in the substrate, as determined by CNS analysis. This mass is further corrected for the biodegradation potential as

determined by EAS testing, to yield an actual mass requirement for each substrate (Table 4.3). No attempt has been made to quantify potential losses, as DOC or POC, to effluent waters.

Table 4.3: Organic substrate mass requirements per reactor.

Substrate	Carbon %	Mass Required (g)	EAS %	Corrected Mass Required (g)
Poultry	35.13	14.63	70.5	20.75
Sheep	45.25	11.36	28.9	39.29
Leaves	40.46	12.70	36.6	34.70
Hay	41.60	12.35	34.5	35.80

The requirement for zero valent iron was calculated in a similar fashion to the substrate requirements. The molar requirement of iron for the precipitation of FeS over six months, at a flow rate of 0.1 mL/min was determined to be 23.88 g per reactor. This value was adjusted to reflect the fact that only the surface of the iron spheres will be available for dissolution and that over the course of the experiment only a limited segment of the diameter may dissolve. It was determined that under a conservative scenario only 18% of the iron may dissolve, and therefore 132.67 g of iron should be placed within each reactor. This conservative dissolution estimate is based upon equal 0.2 mm dissolution around the circumference of a 3.18 mm diameter iron sphere, and calculating the percent mass loss under that scenario. Similar to organic substrates, no attempt has been made to quantify potential losses to effluent, and increased proportions would likely be required for a long term field operation.

The final reactive mixture design is presented in Table 4.4. Each organic reactor had one replicate, with one control reactor simulating natural aquifer conditions, and one other control reactor testing the impact of zero valent iron only, in order to be able to quantify abiotic versus biotic sulphate reduction. The experimental setup only allowed for a total of eight reactors, therefore there could only be three organic reactor mixtures, since each mixture will be used

twice. Given this limitation, it was determined that the group of three different mixtures would test two manure substrates as well as two plant substrates. The higher rated leaves and poultry were used twice, while hay and sheep were only used once. Matrix support and creek sediment were used in sufficient mass to fill the reactors, with matrix support being the primary constituent in order to ensure porosity was maintained. Silica sand was selected for use as matrix support as it was expected to remain unreactive in the conditions present during the flow-through reactor experiments.

Table 4.4: Reactive mixtures for flow-through reactor experiments.

Reactor 1	g	Reactor 2	g	Reactor 3	g	Reactor 4	g
Leaf compost	35	Leaf compost	35	Hay	36	Matrix support	850
Poultry	21	Sheep	36	Poultry	21	Creek sediment	320
Matrix support	400	Matrix support	400	Matrix support	360	Zero-valent iron	133
Creek sediment	200	Creek sediment	200	Creek sediment	180		
Zero-valent iron	133	Zero-valent iron	133	Zero-valent iron	133		
Reactor 5	g	Reactor 6	g	Reactor 7	g	Reactor 8	g
Leaf compost	35	Leaf compost	35	Hay	36	Matrix support	840
Poultry	21	Sheep	36	Poultry	21	Creek sediment	340
Matrix support	400	Matrix support	400	Matrix support	360		
Creek sediment	200	Creek sediment	200	Creek sediment	180		
Zero-valent iron	133	Zero-valent iron	133	Zero-valent iron	133		

Part 2: Flow-Through Reaction Experiments

Chapter 5: Flow-Through Reactor Methods and Design

5.1 Reactor Setup

The reduction-oxidation cell pairs utilized in the flow-through experiments were designed to simulate the behaviour of a permeable reactive barrier (PRB) system, combined with a settling/oxidation pond. This system aimed to encourage the biochemical reduction of dissolved sulphate from the influent water, resulting in the precipitation of iron sulphides. This treatment should produce effluent water which has a much lower sulphate concentration, and is potentially suitable for release into the local environment adjacent to a field PRB installation. Stock water representing the toxic mine pit waters is pumped via peristaltic pump into each of the reduction cells for sulphate removal. Reduction cell effluent then flows to the oxidation cells for settling and oxidation of organics, before flowing to the combined waste collection container (Fig. 5.1).

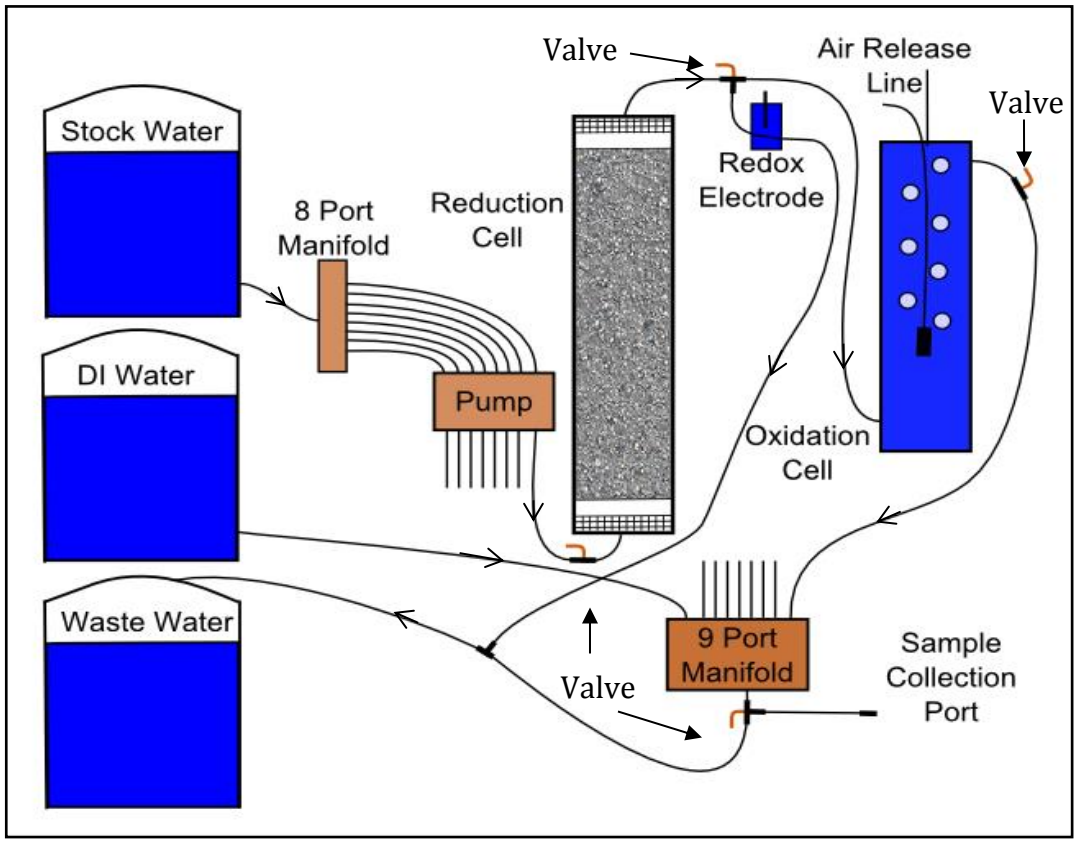

Figure 5.1: Diagram of experimental system.

The experimental setup begins with a stock of the water to be treated. This water was previously collected (2009) from the Hogarth Pit at the Steep Rock site at a water depth of 18 m. All components prior to the oxidation cell were sealed with paraffin film as the system must maintain anaerobic conditions until water reaches the oxidation cell. The conditions are representative of the conditions of a field PRB, and critical to the activity of SRB, which are strictly anaerobic. A peristaltic pump operating at a flow rate of 0.1 mL/min provided a hydraulic gradient throughout the system, pulling water from the stock solution into the eight port manifold where water for each reactive cell pair was separated. The water was pumped into the bottom of each of the eight vertically oriented flow-through reduction cells, in order to operate in an up flow manner, to minimize gravitational settling. Each cell was composed of clear PVC, has a 5.08 cm diameter, with a length of 40 cm, and a volume of 850 ml. Within each cell, a different mixture was prepared to test a variety of reactive mixtures. Six of the reactors contained mixtures of two different organic carbon sources, zero valent iron spheres, silica sand to provide matrix support, and creek sediment as a source of SRB and additional matrix support. Three different organic mixtures were used in order to allow each to have a replicate. Two control reactors were used, consisting of: A) zero valent iron spheres, silica sand, and creek sediment, in order to assess the effectiveness of abiotic sulphate removal by zero valent iron, and B) silica sand and creek sediment as a natural environment control. Each flow-through cell consists of a single reaction chamber with the reactants mixed and distributed throughout the chamber.

The organic components were selected based upon the results of the organic media characterization study (Chapter 4). Equal amounts of organic carbon are supplied by each organic component; however, the actual mass used was determined based upon: 1) the carbon content percentage (as determined by C/N/S combustion); and 2) the availability of the carbon as determined by EAS testing. Therefore, while the mass of each component varied, the organic

carbon available to sulphate reducing bacteria is the same for each substrate. Zero-valent iron accounts for a disproportionate amount of the total mass due to its high density. In contrast, organic materials were of considerably lower density than other materials used and occupied a significant volume despite their limited mass. The mixtures and their mass proportions are given in Table 5.1.

Table 5.1: Reduction cell mixtures and proportions.

Reactor 1	%	Reactor 2	%	Reactor 3	%	Reactor 4	%
Leaf Compost	6	Leaf Compost	6	Hay	7	Silica Sand	65
Poultry Manure	4	Sheep Manure	6	Poultry Manure	4	Creek sediment	25
Silica Sand	49	Silica Sand	48	Silica Sand	48	Zero-valent iron	10
Creek sediment	25	Creek sediment	24	Creek sediment	24		
Zero-valent iron	16	Zero-valent iron	16	Zero-valent iron	17		
Reactor 5	%	Reactor 6	%	Reactor 7	%	Reactor 8	%
Leaf Compost	6	Leaf Compost	6	Hay	7	Silica Sand	71
Poultry Manure	4	Sheep Manure	6	Poultry Manure	4	Creek sediment	29
Silica Sand	49	Silica Sand	48	Silica Sand	48		
Creek sediment	25	Creek sediment	24	Creek sediment	24		
Zero-valent iron	16	Zero-valent iron	16	Zero-valent iron	17		

The two organic carbon sources provided the electron donor for SRB, while zero valent iron provided Fe^{2+} to solution in order for aqueous sulphide produced by the SRB to precipitate as an iron sulphide. The mass of zero valent iron needed was determined based upon a molar calculation of the amount of sulphate to be removed over the course of the experiment, combined with very conservative estimates of the dissolution of zero valent iron. These calculations yielded a value of 132.67 grams of iron to be emplaced into the reduction cell (section 4.2). The iron spheres used have a diameter of 4.7625 mm. SRB are common in the natural environment, and sediment expected to contain SRB was extracted from the anaerobic zone of the McIntyre River on the Lakehead University campus. Manure also commonly contains SRB; however, it is uncertain whether any would be transferred into a PRB with the manure. This is due to the fact

that in a field-scale PRB; emplacement of manure directly in the groundwater flow would raise environmental concerns regarding bacterial contamination of the groundwater. Consequently, it is likely that the manure would have to be treated prior to emplacement in order to neutralize any bacteria present; manure was oven dried in order to be consistent with this requirement. Sheep, poultry, and cow manures, as well as hay, were collected from Sleepy G Farms, Pass Lake, ON. Horse manure was collected at Cryderman Quarter Horses, Murillo, ON. Rabbit manure and leaves were provided courtesy A. Conly. Silica sand, included in order to maintain hydraulic conductivity through the reduction cell, was sub-rounded to sub-angular and had a grain size of 2 to 3 mm.

The components within the reduction cell were mixed and equally distributed throughout the reaction chamber such that sulphate reduction could occur throughout, and equal flow through the reactor is permitted. Consistent and equal mixing is also important to prevent flow channeling which can significantly reduce residence time and limit water interaction with reactants. The reduction cells were wrapped in aluminum foil in order to prevent light from reaching the reaction chamber. This not only reflects the conditions of a field PRB, but also prevents the growth of photolithotrophic bacteria which could impact the results of the experiment. The peristaltic pump maintained a hydraulic gradient throughout the system, and forced water to flow through the reduction cell. At both the inlet and outlet ports of the reduction cells 300 μm nylon mesh screening was installed to prevent the loss of major particles. A 2 cm layer of silica sand was placed between the screening and the reactive mixture in order to maintain permeability in these critical junctions (Fig. 5.2).

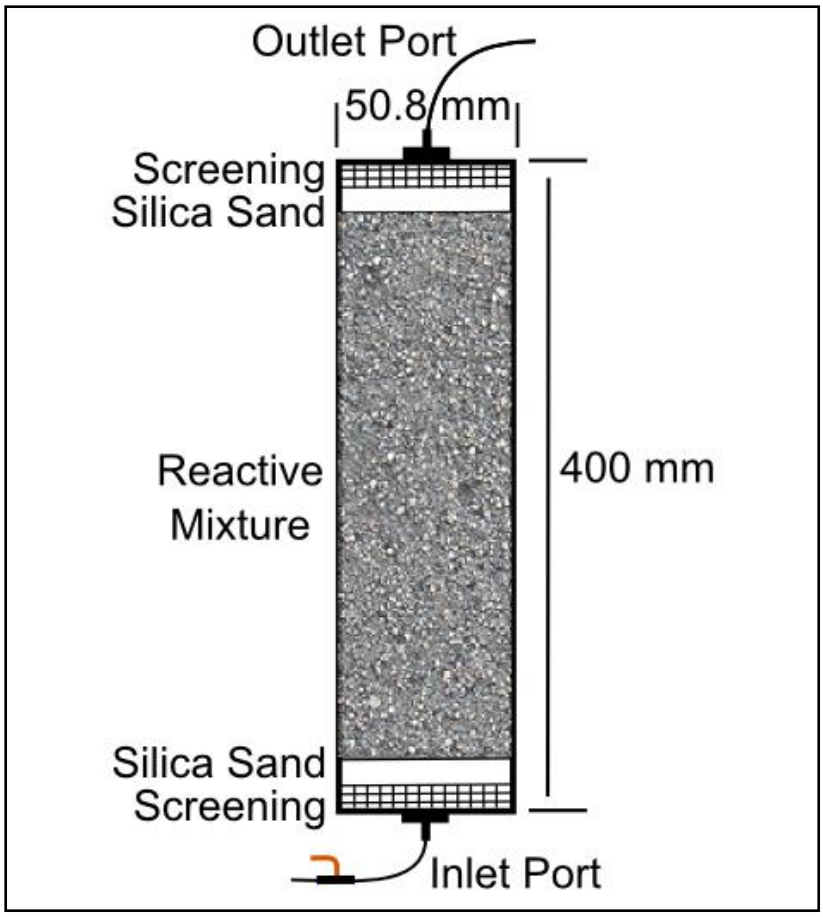

Figure 5.2: Diagram of reduction cell.

From the reduction cell the water flows through the outlet port, and via Tygon tubing is carried to the oxidation cell. On the route to the oxidation cell a valve is present to divert water to a sampling port. This port allows for the measurement of redox potential (Eh), which is an important parameter for the successful growth of sulphate reducing bacteria. The oxidation cell will raise the Eh value and thus it is necessary to be able to measure it at this stage. The oxidation cell exists in order to mitigate the heavy load of organic matter in the reduction cell effluent. This remnant organic matter could pose a threat to the health of a recipient water body if it were discharged directly, in a similar manner to a release of untreated sewage. Such an influx of nutrients could greatly enhance the growth of plants and microorganisms to an unstable level, and these organisms would consume vast quantities of dissolved oxygen. This can lead to the

death of other aquatic organisms such as fish. For these reasons, such a high organic load discharge would not be permitted under environmental regulations such as the Ontario Environmental Protection Act. A bubbler was installed in the oxidation cell in order to create an aerobic environment. In an aerobic environment the oxygen can be used as an electron acceptor in the following reaction: $CH_2O + O_2 \rightarrow CO_2 + H_2O$. The rate of bubbling activity relative to the rate of water flow will ensure that the effluent water remains well oxygenated. Carbon dioxide and air from the bubbler are able to escape via an air release line at the top of the oxidation cell.

The second purpose of the oxidation cell is to act as a settling tank. The effluent water from the reduction cells has a high concentration of total suspended solids (TSS), mostly consisting of organic matter. This is undesirable for release into a natural water body, and thus should be mitigated. The oxidation cell is a vertically oriented cylindrical tube, with inflow near the bottom, and outflow at the top. This arrangement should result in a significantly reduced value for TSS in water exiting the oxidation cell as compared to influent water. The bubbler has a negative impact upon the settling rate; however, the bubbler is placed at the halfway point in the column such that influent water is not initially disturbed. As well, by designing the cell to have a residence time of four days, it is expected that a sufficient reduction in TSS can occur. The settling tank was constructed from PVC tubing, with a diameter of 50.8 mm, and a length of 284.2 mm (Fig. 5.3). One settling tank is provided for the effluent from each reduction cell. At the effluent port, water exits via Tygon tubing to be carried to the sample collection phase.

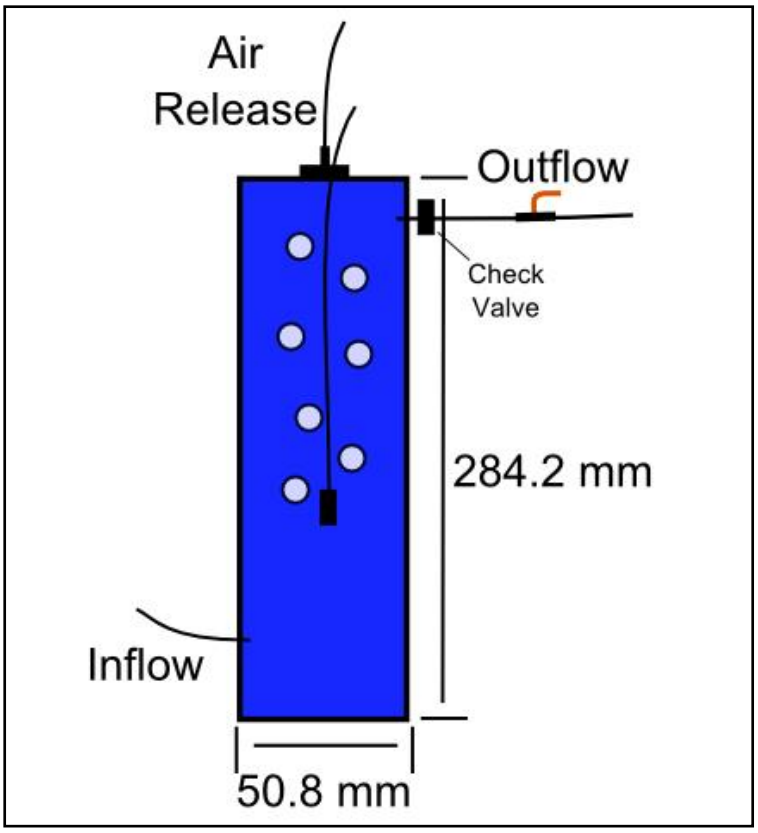

Figure 5.3: Diagram of an oxidation cell.

The effluent water was carried to a nine port manifold at which point it was possible to control which reactor is draining into the final stage of the system; a critical step for accurate sampling. Under operational conditions (as opposed to during sampling) all eight reactors were allowed to drain through the manifold, and all water was directed to the waste water container. In preparation for sample collection, the outlet valves from the oxidation cells were closed. Closing these valves 24 hours in advance of sampling allowed water to build up in the headspace at the top of the oxidation cell, providing sufficient volume of water to be sampled. Before sample collection can occur, the lines must be cleaned in order to ensure an accurate and representative sample was collected. The additional port in the manifold is for de-ionized water, which was run through the manifold and sampling lines after closing the valves. This step was done in order to wash the lines clear of effluent water such that samples were not contaminated by previous water or residuals. Once the manifold and sampling lines were cleaned, each reactors valve was

individually re-opened in order to allow water from that reactor to flow into the collection area. A 3-way valve was adjusted to direct water to the sampling port, rather than from waste collection. These design features are illustrated in Figure 5.1. This process was repeated for each of the eight samples to be taken, with de-ionized water run through between each sample. Each of the eight reduction-oxidation reactor pairs operated concurrently for 23 weeks, with samples collected weekly.

5.2 Flow-Through Reactor Monitoring Methodology

Oxidation-reduction potential (Eh) was measured using an in-line Mettler Toledo LE501 redox electrode, while water samples were collected for all other parameters. All samples to be filtered were centrifuged prior to filtration due to the heavy particulate load. One unfiltered sample was submitted to the Lakehead University Environmental Lab (LUEL) in order to determine alkalinity, conductivity, and pH; while a filtered sample was submitted for ion chromatography (IC) analysis to provide data for sulphate, nitrate, and chloride. Conductivity and pH were measured using a Mettler Toledo SevenMulti, while alkalinity was measured by titration. In the procedure for alkalinity, an automatic titrator was used to titrate the solution with H_2SO_4 (either 0.020 N or 0.100 N) to reach a pH of 4.5. The volume of acid required to reach this pH was used to calculate the alkalinity. The IC analysis was conducted on filtered samples using a Dionex ICS-1100 ion chromatograph. A filtered sample was submitted to LUIL for ICP-AES analysis in order to measure metals and major ions. Each sample for ICP-AES analysis was treated with approximately 0.5 mL nitric acid.

5.3 Post Experiment Analytical Methods

5.3.1 Mineralogical Analyses

The mineralogy of the samples was determined by powder x-ray diffraction (P-XRD) analysis. A small volume of representative material from each sample was hand milled using an

alumina mortar and pestle, with acetone used to expedite the process by keeping the powder from dispersing and creating a slurry to ensure improved milling to a fineness of <75 μm. Silica sand was used to clean the mill between samples. The powder sample was then back loaded into XRD mounts, and it was ensured that the material was non-oriented to prevent bias in the XRD results. The group of samples was assessed at the Lakehead University Instrument Laboratory (LUIL) using the Pananalytical Expert Pro Diffractometer. XRD analysis was conducted on a spinning stage using Cu kα radiation, scanning from 5.0146^{o} to 89.9926^{o}, with a step size of 0.0130^{o}, at a rate of 67.3200 seconds per step, with generator settings of 40 mA and 45 kV. The results from this analysis were provided in a data file for each sample, which was analyzed using XPert Highscore Plus software to determine the composition of each sample.

Selected samples were analyzed using a Hitachi SU-70 scanning electron microscope (SEM) with a beam current of 10,000 volts. Images were taken using back scattered electron (BSE) microscopy. Energy dispersive x-ray spectroscopy (EDS) was utilized to determine semi-quantitative elemental concentrations. Aztek software was used to interpret data received from the instrument and observe spectral peak positions for each element.

5.3.2 Bulk Sample and Sequential Extraction Analyses

Acid digestions were conducted to determine the composition of the reactor materials following completion of the experiment. Four samples were taken within each reactor (5 cm above bottom, 15 cm above bottom, 25 cm above bottom, and 35 cm above bottom) and digestion methodology followed United States Environmental Protection Agency (EPA) method 3050B (1996). Samples were finely milled and oven dried at 65°C for 48 hours. One gram of each sample was added to the digestion tube, 10 ml concentrated HNO_3 was added, and the tube was swirled to create a slurry. The solution was heated to 95°C for 10 minutes, after which time 5 ml of additional HNO_3 was added. If brown fumes appeared, the addition of HNO_3 was

repeated until brown fumes were no longer produced. The digestion was allowed to proceed for 2 hours, or until the solution volume decreased to 5 ml. The samples were removed from heat and allowed to cool after which point 2 ml of DI water and 3 ml of 30% H_2O_2 were added (H_2O_2 added as single drops to prevent overly vigorous reaction). The samples were returned to heat at 95°C, and allowed to digest until effervescence ceased. H_2O_2 was added in 1 ml aliquots until minimal effervescence occurred following addition of H_2O_2 (a maximum of 10 ml H_2O_2 could be added). The solution was digested for two hours, or until the solution was reduced to 5 ml. 10 ml of concentrated HCl was added, and allowed to digest at 95°C for 15 minutes. After cooling, samples were filtered using Whatman #42 filter paper, diluted to 100 ml, and shaken thoroughly to ensure homogeneity. The solutions were transferred to centrifuge tubes, and submitted to the Lakehead University Instrument Lab (LUIL) for ICP-AES analysis to determine the elemental concentrations.

Carbon-nitrogen-sulphur (CNS) combustion analysis was used to determine the carbon, nitrogen and sulphur contents of the post-experiment materials. Sample preparation for this analysis required milling samples to a powder. Samples were submitted to the Lakehead University Instrument Laboratory (LUIL) and analyzed using CHNS Elementar Vario EL analyzer. Samples were loaded into tin boats and then combusted through an automated process at 1150°C. The combustion process results in gasification of the sample, these gases are reduced to N_2, CO_2, and SO_2, and carried in a helium gas stream. CO_2 and SO_2 are adsorbed while passing through the adsorption columns, while N_2 is allowed to reach the detector. Following detection of the N_2 peak, the CO_2 column is heated to release CO_2 and is detected. Finally the SO_2 column is heated and SO_2 is released and detected as well. A computer calculates the elemental concentration from the detector signal and sample weight based upon stored calibration curves (Elementar Vario EL cube technical brochure, undated).

Sequential extractions were conducted in order to assess the different phases and compounds present within the post experiment materials. A six stage extraction was used (modified after Stover et al., 1976 and Rudd et al., 1988), in which the material was placed in a 50 mL centrifuge tube, saturated in a solution, and agitated in a reciprocating rocker for a set period of time (Table 5.2). Following each stage liquids were centrifuged and then decanted into a 15 mL centrifuge tube, taking care to prevent solids loss, and preserved for ICP-AES analysis. De-ionized water was added to the 50 mL centrifuge tube to remove residual chemicals from the previous stage, the sample was then agitated, centrifuged, and decanted. Stage one used de-ionized water to remove salts that may have precipitated from the reactor water during the drying process and agitated for 30 minutes. Stage two used 1 M KNO_3 solution to remove metal fractions designated as "soluble and exchangeable" and was agitated for 16 hours, which is the amount of time used in each of the remaining stages. In stage three 0.5 M KF solution was used to remove adsorbed metals, while stage four used 0.1 M $Na_4P_2O_7$ solution to dissolve organic matter. Stage five utilized 0.1 M EDTA solution to remove the carbonate fraction, while the final stage used 1 M HNO_3 in order to dissolve sulphide species.

Table 5.2: Time periods for sequential extraction steps.

Stage	Time
1. De-ionized water	0.5 hours
2. 1 M Potassium Nitrate	16 hours
3. 0.5 M Potassium Fluoride	16 hours
4. 0.1 M Sodium Pyrophosphate	16 hours
5. 0.1 M EDTA	16 hours
6. 1 M Nitric Acid	16 hours

Chapter 6: Results of Flow-Through Reactor Experiments

6.1 Reactor Monitoring Summary

The reduction cells were constructed based upon the mixtures presented in Table 4.4 (Section 4.2). Each reduction cell was paired with an oxidation cell, and the oxidation cell effluent was collected to provide all data presented in this section, with the exception of ORP (Eh) data, which was collected directly from reduction cell effluent. The reactors were operated for a total of 23 weeks. Full data for the parameters presented below as well as all others collected by IC and ICP-AES for effluent water quality monitoring is available in Appendix C.

During the initial four weeks, many of the results contain highly elevated values as certain components (Cl, Fe, K, Mn, and Na) are rapidly flushed through the system, and the data for some parameters does not appear to follow a clear trend. After this period, most of the data began to follow more apparent trends; although for some parameters a high degree of variability from week to week was still present. Effluent volumes began to progressively decrease following week 10; this was assumed to be due to blockages within the reduction cells; however, it was later determined that precipitates had formed within the influent flow lines and manifold. This caused a drop in the influent flow volume, until the problem was identified and remedied after several flow-through reactors failed to produce sufficient effluent volume in week 18. This problem first impacted only reactor 6, and later reactor 2, which was why the problem was not realized to be located in the intake flow lines. Missing data for these reactors, as well for several other reactors in week 18 is due to this flow issue. As a result of fixing this problem, flow rates increased significantly ahead of week 19 sampling, and several values for week 19 show anomalies associated with this change.

In Figures 6.1 through 6.7, each individual reactor is represented by one line with markers for each data point, while the influent stock water is presented by red diamonds, without connecting lines.

6.1.1 Sulphate and Total Sulphur

All reactors demonstrated an immediate ability to remove sulphate from solution, with reactors 1, 2, and 3 all producing sulphate concentrations below 150 mg/L (Fig. 6.1). By week 3, all reactors (except #5) containing organic substrates produced effluent with sulphate concentrations below 115 mg/L, while influent water contained 1760 mg/L sulphate. These values were generally sustained through week 7, after which time most of the reactors began to lose their capacity for sulphate removal. The sulphate concentration in influent water was also measured to have increased at this point. In week 9, reactors 3 and 7 (replicates) continued to produce high levels of sulphate removal, with 106 mg/L and 426 mg/L, respectively. The other organic amended reactors still removed significant sulphate, with concentrations from 650 mg/L to 900 mg/L. The two control reactors produced very similar results at this point, with reactor 4 measured at 1891 mg/L and reactor 8 measured at 1849 mg/L, while the influent water contained 2342 mg/L sulphate. Most of the reactors continued to show a progressive increase in sulphate concentrations over time, and by the end of the experiment, none of the reactors had concentrations below 1000 mg/L. The highest performing reactor with respect to sulphate removal at the end of the experiment was reactor 1 (poultry manure and leaves), at 1088 mg/L, while reactors 2 (sheep manure and leaves), 3 (poultry manure and hay), 5 (poultry manure and leaves), 6 (sheep manure and leaves), and 7 (poultry manure and hay) all were within the range 1140 to 1210 mg/L. The two control reactors, 4 and 8, were 1791 mg/L and 1588 mg/L, respectively, while influent stock water was measured at 2099 mg/L.

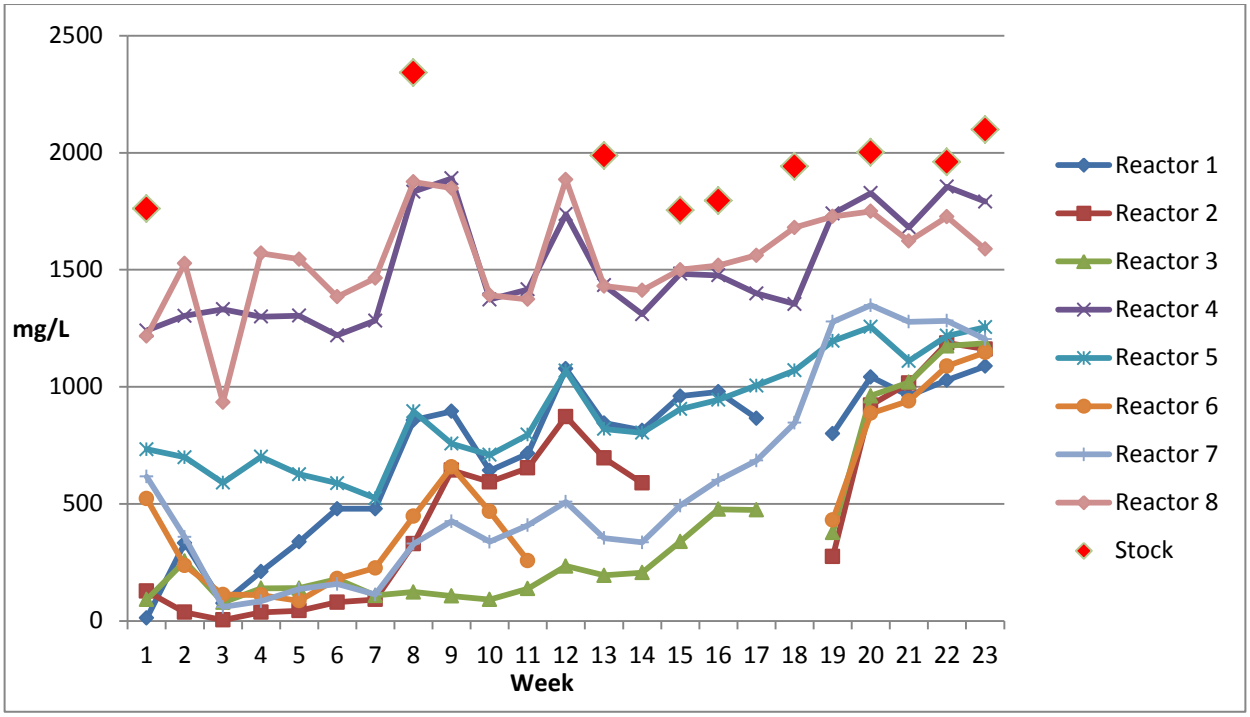

Figure 6.1: Variation in dissolved sulphate content of the effluent over the 23-week duration of the flow-through experiment.

Sulphur values increased progressively during the first half of the experiment, and then more rapidly during the final weeks (Fig. 6.2). It is important to consider the relationship between sulphate and total sulphur in this system. While there does not appear to be a direct relationship between sulphate and sulphur values, there is a long term pattern of rising values for each, with sulphate on average 250 to 450 mg/L higher than sulphur, with the exception of reactors 4 and 8 in which sulphate exceeds sulphur by 1000 mg/L on average (Fig 6.3). Molar concentrations are more similar between sulphur and sulphate for some reactors, while in others there is a strong difference. In reactors 1 and 5 the average sulphate concentration was 8.25 mol/L, while the average sulphur concentration was 13.5 mol/L. In reactors 2 and 6 the average sulphate concentration was 5.10 mol/L, and the average sulphur concentration was 4.40 mol/L. In reactors 3 and 7 the average sulphate concentration was 4.91 mol/L, and the average sulphur concentration was 4.14 mol/L. Finally, in reactors 4 and 8, the average sulphate concentration was 15.87 mol/L, while the average sulphur concentration was 13.28 mol/L

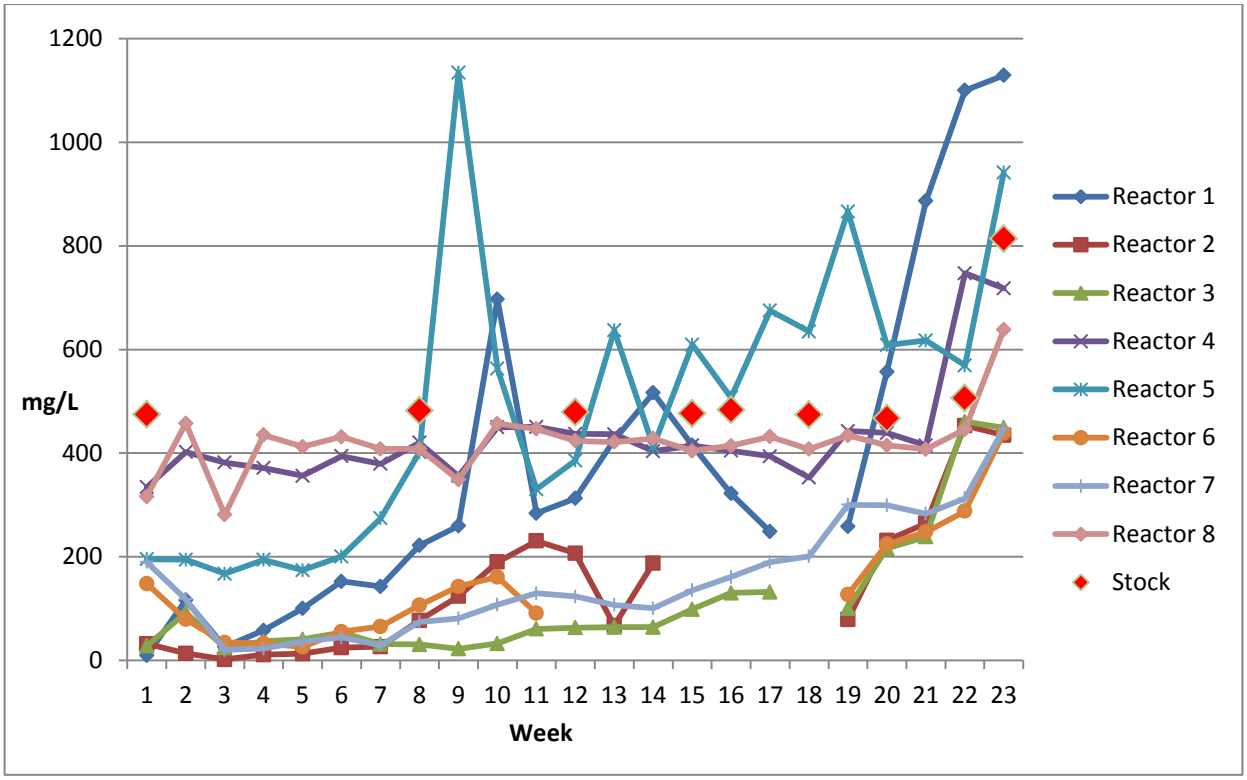

Figure 6.2: Variation in total sulphur content of the effluent over the 23-week duration of the flow-through experiment.

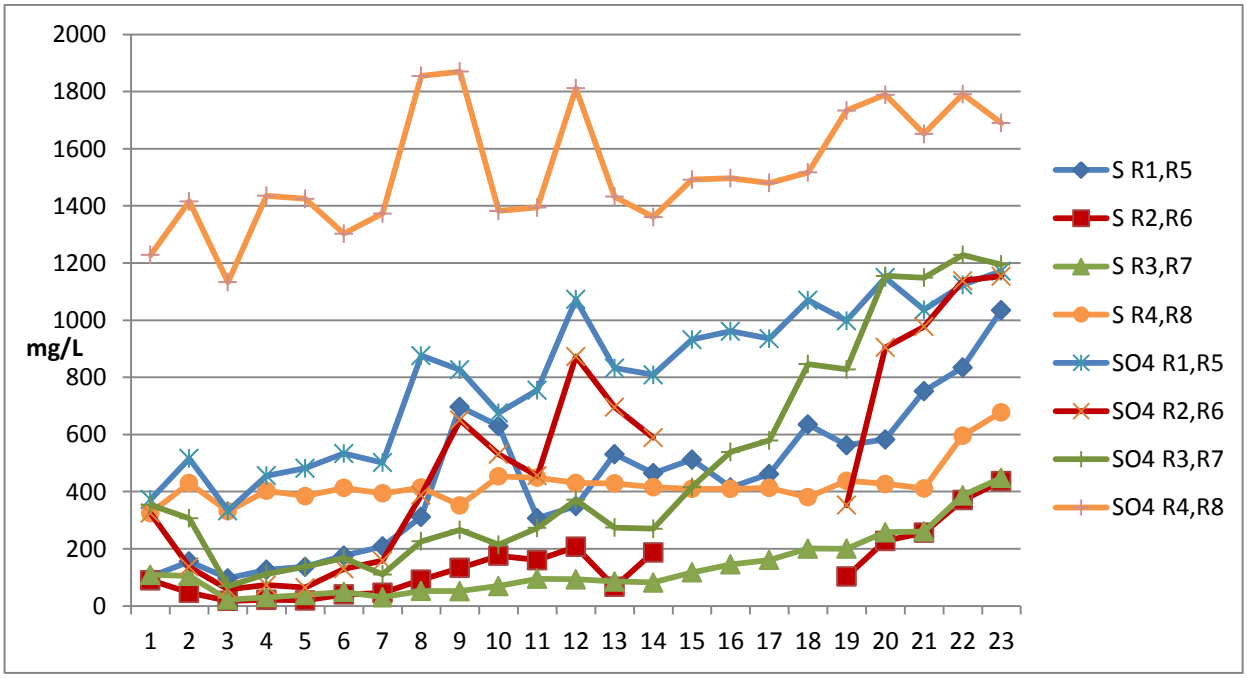

Figure 6.3: Variation in total sulphur and sulphate content for averaged replicate reactors from effluent water over the 23-week duration of the flow-through experiment.

6.1.2 pH and Conductivity

The pH of the effluent waters remained within a relatively narrow range from 7 to 9, while stock water was typically near 8 (Fig. 6.4). Reactor 8, containing only creek sediment and silica sand had a notably lower pH throughout the experiment than the other reactors, reaching a minimum of 6.5 in week 3. In contrast, reactors 2, 3, and 6 had consistently higher pH values, with most results above 8 after week 5.

Values for conductivity are missing for the first four weeks due to equipment failure. Following this point, most reactors had steady values over the course of the experiment, ranging between 2000 to 2500 µs/cm, although reactors 2, 3, and 6 started initially lower at ~1500 µs/cm, before reaching similar values to the other reactors by week 20.

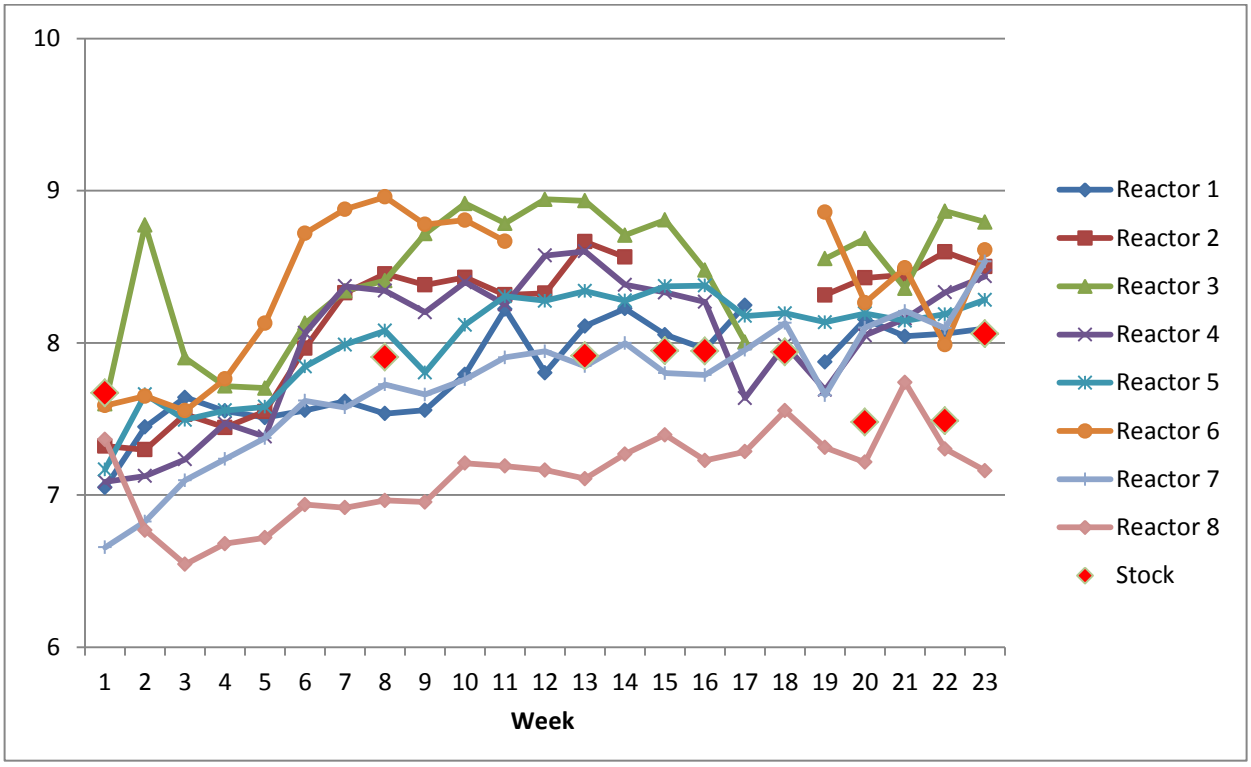

Figure 6.4: Variation in pH of the effluent over the 23-week duration of the flow-through experiment.

6.1.3 Iron

Iron is important because it (or another divalent metal) is required in order to remove sulphide from solution via precipitation of a metal sulphide. If insufficient iron is available, then

sulphide will not be removed from solution. Due to the low concentration of metals in the stock water, iron had to be added to the reactors as iron spheres, which upon reaction with the stock water would contribute iron to solution. Iron concentrations in the effluent waters are significantly elevated during the first three weeks when the fresh iron sphere surfaces were most reactive (Fig. 6.5). Despite a sharp initial drop, a progressive decline in iron concentrations is observed through week 10. Reactor 7 had very high iron values for the first four weeks, and exceeded 100 mg/L for the first two weeks. Reactor 8 maintained higher iron values than all other reactors after week 3. Reactors 1 and 5 generally had the lowest iron concentrations through the duration of the experiment. All reactors contained higher iron content in their effluent than the influent water, with the exception of reactors 1 and 5 in week 13. After week 11 iron concentrations are relatively consistent, with most reactors (excluding #8) near or below 0.1 mg/L.

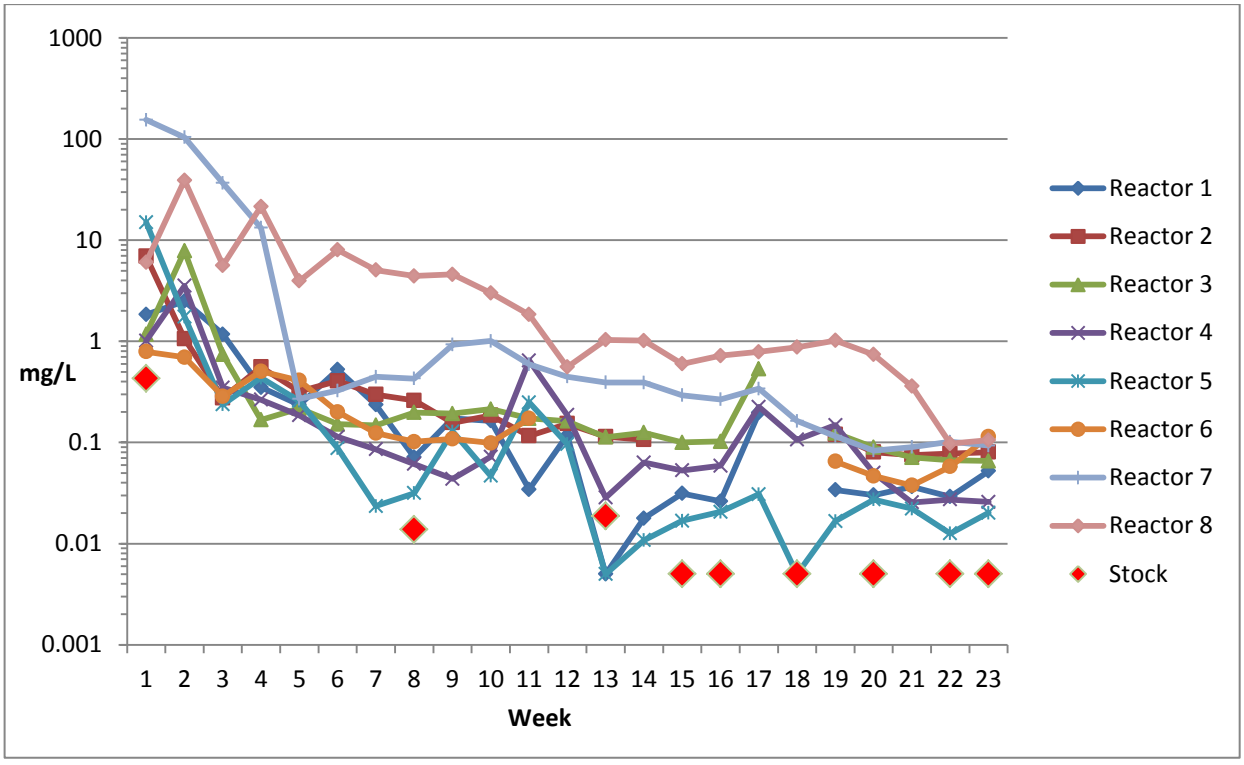

Figure 6.5: Variation in iron content of the effluent over the 23-week duration of the flow-through experiment.

6.1.4 Phosphorus

The two control reactors which contain no added organic matter did not have detectable levels of phosphorus at any time (Fig. 6.6). Reactors 1, 3, 5, and 7 had highly variable phosphorus concentrations over the course of the experiment, ranging from <1 mg/L to 5 mg/L. Reactors 2 and 6 were much more consistent with values below 2 mg/L.

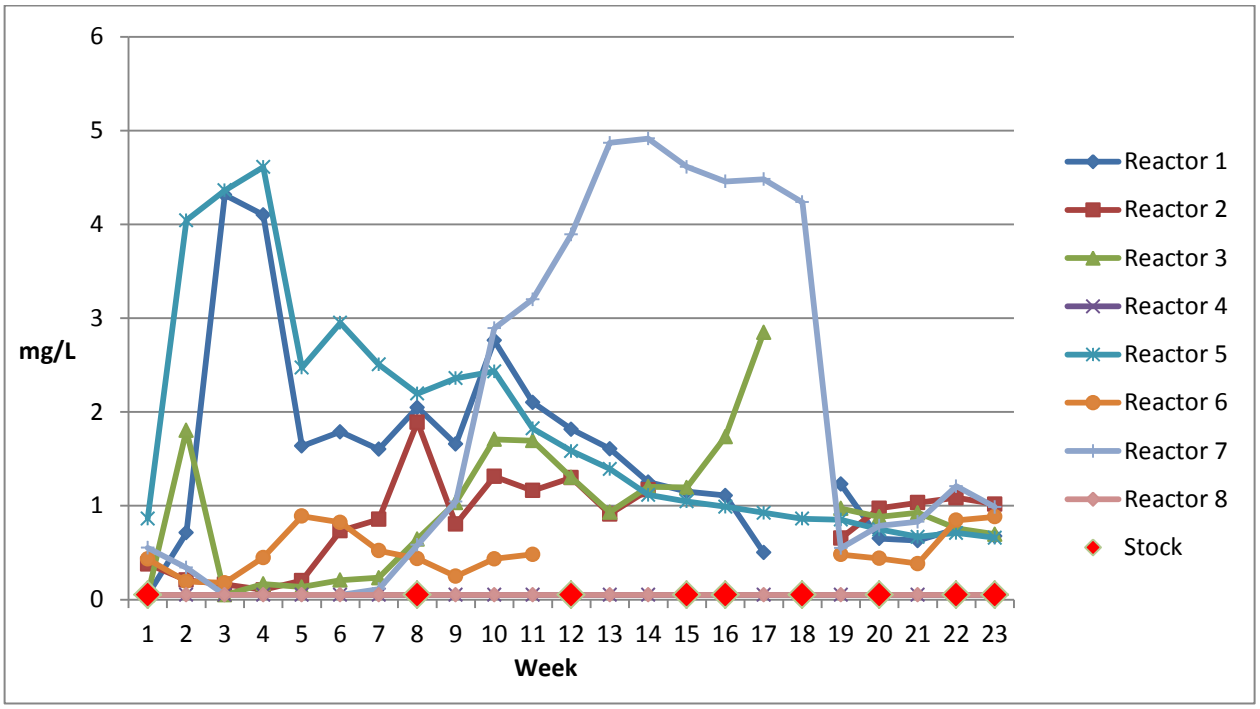

Figure 6.6: Variation in phosphorus content of the effluent over the 23-week duration of the flow-through experiment.

6.1.5 Oxidation-Reduction Potential

Oxidation-reduction potential (ORP), or Eh, is a very important parameter given that sulphate reducing bacteria require reducing conditions, with a redox potential below -100 mV optimal for the growth and activity of SRB (Postgate, 1984). The experiment began with values between zero and -100 mV, and most reactors became more negative in redox potential over the course of the experiment, with the exclusion of reactor 8. Significant spikes to positive values were observed in reactor 6 at week 10, and reactor 7 at week 13. Reactors 1, 2, 3, 4, and 5 were

consistently below -100 mV after week 8. In contrast, influent water was observed to have positive values between zero and 200 mV (Fig. 6.7).

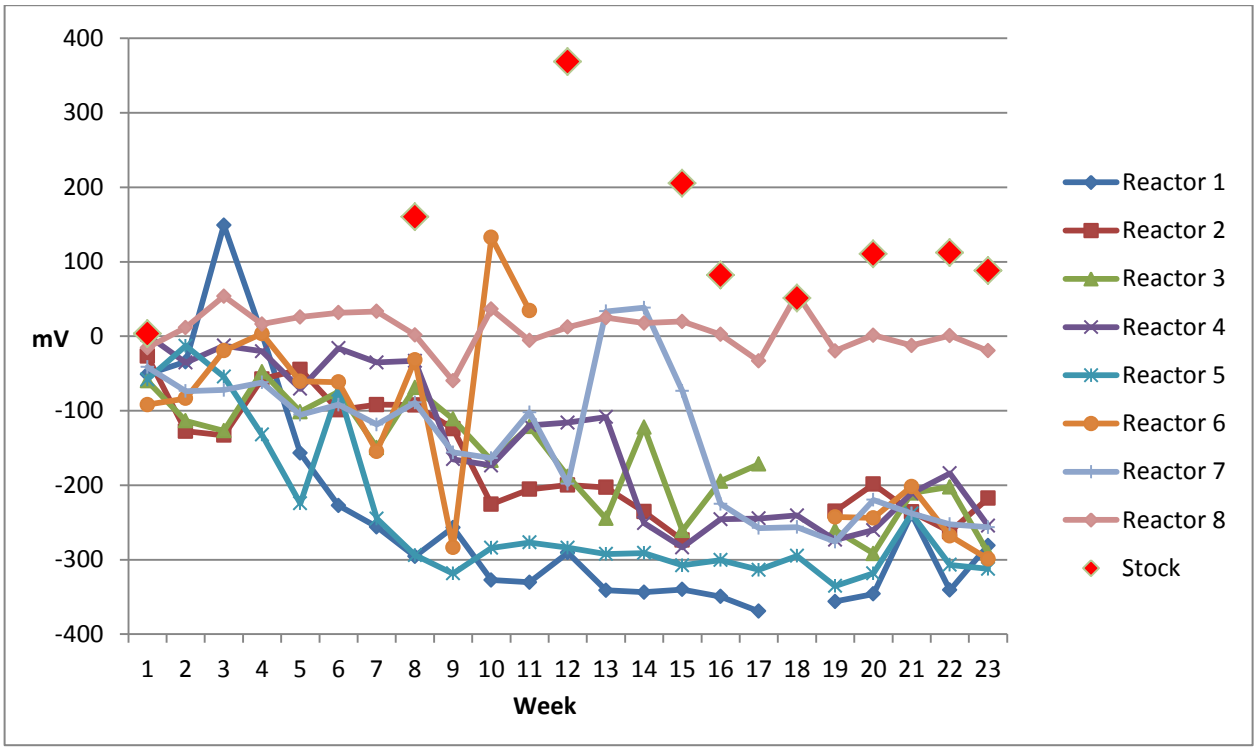

Figure 6.7: Variation in oxidation-reduction potential (Eh) of the effluent over the 23-week duration of the flow-through experiment.

6.1.6 Alkalinity

Total alkalinity values (as mg/L $CaCO_3$) were highly elevated in reactors containing added organic material during the first four weeks, with organic-bearing reactors above 850 mg/L in week 3 and declining to below 600 mg/L in the final four weeks. Reactors 4 and 8, which contained no organic material, were consistently in the range of 100-200 mg/L over the course of the experiment.

6.1.7 Major Cations

Calcium was generally consistent over the course of the experiment, with reactors 1, 4, 5, 7, 8 all within the range 150 to 300 mg/L. Reactors 2, 3, and 6 were more variable, ranging from 50 to 200 mg/L.

Magnesium was also relatively constant over the duration of the experiment. Values for magnesium were slightly lower in most reactors during the first few weeks, except for reactors 4, 5, and 8 which were consistent with later data. After week 9, all reactors consistently produced magnesium concentrations in the range of 150 to 200 mg/L.

Sodium and potassium exhibited similar behaviour, with highly elevated values (>50 mg/L Na and >100 mg/L K) observed during the first three weeks, moderately elevated values (~30 mg\L Na and 7 to 30 mg/L K) from weeks 4 through 10, and finally dropping to a stable level (~20 mg/L Na and ~6 mg\L K) after week 10.

Manganese concentrations were elevated in all reactors, except #3, for the first 4 weeks; with reactors 7 and 8 extremely elevated (up to 14.3 mg/L in week 1). Following this initial period, all reactors (except #8) were below 2 mg/L by week 5 and below 1 mg/L by week 11. Reactor 8 continued to have elevated manganese values relative to the other reactors over the course of the experiment, although these values were below 2 mg/L by week 11.

6.1.8 Anions

Highly elevated chloride concentrations (50-130 mg/L) were observed during the first two weeks, after which values decreased to a generally more consistent in the range of 10 to 30 mg/L. However, several inexplicable spikes and drops were observed in individual weeks, but values returned to typical levels in the following week.

Nitrate values were generally low, with the majority of samples containing less than 0.2 mg/L, and many below detection limit. An anomaly is observed in week 4 with all samples spiking to significantly higher values (highest was 0.943 mg/L in reactor 8); no laboratory error was found, and contamination is a possible explanation.

6.2 Post Experiment Materials Assessment

In order to thoroughly assess the composition of materials within the reactors following completion of the flow through experiment, four samples were taken within each reactor: Sample A represents the lower quarter of the reactor material (influent end); samples B and C represent the lower middle and upper middle quarters, respectively; and, sample D represents the top quarter (effluent end). Efforts were taken to limit the amount of water contained within the collected samples in order to prevent excessive precipitation of compounds during the drying process. However, it is likely that some precipitation did occur as the saturated materials dried. Complete data for all of the post experiment material assessments is provided in Appendix D.

6.2.1 Acid Digestions

In order to assess the behaviour of the flow-through reactor experiments, it was necessary to compare the composition of the materials before and after the experiment. To achieve this, nitric acid digestions were conducted. The results for selected parameters are presented in Figures 6.8 to 6.11, which combine results for samples from replicate reactors. Complete data for these digestions is available in Appendix D.

The digestion results for reactors 1 and 5 are presented in Figure 6.8; these replicate reactors contained leaf compost and poultry manure as the organic components. Iron is the most abundant element detected in each sample, with values ranging between 1.5 (5C) and 2.4 wt% (1C). The concentrations of aluminum, calcium, magnesium, and sulphur are similar to each other (2-5 wt%), with sample 1C having the highest values for aluminum and magnesium, while 1B has the highest values for calcium and sulphur. Potassium, sodium, and phosphorus have notably lower concentrations; the maximum potassium concentration of 5059 mg/kg corresponds to 5B, with 1B yielding the minimum value of 2367 mg/kg. Maximum and minimum sodium concentrations were measured in 1C (2523 mg/kg) and 5C (1470 mg/kg), respectively.

Phosphorus concentrations are highest in sample 1B with a value of 6909 mg/kg, while the minimum was 4218 mg/kg in 5C. Overall, the only apparent trend in this data is lower concentrations in sample 5C, which has the lowest concentration of the four elements.

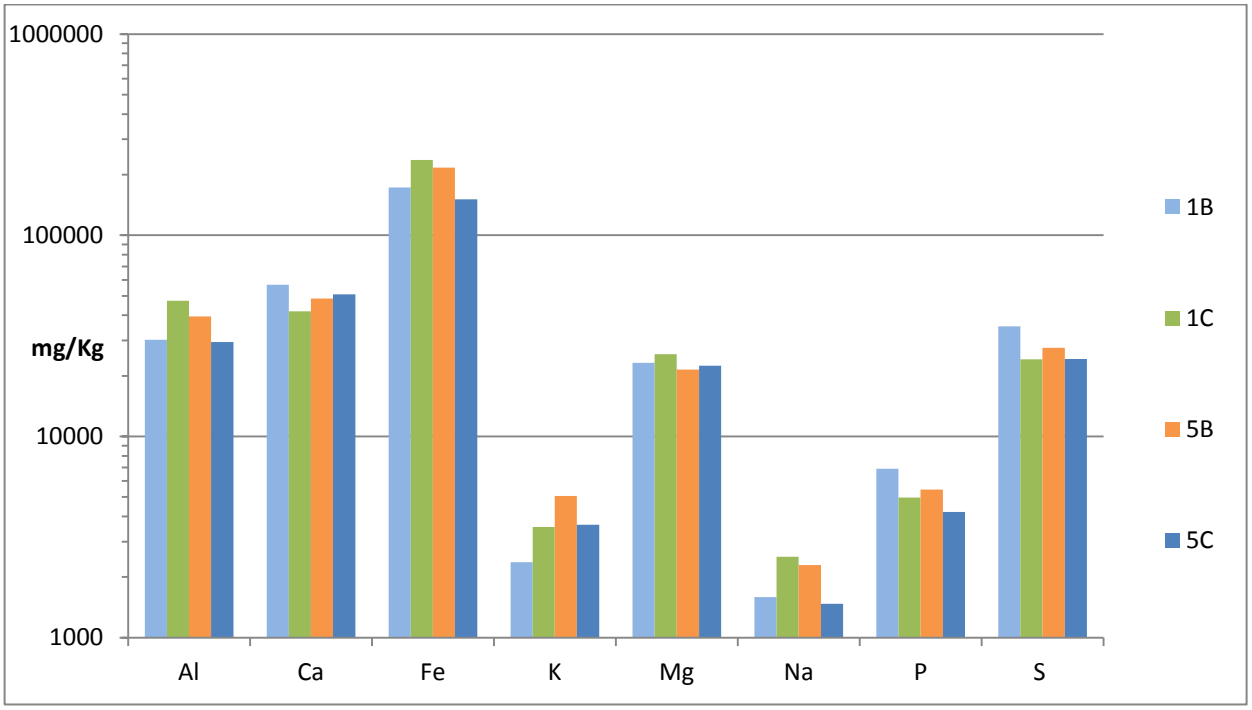

Figure 6.8: Post flow-through experiment digestion results for reactors 1 and 5.

In general, reactors 2 and 6 (Fig. 6.9) follow similar trends to those observed in Figure 4.18. However, phosphorus concentrations are lower, while sulphur concentrations are higher. For reactors 3 and 7 (Fig. 6.10), the general patterns are once again very similar, although phosphorus concentrations returned to the higher levels observed in reactors 1 and 5, while sulphur concentrations rose again, becoming the second most abundant element detected after iron. Overall, little trend is observed between the samples, although sample 3B consistently has higher concentrations than sample 7C.

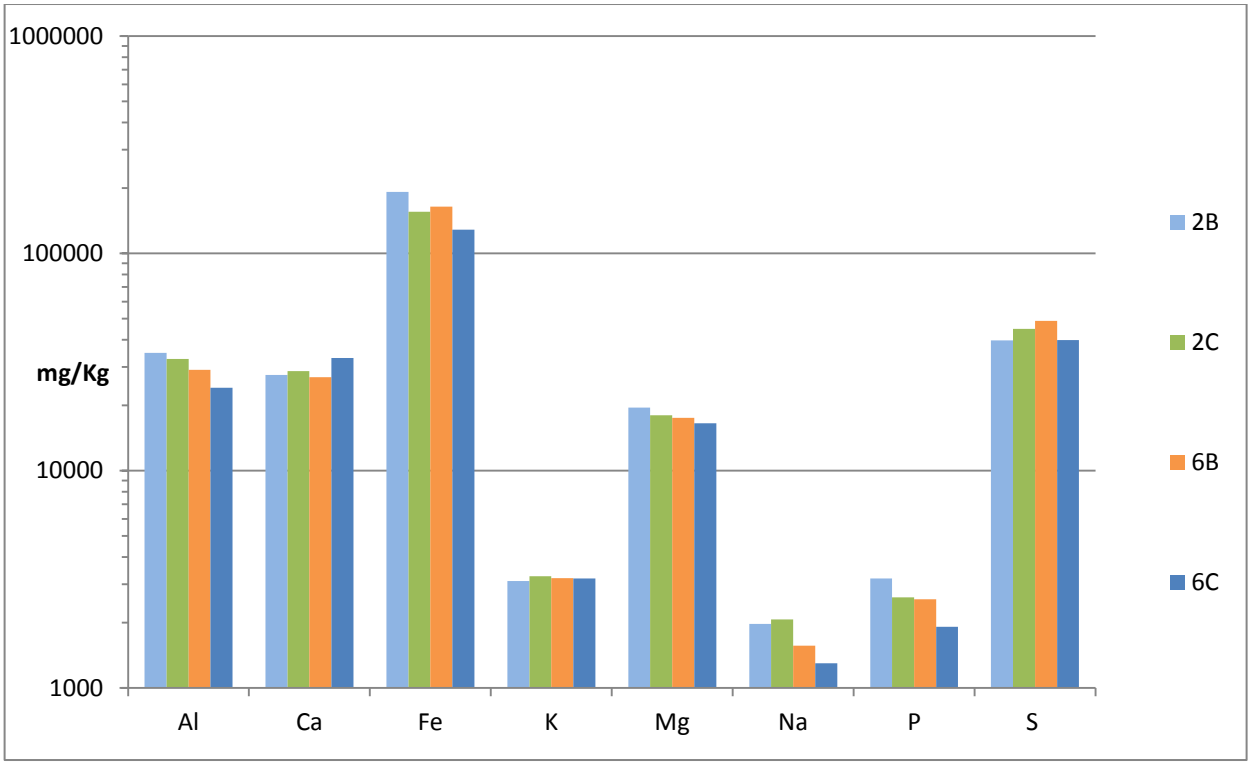

Figure 6.9: Post flow-through experiment digestion results for reactors 2 and 6.

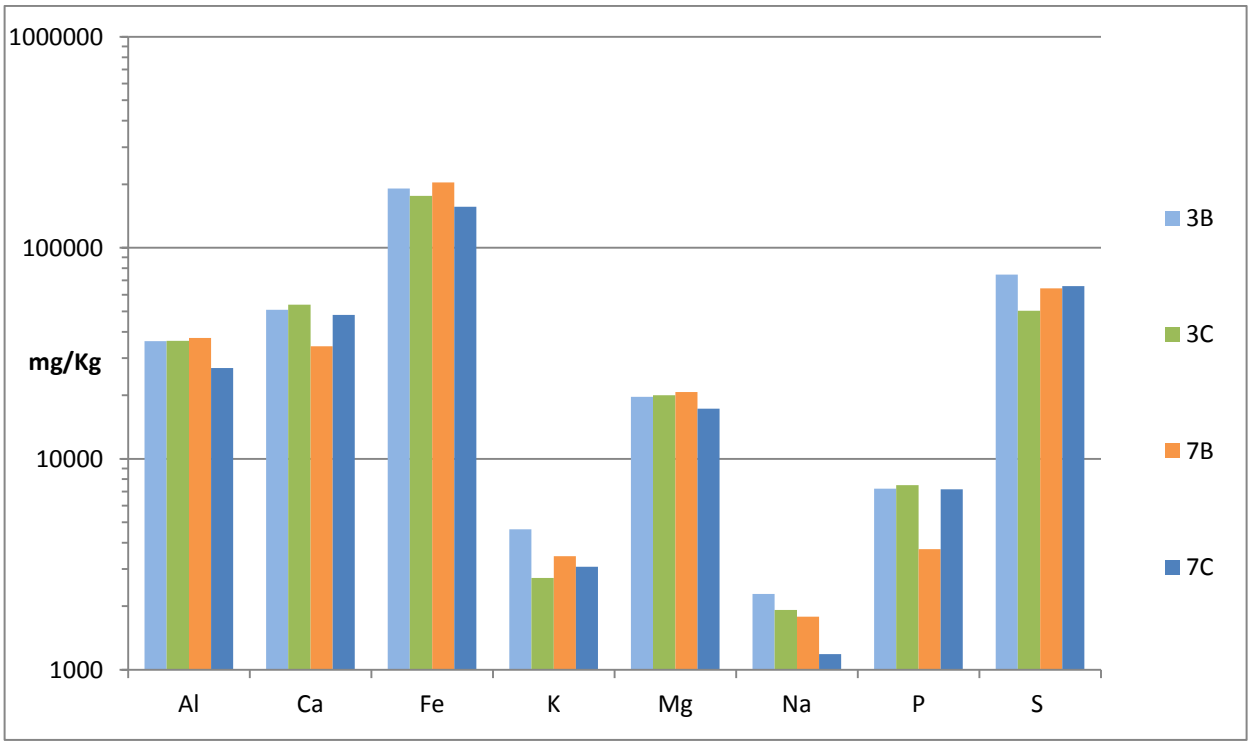

Figure 6.10: Post flow-through experiment digestion results for reactors 3 and 7.

Digestion results for reactors 4 and 8 (Fig. 6.11) show some variation from the previously discussed samples, which is anticipated given that these reactors did not contain any added organic matter. Concentrations of aluminum, calcium, iron, magnesium, and sodium are not significantly different; however, the concentrations of phosphorus and sulphur are significantly lower, with maximum values of 2393 mg/kg and 11800 mg/kg, respectively. In contrast, the concentrations of potassium increased, with a maximum concentration of 6932 mg/kg in sample 4C. Inexplicably, the concentrations of most parameters for samples 4B and 8C are consistently lower than those detected in samples 4C and 8B.

A further technique to assess the chemical behavior of the reactors is to consider how their composition varied within the vertically oriented reactors. In each reactor, the influent flow port was at the bottom, while the effluent flow port was at the top. All four samples collected from each reactor are presented in order to assess these vertical variations, with sample A representing the material near the bottom, sample B the lower-middle portion, sample C the upper-middle portion, and sample D near the top. Sample 1D is noted to diverge substantially from all other samples in iron and potassium concentrations (Figs. 6.12 and 6.13) and is potentially contaminated and may be inaccurate for comparison.

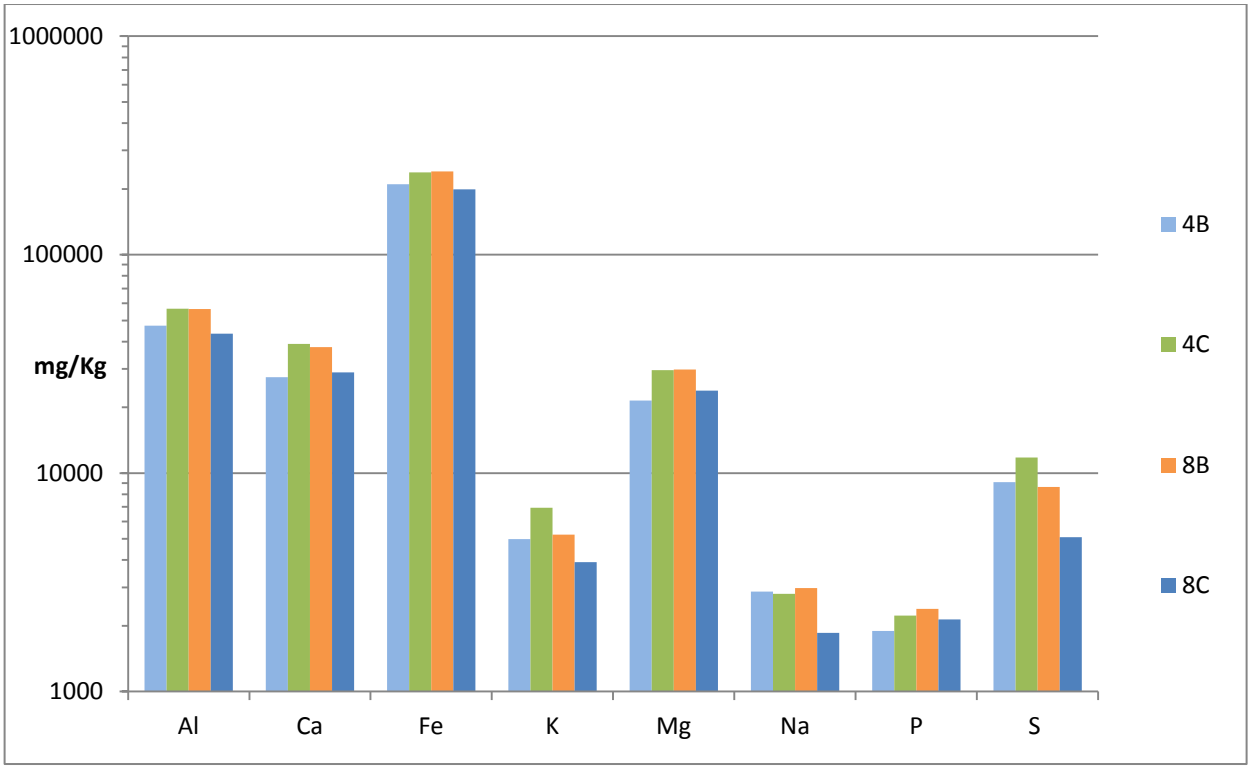

Figure 6.11: Post flow-through experiment digestion results for reactors 4 and 8.

Iron concentrations (Fig. 6.12) did not demonstrate any particular trend with respect to vertical position within each reactor. Sample 1D is of questionably reliability; however, it indicates a dramatic increase in iron concentration at the top of reactor 1. Reactors 2, 5, 6, 7, and 8 are generally consistent from top to bottom. Reactor 3 has a significant concentration increase between the A and B samples, while reactor 4 has progressively decreasing concentrations towards the top.

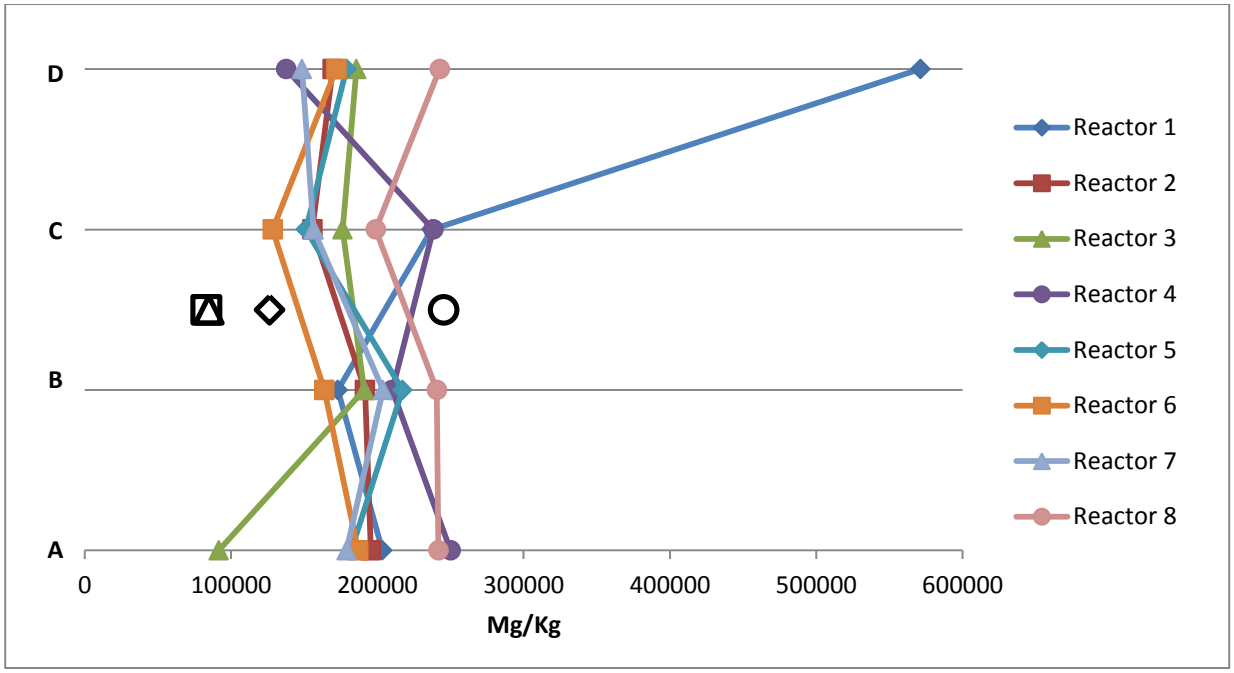

Figure 6.12: Iron concentrations within vertical orientation of reactors. Raw mixture represented as blank symbols corresponding to coloured symbols in legend.

Potassium values (Fig. 6.13) also did not demonstrate any clear trends, although some samples (reactors 3, 5, 6, and 8) demonstrate slight increases from the bottom towards the top of the reactors. Sample 1D once again shows a sharp increase from all other samples at the top of the reactor, while reactors 2 and 4 decrease slightly from the bottom to top, and reactor 7 has slightly higher concentrations in the middle of the reactor.

Sulphur concentrations (Fig. 6.14) have significantly greater variation between reactors than either iron or phosphorus. While there is not a definitive trend, several reactors have lower sulphur concentrations in the upper portion of the reactor (e.g., reactors 2, 4, 5, 6, and 8). Reactor 1 has much lower concentrations in the middle of the reactor, while reactor 3 has a highly elevated concentration in sample B, and reactor 7 has slightly higher concentrations in the middle of the reactor. Overall, the primary trend observed is significantly higher sulphur concentrations in the samples collected after the experiment as compared to the unreacted material. However, this mass increase significantly exceeds the mass of sulphate removed from solution. The amount

of sulphur removed from solution as sulphate only accounts for 59% of the sulphur mass gain in reactors 1 and 5, 41% of the sulphur mass gain in reactors 2 and 6, and 31% of the sulphur mass gain in reactors 3 and 7. The source of this discrepancy is unclear.

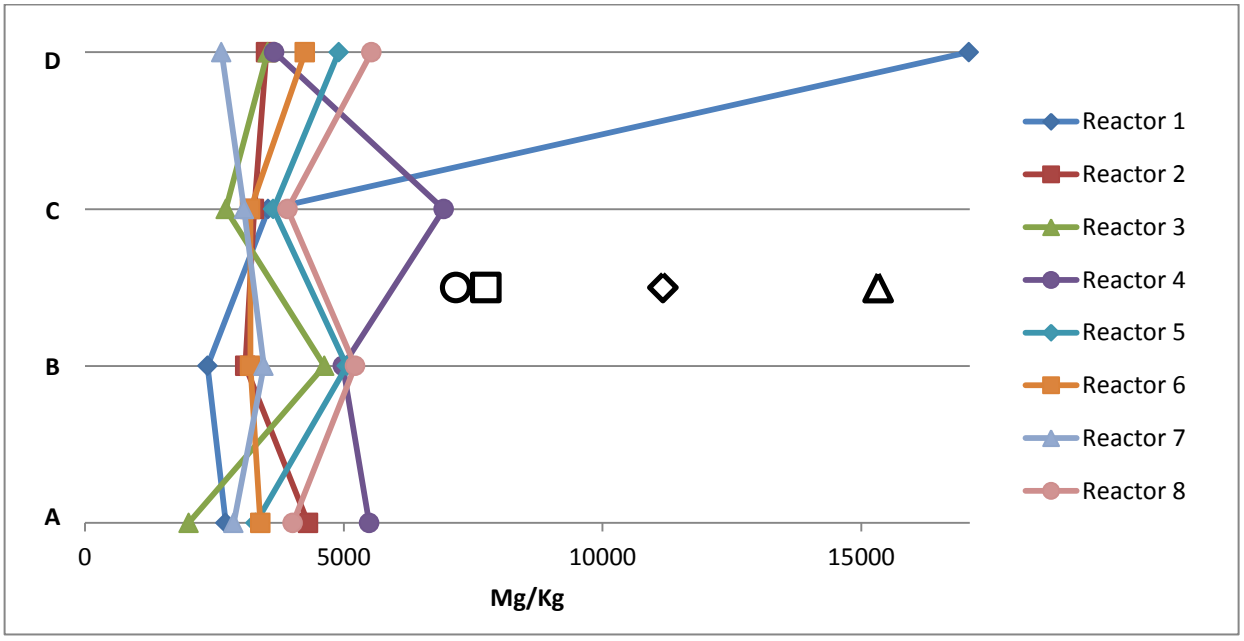

Figure 6.13: Potassium concentrations within vertical orientation of reactors. Raw mixture represented as blank symbols corresponding to coloured symbols in legend.

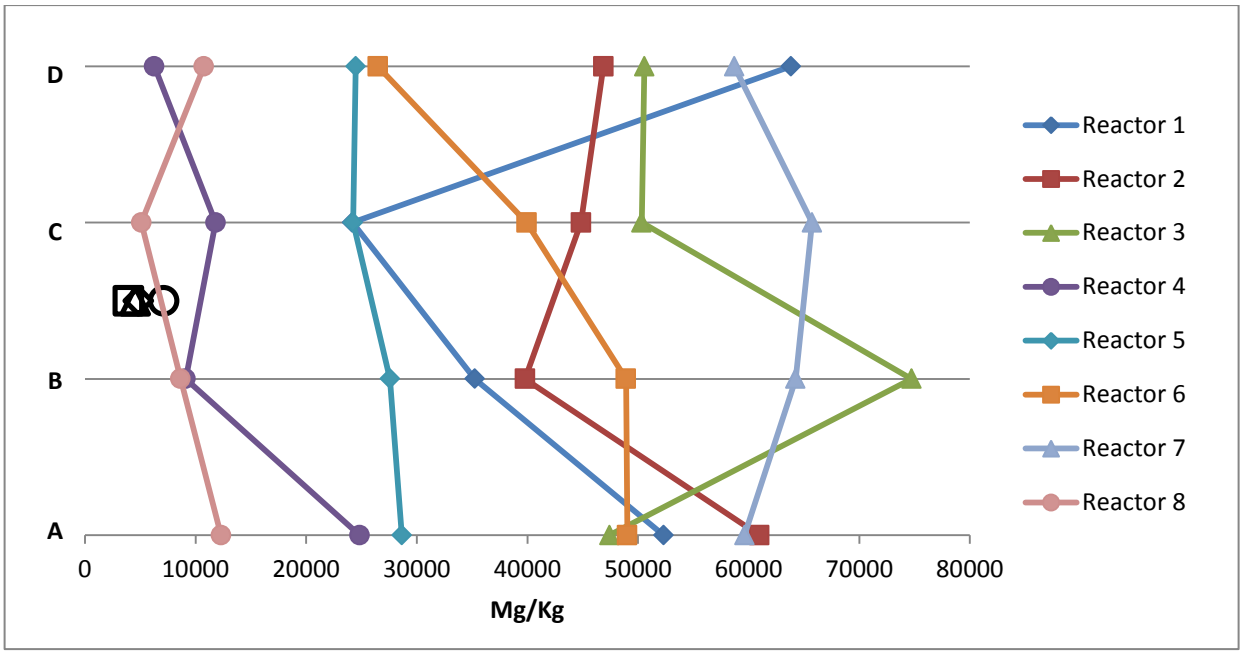

Figure 6.14: Sulphur concentrations within vertical orientation of reactors. Raw mixture represented as blank symbols corresponding to coloured symbols in legend.

Phosphorus does not show any clear vertical variations in reactors 2, 4, 6, and 8 (Fig. 6.15). In contrast, reactors 1, 3, 5, and 7 have higher overall concentrations and greater variation between samples and reactors. Reactor 3 is highly enriched in phosphorus in the middle of the reactor compared to the top or bottom, while only a slightly higher concentration was observed at the top compared to the bottom. Reactors 1, 5, and 7 demonstrated substantial variation between values, with no clear trend evident over the length of the reactor. Overall the vertical plotting of nutrient data did not reveal any clear trends, as the changes in concentration varied dramatically between reactors and different nutrients

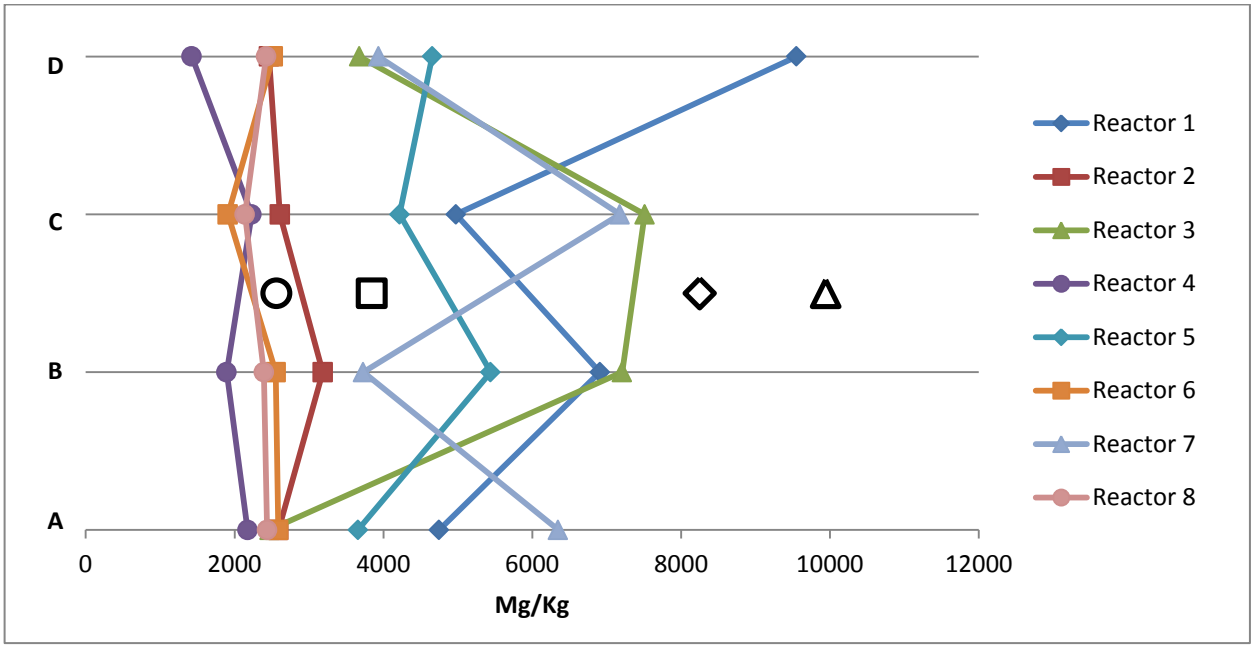

Figure 6.15: Vertical variation of phosphorus concentrations within reactors. Raw mixture represented as blank symbols corresponding to coloured symbols in legend.

6.2.2 Sequential Extractions

Sequential extractions were conducted in order to assess the compounds and phases in which various elements are contained in. In particular, this approach was intended to determine if sulphur contained within the sulphide fraction increased following the experiments, which would provide confirmation of bacterial sulphate reduction. A six stage extraction was used in which the material was saturated and agitated with a solution designed to remove certain phases.

The results of these analyses appear to indicate that targeting of specific phases was not successful (Tables 6.1-6.3). The highest concentrations of aluminum, iron, magnesium, and silicon are consistently in stage six, the final stage of the extraction. Stage 6 is intended to remove the sulphide phase, as most other phases should have been removed by the preceding steps; however, the high concentrations of aluminum, magnesium, and silicon are not consistent with sulphide precipitates that could have formed in the flow-through reactors. Furthermore, the sulphur content is consistently low in stage 6 (typically 1-5 ppm), indicating that the dissolved phases do not contain a significant mass of sulphide minerals. The iron content is typically very high in stage 6, but without corresponding sulphur concentrations the iron is likely derived from oxide phases. Sulphur concentrations are highest in the initial phase treated with only de-ionized water, and are probably reflective of sulphate salts precipitated during the drying process. Calcium is more readily distributed across different stages; however, it is most frequently highest in the second stage, the “soluble and exchangeable” fraction.

Table 6.1: Sequential extraction results for reactors 1-4, values in ppm.

Blank	Al	Ca	Fe	Mg	S	Si	Targeted Fraction
Step 1	BDL	BDL	0.052	BDL	BDL	BDL	Precipitated Salts
Step 2	BDL	BDL	BDL	BDL	BDL	BDL	Soluble/ Exchangeable
Step 3	0.6495	BDL	0.497	BDL	1.5335	9.155	Adsorbed Metals
Step 4	BDL	BDL	0.094	BDL	BDL	BDL	Organically Bound
Step 5	BDL	0.0505	BDL	BDL	6.66	BDL	Carbonates
Step 6	BDL	BDL	BDL	BDL	BDL	0.072	Sulphides
Sample 1A							
Step 1	0.5823	20.2	4.931	11.89	18.44	2.682	Precipitated Salts
Step 2	0.101	76.6	1.3345	18.07	4.5975	1.0445	Soluble/ Exchangeable
Step 3	0.4025	0.227	0.7495	BDL	4.5575	9.885	Adsorbed Metals
Step 4	4.3795	39.815	26.02	7.77	2.7735	8.955	Organically Bound
Step 5	2.155	29.335	47.655	3.522	8.575	7.48	Carbonates
Step 6	37.48	20.42	481.3	33.09	1.243	61.86	Sulphides
Sample 2B							
Step 1	0.3848	18.92	3.908	12.38	21.51	2.944	Precipitated Salts
Step 2	0.101	71.9	2.689	23.64	4.1475	2.124	Soluble/ Exchangeable
Step 3	0.807	0.1675	2.537	0.1575	3.7795	18.665	Adsorbed Metals
Step 4	5	22.7	31.47	7.765	2.381	10.95	Organically Bound
Step 5	3.34	6.755	53.05	3.451	7.945	11.26	Carbonates
Step 6	47.83	19.61	573.2	36.75	1.004	78.66	Sulphides
Sample 3A							
Step 1	0.2009	23.81	2.792	8.524	22.91	1.402	Precipitated Salts
Step 2	0.101	35.335	1.323	4.9815	3.123	0.9765	Soluble/ Exchangeable
Step 3	0.5185	0.0915	1.507	0.0515	3.4555	20.45	Adsorbed Metals
Step 4	2.2095	27.195	13.145	3.632	1.751	6.265	Organically Bound
Step 5	1.3065	7.965	22.51	2.0385	7.48	4.322	Carbonates
Step 6	17.61	12.51	333.7	15.92	2.596	31.94	Sulphides
Sample 4A							
Step 1	0.6779	7.599	5.037	6.073	8.589	2.565	Precipitated Salts
Step 2	0.101	33.085	2.249	13.78	1.724	1.6	Soluble/ Exchangeable
Step 3	0.8795	0.1865	2.78	0.26	2.835	22.455	Adsorbed Metals
Step 4	5.315	11.09	25.475	6.125	1.587	10.81	Organically Bound
Step 5	2.4395	5.635	29.455	3.6705	7.485	7.41	Carbonates
Step 6	38.14	20.58	367.5	30.89	1.651	63.15	Sulphides

Table 6.2: Sequential extraction results for reactors 5-8, values in ppm.

Sample 5A	Al	Ca	Fe	Mg	S	Si	Targeted Fraction
Step 1	0.6239	19.96	5.075	10.72	17.8	2.699	Precipitated Salts
Step 2	0.101	76	1.968	17.14	4.1345	1.578	Soluble/ Exchangeable
Step 3	0.379	BDL	1.0195	BDL	4.184	20.99	Adsorbed Metals
Step 4	4.838	35.22	32.12	7.1	2.6495	9.675	Organically Bound
Step 5	3.2685	10.075	48.3	2.732	8.235	9.85	Carbonates
Step 6	49.72	16.21	512.7	34.02	3.012	74.6	Sulphides
Sample 6B							
Step 1	0.2692	19.94	2.537	13.36	26.2	2.067	Precipitated Salts
Step 2	0.101	87.4	2.8095	30.485	4.5995	2.1655	Soluble/ Exchangeable
Step 3	0.586	BDL	1.919	BDL	2.9125	22.875	Adsorbed Metals
Step 4	5.265	22.52	31.3	6.805	2.501	11.535	Organically Bound
Step 5	3.292	6.155	50.95	2.553	8.515	10.54	Carbonates
Step 6	50.27	18.66	579	37.75	1.138	80.47	Sulphides
Sample 7A							
Step 1	0.4008	27.23	4.963	12	27.28	1.577	Precipitated Salts
Step 2	0.101	56.3	2.51	10.225	5.65	0.9945	Soluble/ Exchangeable
Step 3	0.3045	BDL	0.8395	BDL	3.3075	19.375	Adsorbed Metals
Step 4	2.6655	45	16.88	4.8455	2.167	5.605	Organically Bound
Step 5	1.9535	18.655	40.155	2.6525	8.09	5.965	Carbonates
Step 6	33.44	13.56	539.6	26.63	3.342	58.2	Sulphides
Sample 8B							
Step 1	0.6032	5.976	3.791	3.663	4.007	2.455	Precipitated Salts
Step 2	0.3115	29.83	2.924	9.54	0.5365	2.2045	Soluble/ Exchangeable
Step 3	0.731	0.083	2.4855	0.179	2.018	28.78	Adsorbed Metals
Step 4	5.61	6.415	29.01	2.4035	1.216	11.045	Organically Bound
Step 5	2.1465	3.034	24.275	1.5355	8.105	6.265	Carbonates
Step 6	37.55	15.43	307.4	26.4	1.033	61.35	Sulphides

Table 6.3: Sequential extraction results for raw mixtures, values in ppm.

	Al	Ca	Fe	Mg	S	Si	Targeted Fraction
Mixture 1/5	**Poultry Manure and Leaf Compost**						Precipitated Salts
Step 1	0.2961	10.59	2.545	4.45	8.611	2.751	
Step 2	BDL	90.4	1.0955	14.135	1.7605	6.485	Soluble/ Exchangeable
Step 3	0.2355	BDL	0.7955	BDL	2.228	32.43	Adsorbed Metals
Step 4	3.4835	64.55	24.105	3.949	1.126	9.825	Organically Bound
Step 5	2.1025	13.42	25.565	1.325	7.24	6.855	Carbonates
Step 6	33.41	13.23	279.4	23.01	0.383	59.04	Sulphides
Mixture 2/6	**Sheep Manure and Leaf Compost**						
Step 1	0.2893	11.95	2.059	6.68	3.9	3.406	Precipitated Salts
Step 2	BDL	89	1.3765	24.01	1.2285	9.375	Soluble/ Exchangeable
Step 3	0.6995	0.1825	2.3835	0.166	1.946	44.73	Adsorbed Metals
Step 4	3.442	23.74	24.2	4.2305	1.0115	10.87	Organically Bound
Step 5	1.801	4.4065	23.58	1.258	6.875	7.14	Carbonates
Step 6	33.06	13.97	277.4	23.76	0.5157	60.35	Sulphides
Mixture 3/7	**Poultry Manure and Hay**						
Step 1	1.228	19.6	9.963	12.07	18.86	5.691	Precipitated Salts
Step 2	BDL	79.1	1.764	18.055	4.635	17.98	Soluble/ Exchangeable
Step 3	0.412	0.142	1.6045	BDL	2.9735	37.135	Adsorbed Metals
Step 4	3.878	84.35	28.745	3.56	1.519	11.515	Organically Bound
Step 5	2.7835	33.825	31.295	1.565	7.485	9.4	Carbonates
Step 6	41.74	19.36	324.5	29.34	1.662	69.33	Sulphides
Mixture 4/8	**Control – No Organics**						
Step 1	0.6629	8.518	4.788	3.732	3.766	2.928	Precipitated Salts
Step 2	BDL	28.785	1.978	8.11	0.9535	2.372	Soluble/ Exchangeable
Step 3	1.0055	0.115	3.185	0.208	2.511	40.725	Adsorbed Metals
Step 4	6.075	5.265	32.86	1.9975	1.461	11.44	Organically Bound
Step 5	2.147	1.953	21.855	1.0325	7.685	6.42	Carbonates
Step 6	34.97	13.13	279.7	22.61	2.311	60.89	Sulphides

6.2.3 C/N/S Analysis

Among carbon, nitrogen, and sulphur, carbon is consistently the dominant fraction, with carbon concentrations in reactors with added organic matter in a range from 2-6%. Sulphur and nitrogen concentrations are lower, typically below 1%. In reactors 1 and 5 (Fig. 6.16) the carbon content is 3.88% C in sample 1B, while only 2.06% C is found in sample 5B. Sulphur values are considerably lower, with 0.66% S in sample 1B, and 0.34% in 1C. Nitrogen values are lower

than sulphur values, and demonstrate considerable variation on an individual basis. 1B has the highest value, with 0.22% N, while 5B had only 0.12% N.

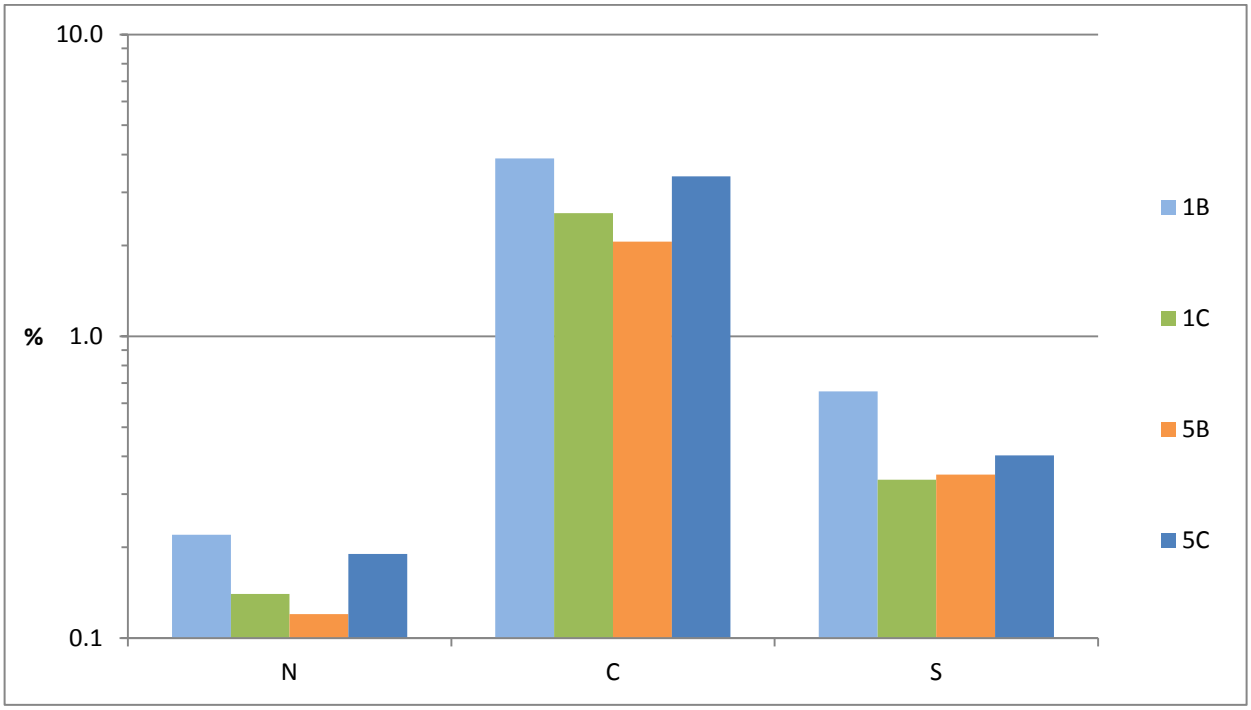

Figure 6.16: C/N/S results for reactors 1 and 5.

In reactors 2 and 6 (Fig. 6.17), concentrations for all three elements was notably higher than in the samples from reactors 1 and 5. Carbon concentrations are generally consistent around 5%, while sulphur concentrations ranged from 0.76% to 1.07%, and nitrogen values ranged from 0.26% to 0.32%.

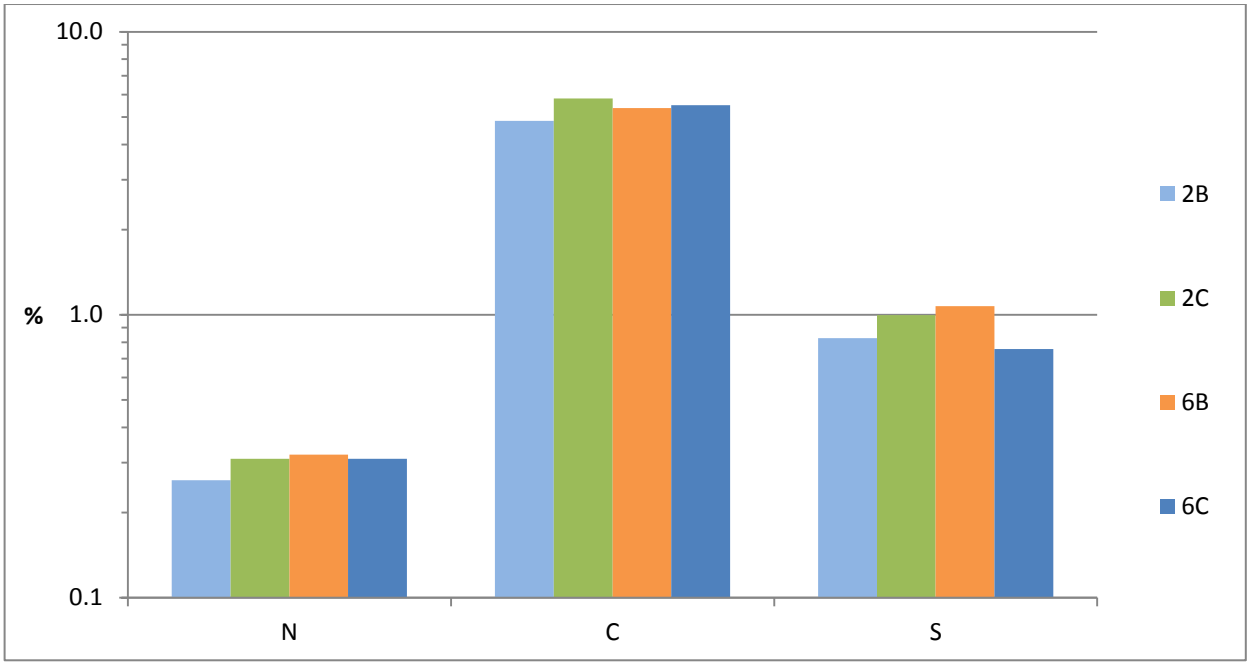

Figure 6.17: C/N/S results for reactors 2 and 6.

Reactors 3 and 7 (Fig. 6.18) demonstrate similar results for carbon to reactors 1 and 5. Carbon concentrations are lower in comparison to reactors 2 and 6, with carbon content ranging from 2.7 to 3.7%. Sulphur results are similar to reactors 2 and 6 and range from 0.95 to 1.25%. Nitrogen concentrations range from 0.16 to 0.21%, which are higher than in reactors 1 and 5, but lower than in reactors 2 and 6.

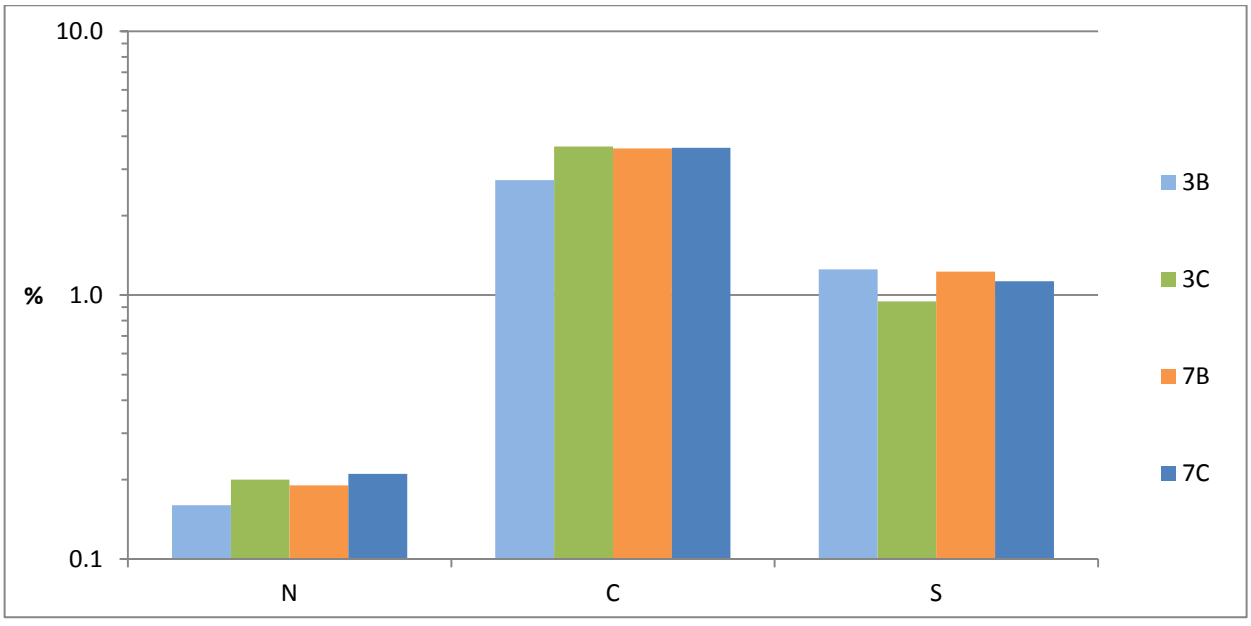

Figure 6.18: C/N/S results for reactors 3 and 7.

In reactors 4 and 8 (Fig. 6.19), no organic material was added to the reactors, and thus it is not surprising to observe that carbon, nitrogen and sulphur concentrations are much lower in these samples. Carbon is still more abundant than either nitrogen or sulphur, but is considerably lower in these samples, ranging from 0.76% to 1.16%. Sulphur and nitrogen concentrations are also low, in a range from 0.04 to 0.11%.

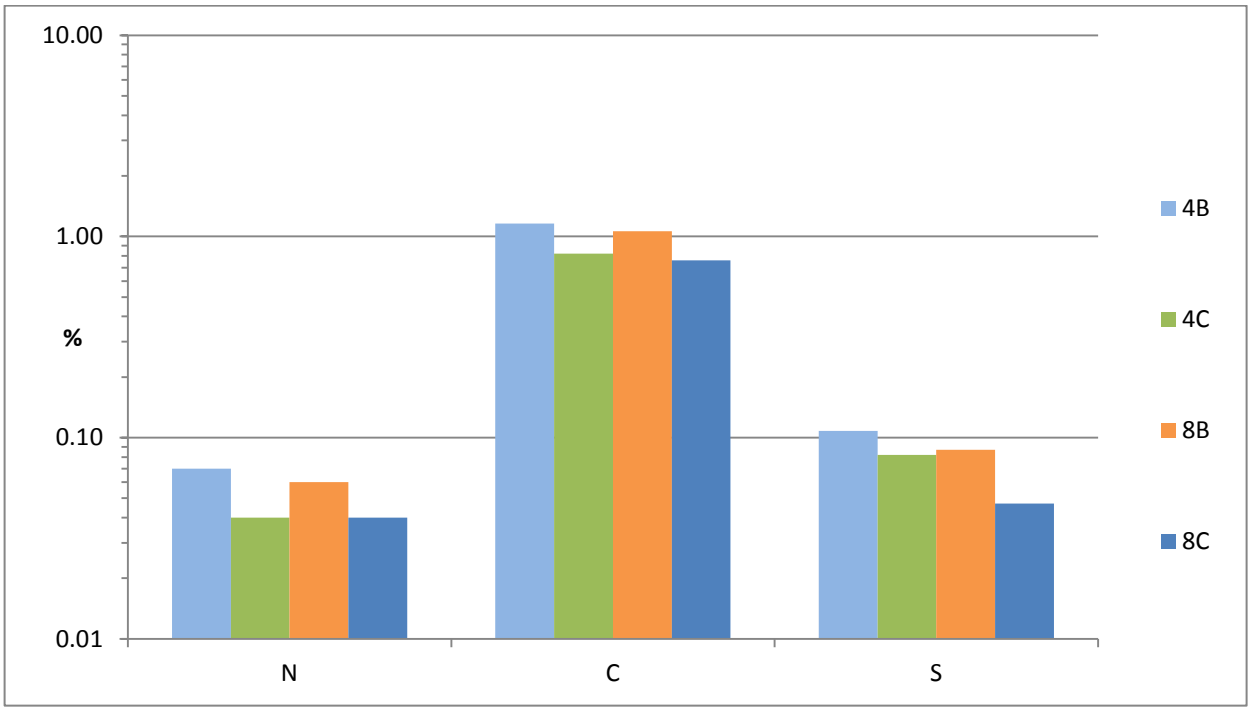

Figure 6.19: C/N/S results for reactors 4 and 8.

With respect to the vertical distribution of materials within the reactors, carbon concentrations do not follow a uniform pattern, although several reactors do have slightly greater carbon concentrations at the bottom than at the top (Fig. 6.20). Reactors 1 and 6 show this pattern most sharply, while the decline in carbon contents in reactors 4, 7, and 8 is less pronounced. In contrast, carbon concentrations are higher in reactors 2, 3, and 5.

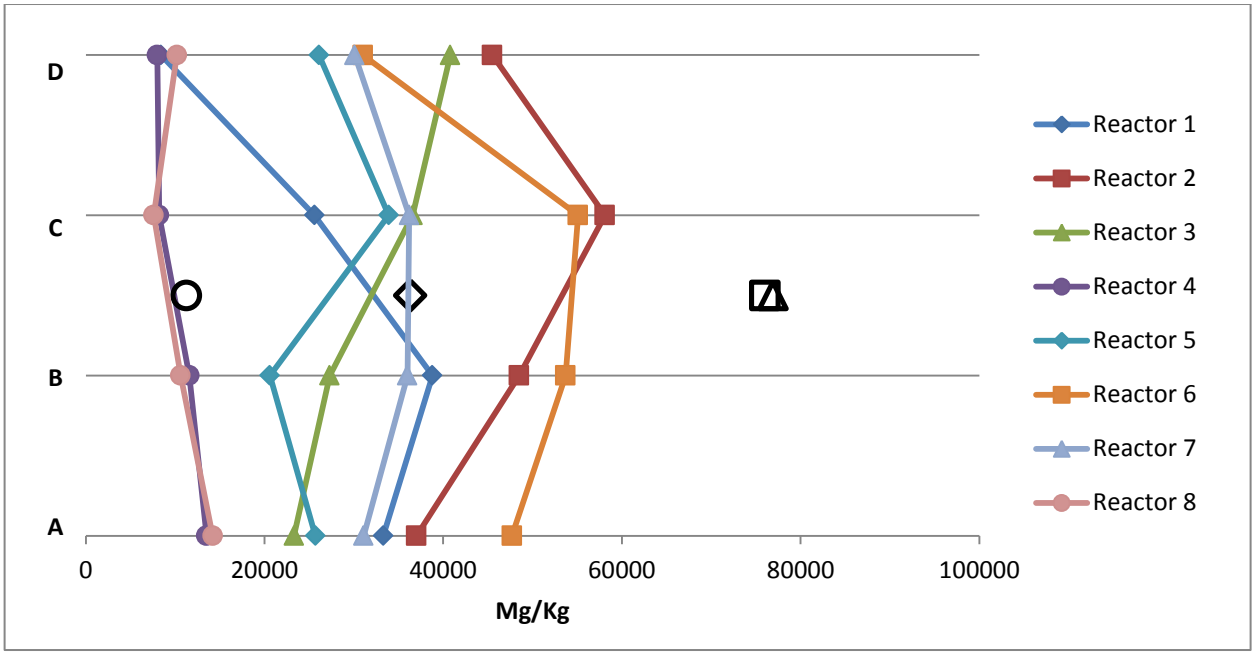

Figure 6.20: Vertical variation of carbon concentrations within reactors. Raw mixture represented as blank symbols corresponding to coloured symbols in legend.

Nitrogen concentrations do not demonstrate any clear trends with respect to vertical variation (Fig. 6.21). Reactors 1 and 6 have significantly higher concentrations at the bottom of the reactor, while reactors 4 and 8 are relatively uniform throughout. In contrast, reactors 2 and 3 have significantly higher nitrogen concentrations at the top of the reactor, while reactor 5 has a slightly higher concentration at the top. Reactor 7 has its highest concentrations in the middle of the reactor, while concentrations at the top and bottom are slightly lower and nearly identical to each other.

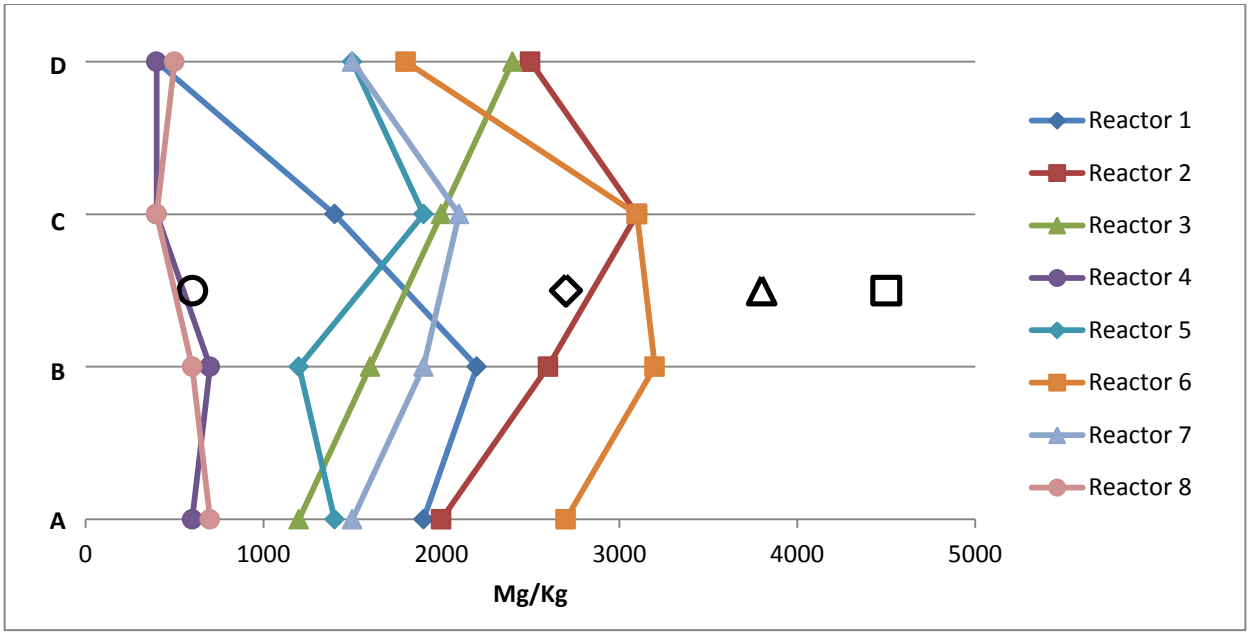

Figure 6.21: Vertical variation of nitrogen concentrations within reactors. Raw mixture represented as blank symbols corresponding to coloured symbols in legend.

6.2.4 X-Ray Diffraction

In order to determine minerals present in the reactor materials, samples were dried and milled for powder XRD analysis. The large volume of silica sand utilized in the reactor mixtures dominates the results, along with the lesser, although still significant, amount of creek sediment. Quartz was identified as the dominant mineral present in every sample, as was anticipated based on the volume of silica sand, and creek sediment would also be a significant source of quartz. The only other significant mineral present in every sample were feldspars, including anorthite and albite, which was consistent with XRD analysis of creek sediment alone, which was found to be quartz dominant. For most samples the XRD patterns are very consistent. A typical pattern is represented by sample 1A (Fig. 6.22) with quartz as the dominant fraction with lesser amounts of albite, while sample 8D (Fig. 6.23) was also dominated by quartz while anorthite represented the feldspar fraction. No evidence of precipitation or alteration products from the experimental procedure was found. The XRD technique is limited to detection of mineral species present with

at least 2% abundance in the sample; consequently trace mineral phases may not have been detected.

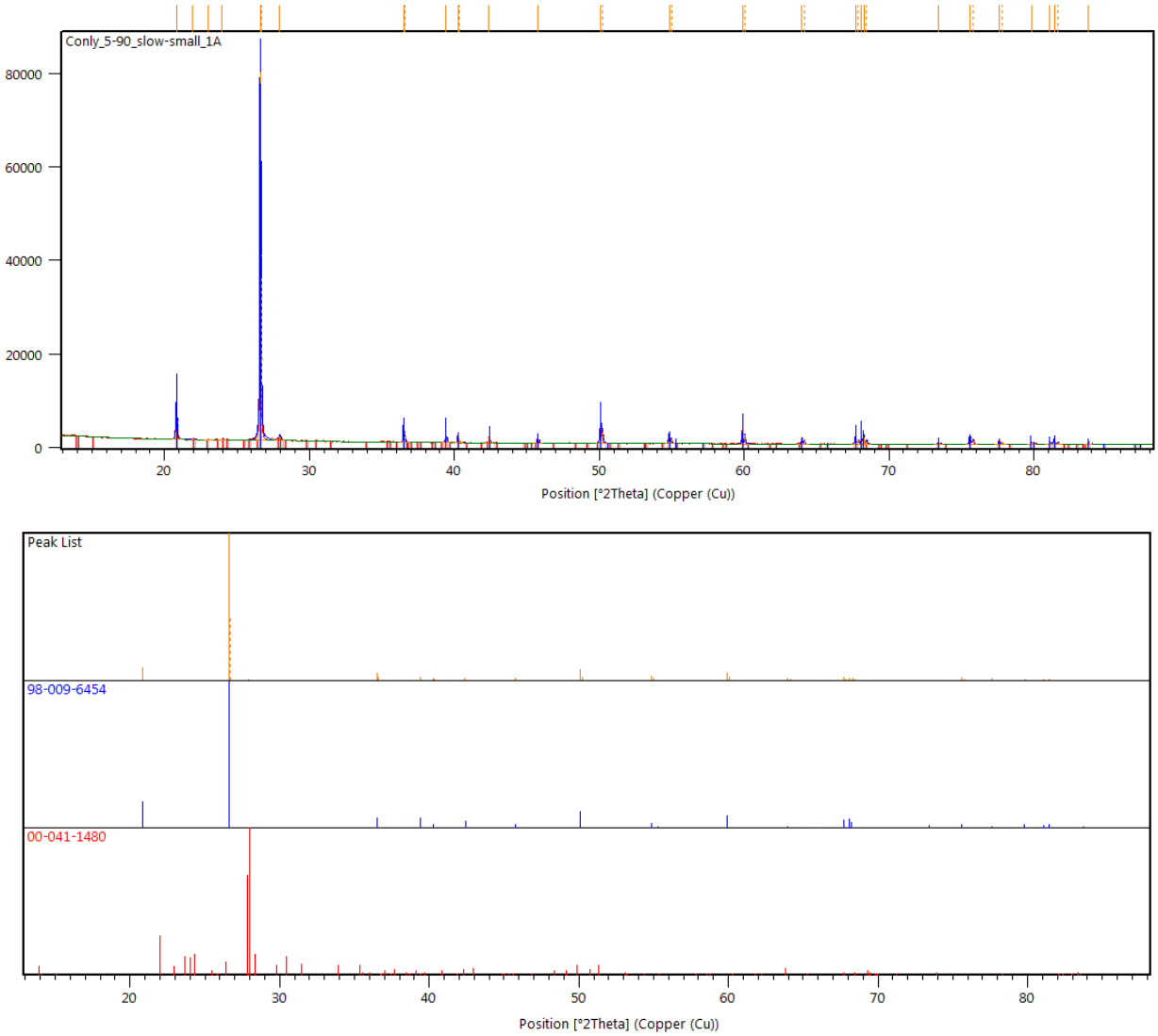

Figure 6.22: XRD profile and reference patterns for sample 1A. Quartz in blue, albite in red.

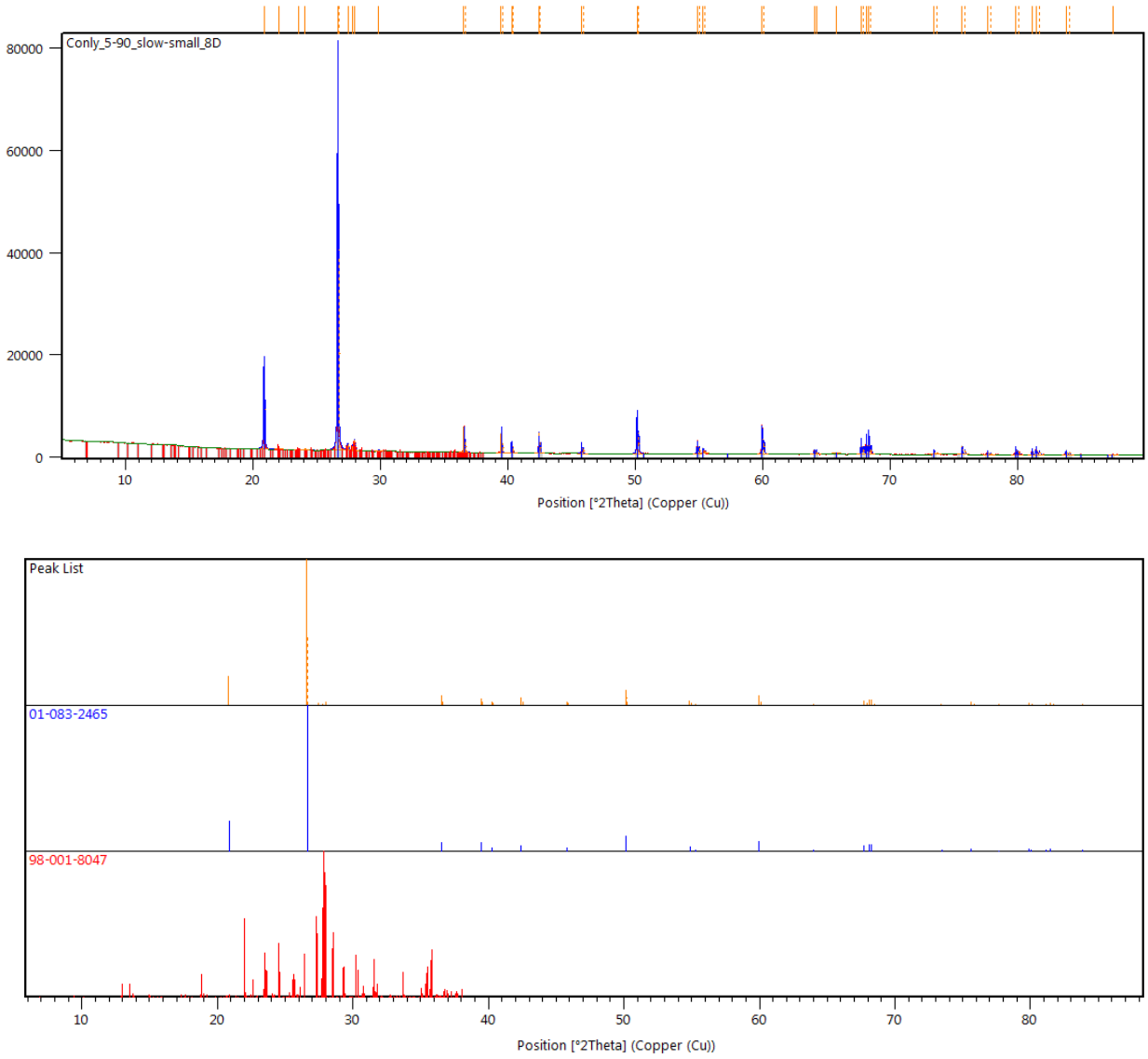

Figure 6.23: XRD profile and reference patterns for sample 8D. Quartz in blue, anorthite in red.

6.2.5 Scanning Electron Microscopy

Scanning electron microscopy (SEM) analysis was conducted on selected samples of dried reactor materials in order to identify trace phases that precipitated as a result of reactions resulting in removal of aqueous sulphate. It is important to note that the elemental concentrations derived from this method are semi-quantitative, but are applicable for phase identification. Due to the very large proportion of silica sand and creek sediment within the mixtures, these materials

were expected to be dominant throughout most areas assessed. Several sites supported this expectation with high concentrations of silicon present, and lesser amounts of other elements that would be contained within a feldspar or mica, such as aluminum, calcium, iron, magnesium, potassium, and sodium. A typical area of material representing these quartz and silicate grains is seen in Figure 6.24. The spectrum 1 site corresponds to quartz crystals, while spectrums 2, 3, and 4 represent feldspar or mica, based on the presence of silicon, aluminum, calcium, iron and magnesium.

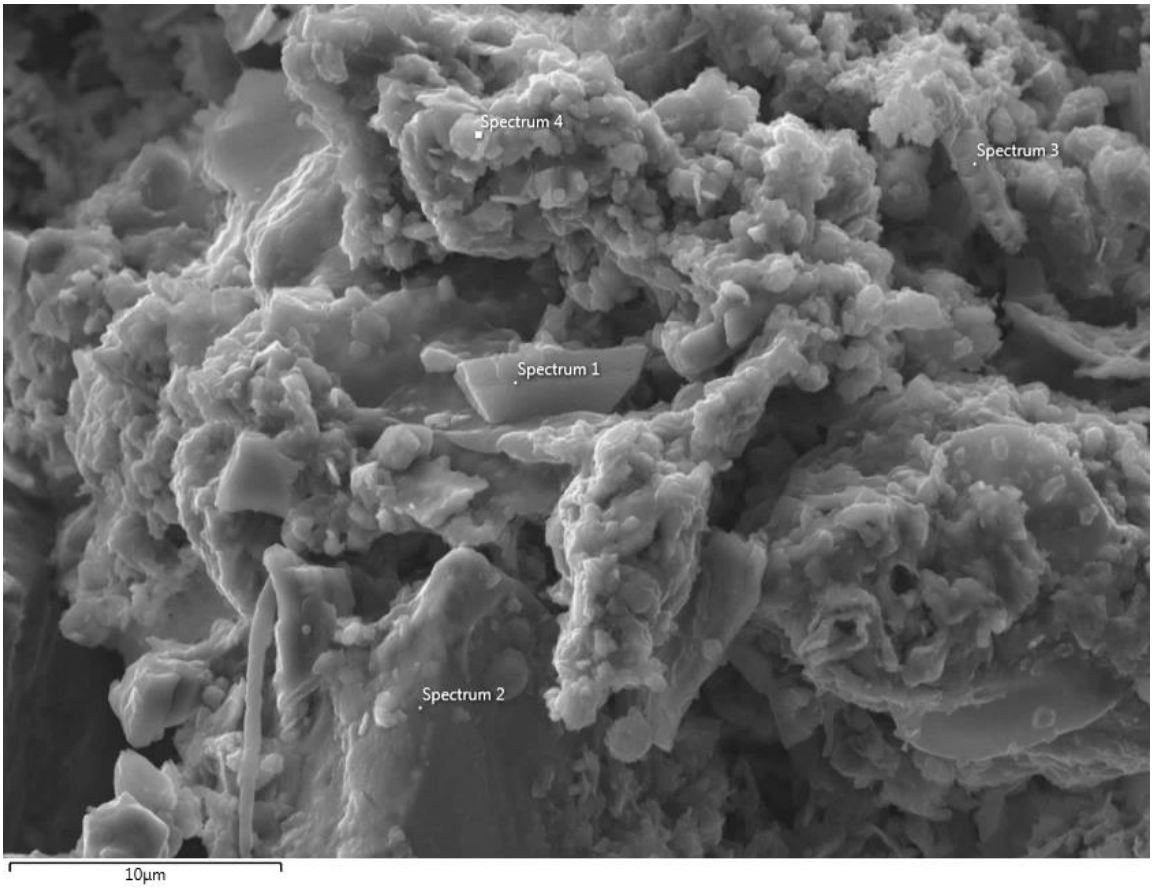

Figure 6.24: Secondary electron image of sample 2C showing quartz and silicate grains of the silica sand and creek sediment.

Organic matter was found throughout the samples, and the organic structures were often easily identified as distinct from the inorganic materials. An example is presented in Figure 6.25, showing a fragment of organic material (spectrum sites 9 and 10) which dominates the field of

view and is surrounded by silicate detritus at spectrum site 11. A rib like structure which is probably plant matter is visible along the bottom of this material (spectrum 10), while the upper face is smooth (spectrum 9). At both spectrum 9 and 10 sites, carbon values are very high while oxygen was also detected along with low levels of iron, calcium, and sulphur. Carbon values are impacted by the carbon coating on all samples; however, the very high counts as compared to other samples indicate that this material is carbon rich, consistent with organic matter (G. Wu, personal communication, January 6, 2015). Spectrums 9 and 10 have very similar compositions, although higher counts for carbon, oxygen, and iron were detected in spectrum 10. Spectrum 11 corresponds to silicates previous observed and is a feldspar or mica.

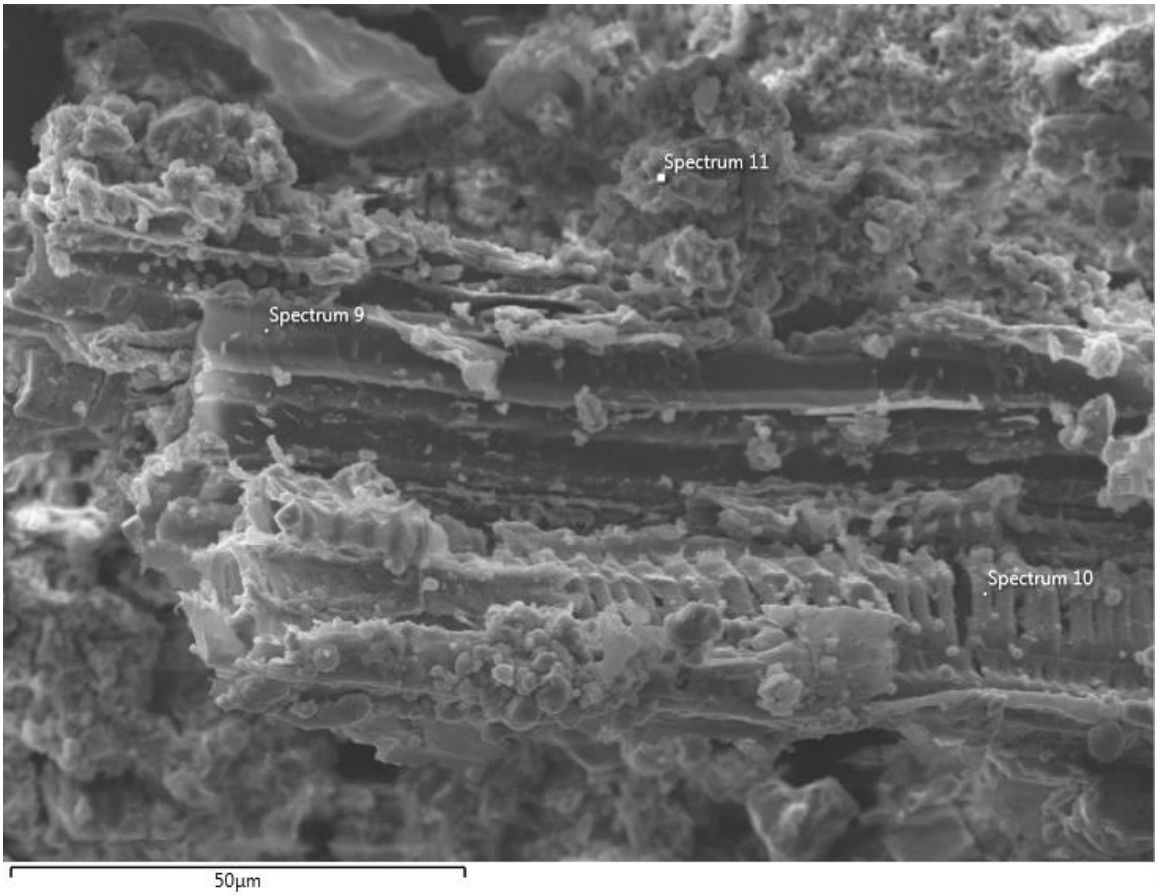

Figure 6.25: Secondary electron image of organic matter surrounded by typical silicate grains in sample 1B.

In Figure 6.26 very fine spherical crystals have formed all along the underlying substrate, and all three sites within the field of view were found to be rich in iron and sulphur (Fig. 6.27), with an iron to sulphur ratio of 3.8:1. The high concentration of iron indicates that iron oxides are present, with a lesser amount of iron sulphide or sulphate possibly accounting for the sulphur content. This is consistent with qualitative observations of the reactor materials which sometimes appeared rust coloured, and rust like staining was also left on the reactor walls following deconstruction.

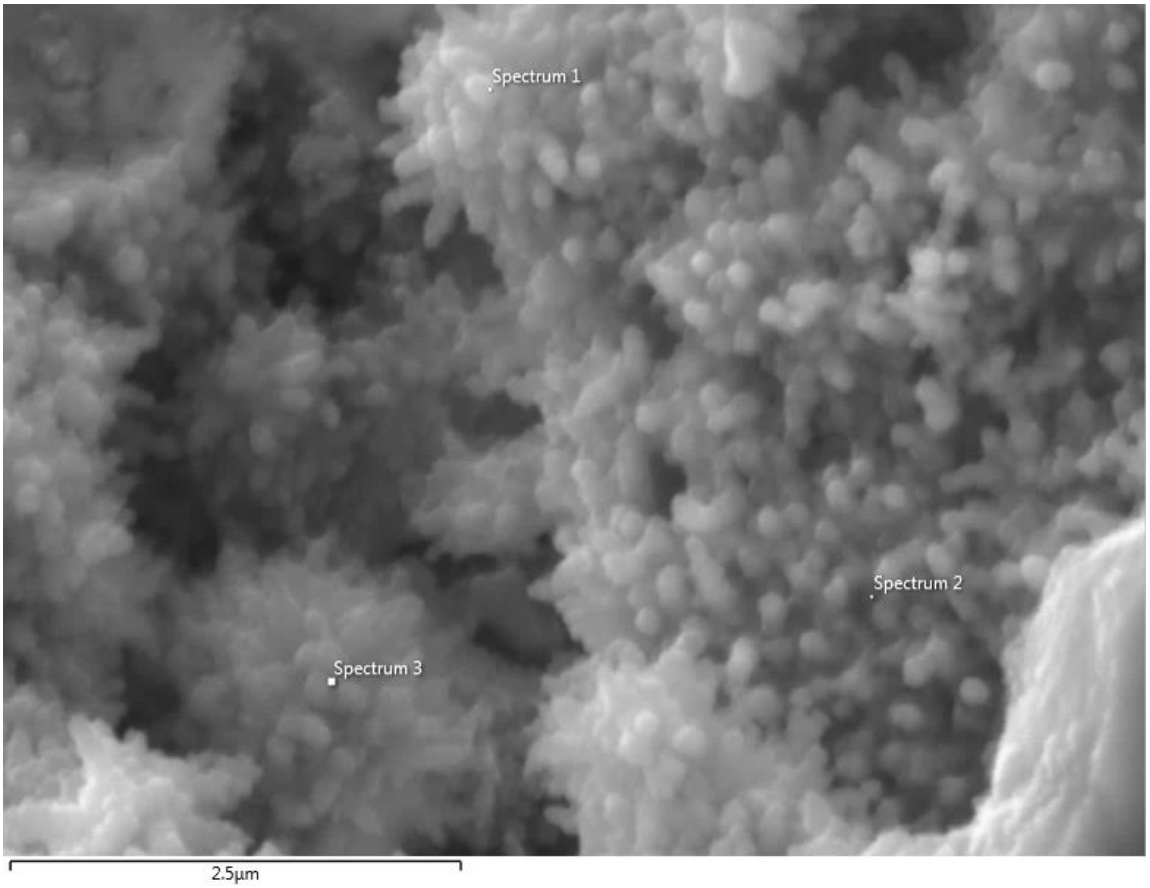

Figure 6.26: Secondary electron image of fine iron precipitates in sample 1B.

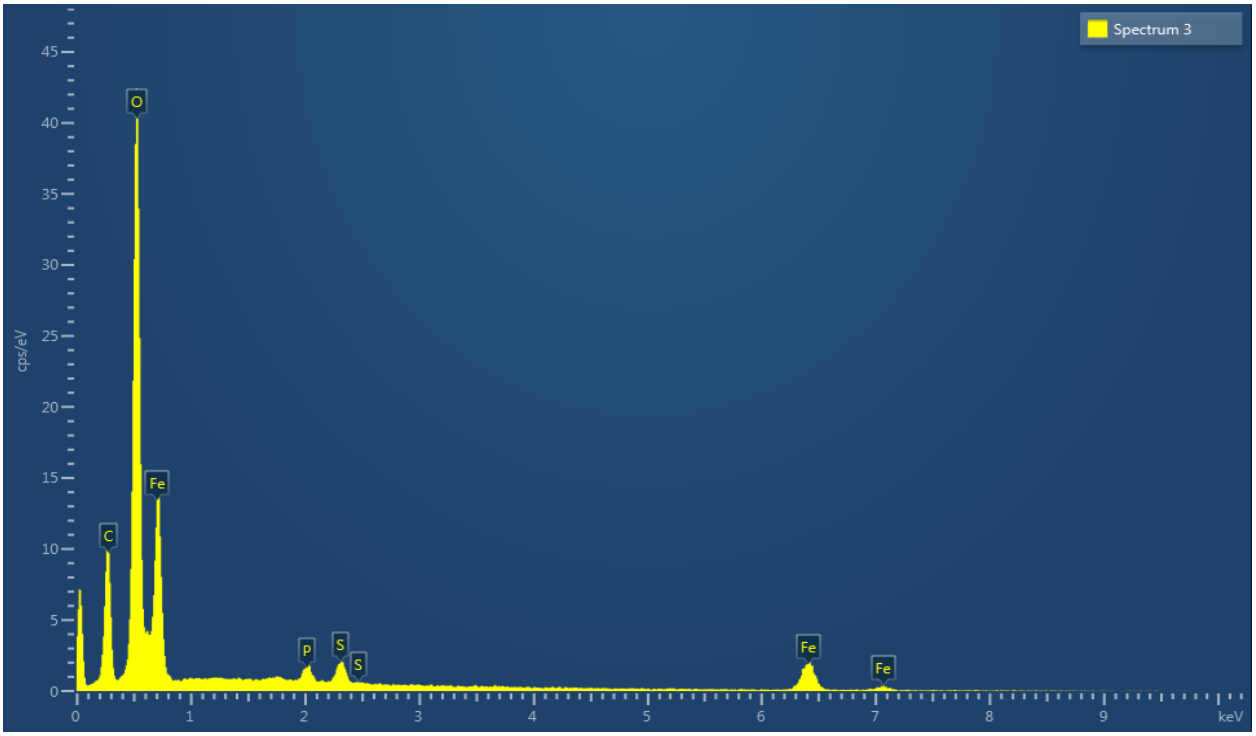

Figure 6.27: Energy-dispersive x-ray spectrum #3, sample 1B.

Mineral grains containing high concentrations of phosphorus were also found. In Figure 6.28, phosphorus was found to be most abundant element in two well defined mineral grains (spectrum sites 12 and 13), which were notably larger than other grains in the surrounding matrix. These are possibly a phosphate mineral, and also contain limited amounts of iron and magnesium in similar proportions in spectrums 12 and 13 (Fig. 6.29). Phosphorus may have been derived from organic material, the small quantity of phosphorus known to be present in the iron spheres, or it may have been present in creek sediment prior to emplacement in the reactors. Spectrum site 15, a finer mineral grain attached to the larger phosphorus rich grain was found to contain significant concentrations of calcium and phosphorus; this likely corresponds to apatite.

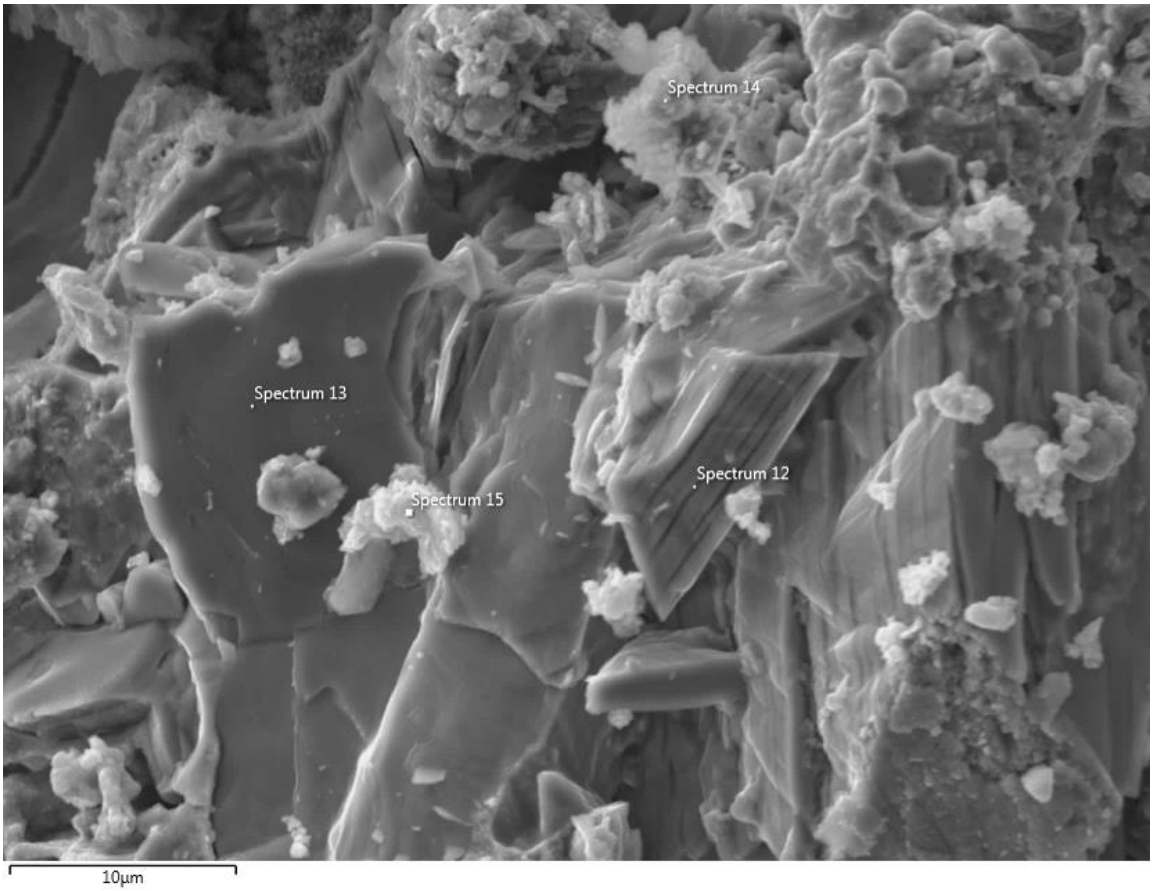

Figure 6.28: Secondary electron image of coarse grained phosphorus bearing minerals in sample 1B. Finer grained typical silicate detritus at spectrum 14.

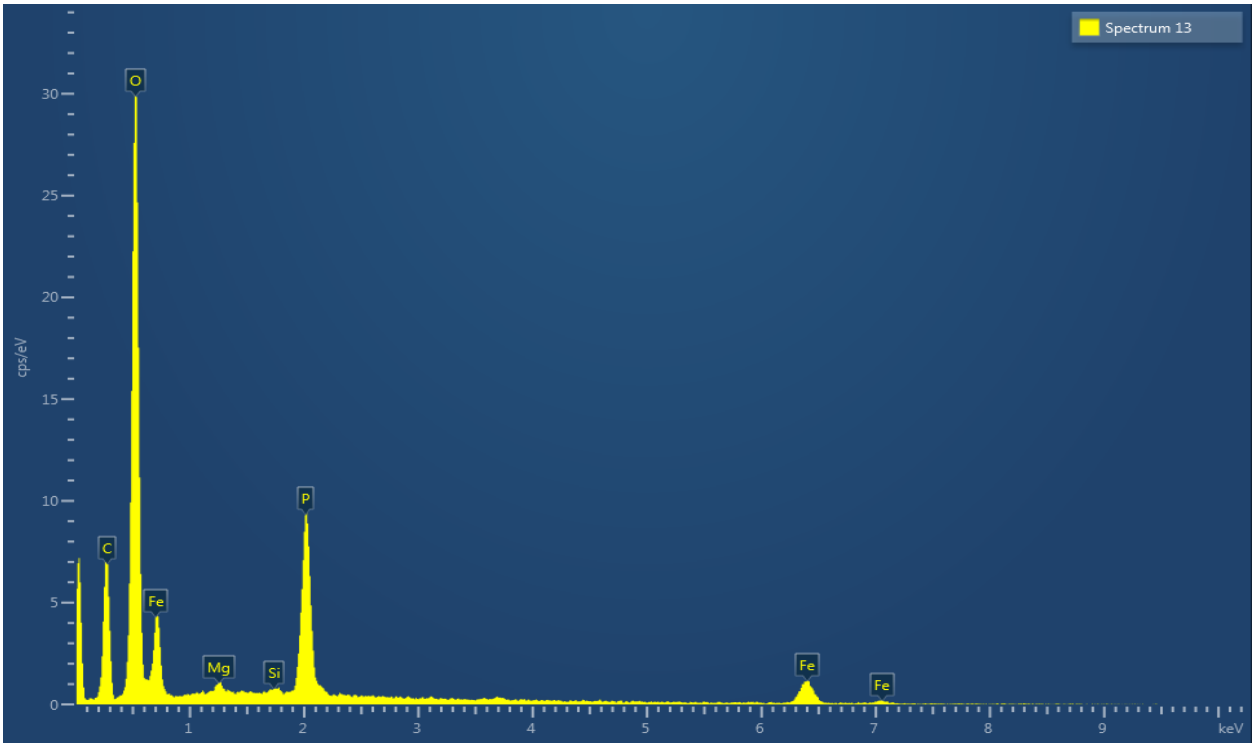

Figure 6.29: Energy-dispersive x-ray spectrum #13, sample 1B.

A final possible precipitate was found in sample 7A and is shown in Figure 6.29. It is observed to have a very rough, yet defined structure with a vaguely triangular base, while a spherical growth with jagged edges appears to rise from the center of the triangle. This spherical growth is similar to the structure of a sulphate rosette, while also vaguely resembling the structure of framboidal pyrite. Both sites analyzed were most abundant in sulphur, followed by iron, with trace amounts of silica, calcium and magnesium (Fig. 6.30). Sulphur and iron are present in a 1.67:1 ratio, which could potentially indicate a mixture of iron sulphides such as mackinawite (FeS) and pyrite (FeS_2).

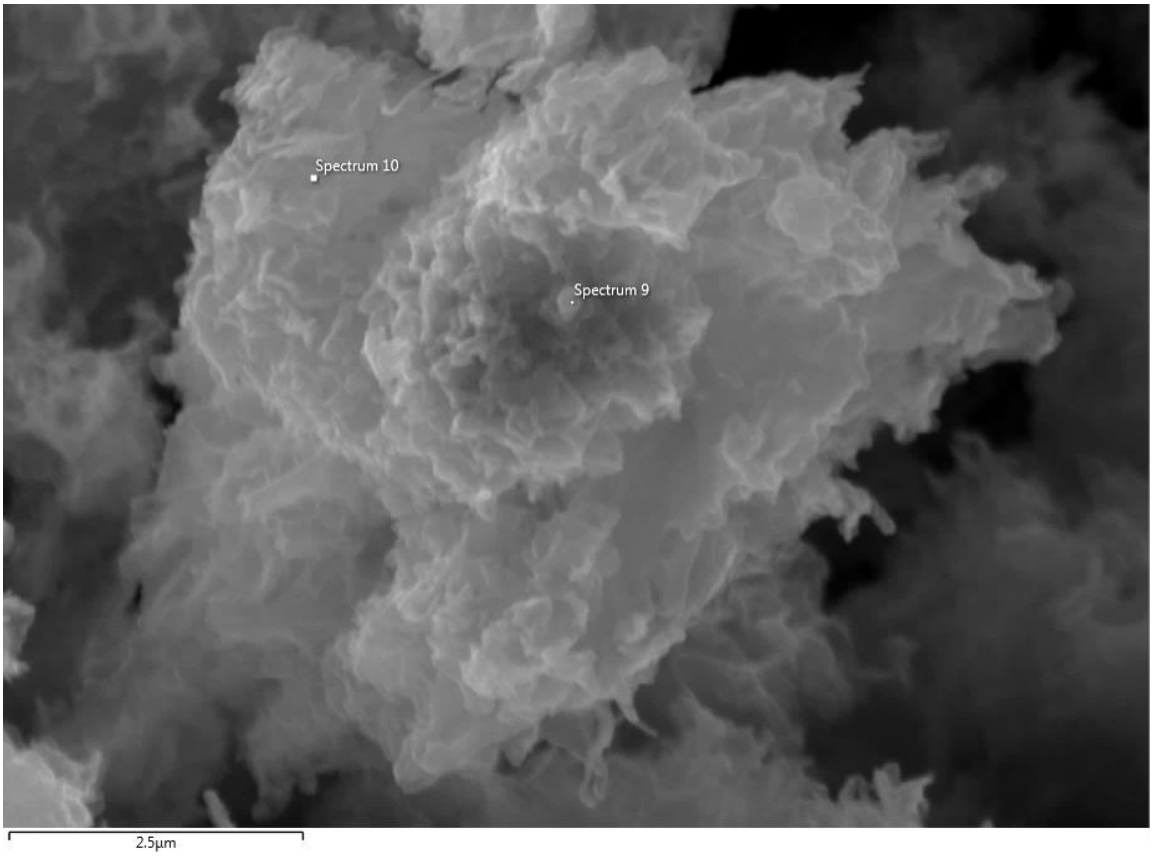

Figure 6.30: Secondary electron (BSE) image of sulphur bearing mineral in sample 7A.

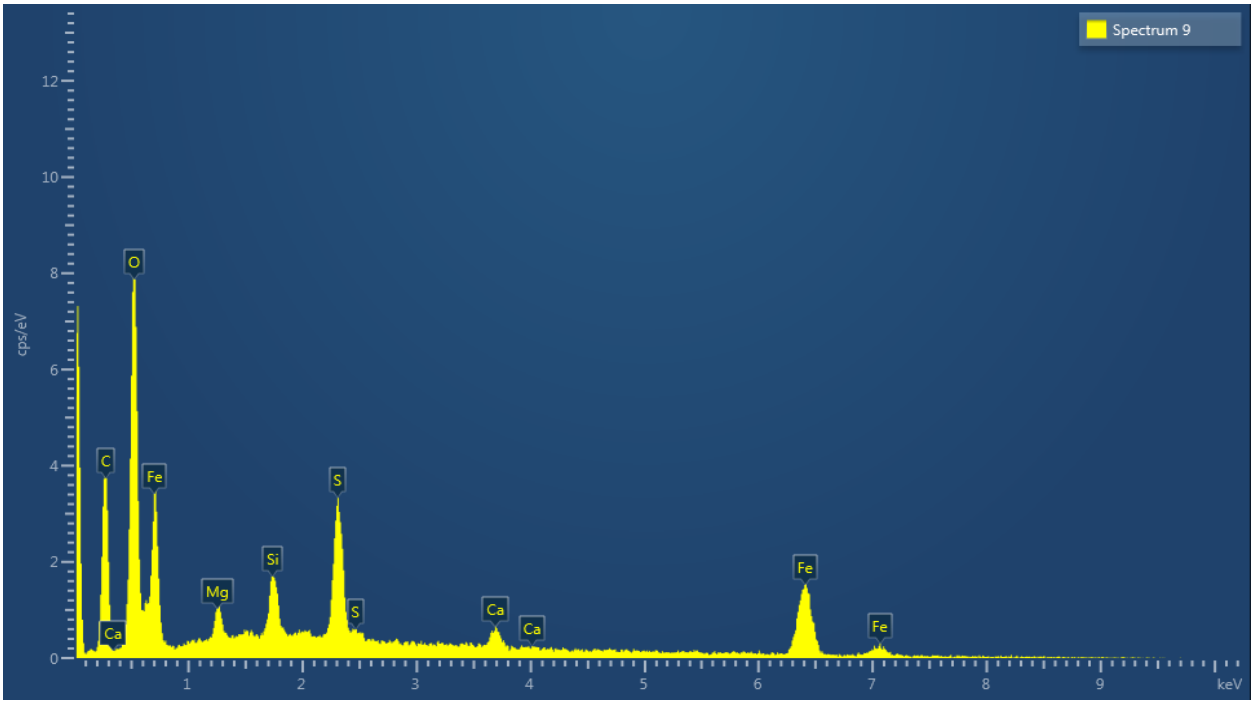

Figure 6.31: Energy-dispersive x-ray spectrum #9, sample 7A.

Chapter 7: Behaviour and Effectiveness of Reactors

7.1 Evaluation of Flow-Through Reactor Performance

7.1.1 Sulphate Removal Efficiency

The primary performance measure of the flow-through reactor experiment is removal of sulphate from Steep Rock pit lake waters. In this regard, all organic amended reactors were very successful for the first eleven weeks. Performance began to decline in week 12, although reactors 3 and 7 maintained >80% sulphate removal through week 14. Following week 14, performance in all organic amended reactors underwent a progressive and significant decline in performance. Non-organic amended reactors (4 and 8) had significantly lower sulphate removal, and did not undergo as significant of long term changes in performance (Fig. 7.1). Complete reactor monitoring data is available in Appendix C. Sulphate removal % was calculated by subtracting the measured effluent sulphate concentration from the most recent influent sulphate concentration data. The resulting value was then divided by the influent sulphate concentration and multiplied by 100.

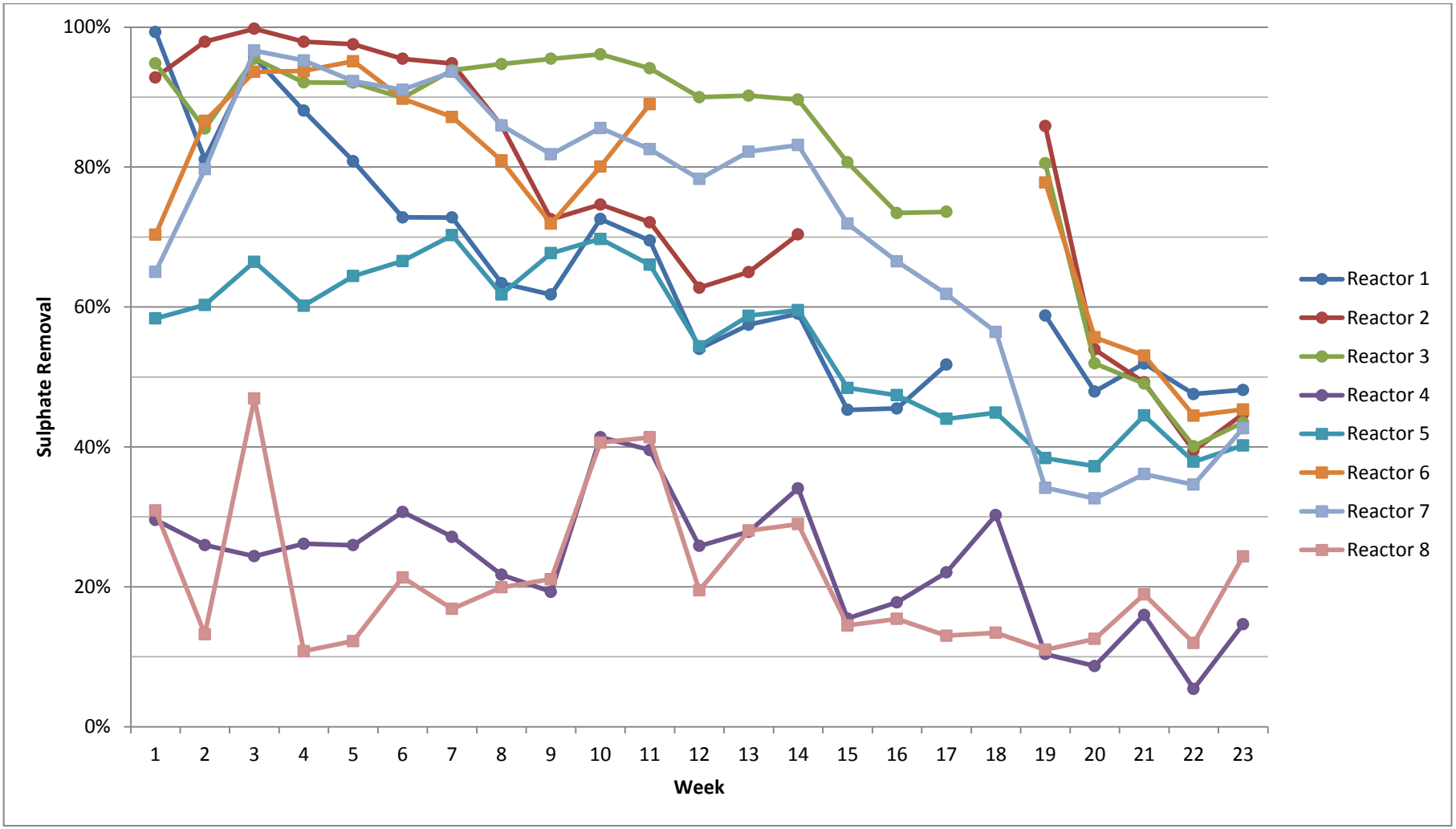

Figure 7.1: Percent sulphate removed over the duration of the flow-through reactor experiments.

While in other studies (e.g., Waybrant et al., 1998; Gibert et al., 2004; Neculita et al., 2011; Shankie, 2011) batch reactor setups (no flow) have been able to exceed this level of sulphate removal, rarely have continuous flow reactors (without external chemical or nutrient feed) been able to achieve such high levels of sulphate removal. A variety of lab- and field-scale PRB systems using natural organic materials to stimulate SRB have only been able to achieve sulphate removal in the 40 to 60% range (e.g., Waybrant et al., 1998; Gibert et al., 2004; Caraballo et al., 2010; Neculita et al., 2011; Song et al., 2012). Consequently, while sustaining sulphate removal at a high level remains a challenge, the performance achieved here, particularly in reactors 3 and 7 (poultry manure and hay), is promising.

Reactor 5 was unable to achieve the high rates of sulphate removal initially produced by the other organic reactors, although from weeks 7 to 16 there was excellent consistency in sulphate reduction values between reactor 5 and its replicate, reactor 1 (poultry manure and leaf compost). There is no clear explanation for the lower initial performance, although preferential flow channelling is a possibility. Reactors 2 and 6 (sheep manure and leaf compost) had intermediate levels of average performance between the best performing reactor pair, 3 and 7, and the poorest, 1 and 5.

Reactors 4 and 8 did not contain any added organic material, and as expected sulphate removal rates were much lower than in the organic amended reactors. Reactor 4 contained zero valent iron (ZVI), while reactor 8 did not (allowing assessment of the ability of ZVI as a sulphate remediation tool on its own). Blowes et al. (2000) and Philips et al. (2000) have suggested that ZVI may be able to remediate sulphate on its own, with sulphate corroding the ZVI to release ferrous iron and convert sulphate to hydrogen sulphide, which can then react to precipitate an iron sulphide, resulting in the removal of both iron and sulphur. Reactor 4 was able to achieve a

slightly higher average sulphate removal, with an average rate of 23% over the duration of the experiment, while reactor 8 was able to achieve an average sulphate removal value of 21%. This relatively small difference does not support the concept of ZVI as a remediation tool on its own, at least under the conditions present within this study. However, this does not diminish the quality of ZVI as a useful tool in combination with sulphate reducing bacteria.

Shankie (2011) conducted batch experiments to assess the capacity of candidate reactive mixtures prior to conducting flow through experiments. The study by Shankie (2011) utilized the same water source as used in the current study, providing an excellent comparison. In the batch experiments conducted by Shankie (2011), three mixtures were assessed, with treatment #1 (wood chips and horse manure) the most effect mixture, achieving 99% sulphate removal. However, when this mixture was utilized in several flow-through reactors using different orientations of separated reaction cells within the reactor, the most effective reactor was only able to attain an average sulphate removal of 49%. Despite the use of wood chips in the study by Shankie (2011), it was not selected for assessment in the current study due to the high C:N ratio reported in several studies (Waybrant et al., 1998; Zagury et al., 2006; Neculita et al., 2008; Shankie, 2011). Shankie (2011) identified the lack of divalent metals available for the removal of sulphide as metal sulphide precipitates as a potential limiting factor for sulphate removal. This finding prompted the use of ZVI within the reaction mixtures in the current study in order to provide sufficient iron to solution. A more detailed substrate analysis was also conducted in order to ensure the most effective combination of carbon, nitrogen, and phosphorus would be available to SRB. These refinements are reflected in the significantly improved sulphate removal results in the current study compared to those achieved in the flow-through experiments by Shankie (2011); (Tables 7.1 and 7.2). Note that all flow-through reactors in Shankie (2011) utilize the same horse manure and wood chip organic source, with different internal structure.

Table 7.1: Comparison of maximum sulphate removal in current study vs. Shankie (2011).

This study; Reactor #1, wk 1	This study; Reactor #2, wk 3	This study; Reactor #3, wk 10	This study; Reactor #4, wk 10
99 % Poultry/Leaves	99 % Sheep/Leaves	96 % Poultry/Hay	41 % No Organic
This study; Reactor #5, wk 7	**This study; Reactor #6, wk 5**	**This study; Reactor #7, wk 3**	**This study; Reactor #8, wk 3**
70 % Poultry/Leaves	95 % Sheep/Leaves	97 % Poultry/Hay	47 % No Organic

Shankie (2011) Reactor #1, wk 4	Shankie (2011) Reactor #2, wk 7	Shankie (2011) Reactor #3, wk 3	Shankie (2011) Reactor #4, wk 6
86 %	51 %	47 %	44 %
Shankie (2011) Reactor #5, wk 3	**Shankie (2011) Reactor #6, wk 9**	**Shankie (2011) Reactor #7, wk 7**	**Shankie (2011) Reactor #8, wk 6**
70 %	57 %	55 %	46 %

Shankie (2011) Batch #1	Shankie (2011) Batch #2	Shankie (2011) Batch #3
99 % Horse/Wood Chips	99 % Organics w/o creek sed.	0 % Molasses

Table 7.2: Comparison of average sulphate removal in current study vs. Shankie (2011).

This study; Reactor #1	This study; Reactor #2	This study; Reactor #3	This study; Reactor #4
65 % Poultry/Leaves	76 % Sheep/Leaves	81 % Poultry/Hay	23 % No Organic
This study; Reactor #5	**This study; Reactor #6**	**This study; Reactor #7**	**This study; Reactor #8**
55 % Poultry/Leaves	76 % Sheep/Leaves	71 % Poultry/Hay	21 % No Organic

Shankie (2011); Reactor #1	Shankie (2011); Reactor #2	Shankie (2011); Reactor #3	Shankie (2011); Reactor #4
40 %	32 %	36 %	33 %
Shankie (2011); Reactor #5	**Shankie (2011); Reactor #6**	**Shankie (2011); Reactor #7**	**Shankie (2011); Reactor #8**
44 %	35 %	35%	36 %

7.1.2 Limitations on Sulphate Removal

The decline in performance is a common problem with permeable reactive barrier systems, in either bench or field-scale tests. A variety of problems can contribute to this decline,

including but not limited to: development of preferential flow paths, loss of permeability, armouring of reactive substrates with precipitates, inadequate residence time, unsuitable conditions for microbial activity (including nutrients, pH, and Eh), and insufficient availability of divalent metals for sulphide removal (Neculita et al., 2007; Sheoran et al., 2010). In the development of the experimental design for this study preventing loss of porosity was an important design consideration. Silica sand was used as the primary mixture component, as well as utilizing silica sand layers at the influent and effluent ports in order to maintain porosity. In contrast, preventing the development of preferential flow paths is more difficult, as flowing water can carve out these paths over time even without any pre-existing weaknesses in the distribution of materials. Armouring of reactive substrates (including organic matter and ZVI spheres) is also a possible factor contributing to the decline in performance. In the initial weeks, this fresh material would have been well exposed and highly reactive; however, it is likely that over time precipitates formed on the surfaces of these materials (Bartzas and Komnitsas, 2010), which limited their reactivity and ability to contribute necessary nutrients for microbial nutrition, or for ZVI to release iron to solution. This factor is confirmed by visual inspection of the ZVI spheres which have significant iron oxide formation on their surfaces following completion of the flow-through experiments (Fig. 7.2). These spheres were originally smooth, round, shiny, and grey in colour.

Figure 7.2: Oxidized iron spheres collected from post-experiment materials.

The conditions for microbial activity appear to have been suitable, with steady near neutral pH conditions, and sufficiently negative Eh values. However, despite sufficiently reducing conditions for the activity of SRB, a problem arises due to the Eh being too high for the stability of aqueous sulphide produced by SRB (Fig. 7.3). Consequently, any aqueous sulphide produced by SRB may have been immediately converted to sulphate. After completion of the flow-through experiments, nutrient concentrations in the reactors were found to have declined significantly compared to the initial mixtures, which may have been a significant factor in the decline in sulphate removal effectiveness. Such a decline in nutrient availability has been cited in other studies as a factor limiting reactor performance (e.g., Waybrant et al., 2002; Neculita et al., 2007). The overall balance of nutrient supply will be assessed in section 7.1.3.

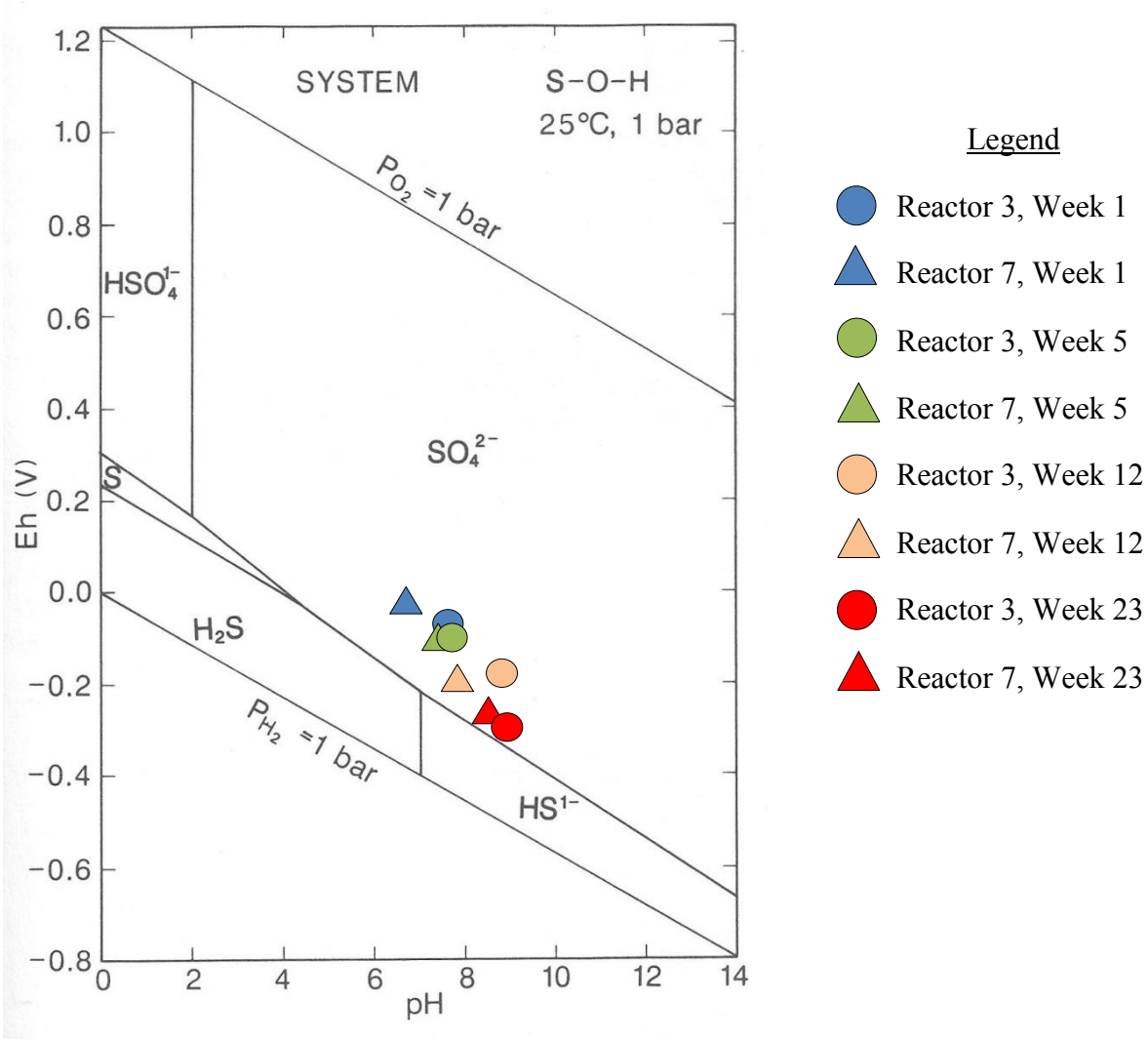

Figure 7.3: Eh/pH diagram for the S-O-H system at 25°C. Modified after Brookins (1988).

The decline in performance could also be related to alternative sulphate removal mechanisms which were effective in the initial weeks, but became less effective over time. For example, sulphate can be adsorbed onto soils (Curtin and Syers, 1990), although the capacity for this adsorption is limited and would likely be exhausted quickly in this system given the high sulphate concentrations. An additional factor which could reduce performance is related to the suppression of SRB activity. Excess H_2S and HS^- have been reported to have toxic effects on bacteria, and consequently a lack of sulphide removal can also depress the activity of SRB (Nagpal et al., 2000). Unreacted free sulphide will ultimately be re-oxidized back to sulphate if

oxidizing conditions are encountered (INAP, 2003), or it is also possible for H_2S to escape solution in gaseous form (Benner et al., 2002); both of these conditions are possible as the effluent entered the oxidation cell. A pungent odour resembling H_2S was observed within the area of the experimental setup during operation, consistent with H_2S off gassing.

Declining iron concentrations in the effluent point to a potential limiting factor for sulphate removal. The highest iron concentrations coincide with the highest rates of sulphate removal, and with the exceptions of reactors 7 and 8, all reactor effluent generally had iron concentrations at or below 0.1 mg/L after week 12 (Fig. 7.4). Reactor 8 (natural aquifer control) consistently had the highest iron concentrations in effluent samples; a significant finding given that no iron spheres were added to the reactor 8 mixture, where any iron above what is already present in influent water must have been derived from the creek sediment. The significantly lower sulphate removal in this reactor may partially explain this; however, reactor 4 does not have the similarly elevated iron concentrates, while having similar sulphate removal rates due to the lack of organic carbon amendments. Other metals such as arsenic, cadmium, copper, nickel, lead, and zinc can also take the place of iron for metal sulphide precipitation (Benner et al., 1997; Neculita et al., 2007); however, these metals were almost always below detection limits for the duration of the experiment. Low iron concentrations are most likely due to precipitation of iron oxides, which have been observed visually as well as by SEM. Calculation of saturation indices using PHREEQC demonstrated that effluent solutions over the entire duration of the experiment, in all reactors, were oversaturated with respect to goethite and hematite. This finding accounts for the low iron concentrations, as precipitation of iron oxides was geochemically favoured. Precipitation of iron oxides accounts for the dramatic increase in iron concentrations in post-experiment reactor materials. In reactor 1 and 5, the average iron concentration increase is 54%, in reactor 2 and 6 the average increase is 92%, in reactor 3 and 7 the average increase is 115%,

while in reactor 4 and 8, a small decline of 10% is the average change. Saturation index calculations also found that iron sulphides such as pyrite and mackinawite were highly under saturated in all effluent waters, and precipitation of these iron sulphides was not geochemically favoured. As a consequence of these findings, it appears that iron sulphide precipitation was not responsible for sulphate removal in any meaningful quantity. An additional source of iron precipitation may be as jarosite, which was also found to be slightly oversaturated in most reactor effluent samples, and may be responsible for some sulphate removal. See Appendix D for saturation index data.

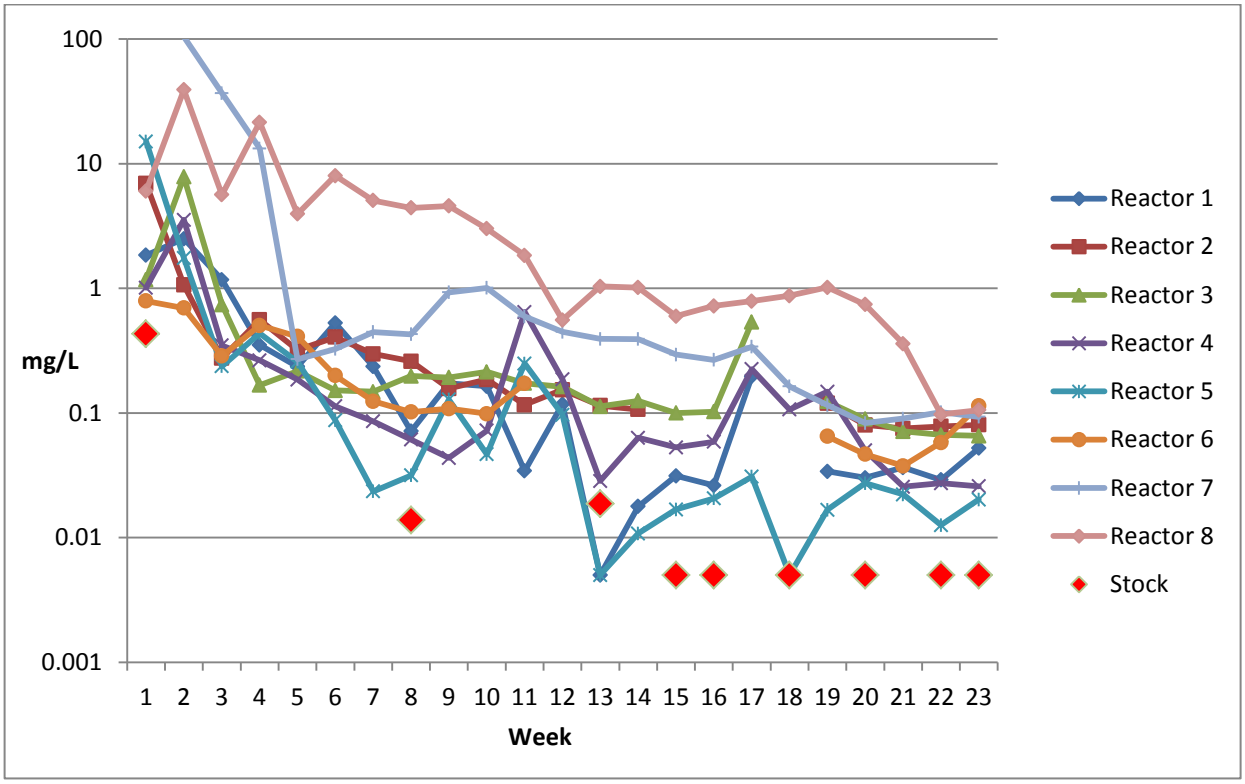

Figure 7.4: Iron concentration by week.

7.1.3 Nutrient Balance

One of the key goals of this study was the refinement of procedures for reactive material selection and determination of requirements for bacterial nutrition. Very few published studies have attempted to compare the availability of nutrients both before and after the operation of a

passive treatment system using natural organic materials to stimulate SRB. Comparing the concentrations of the key nutrients for microbial activity (carbon, nitrogen, and phosphorus) before and after operation of the reactors helps to refine requirements for organic materials. Complete data for nutrient concentrations in post experiment materials is available in Appendix D.

Carbon concentrations are generally lower in post experiment samples as compared to the original mixtures (Fig. 7.5). This result was expected given that organic carbon is required as an electron donor for bacterial sulphate reduction where it is converted to bicarbonate (Cocos et al., 2002; Neculita et al., 2007), and lost to effluent waters. A significant relationship is observed between sulphate removal percentages and the decrease in carbon content. Aside from a few outliers, the post-experiment samples are consistent in a relationship of approximately 2 mg/Kg gain in sulphur for each 1 mg/Kg loss of carbon. The carbon consumption may be related to a variety of bacterial processes, including sulphate reducers, iron oxidizers, and organic decomposers. The most effective reactors for sulphate removal were replicate reactors 3 and 7 (poultry manure and hay), and similarly these reactors had the greatest decline (52-64%) in carbon concentration. Reactors 2 and 6 (rabbit manure and leaf compost) were the second most effective for sulphate removal and carbon concentrations decreased by 24-36%. Reactors 1 and 5 (poultry manure and leaf compost) were the least effective organic amended reactors and had carbon content change in the range +6.9% to -43%. The control reactors 4 and 8 without added organic matter had carbon concentrations change by +3.1% to -32.4%. In the control reactors, no organic matter was added; however, it is likely that a limited amount of organic material was contained in the creek sediment. This relationship between sulphate removal and carbon loss provides support to a bacterial link for sulphate removal, given that higher rates of bacterial activity would result in greater consumption of organic carbon. With more than half of all carbon

lost in the most effective reactors, and an expectation that not all organic carbon will be available to bacteria, availability of organic carbon may have been a limiting factor in the later part of the experiments. This evidence also indicates that a greater mass of organic carbon would be required in order to sustain high rates of sulphate removal over a longer term treatment program.

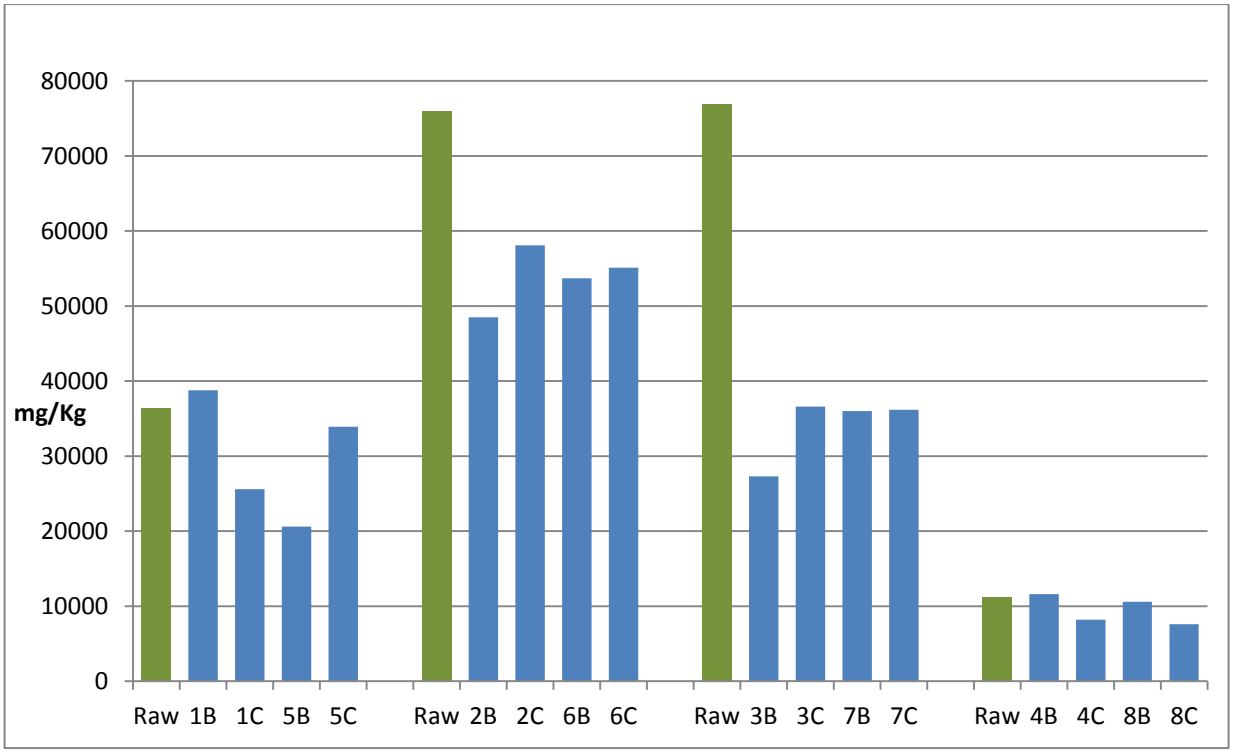

Figure 7.5: Changes in carbon concentrations from raw mixtures to post-experiment materials. Poultry manure and leaves in 1 and 5, sheep manure and leaves in 2 and 6, poultry manure and hay in 3 and 7, no organics added in 4 and 8.

Nitrogen is another important nutrient for microbial nutrition, with many publications citing a C:N ratio of 10:1 as ideal for the growth of bacteria such as SRB (Reinertson et al., 1984; Bechard et al., 1994; Prasad et al., 1999; Zagury et al., 2006). Similar trends in nitrogen loss are observed as those seen for carbon. The greatest decline in nitrogen concentration occurred in replicate reactors 3 and 7, where nitrogen decreased by 45 to 58% (Fig. 7.6). The most significant decline in nitrogen occurs in the same reactors which had the greatest declines in carbon content and effluent sulphate concentration, which further supports the expectation that

bacterial activity is related to sulphate removal. Reactor pairs 1 and 5, and 2 and 6, had intermediate levels of nitrogen loss, with losses in a range from 19 to 56% and 29 to 42%, respectively. Reactors 4 and 8 which did not contain added organic material had smaller changes in nitrogen concentration, ranging from a 17% gain in sample 4B to a 33% loss in sample 4C. The significant nitrogen loss in the most effective reactors for sulphate removal is consistent with the loss in carbon content, and provides further evidence that a greater mass of organic material would be required to support longer term testing. The loss of >50% of nitrogen also suggests that availability of nitrogen may have become an issue in the later stages of the reactor experiments within this study.

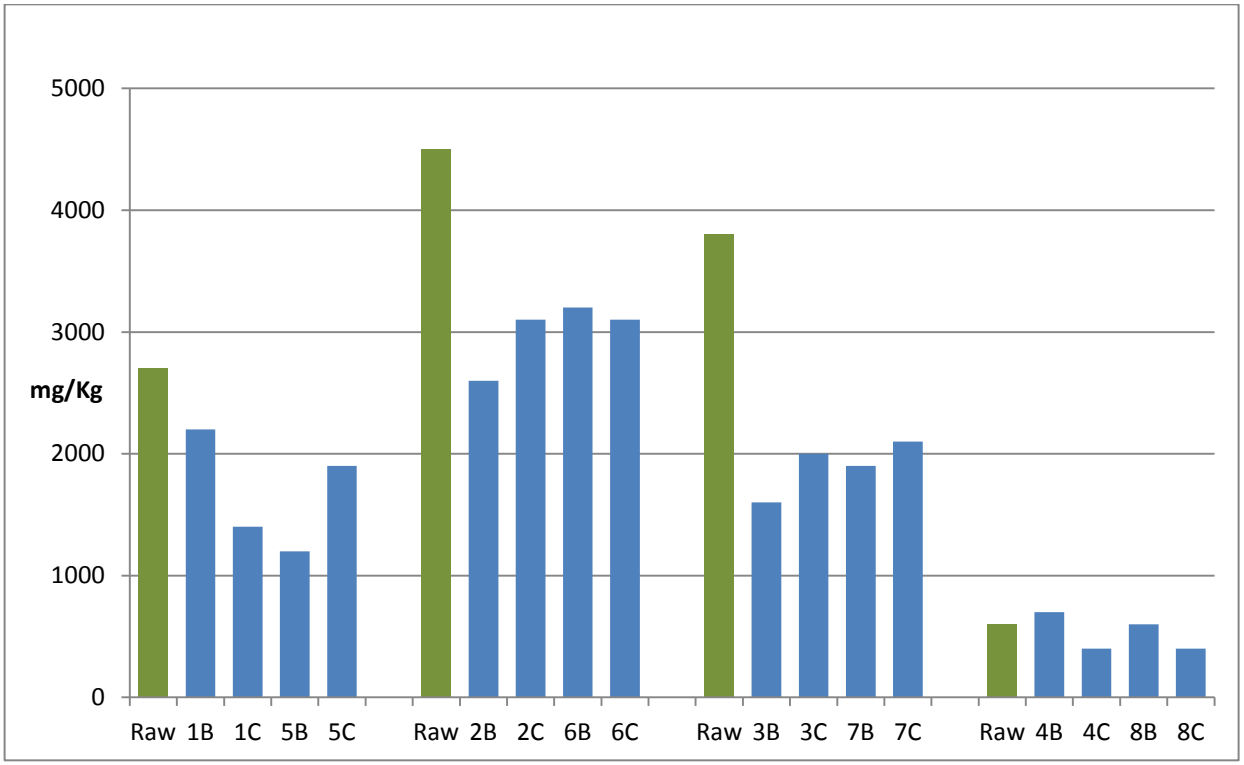

Figure 7.6: Changes in nitrogen concentrations from raw mixtures to post-experiment materials. Poultry manure and leaves in 1 and 5, sheep manure and leaves in 2 and 6, poultry manure and hay in 3 and 7, no organics added in 4 and 8.

Phosphorus is the final nutrient considered for supporting the growth and activity of SRB. A C:N:P ratio of 110:7:1 has been cited as important for supporting high rates of SRB activity

(Kuyucak and St-Germain, 1994; Cocos et al., 2002). The patterns of change in phosphorus content are consistent with those for both carbon and nitrogen; and the highest nutrient loss is linked to the highest rates of sulphate removal. The relationship between nutrient loss and sulphate removal is strong evidence for bacterial activity within the flow-through reactor experiments. The most significant phosphorus loss occurred in reactors 3 and 7, with a loss from 24-62% (Fig. 7.7). Reactors 1 and 5, and 2 and 6, had nearly identical ranges of phosphorus loss, with ranges from 16-49% and 17-50%, respectively. Finally the non-organic amended reactors 4 and 8 had phosphorus losses from 7-26%.

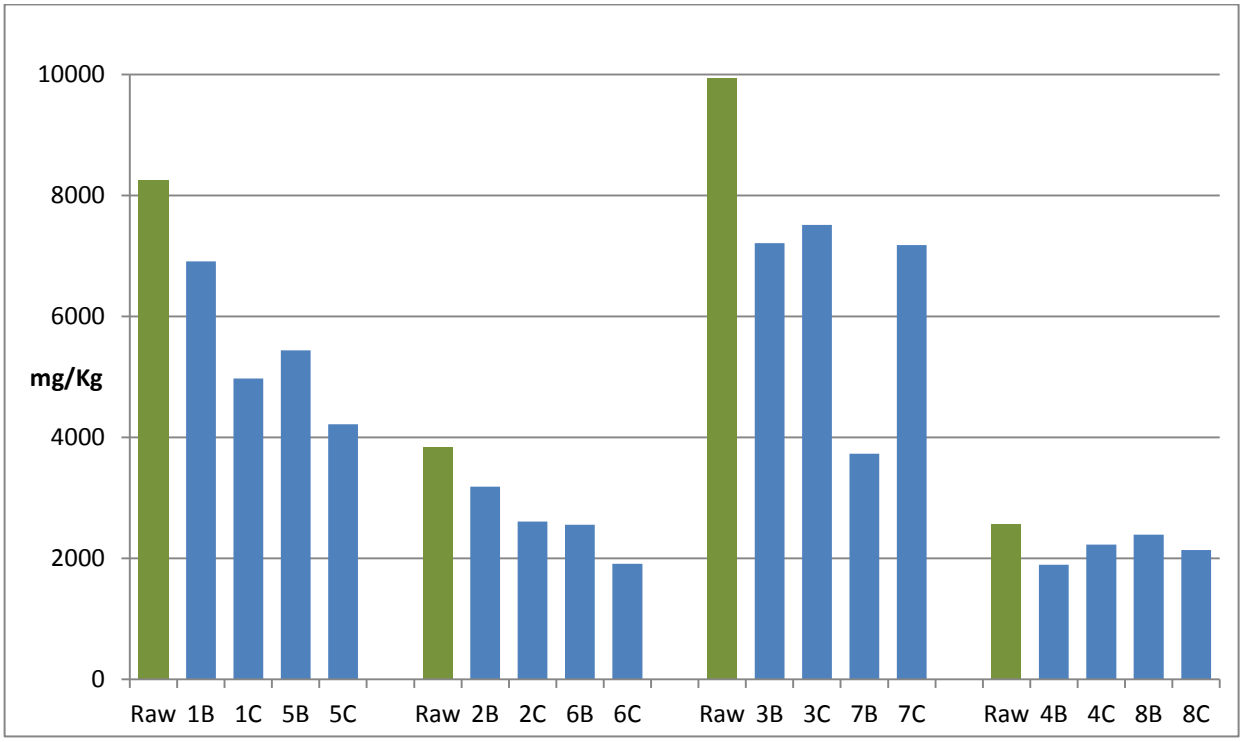

Figure 7.7: Changes in phosphorus concentrations from raw mixtures to post-experiment materials. Poultry manure and leaves in 1 and 5, sheep manure and leaves in 2 and 6, poultry manure and hay in 3 and 7, no organics added in 4 and 8.

7.1.4 Mechanisms of Sulphate Removal

The change in nutrient contents presented in section 7.1.3 is strong evidence for a connection between bacterial activity and sulphate removal. Consistently, carbon, nitrogen, and phosphorus demonstrated highest losses in reactors which had the greatest sulphate removal,

while the smallest losses occurred in reactors with the least sulphate removal. PHREEQC software was utilized in order to determine saturation indices for minerals which could be expected to precipitate from solution. The calculated saturation indices demonstrated that iron sulphides such as pyrite and mackinawite were highly under saturated in all effluent waters. Therefore, iron sulphide precipitation appears unlikely to be a relevant mechanism for sulphate removal. In contrast, sulphate minerals including barite, gypsum, and jarosite were determined to be at saturation or slightly oversaturated in most effluent water samples. Precipitation of these minerals was geochemically favoured, and precipitation of these sulphate minerals presents a plausible alternative mechanism for sulphate removal from solution. Biogenic barite precipitation is widely reported in marine environments (Klump et al., 2000; Torres et al., 2003; Torres-Crespo et al., 2015); however, given the low concentration of barite present in the mixture materials and influent water, it appears unlikely that barite could be a major sink for sulphate. In contrast, calcium is present at much higher concentrations, and precipitation of gypsum is consistent with 150-50 mg/L declines in calcium concentrations in effluent waters compared to influent water. Biomineralization of gypsum has been reported by Thompson and Ferris (1990) in mildly alkaline lake waters.

In the digestions of post experiment materials in organic amended reactors, iron concentrations were consistently higher than in the prepared mixtures, while in non-organic amended reactors the concentrations were slightly lower. The increase in iron values during the flow-through experiments was due to iron derived from the iron spheres, which were not included in the acid digestions. The fact that there was a significant increase in iron concentration in organic-amended reactors, but not in the non-organic reactors implies that iron oxidizing bacteria were stimulated by the presence of organic matter. The greatest iron increase (sample 7B) occurred in one of the top performing reactors for sulphate removal, while the

minimum increase in organic reactors (sample 5C) was in one of the poorest performing reactors. Reactors 2, 3, 6, and 7 all had higher concentrations of both iron and sulphur. Comparing the iron-sulphur relationship, it is found that on average, sulphur increases 1.88 mg/Kg for each 1 mg/Kg increase in iron. The rejection of the possibility of iron sulphide precipitation means this iron was not derived from iron sulphides. Increases in iron concentrations are most likely due to precipitation of iron oxides, which were found to be oversaturated in solution, and may be driven by iron oxidizing bacteria. Bacterially mediated iron oxidation can occur in aerobic or anaerobic environments, and anaerobic, non-light exposed, nitrate dependant oxidation of iron has been reported (Weber et al., 2006). Assuming sulphate mineral precipitation is the dominant mechanism for sulphate removal, a possible cause for the link between iron and sulphate removal could be jarosite precipitation. Jarosite is slightly oversaturated in most effluent water samples, and its chemical formula contains both iron and sulphate; consequently substantial precipitation of jarosite would result in high levels of both iron and sulphate deposition. However, based on visual observation and geochemical data, it is probable that jarosite only accounts for a limited portion of the deposited iron, with a majority in the form of iron oxides. The chemical formula for jarosite contains two molecules of sulphate and one molecule of iron; a ratio that is relatively close to the 1.88 S:Fe increase ratio reported above.

Over the duration of the experiment, measured values for ORP, or Eh, became increasingly negative; after initially starting near or slightly below zero, values reached a range between -200 mv and -300 mv by week 18 (Fig. 7.8). The one exception to this is reactor 8, which was consistently near zero for the duration of the experiment. Other than reactor 8, the conditions are consistent with those necessary for SRB activity, which are known to require an anaerobic, reducing environment with a redox potential lower than -100 mv (Postgate, 1984). A dramatic spike observed in reactor 6 at week 10 was due to an equipment failure that allowed

oxygen to enter the influent flow line. An Eh/pH diagram for the Fe-S-O-H system presenting the water chemistry of the top performing reactor pair (3 and 7) is presented in Figure 7.8. Data is presented for the initial composition at week 1, after initial acclimatization at week 5, mid-experiment at week 12, and final composition at week 23. Over the duration of the experiment the water was found to evolve towards a higher pH and lower Eh within the lower part of the Fe_2O_3 stability field, loosely following the slope of the phase boundary between Fe_2O_3 and FeS_2. This finding indicates that while conditions were suitable for SRB activity, the formation of iron oxides is chemically favoured over iron sulphides.

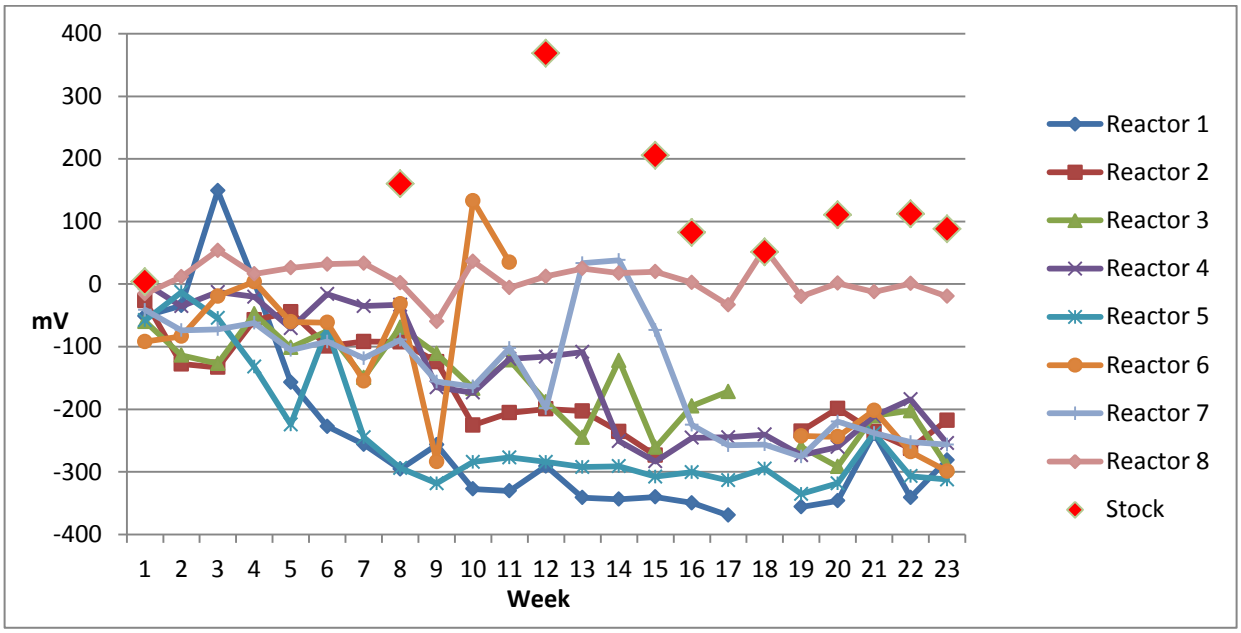

Figure 7.8: Variation in redox potential by week.

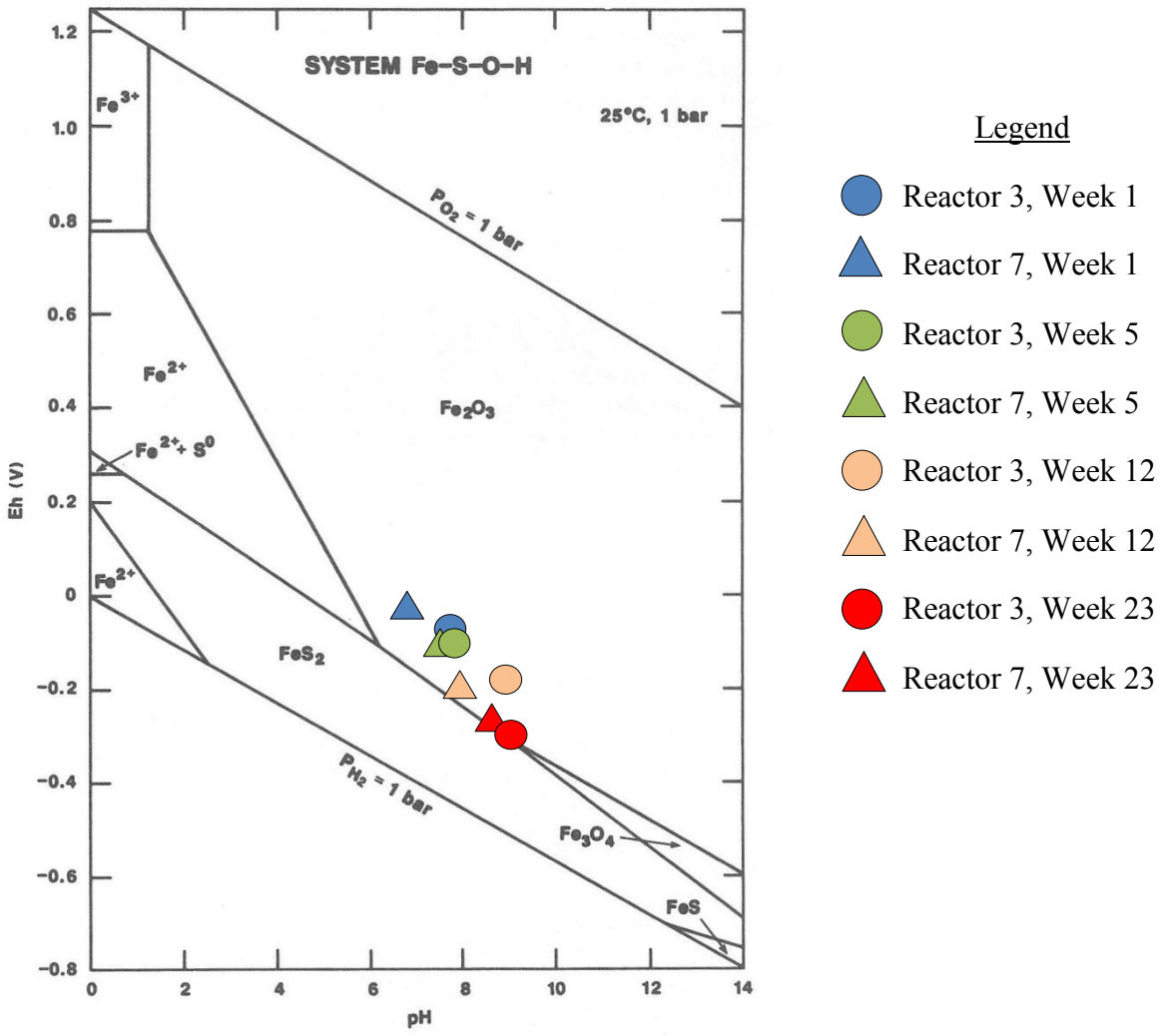

Figure 7.9: Eh/pH diagram for the Fe-S-O-H system at 25°C. Modified after Brookins (1988).

In Figure 7.10, the equivalent Eh/pH data for the study by Shankie (2011) is presented. In this Eh/pH diagram, the two best performing reactors for sulphate removal are plotted using the data for the same weeks as used in Figure 7.9 for the present study. These reactors are 1 and 5, which used a mixture of horse manure and wood chips. This diagram shows that the Eh/pH conditions were very similar between the two studies, with results initially plotting above the sulphide/oxide boundary, with an evolution towards higher pH and lower Eh towards the end of the experiment. In Shankie (2011), one data point (reactor 1, week 20) does plot within the sulphide field; however, at this point in the experiment sulphate removal was poor. During the

most effective weeks for sulphate removal, weeks 3 to 7, the values plot well within the oxide field, consistent with the present study. These results indicate that in both studies the conditions were suitable to support SRB, but did not support sulphide formation, although the conditions in Shankie (2011) may have been more supportive as the Eh/pH values plot closer to the sulphide/oxide boundary. This also indicates that the use of zero valent iron in the present study did not have substantial impacts upon the Eh/pH conditions within the flow-through reactors.

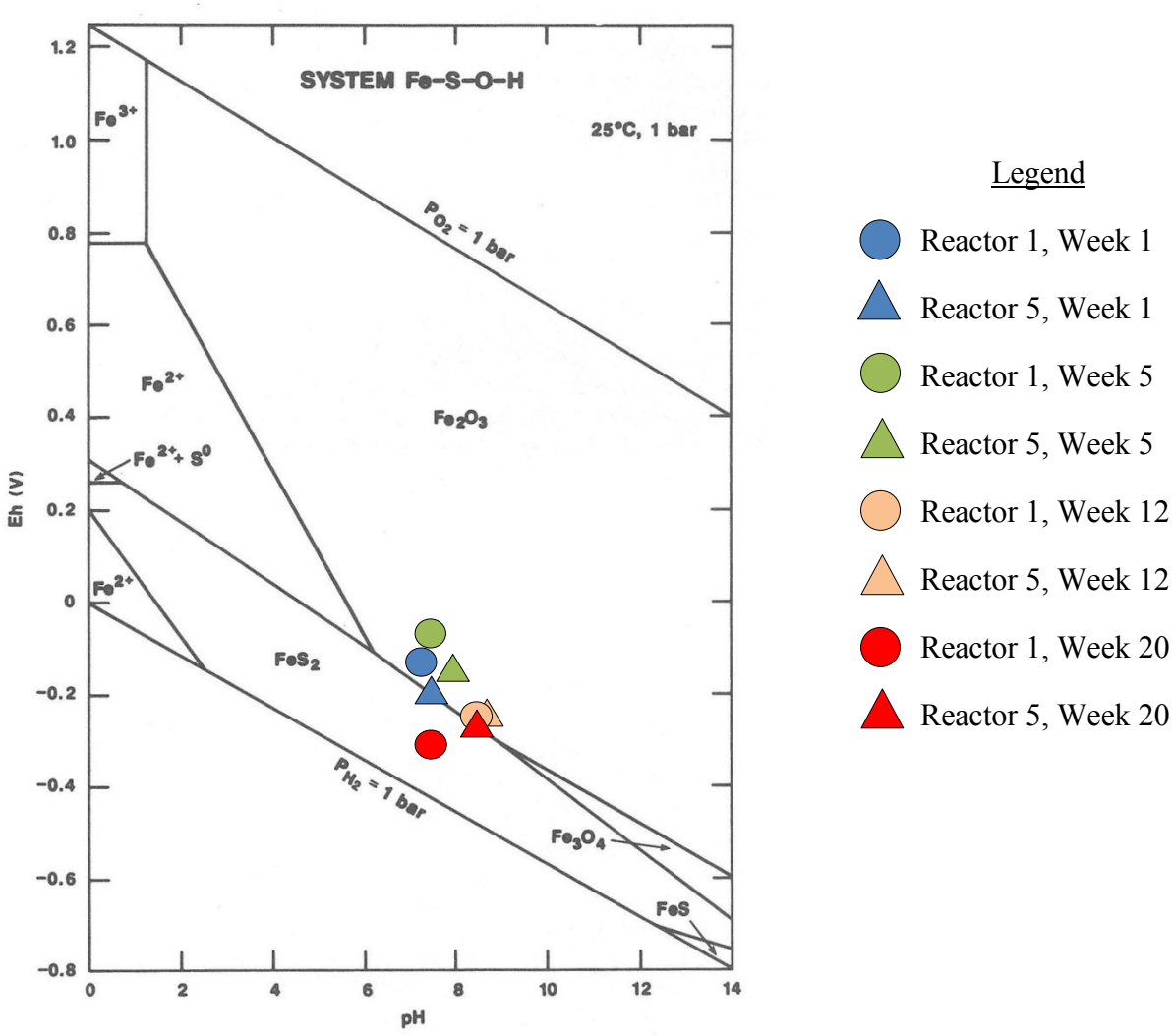

Figure 7.10: Eh/pH diagram for the Fe-S-O-H system at 25°C. Results from Shankie (2011). Modified after Brookins (1988).

The XRD results for the reactor materials were consistent with findings for the original mixtures, which were dominated by silica sand and creek sediment and in mineralogy by quartz and feldspar. No evidence for the formation of additional mineral species during reactor operation was found. XRD is limited to a minimum 2% abundance for detection, and it is possible that small amounts of minerals may have formed without being detected by XRD.

SEM analysis was consistent with creek sediment, silica sand, and organic matter. Fine iron spheres were detected and are probably mostly iron oxides, as the iron to sulphur ratio is 3.8:1. These structures could have also formed prior to the experiment. Larger sulphur rich structures were also located, as seen in Figure 6.29; sulphur and iron are present in a 1.67:1 ratio, which could potentially indicate a mixture of iron sulphides such as mackinawite (FeS) and pyrite (FeS_2), although the structure of the crystals more strongly resembles sulphate rosettes (A. Conly, personal communication). Because the work was conducted in a primarily qualitative manner, with only semi-quantitative data collected, it is not possible to make definitive determinations of specific mineral species.

The sequential extraction results do not appear to have been completely effective at targeting the intended phases. As presented in Tables 6.1 to 6.3, the final stage using 1.0 M nitric acid contained significantly higher concentrations for several parameters, including elements such as silicon (Fig. 7.12) which are not likely to constitute a sulphide phase. The sulphide phase appears to be very small based on the low sulphur concentrations present in the extract from stage six. Sulphur concentrations in stage six (Fig. 7.13) are less than 1% of iron concentrations (Fig. 7.11), which suggests that iron sulphide was not a significant source for the iron dissolved in this phase. Furthermore, most sulphur in the organic amended reactors was extracted during the first stage, a stage in which very little iron (2-5 ppm) was extracted.

Sulphur concentrations in the non-organic amended reactors (4 and 8) are presented in Figure 7.14, and significantly less sulphur was extracted in the first step, totalling 36% of total sulphur in reactor 4 (ZVI amended) and 24% in reactor 8 (creek sediment and silica sand only). In the organic amended reactors the first step extracted 44 to 54% of total sulphur; in the other steps the relative proportions of sulphur are similar between organic and non-organic amended reactors. Sulphur from the first stage is believed to represent sulphate salts which precipitated from sulphate rich waters during the drying process following experiment completion. However, the significant variation between organic and non-organic amended reactors implies that salts from the drying process represent only a portion of the sulphur. The higher sulphur in the organic amended reactors implies that a significant portion of this sulphur is derived from sulphate minerals that formed due to bacterial processes which were stimulated by the presence of organic materials.

In the final step of the sequential extractions the high concentrations of iron and silicon combined with low concentrations of sulphur indicates that earlier stages failed to entirely remove their target phases, and that the final step dissolved non-sulphide phases that should have been removed in the previous steps. The high iron in stage six is likely indicative of iron oxides, which is supported by Eh/pH data as well as visual observation of rust discolouration on post flow-through experiment materials. These results imply that very little iron sulphides formed, although it is not clear that complete dissolution of iron sulphides (if present) was achieved.

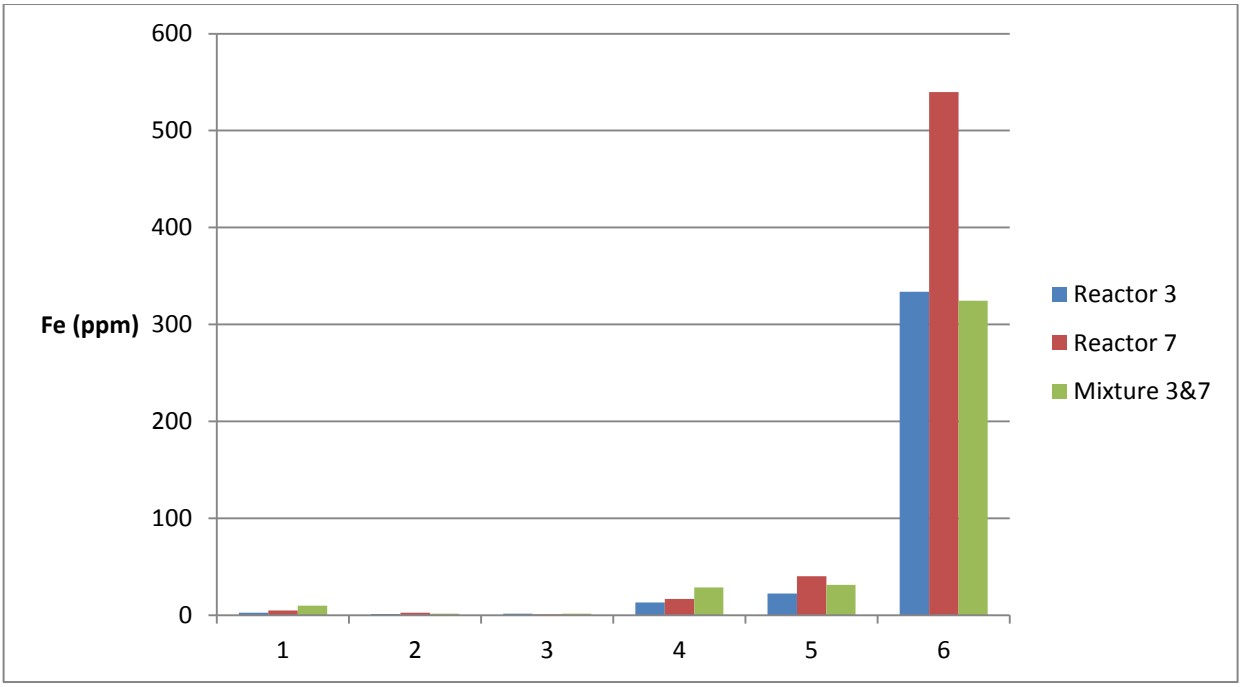

Figure 7.11: Iron concentrations in sequential extractions for reactors 3 and 7. Step 1 targeted salt precipitates; step 2 the soluble/ exchangeable fraction; step 3 adsorbed metals; step 4 organically bound metals; step 5 carbonates, and step 6 sulphides. Step 6 actually removed silicates and iron oxides.

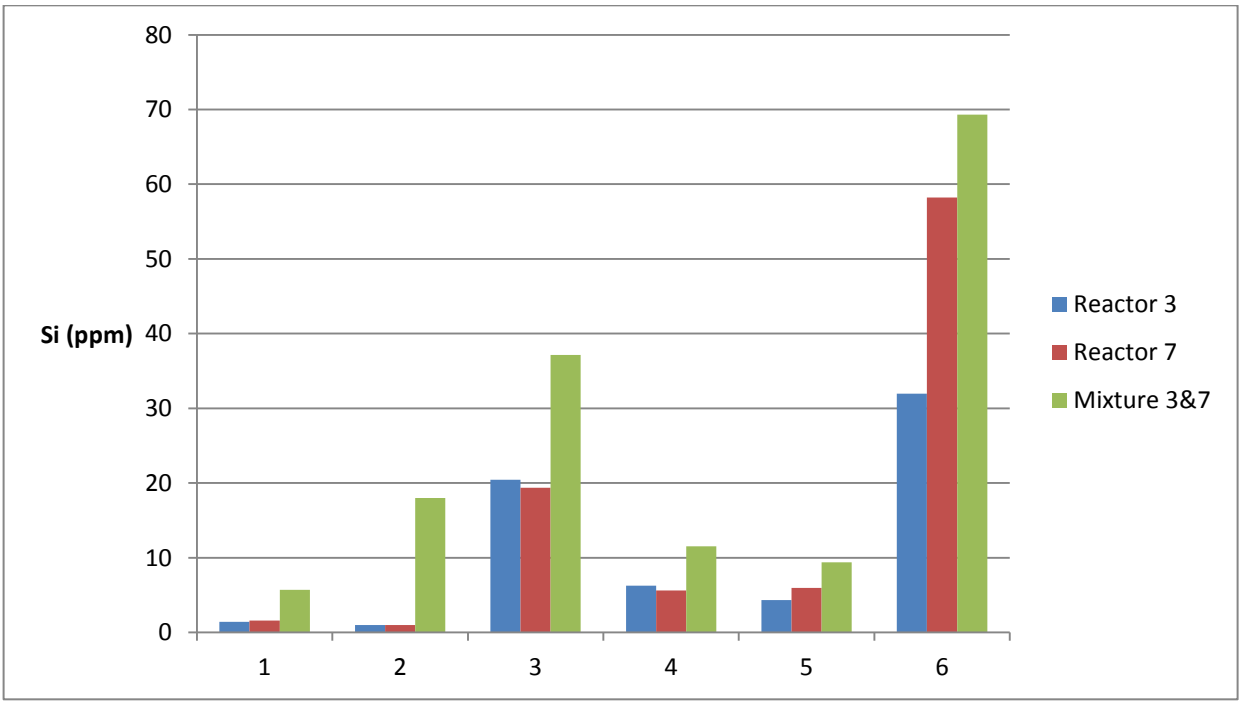

Figure 7.12: Silicon concentrations in sequential extractions for reactors 3 and 7. Step 1 targeted salt precipitates; step 2 the soluble/ exchangeable fraction; step 3 adsorbed metals; step 4 organically bound metals; step 5 carbonates, and step 6 sulphides. Step 6 actually removed silicates and iron oxides.

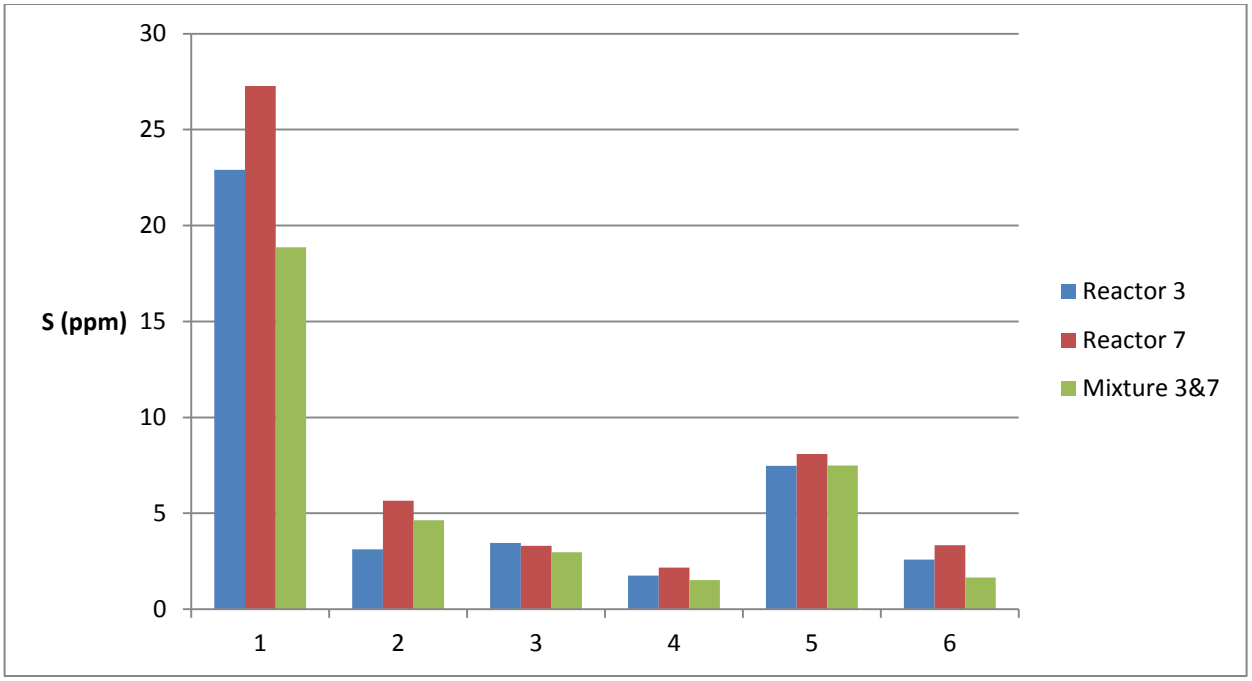

Figure 7.13: Sulphur concentrations in sequential extractions for reactors 3 and 7. Step 1 targeted salt precipitates; step 2 the soluble/ exchangeable fraction; step 3 adsorbed metals; step 4 organically bound metals; step 5 carbonates, and step 6 sulphides. Step 6 actually removed silicates and iron oxides.

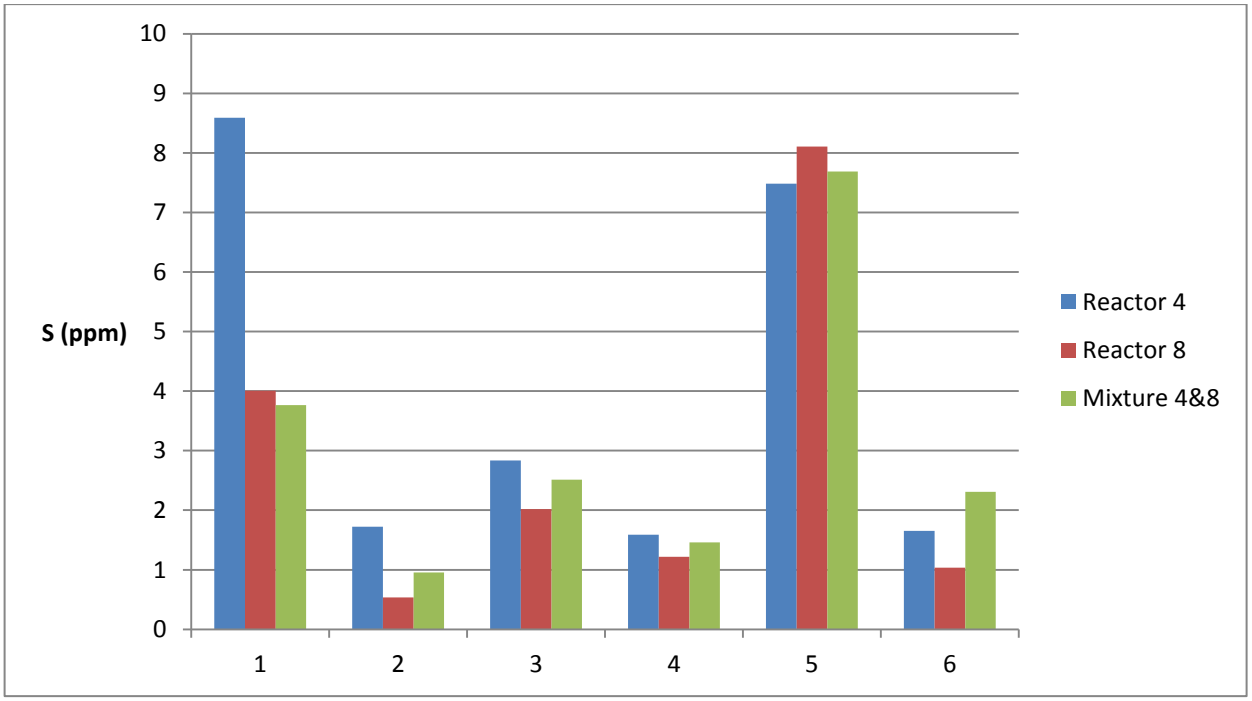

Figure 7.14: Sulphur concentrations in sequential extractions for reactors 4 and 8. Step 1 targeted salt precipitates; step 2 the soluble/ exchangeable fraction; step 3 adsorbed metals; step 4 organically bound metals; step 5 carbonates, and step 6 sulphides. Step 6 actually removed silicates and iron oxides.

A significant problem with the sequential extraction results is that it appears that the majority of sulphur was not dissolved during any stage of the sequential extractions. Sulphur concentrations in post-experiment samples assessed by the sequential extraction procedure produced values only slightly greater than the concentration of sulphur in the pre-experiment mixtures, up to a maximum 33% increase. This result is in disagreement with the up to 1,549% increases in sulphur concentrations in post-experiment materials found by acid digestions (Fig. 7.15). As well, comparison of the CNS analysis of the materials before and after the sequential extraction procedure confirms that a significant mass of sulphur remained following the sequential extraction. Only 7 to 15% of the original mass of material was consumed in the sequential extractions, and of this remaining residual material, maximum sulphur content loss of 35% is observed (Table 7.3). In control reactor 8, the sulphur loss was -79%, meaning that the sulphur in this reactor (which comprised a much smaller portion than in the other reactors) was relatively immobile compared to other phases, and as a result comprises a greater % of the total proportion after these other phases were removed. This result means that while the sequential extractions correctly imply a significant iron phase that is not associated with sulphur, the majority of both iron and sulphur were not dissolved during the sequential extraction procedure. As measured by acid digestion, in samples 3B, 3C, 7B, and 7C, the iron to sulphur ratios are 2.56:1, 3.50:1, 3.17:1, and 2.38:1, respectively. While these ratios are not indicative of dominant iron sulphide phases, which would require 1:1 or 1:2 ratios, they do indicate that the concentrations of these phases is much closer than indicated by the sequential extractions, particularly due to missing sulphur in the sequential extraction results.

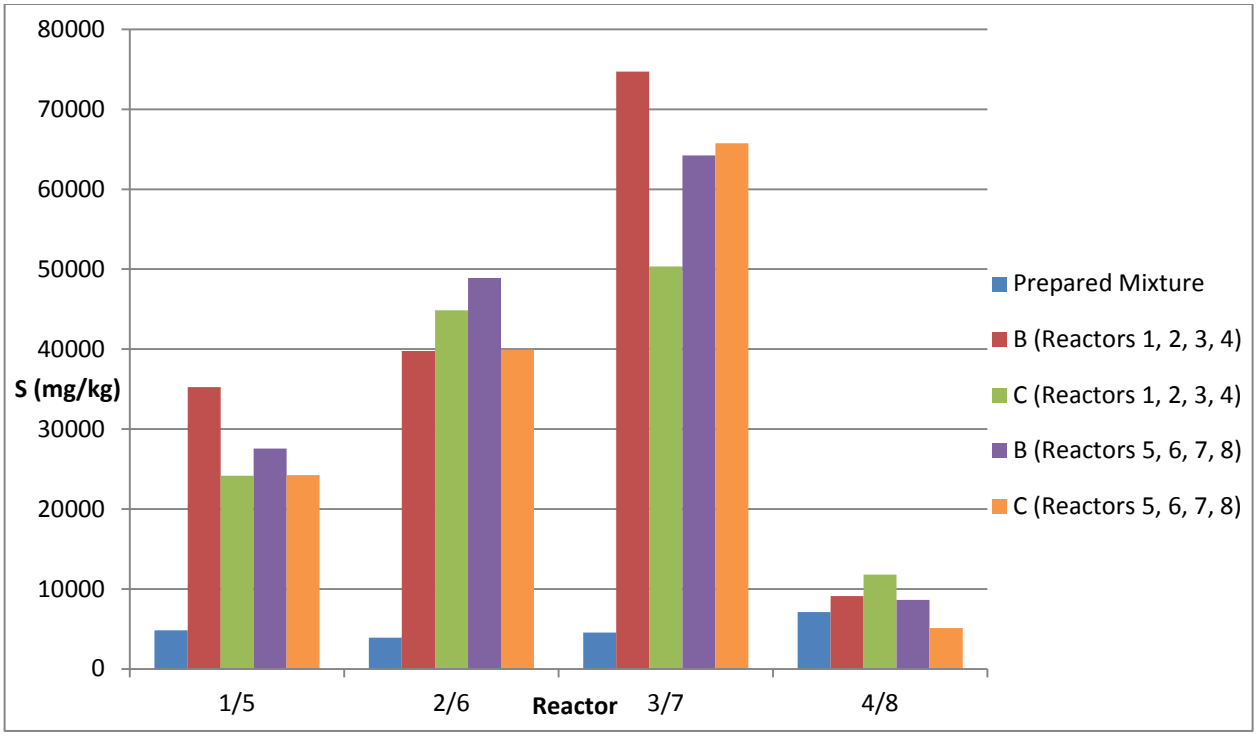

Figure 7.15: Sulphur concentrations in post flow-through reactor materials and prepared mixtures.

Table 7.3: Comparison of CNS results before and after sequential extraction.

Mix type	Post Flow-Through Materials					Post Sequential Materials				% Loss of S
	Sample	N%	C%	S%		Sample	N%	C%	S%	
organic	1A	0.190	3.330	0.831		1A	0.15	1.99	0.542	34.78
organic	2B	0.260	4.850	0.826		2B	0.30	4.13	0.627	24.09
organic	3A	0.120	2.330	0.865		3A	0.15	2.11	0.672	22.31
organic	3C	0.200	3.660	0.946		3C	0.30	3.36	1.026	-8.46
control	4A	0.060	1.350	0.266		4A	0.09	0.90	0.228	14.29
organic	5A	0.140	2.570	0.531		5A	0.22	2.07	0.359	32.39
organic	6B	0.320	5.370	1.074		6B	0.34	4.83	0.831	22.63
organic	7A	0.150	3.110	0.967		7A	0.17	2.84	0.710	26.58
control	8B	0.060	1.060	0.087		8B	0.08	0.69	0.156	-79.31

The nature of the missing sulphur phase is not entirely clear. No sulphur bearing phases were detected by XRD, while SEM found indications of both iron oxides and an iron-sulphur phase. The concentration of sulphur detected by ICP-AES (5-8% of total mass in reactors 3 and 7) proves that there is a significant sulphur phase that was not detected by XRD. However, if this

sulphur is contained in multiple phases it could fall below XRD detection limits, or it could also evade detection if the material is not sufficiently crystalline. In order to not be broken down by the nitric acid step in the sequential extraction, the sulphur bearing phase would have to be relatively immobile. Sulphur at some stage may have combined with organic material to form organic sulphur complexes. Such organic sulphur complexes are relatively immobile, and less susceptible to dissolution (Scherer, 2009). The sulphur phase is also found to have the highest concentrations in the reactors which achieved the highest levels of sulphate removal, confirming a link between sulphate removal and sulphur precipitation. The very high sulphate removal achieved in these reactors which were designed to stimulate the activity of SRB leads to the assumption that organic matter was successful in stimulating bacterial process which removed or favoured reactions removing sulphate from solution. The Eh/pH plots (Figs. 7.3 and 7.9) indicate that conditions were not sufficiently reducing in order to achieve iron sulphide formation.

Alternative mechanisms of sulphate removal such as adsorption of sulphates do not appear to present a viable alternative for the high levels of sulphate removal. The levels of sulphate removal achieved here have rarely been duplicated by other researchers, and no efforts were made to increase adsorption rates relative to other research. If adsorption was the primary mechanism, higher rates of sulphate removal would likely have been observed in the non-organic amended reactors as well. Multiple lines of evidence have demonstrated that iron sulphide precipitation did not occur as intended in the experimental design. Instead, organic matter stimulated iron oxidizing bacteria as well as bacteria which supported sulphate mineral precipitation. In reactors with high levels of sulphate removal, jarosite appears to have been a significant precipitate, and accounts for a connection between high levels of iron and sulphur precipitation.

In comparison to other published studies which have utilized a mixture of organic carbon and zero valent iron to remove sulphate, it is unclear why sulphate reducing conditions were not achieved. In these studies, the authors consistently concluded that sulphate reducing bacteria were the responsible mechanism for sulphate removal (Phillips et al., 2000; Gandhi et al., 2001; Wilkin et al., 2002). The primary problem appears to be the Eh/pH relationship, in which at a neutral pH, the solution was not significantly reducing to support the stability of sulphides. This is also represented in the saturation index calculations, in which iron sulphides such as pyrite and mackinawite were highly under saturated. In several other studies, e.g. Guo and Blowes, 2009; Ludwig et al., 2009; the pH was lower, and the sloping nature of the oxide/sulphide stability field boundary (Fig. 7.9) resulted in conditions supportive of sulphide stability. Decomposition of organic matter and emplacement of zero valent iron have both been cited as supportive of strongly reducing conditions (Wilkin et al., 2002) however, in the current study these do not appear to have been sufficient. Future work in this area will need to investigate how to produce more strongly reducing conditions (more negative Eh) in a neutral pH environment.

7.2 Evaluation of Reactor Effluent Relative to the Natural Environment

An overall goal of this study was to find methods for passive remediation of contaminated water from the Steep Rock site, near Atikokan, Ontario. In order to assess the effectiveness of the work completed here, the water quality in treated effluent can be compared to natural waters in the Atikokan area. The Piper diagrams (Figs. 7.16-7.18) illustrate the compositions of five regional water samples, the eight reactor samples, and the contaminated water. Three sets of Piper diagrams are presented, utilizing reactor effluent data from weeks 5, 10, and 20, to give perspective of the relative effectiveness of the reactors at different levels of performance. The five regional water samples (black circles) plot very closely together, as calcium type waters on the cation plot and as bicarbonate type waters on the anion plot. The

influent contaminated mine water plots as sulphate type water on the anion plot, while plotting as a calcium bearing magnesium type water on the cation plot due to the higher proportion of calcium over sodium and potassium, and a significantly higher magnesium concentration than the regional water samples.

In the week five diagram (Fig. 7.16), the organic amended effluent waters plot relatively close to the regional water samples on the anion and combined plots due to the significantly reduced sulphate content. On the cation plot the effluent waters plot close to the influent water as magnesium type waters given that magnesium remains high, although reactor 3 actually plots above the influent water due to a drop in the calcium concentration. Reactors 4 and 8 which did not have added organic material plot very close to the influent water, as the water has not been substantially remediated. These plots illustrate that the water quality has dramatically improved following the reactor treatments, and is much closer to the regional water samples than the influent contaminated water.

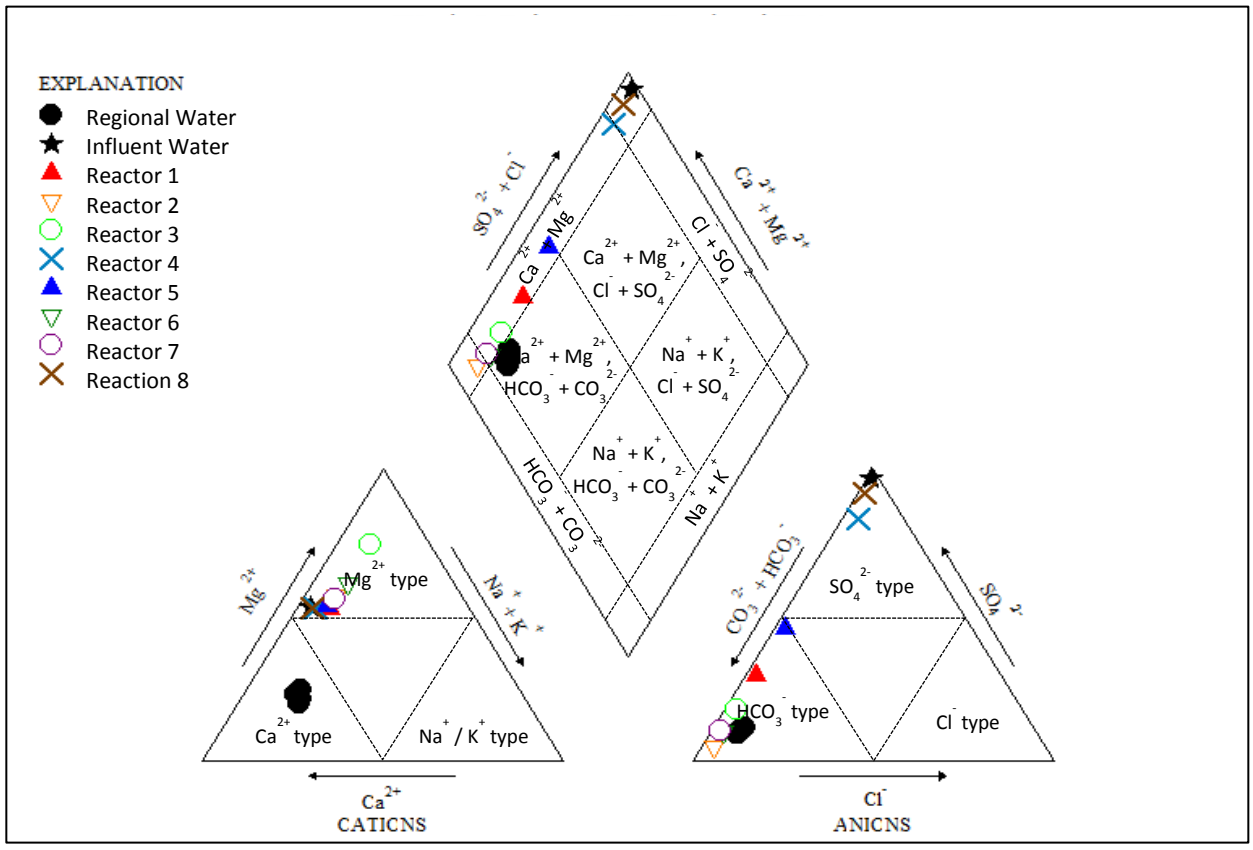

Figure 7.16: Piper diagram comparing reactor effluent waters, week 5, and regional waters. Regional water data from A. Conly and P. Lee (2010), unpublished data.

In week 10, the ternary plots within the Piper diagram are similar to week 5; however, the organic amended effluent waters have moved upwards on the anion plot into sulphate type waters, and have moved upwards within the calcium/magnesium field on the combined plot due to the increasing sulphate concentrations (Fig. 7.17). The cation plot is unchanged compared to week 5, with the exception of reactor 6 rising towards the top of the plot due to a decline in calcium.

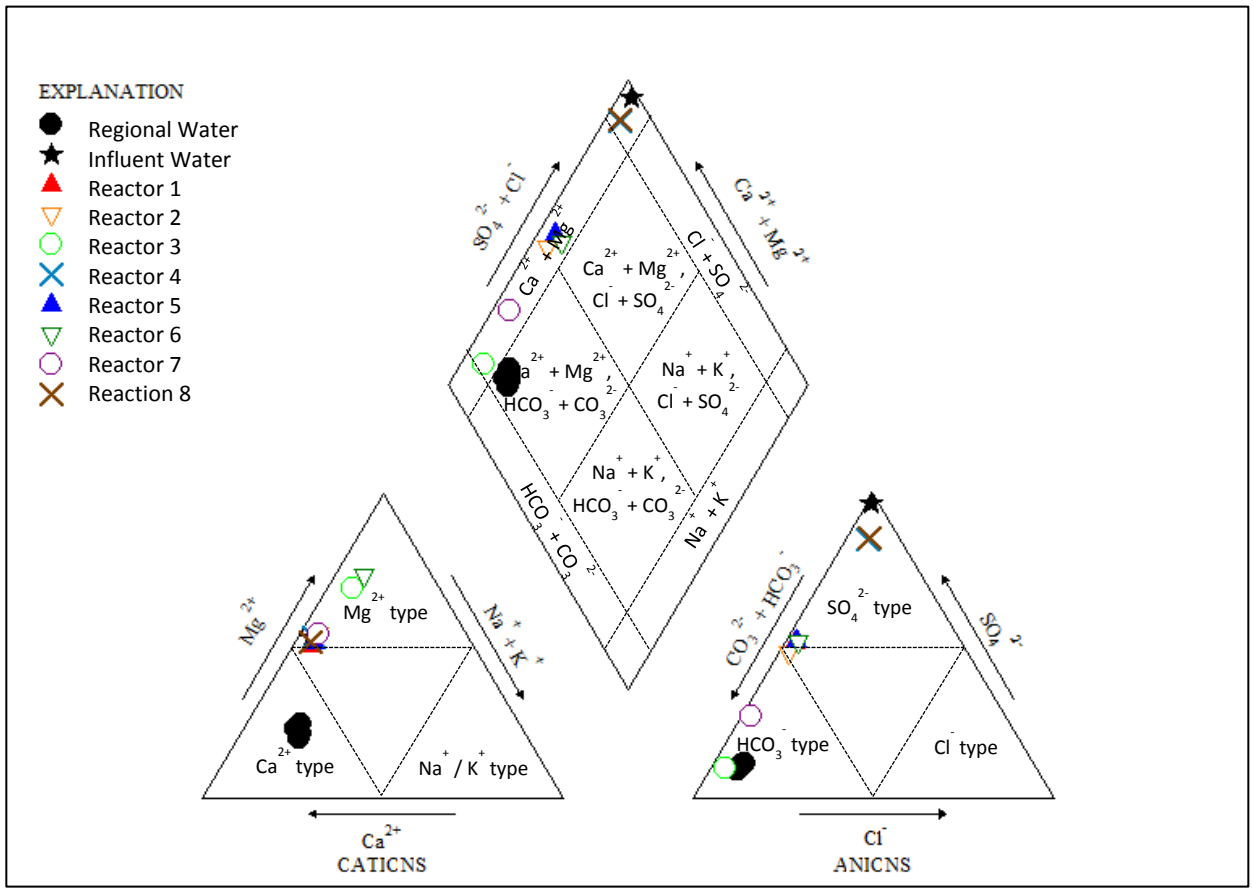

Figure 7.17: Piper diagram comparing reactor effluent waters, week 10, and regional waters. Regional water data from A. Conly and P. Lee (2010), unpublished data.

At week 20, the organic amended effluent waters have returned to plot much closer to the influent water (Fig. 7.18), while the reactors without added organic material show little change from the previous diagrams. The greater sulphate concentrations are largely responsible for the movement of the reactors upwards toward sulphate dominant fields on the anion and combined plots, while the cation plot is largely unchanged. These Piper diagrams illustrate that the reactor experiments were successful in improving water quality to levels much more comparable to local natural waters present in the general area of the study site, at least during periods of high sulphate removal. Sulphate is the primary control on the position within the ternary plots, while consistently high calcium and magnesium concentrations are also relevant factors.

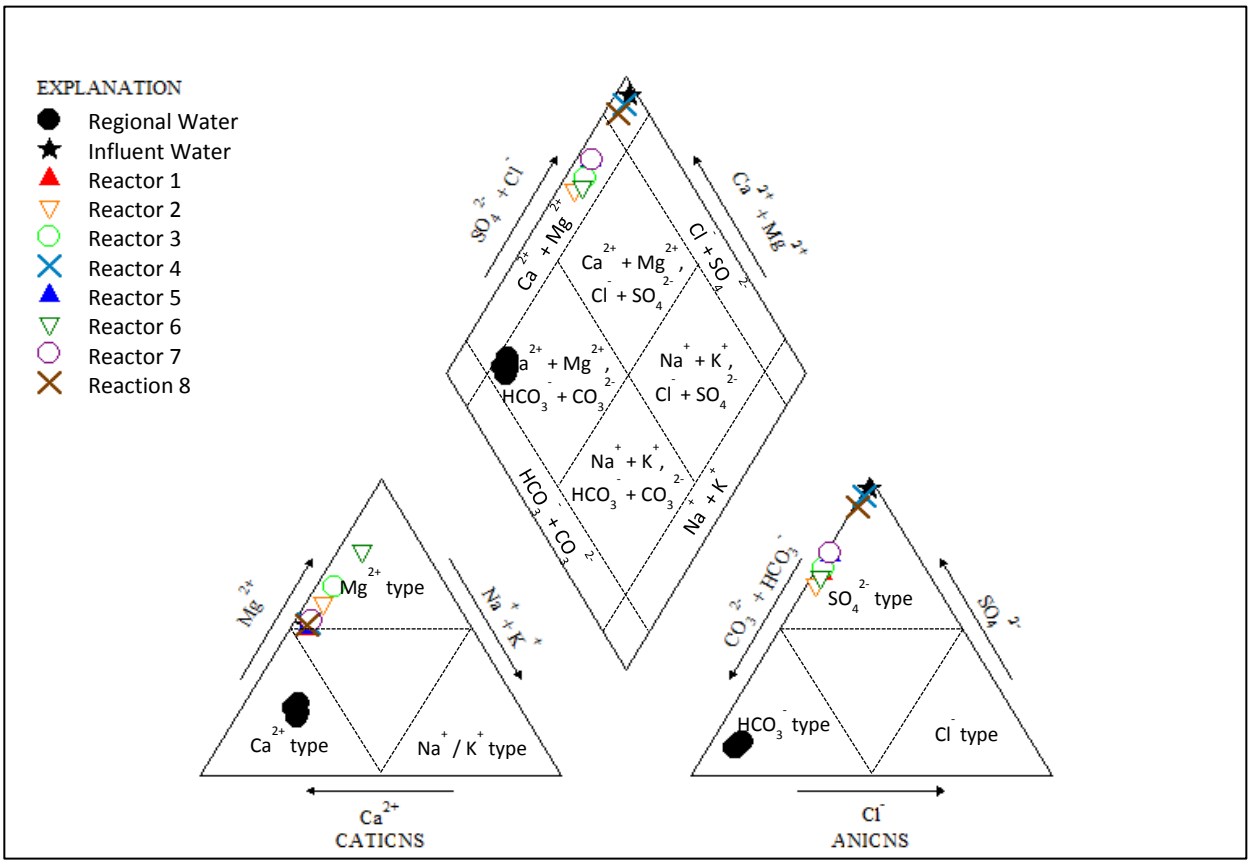

Figure 7.18: Piper diagram comparing reactor effluent waters, week 20, and regional waters. Regional water data from A. Conly and P. Lee (2010), unpublished data.

The reactor experiments were somewhat less successful in producing water with similar alkalinity and pH conditions to local waters (Table 7.3). Alkalinity is dramatically higher than local waters, with concentrations ten to thirty times the values measured in regional water samples. Effluent pH values were also notably higher, with values in the most effective reactor for sulphate removal, reactor 3, approaching a pH of 9, compared to regional waters in with pH values from 6.5 to 6.9.

Table 7.4: Alkalinity and pH of influent, effluent, and regional water samples. Regional water data from A. Conly and P. Lee (2010), unpublished data.

Water Source	Alkalinity (mg/L $CaCO_3$)	pH
Influent	50	7.91
Reactor 1 Effluent (Week 10)	600	7.93
Reactor 2 Effluent (Week 10)	636.6	8.43
Reactor 3 Effluent (Week 10)	795.9	8.92
Reactor 4 Effluent (Week 10)	149.4	8.40
South Marmion Lake	36.7	6.88
Raft Lake Dam - North	15.4	6.56
Raft Lake Dam - South	25.5	6.70
Perch Lake	17.7	6.57
Finlayson Lake	16.1	6.64

Chapter 8: Summary and Conclusions

A thorough analysis of the life-cycle of this lab-scale PRB system has permitted significant insight into the development of effective reactive mixture selection, the evolution of reactor effluents over time, and the consequent changes in composition of materials after experiment operation. This provides improved reactive mixture selection priorities in order to maximize sulphate removal rates, and can aid in the further refinement of PRB technology. Furthermore, this passive treatment system and the tested reactive mixtures have demonstrated considerable promise for sulphate removal from neutral pH, metal-poor mine waters. Despite the high sulphate removal performance of this system; the mechanisms of sulphate removal appear to be different from the design intention, with bacterial sulphate reduction replaced by biogenically driven sulphate mineral precipitation. It appears that sulphate was removed from solution via precipitation of sulphate minerals, such as gypsum, jarosite, and possibly to a limited extent, barite. Iron produced by the ZVI spheres was largely converted to iron oxides, while in the most highly effective reactors, higher iron concentrations are observed, and this may be attributable to jarosite precipitation.

In the process for determining ideal mixture substrates, combinations, and final mixture proportions; the concentrations, availability, and proportions of nutrients were important considerations. The accuracy and effectiveness of this approach has been assessed against final nutrient concentrations and the relative sulphate removal effectiveness of each reactor. A variety of tools were utilized to assess the potential substrates, including C:N ratio, C:N:P ratio, relative biodegradability via EAS testing and the relative change in nutrient concentrations following EAS testing. The targeted C:N ratio of 10 was only closely matched by poultry manure, with a ratio of 11, while leaves were relatively close at 18.2. Poultry manure was the closest substrate to achieving the desired C:N:P ratio of 110:7:1, at 1772:160:1, while all other substrates were much

worse, with sheep manure at 7730:325:1, hay at 16183:394:1, and leaves at 17869:980:1. Regarding the relative biodegradability of each substrate, poultry manure was found to be the most readily degradable in the EAS testing, with 71% of the original mass lost, while leaves, hay, and sheep lost 37%, 35%, and 29%, respectively. The remaining material following EAS testing was assessed to determine if certain nutrients were more or less mobile. The poultry manure lost the greatest portion of its phosphorus fraction, with a 93% phosphorus loss; a proportion much greater than the overall mass loss, indicating that phosphorus is highly available for biodegradation. Sheep manure and hay lost 82% of their phosphorus content, indicating that phosphorus is highly mobile in these substrates as well. Leaf compost lost 78%, indicating that phosphorus is still highly mobile, but not to the same extent as in the other substrates.

Reactors 3 and 7 were the most effective for sulphate removal, and utilized a mixture of poultry manure and hay. These reactors were found to have the highest sulphur concentrations in post-experiment materials, confirming a connection between the amount of sulphate removal and the amount of sulphur deposition. This result supports the substrate testing procedure for the manures, as poultry was easily the highest scoring candidate substrate and was consequently used in two pairs of flow-through reactors. Poultry manure was also used in reactors 1 and 5, which exhibited much poorer sulphate removal effectiveness. However, reactors 3 and 7 used hay as the plant-based substrate, while reactors 1 and 5 used leaf compost. The significant difference in performance between these reactor pairs indicates that hay was considerably more effective than leaf compost in promoting sulphate removal. Results were mixed in the substrate testing, with no clear expectation of either hay or leaf compost performing better. The tests in which hay performed better than leaf compost were the C:N:P ratio and the proportion of phosphorus lost during EAS testing (and therefore assumed bioavailability of phosphorus). The higher performance of the mixture utilizing hay indicates that phosphorus is a highly important

component in substrate selection, and that phosphorus content and availability should be a significant factor in substrate selection procedures for similar systems.

The balance of available nutrients is an important component of this study in order to ensure that the availability of nutrients is not a limiting factor for sulphate removal. The most effective reactors for sulphate removal were replicate reactors 3 and 7, and these reactors had the greatest decline (52-64%) in carbon concentration. Similarly to carbon, the greatest decline in nitrogen concentration occurred in replicate reactors 3 and 7, where nitrogen decreased by 45-58%. For phosphorus the pattern is maintained, with the most significant phosphorus loss occurring in reactors 3 and 7, with a loss from 24-62%. The relationship between carbon consumption and sulphate removal is strong evidence for a bacterial driven reaction leading to sulphate mineral precipitation. It is unknown how much of the remaining organic material is readily available to bacteria; however, such a substantial decline requires consideration of a lack of available organic matter as a major cause of the decline in reactor performance. Additionally, this level of carbon, nitrogen, and phosphorus loss indicates that a significantly greater % of the total reactive mixture mass would need to be comprised of organic material to support bacterial activity in a longer term field PRB.

A major problem preventing the intended removal of sulphur as iron sulphide precipitates may have been the Eh/pH relationship. While conditions were sufficiently reducing to support the activity of SRB, most effluent water samples indicate conditions above the sulphide/sulphate boundary, suggesting that sulphides may not have been stable and could have been converted back to sulphate. Additionally, saturation index calculations indicated that iron sulphides were strongly under saturated in effluent waters. Lower values for either Eh or pH would have resulted in conditions that favour sulphide stability. Alternatively, the availability of metals could also be

a contributing factor to declining performance. Aqueous sulphide produced by SRB will only be removed if sufficient divalent metals are available for it to react and precipitate with. The highest iron concentrations coincide with the highest rates of sulphate removal, and with the exceptions of reactors 7 and 8, all reactor effluent generally had iron concentrations at or below 0.1 mg/L after week 12. The mass of iron does not appear to have been a factor, as the iron spheres did not demonstrate substantial degradation. Using finer iron material (such is iron filings) could be an effective way to increase reactivity via increased surface area. Armouring and surface oxidation of the iron is a problem, as the iron spheres were observed to be covered in oxidation products following experiment completion. The development of preferential flow channels is another common problem impacting PRB performance.

The effectiveness of the flow-through reactor system studied here demonstrates an effective experimental design and rationale for reactive substrate selection on the basis of sulphate removal. However, the system was ineffective at reducing sulphate to iron sulphide precipitates, and instead precipitated sulphate minerals; probably primarily gypsum and jarosite, with possibly limited amounts of barite. These minerals are at greater risk of re-mobilization in the future, and may not present a viable solution for a long term, field-scale PRB. Comparison of effluent waters to natural waters in the area of the study site has demonstrated that at peak treatment effectiveness, effluent water compositions were much closer in composition to natural waters. In particular, the ability of reactors 3 and 7 to maintain sulphate removal at levels greater than 80% for 14 weeks is a significant achievement compared to similar systems previously constructed by other researchers. This result presents the combined use of poultry manure and hay as reactive organic substrates to be highly effective materials for the removal of sulphate. Further improvements of similar PRB systems will need to address the longevity problems, and assess the impact of increasing the mass of organic substrates. If improvements can be made to

sustain high rates of sulphate removal over a period of years, such a design could present a viable treatment system for removal of sulphate in field settings. Such a development would offer a valuable alternative to capital intensive chemical treatment plants presently in operation, particularly at remote, abandoned mine sites with limited resources available. This study utilized a relatively small mass of organic matter, and greater masses should be tested to determine if nutrient loss was a critical factor in the declining sulphate removal rates. As well, ensuring a constant flow rate over time without interruption from equipment problems over time is critical to ensure the validity of the results. Most critically, further studies will need to find methods to create more strongly reducing conditions supportive of iron sulphide stability, in order to ensure that the primary sulphur sink is a stable, immobile form such as pyrite, rather than sulphate minerals which are at greater risk of re-mobilization.

References

Akcil, A., and Koldas, S. 2006. Acid Mine Drainage (AMD): causes, treatment and case studies. Journal of Cleaner Production. Vol. 14, pp. 1139-1145.

Bartzas, G., and Komnitsas, K. 2010. Solid phase studies and geochemical modelling of low-cost permeable reactive barriers. Journal of Hazardous Materials. V. 183, pp. 301-308.

Bechard, G., Yamazaki, H., Gould, W.D., Bedard, P. 1994. Use of cellulosic substrates for the microbial treatment of acid mine drainage. Journal of Environmental Quality V. 23, pp. 111-116.

Benner, S.G., Blowes, D.W., Ptacek, C.J. 1997. A full-scale porous reactive wall for prevention of acid mine drainage. Groundwater Monitoring and Remediation. V. 17, pp. 99-107.

Benner, S.G., Blowes, D.W., Ptacek, C.J., Mayer, K.U. 2002. Rates of sulphate reduction and metal sulfide precipitation in a permeable reactive barrier. Applied Geochemistry. V. 17, pp. 301-320.

Blowes, D.W., Ptacek, C.J., Benner, S.G., McRae, C.W.T., Bennett, T.A., Puls, R.W. 2000. Treatment of Inorganic Contaminants using Permeable Reactive Barriers. Journal of Contaminant Hydrology. V. 45, pp. 123-137.

Brookins, D.G. 1988. Eh-pH diagrams for geochemistry. New York, NY: Springer-Verlag.

Caraballo, M., Santofimia, E., Jarvis, A. 2010. Metal retention, mineralogy, and design considerations of a mature permeable reactive barrier (PRB) for acidic mine water drainage in Northumberland, UK. American Mineralogist. V. 95, pp. 1642-1649.

Castro, J.M. and Moore, J.N. 2000. Pit lakes: their characteristics and the potential for their remediation. Environmental Geology. V. 39, pp. 1254-1260.

Catalan, L.J.J., and Kumari, A. 2005. Efficacy of lime mud residues from kraft mills to amend oxidized mine tailings before permanent flooding. J. Environ. Eng. Sci. V. 4, pp. 241-256.

Cocos, I.A., Zagury, G.J., Clement, B., Samson, R. 2002. Multiple factor design for reactive mixture selection for use in reactive walls in mine drainage treatment. Water Research. V. 32, pp. 167-177.

Conly, A.G., Cockerton, S., Goold, A., and Lee, P. 2007. Source and nature of sulphate toxicity of two pit lakes at the former Steep Rock iron mine, northwestern Ontario. Paper presented at 2007 GSA Annual Meeting, Denver, CO.

Curtin, D., and Syers, J.K. 1990. Mechanism of sulphate adsorption by two tropical soils. Journal of Soil Science. V. 41, pp. 295-304.

Dvorak, D.H., Hedin, R.S., Edenborn, H.M., McIntire, P.E. 1992. Treatment of metal-contaminated water using bacterial sulfate reduction: Results from pilot-scale reactors. Biotechnology and Bioengineering. V. 40, pp. 609-616.

Eary, L.E., 1999. Geochemical and equilibrium trends in mine pit lakes. Applied Geochemistry. V. 14, pp. 963-987.

Egiebor, N.O. and Oni, B. 2007. Acid rock drainage formation and treatment: A review. Asia-Pacific Journal of Chemical Engineering V. 2, pp. 47-62.

Elementar Vario EL cube technical brochure. Undated. Elementar Analysensysteme GmbH. Hanau, Germany.

Fortin, D., Goulet, R., Roy, M. 2000. Seasonal cycling of Fe and S in a constructed wetland: the role of sulphate reducing bacteria. Geomicrobiology Journal. V. 17, pp. 221-235.

Gandhi, S., Oh, B.T., Schnoor, J.L., Alvarez, P.J.J. 2002. Degradation of TCE, Cr (VI), sulfate, and nitrate mixtures by granular iron in flow-through columns under different microbial conditions. Water Research. V. 36, pp. 1973-1982.

Gazea, B., Adam, K., Kontopoulos, A. 1996. A review of passive systems for the treatment of acid mine drainage. Minerals Engineering. V. 9, pp. 23-42.

Gibert, O., de Pablo, J., Cortina, J.L., Ayora, C. 2004. Chemical characterisation of natural organic substrates for biological mitigation of acid mine drainage. Water Research. V. 38, pp. 4186-4196.

Gibert, O., Rotting, T., Cortina, J.L., de Pablo, J., Ayora, C., Carrera, J., Bolzicco, J. 2011. In-situ remediation of acid mine drainage using a permeable reactive barrier in Aznalcollar (sw Spain). Journal of Hazardous Materials. V. 191, pp. 287-295.

Godwin, A., 2009. Geochemical and toxicological investigation of the Hogarth and Caland Pit Lakes, former Steep Rock iron mine site. M.Sc. Thesis, Lakehead University, Thunder Bay, Ontario. 105 p.

Goold, A.R., 2008. Water quality and toxicity investigations of two pit lakes at the former Steep Rock iron mines, near Atikokan, Ontario. M.Sc. Thesis, Lakehead University, Thunder Bay, Ontario. 90 p.

Guo, Q., and Blowes, D.W. 2009. Biogeochemistry of two types of permeable reactive barriers, organic carbon and iron-bearing organic carbon for mine drainage treatment: column experiments. Journal of Contaminant Hydrology. V. 107, pp. 128-139.

Harris, M.A. and Ragusa, S. 2001. Bioremediation of acid mine drainage using decomposable plant material in a constant flow bioreactor. Environmental Geology. V. 40, pp. 1192-1204.

Hoffert, J.R. 1947. Acid mine drainage. Industrial and Engineering Chemistry. V. 39, #5, pp. 642-646.

Hseu, Z.Y. 2004. Evaluating heavy metal contents in nine composts using four digestion methods. Bioresource Technology. V. 95, pp. 53-59.

International Network for Acid Prevention (INAP). 2003. Treatment of Sulphate in Mine Effluents. Lorax Environmental. Vancouver, British Columbia.

Jarvis, A.P., Moustafa, M., Orme, P.H.A., Younger, P.L. 2006. Effective remediation of grossly polluted acidic, and metal rich, spoil heap drainage using a novel, low-cost, permeable reactive barrier in Northumberland, UK. Environmental Pollution. V. 143, pp. 261-268.

Johnson, D.B. 2003. Chemical and microbiological characteristics of mineral spoils and drainage waters at abandoned coal and metal mines. Water, Air, and Soil Pollution. V. 3, pp. 47-66.

Johnson, D.B. and Hallberg, K.B. 2005. Acid mine drainage remediation options: a review. Science of the Total Environment. V. 338, pp. 3-14.

Kepler, D.A., McCleary, E.C. 1994. Successive alkalinity producing systems (SAPS) for the treatment of acidic mine drainage. Proceedings of the International Land Reclamation and Mine Drainage Conference and the 3rd International Conference on the Abatement of Acidic Drainage. V. 1, pp. 195– 204.

Klump, J., Hebbeln, D., Wefer, G. 2000. The impact of sediment provenance on barium-based productivity estimates. Marine Geology. V. 169, pp. 259-271.

Krishnakumar, B. and Manilal, V.B. 1999. Bacterial oxidation of sulphide under denitrifying conditions. Biotechnology Letters. V. 21, pp. 437-440.

Kumar, N., Millot, R., Battaglia-Brunet, F., Negrel, P., Diels, R., Rose, J., Bastiaens, L. 2013. Sulfur and oxygen isotope tracing in zero valent iron based In situ remediation system for metal contaminants. Chemosphere. V. 90, pp. 1376-1371.

Kusky, T.M. and Hudleston, P.J. 1999. Growth and demise of an Archean carbonate platform, Steep Rock Lake, Ontario, Canada. Canadian Journal of Earth Science. V. 36, pp. 565-584.

Kuyucak, N., and St-Germain, P. 1994. In situ treatment of acid mine drainage by sulphate reducing bacteria in open pits: scale up experiences. Proceedings of the International Land Reclamation and Mine Drainage Conference and the 3rd International Conference on the Abatement of Acidic Drainage. pp. 303-310.

Lindsay, M.B.J., Blowes, D.W., Condon, P.D., Ptacek, C.J. 2009. Managing pore-water quality in mine tailings by inducing microbial sulphate reduction. Environmental Science and Technology. V. 43, pp. 7086-7091.

Ludwig, R.D., McGregor, R.G., Blowes, D.W., Benner, S.G., Mountjoy, K. 2002. A permeable reactive barrier for treatment of heavy metals. Ground Water. V. 40, pp. 59-66.

Ludwig, R.D., Smyth, D.J.A, Blowes, D.W., Spink, L.E., Wilkin, R.T., Jewett, D.G., Weisener, C.J. 2009. Treatment of arsenic, heavy metals, and acidity using a mixed ZVI – compost PRB. Environmental Science and Technology. V. 43, pp. 1970-1976.

MacDonald, J.C., 2005. An integrated mineralogy, geochemistry, and stable isotope investigation into potential sulphate sources of the Hogarth Pit Lake, Steep Rock Iron Mine, Atikokan. B.Sc. Thesis, Lakehead University, Thunder Bay, Ontario, 52 p.

Mikkelsen, L. 2012. Preliminary hydrodynamic modelling of the Steep Rock pit lakes, Atikokan, Ontario. M.Sc. Thesis, Lakehead University, Thunder Bay, Ontario, 197 p.

Nagpal, S., Chuichulcherm, S., Livingston, A., Peeva, L. 2000. Ethanol utilization by sulfate-reducing bacteria: An experimental and modeling study. Biotechnology and Bioengineering. V. 70, pp. 533-543.

Neculita, C.M., Zagury, G.J., Bussiere, B. 2007. Passive treatment of acid mine drainage in bioreactors using sulfate reducing bacteria: Critical review and research needs. Journal of Environmental Quality. V. 36, pp. 1-16.

Neculita, C.M., Zagury, G.J. 2008. Biological treatment of highly contaminated acid mine drainage in batch reactors: long term treatment and reactive mixture characterization. Journal of Hazardous Materials. V. 157, pp. 358-366.

Neculita, C.M., Yim, G.J., Lee, G., Ji, S.W., Jung, J.W., Park, H.S., Song, H. 2011. Comparative effectiveness of mixed organic substrates to mushroom compost for treatment of mine drainage in passive bioreactors. Chemosphere. V. 83, pp. 76-82.

Olem, H. and Unz, R.F. 1980. Rotating-disc biological treatment of acid mine drainage. Journal of Water Pollution Control Federation. V. 52, pp. 257-269.

Perusse, C., 2009. Hydrogeoloical and geochemical assessment of two tailings impoundments at the former Steep Rock iron mine Atikokan, Ontario. H.B.Sc. Thesis, Lakehead University, Thunder Bay, Ontario, 39 p.

Peters, J. (ed.) 2003. Recommended methods of manure analysis (A3769). University of Wisconsin – Extension. Madison, WI. 58 p.

Phillips, D.H., Gu, B., Watson, D.B., Roh, Y., Liang, L., Lee, S.Y. 2000. Performance evaluation of a zerovalent iron reactive barrier: Mineralogical characteristics. Environmental Science and Technology. V. 34, pp. 4169-4176.

Postgate, J.R., 1984. The Sulphate Reducing Bacteria, second ed. Cambridge University Press, Cambridge, UK. 222 p.

Prasad, D., Wai, M., Berube, P., Henry, J.G. 1999. Evaluating substances in the biological treatment of acid mine drainage. Environmental Technology. V. 20, pp. 449-458.

Reinertson, S.A., Elliott, F., Cochran, V.L., Campbell, G.S. 1984. Role of available carbon and nitrogen in determining the rate of wheat straw decomposition. Soil Biology and Biochemistry. V. 16, pp. 459-464.

Rudd, T., Campbell, J.A., Lester, J. N. 1988. The use of model compounds to elucidate metal forms in sewage sludge. Environmental Pollution. V. 50, pp. 225-242.

Scherer, M.M., Richter, S., Valentine, R.L., Alvarez, P.J.J. 2000. Chemistry and microbiology of permeable reactive barriers for in situ groundwater cleanup. Critical Reviews in Microbiology. V. 26, pp. 221-264.

Scherer, H.W. 2009. Sulfur in Soils. Journal of Plant Nutrition and Soil Science. V. 172, pp. 326-335.

Shankie, S.J. 2011. Assessment of Permeable Reactive Barriers for Sulphate Reduction at the Former Steep Rock Iron Mine Site, Atikokan, Ontario. Unpublished M.Sc. Thesis. Lakehead University. 152 p.

Sheoran, A.S., Sheoran, V., Choudhary, R.P. 2010. Bioremediation of acid-rock drainage by sulphate reducing prokaryotes: a review. Minerals Engineering. V. 23, pp. 1073-1100.

Shevenell, L., Connors, K.A., Henry, C.D. 1999. Controls on pit lake water quality at sixteen open-pit mines in Nevada. Applied Geochemistry. V. 14, pp. 669-687.

Song, H., Yim, G.J., Ji, S.W., Nam, I.H., Neculita, C.M., Lee, G. 2012. Performance of mixed organic substrates during treatment of acidic and moderate mine drainage in column bioreactors. Journal of Environmental Engineering. V. 138, pp. 1077-1084.

Sowa, V.A. 2002. Steep Rock Iron Mines: Dredging and draining of Steep Rock Lake and some effects after 45 years. *in* Tailings and Mine Waste ’02: Proceedings of the Ninth Annual Tailings and Mine Waste Conference. Balkema. Pp. 393-402.

Stover, R.C., Sommers, L.E., Silviera, D.J. 1976. Evaluation of metals in wastewater sludge. Water Pollution Control Federation. Vol. 48, pp. 2165-2175.

Taylor, B. 1978. Steep Rock: The men and the mines. Quetico Publishing: Atikokan, Ontario. 144 p.

Thompson, J.B. and Ferris, F.G. 1990. Cyanobacterial precipitation of gypsum, calcite, and magnesite from natural alkaline lake water. Geology. V. 18, pp. 995-998.

Torres, M.E., Bohrmann, G., Dube, T.E., Poole, F.G. 2003. Formation of modern and Paleozoic stratiform barite at cold methane seeps on continental margins. Geology. V. 31, pp. 897-900.

Torres-Crespo, N., Martinez-Ruiz, F., Gonzalez-Munoz, M.T., Bedmar, E.J., De Lange, G.J., Jroundi, F. 2015. Role of bacteria in in marine barite precipitation: A case study using Mediterranean seawater. Science of the Total Environment. V. 512-513, pp. 562-571.

Tsukamoto, T.K., Killion, H.A., Miller, G.C. 2004. Column experiments for microbiological treatment of acid mine drainage: Low temperature, low-pH and matrix investigations. Water Research. V. 38, pp. 1405-1418.

United States Environmental Protection Agency. 1998. Permeable reactive barrier technologies for contaminant remediation. EPA/600/R-98/125. Washington, DC. 94 p.

United States Environmental Protection Agency. 1996. Method 3051A: Microwave assisted acid digestion of sediments, sludges, soils, and oils. Washington, DC. 30 p.

Vancook, M. 2005. The limnology and remediation of two proximal pit lakes in northwestern Ontario. Unpublished MSc thesis, Lakehead University, Thunder Bay, ON, Canada, 105 p.

Wang, H.L., Shang, J.Q., Kovac, V., Ho, K.S. 2006. Utilization of Atikokan coal fly ash in acid rock drainage control from Musselwhite Mine tailings. Canadian Geotechical Journal. V. 43, pp. 229-243.

Waybrant, K.R., Blowes, D.W., Ptacek, C.J. 1998. Selection of reactive mixtures for use in permeable reactive walls for treatment of mine drainage. Environmental Science and Technology. V. 32, pp. 1972-1979.

Waybrant, K.R., Ptacek, C.J., Blowes, D.W. 2002. Treatment of mine drainage using permeable reactive barriers: column experiments. Environmental Science and Technology. V. 36, pp. 1349-1356.

Weber, K.A., Achenbach, L.A., Coates, J.D. 2006. Microorganisms pumping iron: Anaerobic microbial iron oxidation and reduction. Nature Reviews Microbiology. V. 4, pp. 752-764.

Wilkin, R.T., Puls, R.W., Sewell, G.W. 2002. Long-term performance of permeable reactive barriers using zero-valent iron: geochemical and microbiological effects. Groundwater. V. 41, pp. 493-503.

Willow, M.A., and Cohen, R.R.H. 2003. pH, dissolved oxygen, and adsorption effects on metal removal in anaerobic bioreactors. Journal of Environmental Quality. V. 32, pp. 1212–1221.

Wu, J., Lu, J., Chen, T., He, Z., Su, Y., Jin, X., Yao, X. 2010. In Situ Biotreatment of Acidic Mine Drainage using Straw as Sole Substrate. Environmental Earth Science. V. 60, pp. 421-429.

Younger, P.L., Jayaweera, A., Elliot, A., Wood, R., Amos, P., Daugherty, A.J. 2003. Passive treatment of acidic mine waters in subsurface flow systems: exploring RAPS and permeable reactive barriers. Land Contamination and Reclamation. V. 11, pp. 127– 135.

Zagury, G.J., Kulnieks, V.I., Neculita, C.M. 2006. Characterization and reactivity assessment of organic substrates for sulphate reducing bacteria in acid mine drainage treatment. Chemosphere. V. 64, pp. 944-954.

Zaluski, M.H., Trudnowski, J.M., Harrington-Baker, M. A., Bless, D.R. 2003. Post-mortem findings on the performance of engineered SRB field-bioreactors for acid mine drainage control. pp. 845–853. *in* Proceedings of the 6th International Conference on Acid Rock Drainage.

Ziemkiewicz, P.F., Skousen, J.G., Simmons, J. 2003. Long-term performance of Passive Acid Mine Drainage Treatment Systems. Mine Water and the Environment. V. 22, pp. 118-129.

Appendices

Abbreviations used in Appendices:

<DL, BDL: Below Detection Limit

EXC: Excluded due to interference from chemical solution in procedure.

MDL: Minimum Detection Limit

ND: Not Detected

Appendix A: Raw Material Testing Results

Digested Raw Substrates

Sample	MDL	Blank 1	Blank 2	Cow	Horse	Hay 1	Hay 2	Hay 3	Leaves	Poultry	Sheep	Rabbit 1	Rabbit 2	Rabbit 3
		ppm	ppm	mg/kg	mg/kg	mg/kg	mg/kg	mg/kg	mg/kg	mg/kg	mg/kg	mg/kg	mg/kg	mg/kg
Dry Mass Used (g)		blank	blank	0.2514	0.2493	0.2499	0.2495	0.2506	0.2509	0.2517	0.2506	0.2494	0.2501	0.2504
Al	0.05	0.09	0.06	156.01	3319.29	27.89	28.22	28.29	547.23	456.10	87.71	1404.97	976.01	1222.84
As	0.06	BDL	BDL	BDL	BDL	BDL	BDL	BDL	BDL	BDL	BDL	BDL	BDL	BDL
B	0.04	BDL	BDL	BDL	BDL	BDL	BDL	BDL	72.10	30.12	BDL	BDL	BDL	BDL
Ba	0.005	0.04	BDL	36.71	31.21	9.48	8.74	9.42	37.58	11.04	31.56	42.94	43.02	43.33
Be	0.001	BDL	BDL	BDL	BDL	BDL	BDL	BDL	BDL	BDL	BDL	BDL	BDL	BDL
Ca	0.01	0.29	0.23	11006.36	6522.26	2491.40	2399.20	2569.03	22443.20	82002.38	10375.10	4643.14	4666.13	4928.12
Cd	0.01	BDL	BDL	BDL	BDL	BDL	BDL	BDL	BDL	BDL	BDL	BDL	BDL	BDL
Co	0.008	BDL	BDL	BDL	4.17	BDL	BDL	BDL	5.38	BDL	BDL	BDL	BDL	BDL
Cr	0.008	BDL	BDL	BDL	45.21	6.24	5.09	7.26	5.62	6.99	3.27	5.01	5.20	4.71
Cu	0.005	BDL	0.01	32.50	52.55	24.93	25.57	29.01	15.38	92.93	21.83	32.12	33.07	31.63
Fe	0.01	0.07	0.05	337.95	7220.22	118.09	106.21	122.47	1473.10	560.59	149.24	912.59	830.07	912.54
K	0.1	BDL	BDL	3756.96	4921.78	12132.85	12088.18	11723.86	3035.87	20083.43	8699.12	8448.28	8412.63	8338.66
Li	0.05	BDL	BDL	BDL	BDL	BDL	BDL	BDL	BDL	BDL	BDL	BDL	BDL	BDL
Mg	0.01	0.11	0.05	3195.31	5002.01	1027.21	1000.00	1045.89	3624.95	5184.74	3625.70	2024.86	1912.44	1982.43
Mn	0.002	0.00	0.00	250.52	148.58	113.05	115.03	116.72	191.59	237.74	236.71	111.99	112.71	114.10
Mo	0.02	BDL	BDL	BDL	BDL	BDL	BDL	BDL	BDL	BDL	BDL	BDL	BDL	0.08
Na	0.01	0.48	0.17	2032.62	732.45	78.55	83.57	80.13	131.73	2953.91	522.35	1574.18	1544.18	1560.30
Ni	0.01	BDL	BDL	BDL	19.74	4.64	BDL	BDL	BDL	10.65	BDL	5.69	5.32	4.35
P	0.1	3.55	3.62	5847.26	4275.97	2537.82	2652.91	2520.75	2264.25	19825.19	5853.95	4402.57	4550.18	4408.95
Pb	0.05	BDL	BDL	BDL	BDL	BDL	BDL	BDL	BDL	BDL	BDL	BDL	BDL	BDL
S	0.1	0.12	BDL	1984.49	1093.86	649.86	660.52	684.76	1763.65	5661.50	2019.95	2387.73	2324.27	2381.39
Se	0.1	BDL	BDL	BDL	BDL	BDL	BDL	BDL	BDL	BDL	BDL	BDL	BDL	BDL
Si	0.05	0.05	0.07	42.32	42.80	277.39	43.09	73.62	39.58	42.03	24.62	57.54	52.94	49.96
Sn	0.1	BDL	BDL	BDL	BDL	BDL	BDL	BDL	BDL	BDL	BDL	BDL	BDL	BDL
Sr	0.005	BDL	BDL	22.99	25.39	7.12	6.61	7.18	39.38	179.30	22.39	36.05	36.79	36.70
Ti	0.005	BDL	BDL	3.30	260.49	BDL	BDL	BDL	40.02	3.26	BDL	8.54	6.08	7.39
V	0.05	BDL	BDL	BDL	BDL	BDL	BDL	BDL	BDL	BDL	BDL	BDL	BDL	BDL
W	0.04	BDL	BDL	24.70	BDL	BDL	BDL	BDL	BDL	BDL	BDL	BDL	BDL	BDL
Y	0.01	BDL	BDL	BDL	BDL	BDL	BDL	BDL	BDL	BDL	BDL	BDL	BDL	BDL
Zn	0.01	BDL	BDL	140.33	114.68	26.65	25.89	33.68	171.54	207.63	108.22	173.42	165.13	167.13
Zr	0.01	BDL	BDL	BDL	BDL	BDL	BDL	BDL	BDL	BDL	BDL	BDL	BDL	BDL

Sample	MDL	Blank 1	Blank 2	Cow	Horse	Hay 1	Hay 2	Hay 3	Leaves	Poultry	Sheep	Rabbit 1	Rabbit 2	Rabbit 3
		ppm	ppm	mg/kg	mg/kg	mg/kg	mg/kg	mg/kg	mg/kg	mg/kg	mg/kg	mg/kg	mg/kg	mg/kg
Dry Mass Used (g)		blank	blank	0.2514	0.2511	0.2493	0.2501	0.2498	0.2503	0.2499	0.2514	0.2516	0.2512	0.2506
Al	0.05	BDL	BDL	163.96	2077.66	22.94	24.47	21.58	459.05	666.67	82.66	1746.42	1535.43	1235.83
As	0.06	BDL	BDL	BDL	BDL	BDL	BDL	BDL	BDL	BDL	BDL	BDL	BDL	BDL
B	0.04	BDL	BDL	BDL	BDL	BDL	BDL	BDL	BDL	BDL	BDL	BDL	BDL	BDL
Ba	0.005	BDL	BDL	2.47	6.65	BDL	BDL	BDL	3.68	5.64	BDL	3.14	2.71	3.27
Be	0.001	BDL	BDL	BDL	BDL	BDL	BDL	BDL	BDL	BDL	BDL	BDL	BDL	BDL
Ca	0.01	0.13	0.09	461.81	1353.64	243.96	309.84	262.61	1050.34	5026.01	312.37	164.59	147.05	232.52
Cd	0.01	BDL	BDL	BDL	BDL	BDL	BDL	BDL	BDL	BDL	BDL	BDL	BDL	BDL
Co	0.008	BDL	BDL	BDL	BDL	BDL	BDL	BDL	BDL	BDL	BDL	BDL	BDL	BDL
Cr	0.008	BDL	BDL	BDL	42.85	6.06	5.64	5.08	7.71	8.24	3.50	BDL	BDL	BDL
Cu	0.005	BDL	BDL	10.78	31.54	24.83	8.16	17.85	6.15	130.45	14.20	73.69	21.06	10.61
Fe	0.01	0.02	0.02	180.19	2899.64	93.34	77.85	84.83	536.56	458.58	93.00	474.96	392.28	396.37
K	0.1	BDL	BDL	75.82	364.72	843.56	1316.27	1058.85	147.38	184.59	95.98	171.58	209.91	311.01
Li	0.05	BDL	BDL	BDL	BDL	BDL	BDL	BDL	BDL	BDL	BDL	BDL	BDL	BDL
Mg	0.01	0.04	0.03	153.98	878.53	87.16	120.71	99.20	242.39	247.94	108.91	310.02	277.67	263.13
Mn	0.002	0.004	0.003	16.11	31.94	10.55	14.39	11.97	11.07	18.73	10.38	5.37	4.86	6.54
Mo	0.02	BDL	BDL	BDL	BDL	BDL	BDL	BDL	BDL	BDL	BDL	BDL	BDL	BDL
Na	0.01	0.18	0.17	119.77	312.35	56.76	42.30	34.11	76.07	70.55	89.50	76.11	66.24	89.94
Ni	0.01	BDL	BDL	BDL	14.18	BDL	BDL	BDL	BDL	4.60	BDL	BDL	BDL	BDL
P	0.1	0.29	0.26	1002.39	602.15	436.02	456.22	402.32	485.02	1496.60	982.90	340.98	352.47	406.62
Pb	0.05	BDL	BDL	BDL	BDL	BDL	BDL	BDL	BDL	BDL	BDL	BDL	BDL	BDL
S	0.1	BDL	BDL	2085.92	1371.17	659.45	637.74	633.71	2096.28	5498.20	2223.15	2159.78	2251.59	2232.24
Se	0.1	BDL	BDL	BDL	BDL	BDL	BDL	BDL	BDL	BDL	BDL	BDL	BDL	BDL
Si	0.05	BDL	BDL	32.26	38.39	61.77	37.03	33.99	30.76	33.77	30.47	50.00	43.39	36.43
Sn	0.1	BDL	BDL	BDL	BDL	BDL	BDL	BDL	BDL	BDL	BDL	BDL	BDL	BDL
Sr	0.005	BDL	BDL	BDL	5.26	BDL	BDL	BDL	2.44	10.36	BDL	BDL	BDL	BDL
Ti	0.005	BDL	BDL	9.35	258.58	6.30	5.56	6.89	64.92	10.64	5.21	21.58	17.56	18.08
V	0.05	BDL	BDL	BDL	BDL	BDL	BDL	BDL	BDL	BDL	BDL	BDL	BDL	BDL
W	0.04	BDL	BDL	BDL	23.70	37.34	BDL	BDL	BDL	17.77	23.51	BDL	18.87	BDL
Y	0.01	BDL	BDL	BDL	BDL	BDL	BDL	BDL	BDL	BDL	BDL	BDL	BDL	BDL
Zn	0.01	BDL	BDL	9.23	22.42	4.33	4.60	4.64	10.83	21.81	6.80	10.17	8.52	10.97
Zr	0.01	BDL	BDL	BDL	4.10	BDL	BDL	BDL	BDL	BDL	BDL	BDL	BDL	BDL

Creek Sediment Digestion Data

		Untreated			EAS Treated		
Sample	MDL	1	2	3	1	2	3
Dry Mass Used (g)		1.0099	1.0026	1.0027	1.0045	1.0062	1.0078
		mg/kg	mg/kg	mg/kg	mg/kg	mg/kg	mg/kg
As	0.06	BDL	8.92	6.13	7.74	7.30	6.44
Ba	0.005	91.67	93.21	93.03	18.76	19.28	20.48
Be	0.001	0.455	0.469	0.459	0.119	0.119	0.119
Ca	0.01	4780.7	5100.7	5019.4	1697.4	1928.0	1870.4
Cd	0.01	BDL	BDL	BDL	BDL	BDL	BDL
Co	0.008	BDL	BDL	BDL	BDL	BDL	BDL
Cr	0.008	20.92	22.47	22.51	20.47	18.33	20.20
Cu	0.005	20.39	20.76	21.05	7.21	6.28	6.74
Fe	0.01	46242.2	47895.5	47691.2	26769.5	26982.7	27832.9
K	0.1	483.51	559.74	521.09	523.05	477.44	507.44
Li	0.05	11.24	11.50	11.45	9.00	8.26	8.51
Mg	0.01	5023.3	5199.5	5198.0	3149.8	3082.9	3224.8
Mn	0.002	510.84	532.42	535.45	106.12	106.94	112.52
Mo	0.02	BDL	BDL	BDL	BDL	BDL	BDL
Na	0.01	598.87	688.61	631.20	353.91	419.90	395.61
Ni	0.01	14.90	15.53	15.55	9.40	9.11	9.75
S	0.1	2269.53	2354.88	2398.52	2288.70	1886.30	1998.41
Si	0.05	5.46	9.43	7.20	20.58	19.18	6.64
Sr	0.005	12.60	13.91	13.65	5.66	6.57	6.56
Ti	0.005	234.97	285.76	257.21	237.63	235.94	226.33
V	0.05	44.32	49.89	46.67	33.70	37.29	38.91
Y	0.01	4.94	5.17	5.04	1.43	1.45	1.57
Zn	0.01	85.49	90.14	90.07	23.48	25.09	25.46
Zr	0.01	8.54	9.69	9.09	9.39	8.43	8.51

Carbon, Nitrogen, Sulphur Combustion Results

Sample	N%	C%	S%
Raw Substrates			
Creek Sed 1	0.20	3.83	0.286
Creek Sed 2	0.19	3.18	0.278
Creek Sed 3	0.18	3.21	0.287
Cow	1.75	45.64	0.221
Horse	1.34	36.84	0.141
Hay 1	1.08	41.45	0.069
Hay 2	0.91	41.72	0.051
Hay 3	1.05	41.63	0.049
Leaves	2.22	40.46	0.144
Poultry	3.18	35.13	0.546
Rabbit 1	1.95	44.50	0.245
Rabbit 2	1.91	44.61	0.228
Rabbit 3	1.95	44.37	0.235
Sheep	1.90	45.25	0.198
EAS Residues			
Creek Sed 1	0.20	2.66	0.190
Creek Sed 2	0.17	2.40	0.203
Creek Sed 3	0.17	2.33	0.189
Cow	1.92	47.90	0.289
Horse	1.31	37.87	0.172
Hay 1	1.41	47.91	0.124
Hay 2	1.52	47.73	0.110
Hay 3	1.22	47.22	0.103
Leaves	2.92	49.88	0.226
Poultry	2.38	48.03	0.582
Rabbit 1	1.90	44.72	0.275
Rabbit 2	2.05	44.79	0.270
Rabbit 3	2.01	45.03	0.264
Sheep	1.98	47.47	0.238

Easily Available Substances Testing

Experiment Set 1						
Sample	Initial Mass (g)	Empty Dish (g)	Full Dish (g)	Remaining Mass (g)	Mass Lost (g)	**EAS %**
Hay 1	2.006	1.031	2.374	1.343	0.663	33.1
Hay 2	2.018	1.042	2.407	1.365	0.653	32.4
Hay 3	Experiment Error					
Leaves	Experiment Error					
Cow	2.021	1.031	2.693	1.662	0.359	17.8
Poultry	2.015	1.035	1.605	0.57	1.445	71.7
Horse	2.012	1.052	2.679	1.627	0.385	19.1
Sheep	2.011	1.041	2.569	1.528	0.483	24.0
Rabbit 1	Experiment Error					
Rabbit 2	2.021	1.051	2.483	1.432	0.589	29.1
Rabbit 3	2.014	1.047	2.410	1.363	0.651	32.3
Creek Sed 1	5.028	1.041	5.474	4.433	0.595	11.8
Creek Sed 2	4.998	1.040	5.445	4.405	0.593	11.9
Creek Sed 3	4.999	1.044	5.466	4.422	0.577	11.5
Experiment Set 2						
	Initial Mass (g)	Empty Dish (g)	Full Dish (g)	Remaining Mass (g)	Mass Lost (g)	**EAS %**
Hay 1	2.0141	1.016	2.2778	1.262	0.7523	37.4
Hay 2	2.0137	1.0248	2.318	1.293	0.7205	35.8
Hay 3	2.0007	1.0425	2.3272	1.285	0.716	35.8
Leaves	2.0026	1.0094	2.2624	1.253	0.7496	37.4
Cow	2.0061	1.0634	2.5782	1.515	0.4913	24.5
Poultry	2.0071	1.028	1.5664	0.538	1.4687	73.2
Horse	1.9997	1.0164	2.5526	1.536	0.4635	23.2
Sheep	2.0049	1.0574	2.3847	1.327	0.6776	33.8
Rabbit 1	1.9963	1.0508	2.3981	1.347	0.649	32.5
Rabbit 2	2.0041	1.0558	2.4338	1.378	0.6261	31.2
Rabbit 3	1.9967	1.0504	2.421	1.370	0.6265	31.4
Creek Sed 1	2.0037	1.0235	2.3714	1.348	0.6558	32.7
Creek Sed 2	2.0004	1.0254	2.3098	1.284	0.716	35.8
Creek Sed 3	2.0008	1.0096	2.3559	1.346	0.6545	32.7

Appendix B: Reactive Mixture Calculations

Organic Carbon Requirements

Influent Water			Calculation Data		Flow Rates	
1585	mg/L SO4		96	molar mass SO4 (g)	0.1	mL/min
1.585	g/L SO4		32	molar mass S (g)	6	mL/hr
0.52833	g/L S		0.33333	S fraction of SO4	144	mL/day
			12.01	g/mol C	0.144	L/day
0.01651	mol/L SO4		180	days for experiment	25.92	L over 180 days
0.01651	mol/L S					
mol/L * total liters			Therefore:		Therefore:	
0.4280	mol S to be removed		0.8559	mol C required	5.14	g C required per substrate

		Mass Required (g)		Mass Required (g)
Substrate	% Carbon	C req. x C %	EAS %	EAS Factor applied
Poultry	35.13	14.63	70.51	20.75
Rabbit	44.49	11.55	32.61	35.42
Sheep	45.25	11.36	28.91	39.29
Leaves	40.46	12.70	36.61	34.70
Hay	41.6	12.35	34.51	35.80

Appendix C: Flow-Through Reactor Monitoring Data

ICP-AES Results. All values in ppm.

	Al	As	B	Ba	Be	Ca	Cd	Co	Cr	Cu	Fe	K	Mg	Mn	Na	Ni	P	Pb	S	Si	Sr	Ti	V	Zn
MDL	0.05	0.06	0.04	0.005	0.001	0.01	0.01	0.008	0.008	0.005	0.01	0.1	0.01	0.002	0.01	0.01	0.1	0.05	0.1	0.05	0.005	0.005	0.05	0.01
Week 1																								
1	nd	nd	0.1195	0.0314	nd	17.07	nd	nd	nd	nd	1.843	11.49	9.259	0.4506	5.345	nd	nd	nd	9.772	0.541	0.0563	nd	nd	0.0265
2	nd	nd	0.2573	0.1836	nd	174.9	nd	nd	nd	nd	6.93	126.1	117.1	2.301	61.8	0.0114	0.3794	nd	32.3	8.696	0.5702	nd	nd	nd
3	nd	nd	0.1357	0.0191	nd	15.28	nd	nd	nd	nd	1.172	85.22	34.71	0.1446	17.01	nd	nd	nd	28.23	0.8865	0.0842	nd	nd	nd
4	nd	nd	0.158	0.2762	nd	209.7	nd	nd	nd	nd	1.013	9.023	127.2	3.05	77.68	nd	nd	nd	334.5	3.131	0.8979	nd	nd	0.0234
5	nd	nd	0.2723	0.1619	nd	187	nd	nd	nd	nd	15.06	193.7	132.9	2.359	79.73	nd	0.8631	nd	195.5	8.095	0.6879	nd	nd	nd
6	nd	nd	0.309	0.0974	nd	104	nd	nd	nd	nd	0.7916	143.5	111.6	1.181	87.43	0.0116	0.4317	nd	148.4	7.166	0.3982	nd	nd	0.0217
7	nd	nd	0.2293	0.6568	nd	326.9	nd	nd	nd	nd	155.2	466.3	201.7	9.574	90	0.02	0.5516	nd	190	9.966	1.213	nd	nd	0.0617
8	nd	nd	0.14	0.0827	nd	224.3	nd	0.0095	nd	nd	6.027	9.178	99.02	14.3	109.4	0.0112	nd	nd	316.3	5.647	0.675	nd	nd	0.0616
Stock	nd	nd	0.0557	0.0068	nd	253.5	nd	nd	nd	nd	0.4303	6.893	178.5	0.063	24.25	0.0222	nd	nd	475	1.375	1.127	nd	nd	0.0138
Week 2																								
1	nd	nd	0.2805	0.1834	0.002	212.2	nd	nd	nd	nd	2.498	149.1	144.4	3.277	58.78	nd	0.7114	nd	116.4	10.62	0.6305	nd	nd	0.0144
2	nd	nd	0.2074	0.1306	nd	198.9	nd	nd	nd	nd	1.063	106.9	148.4	2.227	45.81	nd	0.2072	nd	13.67	11.25	0.5397	nd	nd	nd
3	nd	nd	0.1916	0.0335	nd	30.17	nd	nd	nd	nd	7.839	291.1	164.5	0.1942	59.43	nd	1.805	nd	92.34	3.636	0.1445	nd	nd	nd
4	nd	nd	0.0591	0.2573	nd	253.8	nd	nd	nd	nd	3.543	14.15	173	2.731	50.11	nd	nd	nd	402.3	3.433	0.957	nd	nd	0.0234
5	nd	nd	0.2249	0.1868	nd	200.3	nd	nd	nd	nd	1.752	119.3	163.8	2.023	50.37	nd	4.043	nd	194.7	9.671	0.6673	nd	nd	nd
6	nd	nd	0.1316	0.1462	nd	183.7	nd	nd	nd	nd	0.6957	140.5	138.6	2.748	39.11	nd	0.1938	nd	79.55	6.483	0.545	nd	nd	nd
7	nd	nd	0.1819	0.2262	nd	255.2	nd	nd	nd	nd	104.1	240.6	183.8	5.946	53.45	nd	0.3407	nd	118.2	13.2	0.8884	0.0054	nd	0.0182
8	nd	nd	0.0859	0.1729	nd	284.5	nd	nd	nd	nd	39.12	9.126	174.2	10.82	51.84	nd	nd	nd	457.6	6.187	0.8955	nd	nd	0.0264
Week 3																								
1	nd	nd	0.2225	0.3038	0.0022	158.5	nd	nd	0.0179	nd	1.174	73.02	121.5	2.33	36.74	nd	4.315	nd	26.44	10.52	0.5542	nd	nd	nd
2	nd	nd	0.179	0.114	0.0013	169	nd	nd	0.0095	nd	0.2755	57.79	120.5	1.713	31.94	nd	0.1631	nd	1.825	10.19	0.4955	nd	nd	nd
3	nd	nd	0.1271	0.0379	nd	45.72	nd	nd	nd	nd	0.74	114.7	149.3	0.4108	33.56	nd	nd	nd	24.63	4.732	0.1943	nd	nd	nd
4	nd	nd	0.0568	0.2849	nd	249.8	nd	nd	nd	nd	0.3482	6.664	169.1	2.851	36.82	nd	nd	nd	382	3.411	0.9686	nd	nd	nd
5	nd	nd	0.1706	0.2955	nd	191.9	nd	nd	nd	nd	0.2373	53.75	143.9	1.833	33.78	nd	4.362	nd	167.4	8.224	0.7206	nd	nd	nd
6	nd	nd	0.125	0.0987	nd	179.9	nd	nd	nd	nd	0.2862	54.29	128.6	2.273	30.83	nd	0.1775	nd	34.53	9.22	0.5406	nd	nd	nd
7	nd	nd	0.1435	0.1089	nd	186.6	nd	nd	nd	nd	36.76	111.6	143.2	3.728	34.12	nd	nd	0.0904	20.36	12.44	0.6861	nd	nd	nd
8	nd	nd	0.0314	0.138	nd	172.4	nd	nd	nd	nd	5.639	3.858	118.5	4.504	23.16	nd	nd	nd	281.3	3.128	0.6103	nd	nd	nd
Week 4																								
1	nd	nd	0.1776	0.3285	nd	168.3	nd	nd	nd	nd	0.3512	49.72	122.1	2.201	31.75	nd	4.101	nd	58.16	8.621	0.6039	nd	nd	nd
2	nd	nd	0.127	0.0969	nd	138.4	nd	nd	nd	nd	0.5578	34.17	107.5	1.393	25.97	nd	0.1034	nd	11.14	9.485	0.4324	nd	nd	nd
3	nd	nd	0.0941	0.0289	nd	46.16	nd	nd	nd	nd	0.1672	53.36	141.2	0.3236	25.57	nd	0.1671	nd	37.18	4.779	0.1608	nd	nd	nd
4	nd	nd	0.05	0.2899	nd	248.7	nd	nd	nd	nd	0.2646	6.017	170.6	2.292	33.86	nd	nd	nd	371.5	3.059	0.9799	nd	nd	nd
5	nd	nd	0.1044	0.255	nd	194.4	nd	nd	nd	nd	0.436	34.55	142.8	1.375	29.95	nd	4.611	nd	194.3	6.197	0.7561	nd	nd	nd
6	nd	nd	0.1022	0.0468	nd	90.88	nd	nd	nd	nd	0.5043	47.64	124	0.2402	29.64	nd	0.4475	nd	32.66	8.624	0.3625	nd	nd	nd
7	nd	nd	0.0896	0.0947	nd	162.8	nd	nd	nd	nd	13.24	62.65	127.1	2.735	26.64	nd	nd	0.0511	22.95	10.62	0.6442	nd	nd	nd
8	nd	nd	0.0487	0.243	nd	269.8	nd	nd	nd	nd	21.48	6.098	181.5	4.946	30.31	nd	nd	nd	435.1	4.55	1.005	nd	nd	0.0143
Week 5																								
1	0.1078	nd	0.1284	0.249	nd	174.3	nd	0.0084	nd	nd	0.2358	34.94	145	1.829	28.6	nd	1.636	nd	100.3	6.414	0.5854	nd	nd	nd
2	0.0601	nd	0.0872	0.0997	nd	128.2	nd	nd	nd	nd	0.3192	23.13	126.8	0.9861	24.24	nd	0.2015	nd	13.17	9.208	0.4005	nd	nd	nd
3	nd	nd	0.0782	0.0383	nd	56.97	nd	nd	nd	nd	0.2167	29.48	157.5	0.3076	21.66	nd	0.134	nd	40.95	5.474	0.2078	nd	nd	nd
4	nd	nd	0.0456	0.3387	nd	240.9	nd	nd	nd	nd	0.1852	6.015	178.9	1.704	29.23	nd	nd	nd	356.2	3.03	0.9576	nd	nd	nd
5	nd	nd	0.0806	0.1921	nd	187.6	nd	nd	nd	nd	0.2575	26.72	156.9	0.9175	26.74	nd	2.473	nd	174.2	5.15	0.7246	nd	nd	nd
6	nd	nd	0.0995	0.0295	nd	106.9	nd	nd	nd	nd	0.4105	34.11	134.2	0.5063	23.16	nd	0.89	nd	26.15	10.01	0.3278	nd	nd	nd
7	nd	nd	0.0656	0.0983	nd	166.1	nd	nd	nd	nd	0.2703	41.42	158.3	1.979	23.92	nd	nd	nd	36.74	10.35	0.6258	nd	nd	nd
8	nd	nd	0.0433	0.2286	nd	256.7	nd	nd	nd	nd	3.948	5.9	187.1	3.631	25.29	nd	nd	0.0571	412.6	4.019	0.9792	nd	nd	nd

	Al	As	B	Ba	Be	Ca	Cd	Co	Cr	Cu	Fe	K	Mg	Mn	Na	Ni	P	Pb	S	Si	Sr	Ti	V	Zn
MDL	0.05	0.06	0.04	0.005	0.001	0.01	0.01	0.008	0.008	0.005	0.01	0.1	0.01	0.002	0.01	0.01	0.1	0.05	0.1	0.05	0.005	0.005	0.05	0.01
Week 6																								
1	nd	nd	0.2171	0.2283	nd	192.4	nd	nd	nd	nd	0.5259	27.32	146.8	1.472	29.32	nd	1.788	nd	152.6	4.942	0.6495	nd	nd	nd
2	nd	nd	0.1779	0.1449	nd	146.1	nd	nd	nd	nd	0.4061	19.13	134.3	0.7539	26.7	nd	0.7328	nd	24.69	8.166	0.4713	nd	nd	nd
3	nd	nd	0.145	0.037	nd	58.59	nd	nd	nd	nd	0.1516	20.64	161.5	0.138	24.65	nd	0.2072	nd	53.82	6.933	0.3036	nd	nd	nd
4	nd	nd	0.1025	0.3918	nd	261.5	nd	nd	nd	nd	0.1133	6.884	183.9	1.683	28.88	nd	nd	nd	394.3	3.369	1.033	nd	nd	nd
5	nd	nd	0.1269	0.1962	nd	200.5	nd	nd	nd	nd	0.0876	25.26	156.7	0.7521	28.98	nd	2.949	nd	200.6	4.588	0.7677	nd	nd	nd
6	nd	nd	0.1385	0.0779	nd	120.9	nd	nd	nd	nd	0.1999	23.02	140.6	0.5157	25.19	nd	0.8227	nd	55.59	9.023	0.4164	nd	nd	nd
7	nd	nd	0.0955	0.1086	nd	176	nd	nd	nd	nd	0.3261	29.12	157.8	1.266	25.28	nd	nd	nd	44.66	10.46	0.6724	nd	nd	nd
8	nd	nd	0.0873	0.267	nd	286.2	nd	nd	nd	nd	8.007	7.415	192.9	3.073	28.02	nd	nd	nd	431.5	4.354	1.099	nd	nd	nd
Week 7																								
1	nd	nd	0.0872	0.2072	nd	179	nd	nd	nd	nd	0.2354	24.18	158.1	1.266	26.32	nd	1.602	nd	142.6	4.33	0.6534	nd	nd	nd
2	nd	nd	0.0781	0.1143	nd	130.9	nd	nd	nd	nd	0.298	16.55	148.9	0.4161	23.56	nd	0.8559	nd	26.5	6.951	0.4692	nd	nd	nd
3	nd	nd	0.0652	0.0343	nd	46.99	nd	nd	nd	nd	0.1481	14.32	163.6	0.0928	21.53	nd	0.2335	nd	31.71	6.253	0.2927	nd	nd	nd
4	nd	nd	0.0464	0.3217	nd	222.5	nd	nd	nd	nd	0.0857	6.234	195.1	1.043	25.33	nd	nd	nd	379.5	3.263	0.9762	nd	nd	nd
5	nd	nd	0.0699	0.1759	nd	176	nd	nd	nd	nd	0.0235	20.93	164.2	0.5898	25.13	nd	2.507	nd	274.4	4.125	0.7266	nd	nd	nd
6	nd	nd	0.0785	0.0622	nd	67.72	nd	nd	nd	nd	0.1239	15.94	149.3	0.2035	21.83	nd	0.5204	nd	65.53	7.42	0.3159	nd	nd	nd
7	nd	nd	0.0533	0.1128	nd	159.9	nd	0.0264	nd	nd	0.446	22.33	165.7	0.9551	22.17	nd	0.1116	nd	29.43	10.14	0.663	nd	nd	nd
8	nd	nd	0.0495	0.25	nd	252.6	nd	0.0195	nd	nd	5.06	6.908	204.8	2.756	24.09	nd	nd	nd	408.3	4.267	1.063	nd	nd	nd
Week 8																								
1	nd	nd	0.0715	0.2179	nd	210.5	nd	nd	nd	nd	0.0714	16.05	153.5	1.025	27.86	nd	2.048	nd	221.9	11.54	0.7602	nd	nd	nd
2	nd	nd	0.0581	0.2106	nd	163	nd	nd	nd	nd	0.2599	10.96	146.1	0.3997	25.31	nd	1.891	nd	77.25	20.74	0.603	nd	nd	nd
3	nd	nd	0.0526	0.0394	nd	51.58	nd	nd	nd	nd	0.198	10.78	141.7	0.057	23.5	nd	0.646	nd	31.01	20.54	0.3242	nd	nd	nd
4	nd	nd	0.0438	0.3696	nd	247.1	nd	nd	nd	nd	0.0612	6.025	193.1	0.745	27.48	nd	0.022	nd	420.2	9.957	1.074	nd	nd	nd
5	nd	nd	0.0563	0.167	nd	192.7	nd	nd	nd	nd	0.0316	14.45	149.2	0.4034	25.56	nd	2.196	nd	401.8	10.44	0.7808	nd	nd	nd
6	nd	nd	0.0627	0.0765	nd	74.23	nd	nd	nd	nd	0.1017	11.52	140.7	0.1577	24.61	nd	0.4367	nd	106.5	20.89	0.3621	nd	nd	nd
7	nd	nd	nd	0.1383	nd	181.3	nd	nd	nd	nd	0.428	14.44	151.7	0.5896	24.22	nd	0.5819	nd	74.32	25.67	0.7318	nd	nd	nd
8	nd	nd	0.0507	0.2711	nd	263	nd	nd	nd	nd	4.422	6.347	191.2	2.368	25.32	nd	nd	nd	408.2	12.61	1.097	nd	nd	nd
Stock	nd	nd	0.0523	0.0051	nd	273.2	nd	nd	nd	nd	0.0138	6.424	202	0.0052	24.34	0.024	nd	nd	482.3	4.266	1.199	nd	nd	nd
Week 9																								
1	nd	nd	0.0519	0.2089	nd	241.2	nd	nd	nd	nd	0.1734	14.14	141.1	1.097	30.92	nd	1.657	nd	259.6	2.74	0.8047	nd	nd	nd
2	nd	nd	nd	0.2141	nd	202.2	nd	nd	nd	nd	0.157	8.925	138.1	0.2749	27.41	nd	0.8046	nd	123.9	4.672	0.6999	nd	nd	nd
3	nd	nd	0.044	0.0488	nd	87.77	nd	nd	nd	nd	0.1929	9.52	129.8	0.057	27.12	nd	1.035	nd	22.48	5.238	0.4012	nd	nd	nd
4	nd	nd	nd	0.3488	nd	274.7	nd	nd	nd	nd	0.0436	6.719	178.1	0.6179	31.94	nd	nd	nd	356.1	2.488	1.082	nd	nd	nd
5	nd	nd	0.0462	0.1999	nd	228.4	nd	nd	nd	nd	0.1282	15.81	140	0.5279	31.78	nd	2.36	nd	1134	2.701	0.8482	nd	nd	nd
6	nd	nd	0.0435	0.0719	nd	84.08	nd	nd	nd	nd	0.1084	10.71	137.2	0.0934	29.2	nd	0.2479	nd	142.8	4.973	0.4126	nd	nd	nd
7	nd	nd	nd	0.1576	nd	201.7	nd	nd	nd	nd	0.9286	12.17	134.3	0.4996	26.91	nd	1.044	nd	81.34	5.412	0.7595	nd	nd	nd
8	nd	nd	nd	0.2557	nd	273.1	nd	nd	nd	nd	4.583	6.414	161.9	2.016	27.67	nd	nd	nd	348.7	3.06	1.035	nd	nd	nd
Week 10																								
1	nd	nd	0.0745	0.2471	nd	249.4	nd	nd	nd	nd	0.1636	11.52	173.2	1.115	28.08	nd	2.763	nd	696.7	11.52	0.9656	nd	nd	nd
2	nd	nd	0.0498	0.2466	nd	213.5	nd	nd	nd	nd	0.1855	8.286	170.1	0.2134	25.98	nd	1.313	nd	190	21.61	0.874	nd	nd	nd
3	nd	nd	0.062	0.0565	nd	90.74	nd	nd	nd	nd	0.2137	8.219	158.4	0.0585	25.05	nd	1.708	nd	32.74	25.4	0.4615	nd	nd	nd
4	nd	nd	0.0505	0.4112	nd	287	nd	nd	nd	nd	0.0723	7.126	216.3	0.7609	31.35	nd	nd	nd	449.7	10.94	1.276	nd	nd	nd
5	nd	nd	0.0615	0.2082	nd	245.8	nd	nd	nd	nd	0.0467	11.67	177.7	0.398	27.95	nd	2.433	nd	563.1	10.92	1.022	nd	nd	nd
6	nd	nd	0.062	0.0731	nd	69.7	nd	nd	nd	nd	0.0986	11.32	168.5	0.0985	29.6	nd	0.4341	nd	161.3	20.96	0.433	nd	nd	nd
7	nd	nd	0.0483	0.2068	nd	213	nd	nd	nd	nd	1.01	9.65	169.5	0.4233	25.65	nd	2.891	nd	107.7	21.84	0.9064	nd	nd	nd
8	nd	nd	0.0591	0.3254	nd	295.2	nd	nd	nd	nd	3.008	6.923	206.1	2.145	27.73	nd	nd	nd	457	13.91	1.264	nd	nd	nd

	Al	As	B	Ba	Be	Ca	Cd	Co	Cr	Cu	Fe	K	Mg	Mn	Na	Ni	P	Pb	S	Si	Sr	Ti	V	Zn
MDL	0.05	0.06	0.04	0.005	0.001	0.01	0.01	0.008	0.008	0.005	0.01	0.1	0.01	0.002	0.01	0.01	0.1	0.05	0.1	0.05	0.005	0.005	0.05	0.01
Week 11																								
1	nd	nd	0.0647	0.1999	nd	232.1	nd	nd	0.0107	nd	0.0343	8.118	167.1	0.7112	28.19	nd	2.102	nd	284.2	9.823	0.9084	nd	nd	nd
2	nd	nd	0.0442	0.2244	nd	201.2	nd	nd	nd	nd	0.1163	6.816	163.6	0.1349	25.18	nd	1.162	nd	230.8	20.06	0.8383	nd	nd	nd
3	nd	nd	0.0611	0.0551	nd	91.73	nd	nd	nd	nd	0.173	6.601	160.4	0.0649	24.65	nd	1.694	nd	60.85	25.65	0.4789	nd	nd	nd
4	0.2959	nd	0.0448	0.3657	nd	259.9	nd	nd	nd	nd	0.6457	6.336	202.9	0.5744	27.18	nd	nd	nd	450.8	8.682	1.165	nd	nd	nd
5	0.1195	nd	0.052	0.1774	nd	234.9	nd	nd	nd	nd	0.249	9.19	173.8	0.3572	24.86	nd	1.824	nd	330.5	9.713	0.9643	nd	nd	nd
6	nd	nd	0.0562	0.0515	nd	56.18	nd	nd	nd	nd	0.1724	9.607	158.4	0.0527	27.49	nd	0.4822	nd	91.05	20.3	0.3714	nd	nd	nd
7	nd	nd	0.0445	0.1921	nd	212.1	nd	nd	nd	nd	0.5934	7.191	170.3	0.3722	23.96	nd	3.2	nd	129.7	19.48	0.8962	nd	nd	nd
8	nd	nd	0.0497	0.2829	nd	267.6	nd	nd	nd	nd	1.84	6.166	194.8	1.824	24.84	nd	nd	nd	446.9	12.43	1.149	nd	nd	nd
Week 12																								
1	nd	nd	0.0504	0.1927	0.0011	237.3	nd	nd	nd	nd	0.1177	7.043	169.8	0.5521	23.61	nd	1.815	nd	312.8	8.74	0.9393	nd	nd	nd
2	nd	nd	0.036	0.2383	nd	213.2	nd	nd	nd	nd	0.1533	7.042	167.4	0.0772	23.5	nd	1.298	nd	206.9	20.95	0.8879	nd	nd	nd
3	nd	nd	0.0571	0.0527	nd	95.79	nd	nd	nd	nd	0.1625	5.959	162.2	0.0623	23.92	nd	1.302	nd	63.4	24.78	0.4771	nd	nd	nd
4	0.0787	nd	nd	0.35	0.0029	257.4	nd	nd	nd	nd	0.1868	6.42	203.5	0.5313	26.99	nd	nd	nd	437.2	8.763	1.157	nd	nd	nd
5	nd	nd	0.0445	0.1683	0.002	232.9	nd	nd	nd	nd	0.0967	8.034	174.7	0.2878	23.6	nd	1.583	nd	385.7	8.942	0.9618	nd	nd	nd
7	nd	nd	0.0445	0.1942	0.001	209	nd	nd	nd	nd	0.4474	6.124	173.3	0.3652	22.65	nd	3.893	nd	123.5	20.16	0.8993	0.0146	nd	nd
8	nd	nd	0.0455	0.2726	nd	255.4	nd	nd	nd	nd	0.557	5.913	189.4	1.646	23.48	nd	nd	nd	423.8	11.68	1.109	nd	nd	nd
Stock	nd	nd	0.0516	0.0072	nd	264.2	nd	nd	nd	nd	0.0187	6.306	200.8	0.0031	23.32	0.0238	nd	nd	479	4.193	1.185	nd	nd	0.0162
Week 13																								
1	nd	nd	0.045	0.1833	nd	245.9	nd	nd	nd	nd	nd	7.008	176.8	0.4085	24.34	nd	1.608	nd	425.7	8.39	0.9834	nd	nd	nd
2	nd	nd	0.0506	0.0409	nd	85.23	nd	nd	nd	nd	0.1144	5.84	160.3	0.0629	23.67	nd	0.9113	nd	67.43	23.55	0.4138	nd	nd	nd
3	nd	nd	0.0483	0.0419	nd	85.49	nd	nd	nd	nd	0.113	5.863	159.7	0.0638	23.7	nd	0.9316	nd	64.16	22.49	0.4245	nd	nd	nd
4	nd	nd	0.04	0.2926	nd	253.7	nd	nd	nd	nd	0.0285	6.659	207.9	0.3659	27.4	nd	nd	nd	436.5	8.335	1.123	nd	nd	nd
5	nd	nd	0.0446	0.1583	nd	238.1	nd	nd	nd	nd	nd	7.693	174	0.2402	23.74	nd	1.392	0.3454	636.8	8.367	0.9603	nd	nd	nd
7	nd	nd	0.0431	0.2001	nd	216.9	nd	nd	nd	nd	0.3925	5.955	174.9	0.3954	22.9	nd	4.869	0.4639	107.2	21.91	0.9256	0.0141	nd	nd
8	nd	nd	0.0415	0.265	nd	264.9	nd	nd	nd	nd	1.036	6.129	191.9	1.534	23.89	nd	nd	nd	421.4	11.68	1.112	nd	nd	nd
Week 14																								
1	nd	nd	0.0464	0.1918	nd	244.3	nd	nd	nd	nd	0.0178	6.852	147.9	0.335	23.81	nd	1.252	nd	516.5	7.464	0.9829	nd	nd	nd
2	nd	nd	nd	0.2083	nd	197.8	nd	nd	nd	nd	0.1066	6.813	139.6	0.0248	22.42	nd	1.17	nd	187.7	20.45	0.8434	nd	nd	nd
3	nd	nd	0.0564	0.0571	nd	111	nd	nd	nd	nd	0.1253	5.764	144.8	0.0783	22.32	nd	1.203	nd	64.22	22.73	0.5506	nd	nd	nd
4	nd	nd	nd	0.3135	nd	237.9	nd	nd	nd	nd	0.0633	6.162	156.9	0.3989	24.26	nd	nd	nd	403.8	7.05	1.04	nd	nd	nd
5	nd	nd	0.0438	0.163	nd	235	nd	nd	nd	nd	0.0108	7.424	149.8	0.2156	23.06	nd	1.116	nd	412.4	7.753	0.9594	nd	nd	nd
7	nd	nd	0.053	0.1903	nd	211.6	nd	nd	nd	nd	0.3913	6.077	151.9	0.4104	22.16	nd	4.915	nd	100.8	22.58	0.9004	0.0147	nd	nd
8	nd	nd	0.0488	0.2763	nd	261.8	nd	nd	nd	nd	1.016	6.394	162	1.417	23.83	nd	nd	nd	428.1	11.27	1.109	nd	nd	nd
Week 15																								
1	nd	nd	0.0437	0.1852	nd	240.6	nd	nd	nd	nd	0.0313	6.462	172.8	0.2919	22.97	nd	1.15	nd	415.2	6.782	0.9692	nd	nd	nd
3	nd	nd	0.053	0.0576	nd	109.5	nd	nd	nd	nd	0.1001	6.016	164.8	0.0725	22.39	nd	1.195	nd	98.91	21.4	0.5414	nd	nd	nd
4	nd	nd	nd	0.308	nd	239.3	nd	nd	nd	nd	0.053	6.004	188.7	0.3859	24.28	nd	nd	nd	414.8	6.801	1.036	nd	nd	nd
5	nd	nd	0.0439	0.1625	nd	238.2	nd	nd	nd	nd	0.0168	6.922	174	0.1991	22.88	nd	1.046	nd	609.4	7.362	0.9602	nd	nd	nd
7	nd	nd	0.0527	0.1815	nd	219.1	nd	nd	nd	nd	0.2939	6.165	174.3	0.3667	22.16	nd	4.613	nd	135.7	21.08	0.9151	0.0131	nd	nd
8	nd	nd	0.0471	0.2556	nd	244.7	nd	nd	nd	nd	0.5986	5.803	185	1.248	21.94	nd	nd	nd	404.4	10.36	1.038	nd	nd	nd
Stock	nd	nd	0.0506	0.0071	nd	253.8	nd	nd	nd	nd	nd	6.136	194.2	0.0054	21.98	0.0208	nd	nd	476.4	3.554	1.097	nd	nd	nd

	Al	As	B	Ba	Be	Ca	Cd	Co	Cr	Cu	Fe	K	Mg	Mn	Na	Ni	P	Pb	S	Si	Sr	Ti	V	Zn
MDL	0.05	0.06	0.04	0.005	0.001	0.01	0.01	0.008	0.008	0.005	0.01	0.1	0.01	0.002	0.01	0.01	0.1	0.05	0.1	0.05	0.005	0.005	0.05	0.01
Week 16																								
1	nd	nd	0.0427	0.1874	nd	233.6	nd	nd	nd	nd	0.0262	6.25	161.7	0.2785	22.69	nd	1.11	nd	322.2	6.673	1.065	nd	nd	nd
3	nd	nd	0.0529	0.0835	nd	134.3	nd	nd	nd	nd	0.1025	5.831	160.3	0.0982	21.96	nd	1.735	nd	130.4	22.67	0.7482	nd	nd	nd
4	nd	nd	0.0351	0.3313	nd	236.1	nd	nd	nd	nd	0.0588	5.789	178.4	0.4005	23.98	nd	nd	nd	404.9	6.389	1.139	nd	nd	nd
5	nd	nd	0.0425	0.1699	nd	237.4	nd	nd	nd	nd	0.0206	6.527	167.4	0.198	23.13	nd	0.9893	nd	507.3	7.306	1.077	nd	nd	nd
7	nd	nd	0.0518	0.1776	nd	215.5	nd	nd	nd	nd	0.2671	5.97	163.8	0.3943	22.01	nd	4.458	nd	161.1	21.07	1.003	0.012	nd	nd
8	nd	nd	0.0489	0.2851	nd	254.1	nd	nd	nd	nd	0.7225	6.012	182.2	1.328	23.57	nd	nd	nd	414.5	11.25	1.199	nd	nd	nd
Stock	nd	nd	0.0559	0.0072	nd	269.3	nd	nd	nd	nd	nd	6.405	194.6	0.0065	24.63	0.0337	nd	nd	483.1	3.924	1.318	nd	nd	0.0162
Week 17																								
1	nd	nd	0.0467	0.1583	nd	199.5	nd	nd	nd	nd	0.1965	5.483	140.9	0.2536	19.73	nd	0.5	nd	248.6	5.902	0.8983	nd	nd	nd
3	nd	nd	0.0539	0.1464	nd	177.6	nd	nd	nd	nd	0.5355	6.08	164.5	0.2565	21.92	nd	2.849	nd	132.2	28.81	0.946	0.0068	nd	nd
4	nd	nd	nd	0.372	nd	244.6	nd	nd	nd	nd	0.2245	5.785	177.2	0.7869	24.04	nd	nd	nd	394	7.138	1.157	nd	nd	nd
5	nd	nd	0.0437	0.1648	nd	233.6	nd	nd	nd	nd	0.0308	6.242	165.9	0.1842	23.39	nd	0.9253	nd	675.1	7.161	1.059	nd	nd	nd
7	nd	nd	0.0516	0.1744	nd	217.7	nd	nd	nd	nd	0.3403	6.099	165.4	0.3811	22.65	nd	4.481	nd	189.8	20.45	1.002	0.012	nd	nd
8	nd	nd	0.0498	0.2813	nd	253.2	nd	nd	nd	nd	0.7885	5.935	183.6	1.246	24.07	nd	nd	nd	431.8	11.43	1.182	nd	nd	nd
Week 18																								
4	nd	nd	nd	0.3375	nd	238.9	nd	nd	nd	nd	0.1066	5.702	170.4	0.6175	23.51	nd	nd	nd	352.9	6.327	1.13	nd	nd	nd
5	nd	nd	0.0452	0.167	nd	236.3	nd	nd	nd	nd	nd	6.246	165.8	0.1735	23.39	nd	0.8617	nd	634.9	6.704	1.074	nd	nd	nd
7	nd	nd	0.0546	0.1754	nd	224.8	nd	nd	nd	nd	0.1635	6.347	167.6	0.3774	23.25	nd	4.235	nd	201.1	19.08	1.035	0.0113	nd	nd
8	nd	nd	0.0528	0.2938	nd	261.6	nd	nd	nd	nd	0.8739	6.139	188.5	1.23	24.52	nd	nd	nd	408	11.3	1.22	nd	nd	nd
Stock	nd	nd	0.0572	0.0074	nd	269.1	nd	nd	nd	nd	nd	6.421	196	nd	24.77	0.0247	nd	nd	474.2	3.792	1.287	nd	nd	0.0125
Week 19																								
1	nd	nd	0.043	0.1587	nd	204.6	nd	nd	nd	nd	0.034	6.7	146.1	0.2212	24.63	nd	1.231	nd	258.7	6.408	0.9354	nd	nd	nd
2	nd	nd	0.0417	0.0994	nd	88.86	nd	nd	nd	nd	0.1199	7.411	158.2	0.0144	23.79	nd	0.6547	nd	78.85	20.98	0.6038	nd	nd	nd
3	nd	nd	0.0554	0.0443	nd	78.54	nd	nd	nd	nd	0.1238	6.676	162.1	0.0574	23.88	nd	0.9716	nd	100.3	17.77	0.4883	nd	nd	nd
4	nd	nd	nd	0.2409	nd	237	nd	nd	nd	nd	0.1482	5.887	180.8	0.2442	25.02	nd	nd	nd	442.8	4.438	1.138	nd	nd	nd
5	nd	nd	0.0443	0.1731	nd	251.3	nd	nd	nd	nd	0.0167	6.422	173.6	0.1645	24.72	nd	0.8515	nd	866.3	6.458	1.142	nd	nd	nd
6	nd	nd	0.0867	0.0448	nd	37.49	nd	nd	nd	nd	0.0649	15	246.8	0.0722	39.18	nd	0.4802	nd	126.8	20.63	0.3787	nd	nd	nd
7	nd	nd	0.0496	0.1014	nd	227.9	nd	nd	nd	nd	0.1156	6.713	175.3	0.1603	24.45	nd	0.5478	nd	300.5	12.28	1.027	nd	nd	nd
8	nd	nd	0.0521	0.2832	nd	258.5	nd	nd	nd	nd	1.019	6.028	183.2	1.105	24.45	nd	nd	nd	434.2	10.95	1.208	nd	nd	nd

	Al	As	B	Ba	Be	Ca	Cd	Co	Cr	Cu	Fe	K	Mg	Mn	Na	Ni	P	Pb	S	Si	Sr	Ti	V	Zn
MDL	0.05	0.06	0.04	0.005	0.001	0.01	0.01	0.008	0.008	0.005	0.01	0.1	0.01	0.002	0.01	0.01	0.1	0.05	0.1	0.05	0.005	0.005	0.05	0.01
Week 20																								
1	nd	nd	0.0431	0.2082	nd	233.1	nd	nd	nd	nd	0.0302	6.279	155.6	0.1618	23.63	nd	0.6514	nd	557	5.562	1.15	nd	nd	nd
2	nd	nd	0.0431	0.2083	nd	176.6	nd	nd	nd	nd	0.0802	7.198	167.5	0.0302	23.35	nd	0.9736	nd	231.7	20.08	0.9872	nd	nd	nd
3	nd	nd	0.0529	0.0794	nd	129.6	nd	nd	nd	nd	0.0894	6.597	163.1	0.0624	23.29	nd	0.8826	nd	216.3	16.31	0.8035	nd	nd	nd
4	nd	nd	nd	0.2826	nd	244.8	nd	nd	nd	nd	0.05	6.343	171.7	0.2185	24.76	nd	nd	nd	438.9	4.657	1.245	nd	nd	nd
5	nd	nd	0.0442	0.181	nd	241	nd	nd	nd	nd	0.0273	6.139	161	0.1491	23.21	nd	0.748	nd	608.5	6.238	1.184	nd	nd	nd
6	nd	nd	0.0778	0.0887	nd	74.72	nd	nd	nd	nd	0.0466	9.597	194.1	0.0815	27.76	nd	0.4399	nd	224.4	21.24	0.6062	nd	nd	nd
7	nd	nd	0.0495	0.1088	nd	223	nd	nd	nd	nd	0.0831	6.585	165.6	0.1354	23.36	nd	0.7865	nd	299.5	12.12	1.084	nd	nd	nd
8	nd	nd	0.0521	0.2955	nd	249.2	nd	nd	nd	nd	0.7408	6.339	170.4	0.9976	23.28	nd	nd	nd	414.9	11.13	1.254	nd	nd	nd
Stock	nd	nd	0.0541	0.0065	nd	256.5	nd	nd	nd	nd	nd	6.046	175.1	nd	23.44	0.0282	nd	nd	467.1	3.673	1.315	nd	nd	nd
Week 21																								
1	nd	nd	nd	0.1851	nd	204.4	nd	nd	nd	nd	0.0365	5.348	148	0.1352	20.37	nd	0.6278	nd	886.4	5.035	1.078	nd	nd	nd
2	nd	nd	nd	0.2125	nd	183.7	nd	nd	nd	nd	0.0751	5.505	160.2	0.0305	20.11	nd	1.032	nd	264.7	19.3	0.9954	nd	nd	nd
3	nd	nd	0.0444	0.0904	nd	144.8	nd	nd	nd	nd	0.0712	5.944	155.6	0.0699	20.3	nd	0.9259	nd	238.6	15.28	0.8624	nd	nd	nd
4	nd	nd	nd	0.248	nd	218.7	nd	nd	nd	nd	0.0256	5.479	169.9	0.183	21.85	nd	nd	nd	415	3.915	1.166	nd	nd	nd
5	nd	nd	0.04	0.1578	nd	211.4	nd	nd	nd	nd	0.0222	5.568	155.2	0.1294	20.51	nd	0.6697	nd	617.5	5.721	1.094	nd	nd	nd
6	nd	nd	0.0679	0.1154	nd	100.4	nd	nd	nd	nd	0.0376	6.557	170.5	0.0831	21.77	nd	0.3822	nd	248.1	20.24	0.7379	nd	nd	nd
7	nd	nd	0.0451	0.0922	nd	189.2	nd	nd	nd	nd	0.0902	5.894	160.3	0.1236	20.34	nd	0.8295	nd	283.1	11.88	0.9838	nd	nd	nd
8	nd	nd	0.0485	0.2615	nd	222	nd	nd	nd	nd	0.3596	5.323	171.7	0.9747	20.56	nd	nd	nd	407.5	10.95	1.186	nd	nd	nd
Week 22																								
1	nd	nd	0.041	0.2059	nd	234.8	nd	nd	nd	nd	0.0291	6.042	159.6	0.1352	23.53	0.0101	0.7508	nd	1100	5.157	1.224	nd	nd	nd
2	nd	nd	0.0448	0.2765	nd	235.2	nd	nd	nd	nd	0.078	5.608	174.4	0.1212	24.2	nd	1.086	nd	453.3	22.3	1.247	nd	nd	nd
3	nd	nd	0.0511	0.1137	nd	193.5	nd	nd	nd	nd	0.0667	7.09	173	0.0827	24.53	nd	0.7574	nd	460.6	15.49	1.097	nd	nd	nd
4	nd	nd	0.0462	0.2901	nd	275.3	nd	nd	nd	nd	0.0273	6.884	188.2	0.2256	27.99	nd	nd	nd	747.1	4.115	1.468	nd	nd	nd
5	nd	nd	0.0452	0.1773	nd	240.7	nd	nd	nd	nd	0.0126	6.282	165.4	0.0305	23.77	nd	0.7108	nd	569.4	6.02	1.236	nd	nd	nd
6	nd	nd	0.0752	0.1927	nd	153.8	nd	nd	nd	nd	0.0578	6.825	179	0.0699	24.54	nd	0.8454	nd	288.1	22.06	1.002	nd	nd	nd
7	nd	nd	0.0531	0.1161	nd	205.6	nd	nd	nd	nd	0.1015	6.778	172	0.183	23.87	nd	1.209	nd	312.7	13.43	1.104	nd	nd	nd
8	nd	nd	0.0544	0.2857	nd	254.5	nd	nd	nd	nd	0.0973	6.068	181.8	0.1294	24.1	nd	nd	nd	445.7	11.29	1.32	nd	nd	nd
Stock	nd	nd	0.0574	0.0073	nd	262.6	nd	nd	nd	nd	nd	6.309	188.8	0.0831	24.48	0.0286	nd	nd	506.4	3.77	1.38	nd	nd	nd
Week 23																								
1	nd	nd	0.0419	0.2054	nd	238.8	nd	nd	nd	nd	0.0522	6.2	159.4	0.149	23.6	nd	0.674	nd	1129	4.852	1.268	nd	nd	nd
2	nd	nd	0.04	0.2655	nd	226.6	nd	nd	nd	nd	0.0803	5.305	169.5	0.0978	23.24	nd	1.018	nd	434.6	21	1.215	nd	nd	nd
3	nd	nd	0.0487	0.1145	nd	186.7	nd	nd	nd	nd	0.0656	6.837	168.2	0.0809	23.65	nd	0.6962	nd	449.1	14.34	1.064	nd	nd	nd
4	nd	nd	0.0429	0.2803	nd	272	nd	nd	nd	nd	0.0258	6.646	187	0.2028	28.33	nd	nd	nd	718	3.836	1.456	nd	nd	nd
5	nd	nd	0.045	0.1844	nd	245.1	nd	nd	nd	nd	0.0202	6.304	163.5	0.1315	24.03	nd	0.66	nd	941.3	5.754	1.284	nd	nd	nd
6	nd	nd	0.0679	0.2274	nd	190.5	nd	nd	nd	nd	0.1141	6.258	170.2	0.2325	24.25	nd	0.8827	nd	438.9	20.05	1.114	nd	nd	nd
7	nd	nd	0.05	0.1171	nd	217.8	nd	nd	nd	nd	0.093	6.519	169	0.1353	23.6	nd	0.9867	nd	447.2	12.92	1.153	nd	nd	nd
8	nd	nd	0.0526	0.2927	nd	257.9	nd	nd	nd	nd	0.1053	6.064	175.9	1.028	24.45	nd	nd	nd	638.1	11.05	1.36	nd	nd	nd
Stock	nd	nd	0.0665	0.0093	nd	299.3	nd	nd	nd	nd	nd	7.125	198.1	0.002	30.9	0.0267	nd	nd	813.4	4.135	1.717	nd	nd	nd

IC and ORP Results.

	Alkalinity	Conductivity	Chloride	Nitrate	Sulphate	pH	ORP
MDL	1	0.2	0.05	0.009	0.03		
Week 1	mg/L	uS/cm	mg/L	mg/L	mg/L		mv
1	112.6	nd	5.17	0.021	12.14	7.05	-51.1
2	1164.8	nd	71.85	0.229	126.62	7.322	-26.7
3	483.3	nd	19.51	0.043	91.32	7.598	-59.8
4	152.5	nd	76.17	<DL	1240.2	7.087	1.5
5	1302.3	nd	126.08	<DL	733.17	7.169	-57.9
6	683.1	nd	133.1	0.033	522.27	7.588	-91.8
7	1191	nd	127.69	<DL	616.02	6.656	-41.4
8	165.3	nd	108.45	0.024	1216.58	7.366	-15.4
9	48.2	nd	14.15	1.083	1760.7	7.671	3.6
Week 2							
1	741.2	nd	51.58	<DL	332.62	7.447	-34.3
2	945	nd	35.88	<DL	36.8	7.298	-127.6
3	1356.4	nd	58.08	0.136	255.43	8.775	-113.5
4	244.1	nd	36.23	<DL	1303.38	7.125	-35.4
5	1236.5	nd	46.34	<DL	699.2	7.662	-12.9
6	1091.4	nd	78.58	0.042	236.22	7.65	-83.5
7	1547.8	nd	56.11	0.236	357.67	6.826	-73.7
8	205.8	nd	34.02	0.017	1527.79	6.769	11.6
Week 3							
1	889.5	nd	35.35	<DL	75.65	7.642	149.2
2	960.9	nd	28.29	<DL	4.12	7.53	-133
3	1143.6	nd	30.5	0.025	79.35	7.901	-126.8
4	227.4	nd	22.3	<DL	1331.65	7.235	-12.7
5	943.7	nd	32.36	<DL	590.6	7.494	-54.2
6	1133.7	nd	25.85	<DL	112.62	7.554	-19.4
7	1581.5	nd	34.31	<DL	59.09	7.097	-72.2
8	67.7	nd	13.71	<DL	934.32	6.545	53.7
Week 4							
1	1166.5	nd	31.56	0.18	210.23	7.552	3.6
2	925.5	nd	19.08	0.258	36.71	7.444	-57.4
3	852.1	nd	25.36	0.733	139.18	7.716	-47.7
4	223.5	nd	21.51	0.303	1300.12	7.471	-20.2
5	788.3	nd	27.28	0.182	701.18	7.556	-132.1
6	806.7	nd	42.36	0.247	110.22	7.763	3.6
7	1357.2	nd	25.17	0.328	83.75	7.237	-62.1
8	130.2	nd	19.96	0.943	1570.6	6.681	16.3
Week 5							
1	794.1	2050	22.48	<DL	337.15	7.509	-156.9
2	844	1564	22.47	<DL	43.27	7.549	-44.5
3	655.7	1404	18.82	0.013	139.61	7.703	-101.3
4	208.6	2160	52.44	0.084	1303.93	7.384	-70.7
5	739.8	2240	26.9	<DL	626.58	7.58	-224.4
6	784	1512	22.78	<DL	85.78	8.128	-60.4
7	1199.7	2280	22.88	0.015	136	7.375	-105.4
8	121.9	2330	17.59	0.058	1545.34	6.72	25.9

	Alkalinity	Conductivity	Chloride	Nitrate	Sulphate	pH	ORP
MDL	1	0.2	0.05	0.009	0.03		
Week 6	mg/L	uS/cm	mg/L	mg/L	mg/L		mv
1	671.8	2010	22.08	<DL	478.74	7.556	-227.3
2	873.9	1628	19.01	<DL	79.75	7.965	-99
3	661.4	1446	18.08	0.018	178.01	8.128	-74.7
4	203.9	2220	16.19	0.048	1220.16	8.065	-16
5	660.9	2070	19.22	<DL	588.58	7.844	-71.8
6	718.1	1442	20.78	0.012	180.12	8.72	-61.6
7	1070.2	2070	18.36	0.026	157.53	7.619	-91.9
8	147.1	2260	18.49	0.052	1384.91	6.937	31.7
Week 7							
1	631.4	1857	26.09	<DL	479.24	7.616	-255.9
2	815.5	1491	0.52	<DL	91.3	8.328	-91.9
3	650.6	1298	0.33	<DL	108.35	8.342	-149.4
4	162.2	2160	18.85	<DL	1282.71	8.372	-35.1
5	710.1	2040	0.57	<DL	523.77	7.989	-244.8
6	558.8	1261	22.87	<DL	226.02	8.878	-154.7
7	1091.5	2010	0.74	<DL	112.46	7.575	-118.4
8	165.9	2400	19.95	<DL	1464.05	6.917	33.4
Week 8							
1	603.2	1995	25.41	<DL	857.32	7.535	-295.6
2	784.6	1636	23.93	<DL	329.53	8.453	-92.4
3	660	1305	22.63	<DL	123.6	8.409	-68.8
4	148.3	2230	22.69	0.039	1833.62	8.343	-33.1
5	657.7	2040	24.28	<DL	895.02	8.08	-293.8
6	477.4	1341	22.82	<DL	446.68	8.959	-31.7
7	937.4	1972	24.53	<DL	329.04	7.727	-89.1
8	164.4	2390	21.63	0.052	1875.62	6.964	1.9
9	49.1	2500	18.81	0.893	2342.57	7.907	160.1
Week 9							
1	518.6	1821	24.18	<DL	895.55	7.557	-256.8
2	624.9	1723	21.93	<DL	643.45	8.381	-124
3	778.3	1400	22.79	0.04	106.08	8.717	-111
4	161.2	2290	23	0.028	1890.79	8.201	-165.1
5	776.1	2240	25.03	0.036	756.88	7.806	-318.4
6	392.7	1476	23.25	0.153	658.03	8.778	-283.5
7	937.5	2060.2	24.5	0.092	425.73	7.66	-155.8
8	146.5	2370	20.08	0.06	1848.8	6.954	-59.8
Week 10							
1	600	2040	24.38	7.498	642.45	7.793	-327.3
2	636.6	1937	22.46	9.106	594.08	8.43	-225.4
3	795.9	1393	28.2	<DL	91.09	8.916	-166.6
4	149.4	2290	70.02	<DL	1373.05	8.399	-173.4
5	635.5	2130	29.46	<DL	709.19	8.119	-284.2
6	406.4	1463	24.05	8.406	467.15	8.806	132.9
7	914.3	2040	20.98	<DL	337.79	7.76	-163.6
8	147.3	2330	70.54	0.107	1391.32	7.209	36.4

	Alkalinity	Conductivity	Chloride	Nitrate	Sulphate	pH	ORP
MDL	1	0.2	0.05	0.009	0.03		
Week 11	mg/L	uS/cm	mg/L	mg/L	mg/L		mv
1	521.6	1915	17.5	<DL	714.75	8.222	-330.4
2	549.4	1872	29.09	0.075	653.25	8.316	-205.6
3	772	1462	0.18	0.011	137.85	8.786	-121.2
4	143.9	2220	15.02	0.046	1416	8.252	-119.6
5	575.3	2160	16.7	0.021	795.5	8.306	-276.8
6	498.1	1337	32.85	<DL	257.75	8.668	34.5
7	886.1	2070	0.35	<DL	408.5	7.904	-102.2
8	152.8	2340	13.98	<DL	1373.5	7.191	-5.8
Week 12							
1	397.1	1775	26.46	<DL	1077.15	7.804	-290.6
2	572.8	1942	26.35	0.048	872.66	8.326	-199.6
3	760.6	1447	20.37	<DL	234.41	8.943	-188
4	151.1	2360	20.56	<DL	1737.4	8.574	-115.9
5	510.9	2130	19.73	<DL	1068.62	8.277	-284
7	895.3	2110	36.9	<DL	508.57	7.944	-198.1
8	151.6	2350	18.53	<DL	1886.04	7.164	12.4
9	50.2	2490	17.79	0.807	1987.65	7.915	368.7
Week 13							
1	509.5	2090	14.53	<DL	845.48	8.11	-341.1
2	499.8	1820	14.07	<DL	695.72	8.665	-202.9
3	695.5	1443	15.25	0.015	194.69	8.934	-244.6
4	122.2	2390	14.99	0.027	1433.74	8.602	-108.4
5	551.7	2250	14.56	0.042	819.78	8.341	-292.2
7	1015.2	2250	23.12	0.059	353.52	7.847	33.4
8	162	2440	13.75	<DL	1430.2	7.108	24.9
Week 14							
1	527.5	2200	14.94	<DL	813.95	8.225	-343.7
2	610.6	1932	14.65	<DL	588.92	8.564	-235.5
3	793.8	1588	14.64	<DL	206.11	8.708	-122
4	151.1	2320	13.9	<DL	1310.12	8.382	-250.8
5	5681	2220	14.34	<DL	803.93	8.278	-291
7	1014.7	2210	18.01	<DL	335.04	7.998	38.3
8	178.7	2450	13.83	<DL	1412.07	7.269	17.6
Week 15							
1	470.1	2060	16.75	<DL	959.85	8.054	-340
3	680.2	1575	16.45	<DL	338.78	8.808	-260.9
4	135.8	2240	17.32	<DL	1483.15	8.331	-283.4
5	542.8	2190	16.59	<DL	904.75	8.372	-307.5
7	932.5	2230	16.64	<DL	492.88	7.801	-73.5
8	170.7	2400	16.68	<DL	1500.45	7.396	19.8
9	50.1	2490	16.72	0.678	1754.4	7.948	205.4

	Alkalinity	Conductivity	Chloride	Nitrate	Sulphate	pH	ORP
MDL	1	0.2	0.05	0.009	0.03		
Week 16	mg/L	uS/cm	mg/L	mg/L	mg/L		mv
1	486.1	2160	16.8	<DL	978.5	7.959	-349.5
3	704.6	1805	17.51	<DL	477	8.479	-194.6
4	145.1	2310	18.43	<DL	1476	8.269	-245.6
5	510	2240	17.31	<DL	944.5	8.376	-300.4
7	838	2230	16.97	<DL	601.25	7.789	-225.1
8	168.3	2360	17.92	<DL	1518.5	7.227	2.4
9	50.5	2530	17.91	0.71	1795	7.946	82.2
Week 17							
1	499.8	2100	15.85	<DL	866	8.247	-369.1
3	754.9	1963	17.92	<DL	474	8.005	-171.5
4	227.7	2220	18.15	<DL	1399	7.637	-244.6
5	496.2	2150	18.01	<DL	1005	8.177	-313.5
7	820.2	2240	15.36	<DL	684.75	7.954	-257.5
8	180.8	2430	17.98	<DL	1561.5	7.285	-33.3
Week 18							
4	294.9	2280	21.01	<DL	1353.85	7.986	-240.5
5	501.1	2200	21.87	<DL	1069.96	8.195	-294.9
7	746.3	2180	25.13	0.068	846.26	8.13	-256.2
8	185.6	2440	19.98	0.043	1680.72	7.554	56.8
9	50	2510	16.61	0.802	1941.44	7.939	51
Week 19							
1	542.9	2030	39.25	0.05	800.04	7.875	-356
2	727.2	1594	5.61	<DL	274.28	8.314	-234.9
3	604.2	1436	24.24	<DL	377.74	8.553	-260.1
4	94.4	2280	68.4	0.051	1739.77	7.691	-273.3
5	482.6	2390	57.89	<DL	1195.93	8.136	-335.2
6	945.3	1965	78.22	<DL	430.99	8.858	-242.6
7	508	2300	27.23	<DL	1278.34	7.656	-275.7
8	178	2450	21.09	<DL	1727.71	7.313	-19.7

	Alkalinity	Conductivity	Chloride	Nitrate	Sulphate	pH	ORP
MDL	1	0.2	0.05	0.009	0.03		
Week 20	mg/L	uS/cm	mg/L	mg/L	mg/L		mv
1	463.5	2140	24.65	<DL	1042.07	8.154	-346.1
2	487.7	1991	24.93	0.119	921.89	8.427	-198.6
3	393.9	1828	16.51	<DL	961.56	8.686	-291.6
4	89.8	2460	16.88	0.063	1827.47	8.049	-260.3
5	416.6	2360	16.73	<DL	1255.97	8.194	-318.2
6	417.1	1926	26.74	<DL	887.33	8.264	-244
7	434.7	2310	17.07	0.053	1348.19	8.1	-219.7
8	169.5	2470	16.3	<DL	1749.63	7.216	1.4
9	48.4	2550	14.9	<DL	2000.92	7.48	110.5
Week 21							
1	460.7	2080	15.67	<DL	962.08	8.043	-238.5
2	483.5	2180	17.01	0.087	1015.95	8.448	-235.7
3	378.4	1906	16.1	0.072	1019.54	8.359	-210.5
4	95.5	2430	16.78	<DL	1681.31	8.16	-210.9
5	429.2	2340	16.93	<DL	1110.7	8.145	-238.2
6	322.8	1929	17.5	<DL	939.31	8.492	-201.8
7	425.4	2250	16.57	0.067	1278.07	8.209	-238
8	164.6	2470	16.15	<DL	1622.49	7.74	-12.4
Week 22							
1	470.6	1985	24.34	<DL	1028.54	8.06	-340.8
2	519.9	2300	24.56	0.226	1187.3	8.597	-262.5
3	399.9	2140	24.26	0.185	1174.55	8.865	-202.2
4	110.4	2650	39.58	0.165	1855.12	8.332	-184.1
5	446.3	2330	24.67	<DL	1218.18	8.188	-306.8
6	358.3	2050	25.24	<DL	1088.94	7.987	-268.1
7	445.1	2250	18.37	<DL	1282.45	8.097	-252.3
8	152.8	2440	35.4	<DL	1726.47	7.303	0.9
9	47.9	2530	30.69	0.831	1961.07	7.488	112
Week 23							
1	451.7	2250	19.56	<DL	1088.2	8.094	-281
2	472.5	2230	18.43	<DL	1160.91	8.502	-217.6
3	370.8	2130	23.92	0.185	1185.82	8.794	-290.7
4	110.3	2660	25.97	<DL	1791.31	8.438	-254.3
5	418.4	2370	24.17	<DL	1254.86	8.283	-312.3
6	406.4	2130	25.02	<DL	1146.95	8.61	-299
7	455.7	2280	21.26	<DL	1203.54	8.535	-256.5
8	174.7	2520	27.86	<DL	1588.04	7.16	-19.5
9	66.7	2870	34.33	1.146	2098.65	8.06	87.9

Appendix D: Post-Experiment Testing Results

Digestion ICP-AES Results

Samples 15A/B, 26A/B, 37A/B, and 48A/B are raw mixtures corresponding to the reactors they were used in.

	Al	As	B	Ba	Be	Ca	Cd	Co	Cr	Cu	Fe	K	Mg
All in mg/kg													
1A	37248	BDL	78.399	286.07	BDL	50342	BDL	BDL	84.1	92.7	203336	2718.9	23486
1B	30229	BDL	77.348	319.34	BDL	56796	BDL	BDL	72.5	93.6	173007	2367.8	23236
1C	47166	BDL	BDL	458.29	BDL	41889	BDL	BDL	101.6	103.7	237097	3541.5	25668
1D	138414	BDL	BDL	1194.59	BDL	106595	BDL	BDL	329.7	254.1	571171	17081.1	69928
2A	41198	BDL	62.338	233.62	BDL	33088	BDL	BDL	78.1	74.7	195527	4310.2	22713
2B	34796	BDL	53.876	301.18	BDL	27569	BDL	BDL	69.5	64.5	191590	3099.9	19514
2C	32624	BDL	62.166	305.86	BDL	28752	BDL	BDL	62.9	57.2	155541	3270.1	17962
2D	34582	BDL	72.080	371.17	BDL	33952	BDL	BDL	64.3	63.6	169511	3502.9	20729
3A	14445	BDL	BDL	86.55	BDL	20556	BDL	BDL	27.9	53.8	91540	2003.0	8071
3C	36185	BDL	46.509	324.79	BDL	53711	BDL	BDL	75.3	89.4	176251	2720.2	20022
3D	43030	BDL	BDL	342.42	BDL	36667	BDL	BDL	91.6	84.0	185690	3532.0	24478
4A	51890	BDL	BDL	301.59	BDL	40202	BDL	BDL	129.0	108.2	250101	5492.1	32958
4B	47307	BDL	BDL	441.55	BDL	27513	BDL	BDL	126.6	85.1	210115	4985.7	21487
4C	56602	BDL	BDL	498.06	BDL	38971	BDL	BDL	137.9	102.9	238301	6932.0	29578
4D	33235	BDL	BDL	308.48	BDL	21483	BDL	BDL	79.7	61.9	137594	3660.0	16560
5A	33553	BDL	BDL	285.03	BDL	36069	BDL	BDL	84.9	77.3	182237	3301.0	19243
5B	39564	BDL	BDL	337.39	BDL	48234	BDL	BDL	60.1	70.4	214335	5006.9	21856
5C	29501	BDL	BDL	298.34	BDL	50776	BDL	BDL	68.2	79.9	151054	3639.6	22458
5D	34198	BDL	BDL	319.90	BDL	44750	BDL	BDL	77.8	89.1	178973	4903.7	19892
6A	31853	BDL	45.778	248.86	BDL	32278	BDL	BDL	74.5	71.2	186830	3389.3	19713
6B	29108	BDL	50.903	265.12	BDL	26907	BDL	BDL	69.8	63.3	163770	3195.3	17494
6C	24075	BDL	BDL	265.41	BDL	32977	BDL	BDL	57.4	54.9	128451	3194.0	16511
6D	34651	BDL	BDL	357.81	BDL	38041	BDL	BDL	78.7	68.3	172021	4250.7	23071
7A	24801	BDL	BDL	184.21	BDL	40862	BDL	BDL	62.3	74.2	179007	2873.9	15701
7B	37359	BDL	BDL	252.42	BDL	34147	BDL	BDL	88.5	81.6	203849	3454.5	20730
7C	26910	BDL	BDL	301.10	BDL	48020	BDL	BDL	71.0	99.2	156465	3073.8	17268
7D	21467	BDL	BDL	208.43	BDL	36535	BDL	BDL	58.3	63.2	148433	2637.9	17929
8A	49132	BDL	BDL	299.07	BDL	36021	BDL	BDL	123.9	116.2	241789	4016.0	30547
8B	56351	BDL	BDL	505.19	BDL	37674	BDL	BDL	139.9	103.4	240716	5220.0	29785
8C	43526	BDL	BDL	455.45	BDL	28910	BDL	BDL	104.7	95.3	198910	3914.2	23815
8D	56761	BDL	BDL	514.86	BDL	32541	BDL	BDL	128.5	110.9	242604	5539.2	27265
15A	32709	BDL	78.019	337.00	BDL	47817	BDL	BDL	62.1	75.2	124365	11493.8	16223
15B	32054	BDL	92.840	349.02	BDL	44815	BDL	BDL	61.5	75.4	128261	10840.3	16428
26A	21608	BDL	59.805	248.75	BDL	23523	BDL	BDL	41.9	44.2	86216	7537.1	12852
26B	20618	BDL	57.675	238.25	BDL	22943	BDL	BDL	40.1	43.2	79922	7952.9	12516
37A	22198	BDL	44.048	219.87	BDL	35522	BDL	BDL	45.8	62.4	85577	14926.7	12179
37B	20138	BDL	40.414	219.82	BDL	35778	BDL	BDL	43.0	66.4	83964	15726.0	11883
48A	67631	BDL	BDL	658.16	BDL	34582	BDL	BDL	127.4	113.2	248312	7032.6	29021
48B	68425	BDL	BDL	658.84	BDL	37044	BDL	BDL	121.5	96.7	242431	7301.1	30718

	Mn	Mo	Na	Ni	P	Pb	S	Si	Sr	Ti	V	Zn	Zr
All in mg/kg													
1A	2168.5	BDL	1931.6	60.72	4749.0	BDL	52310	439.5	208.2	1311.6	BDL	371.14	BDL
1B	2058.4	BDL	1591.2	52.57	6909.2	BDL	35249	467.6	220.8	1012.8	BDL	355.80	BDL
1C	2951.6	BDL	2523.0	68.20	4974.7	BDL	24171	802.5	197.0	1811.1	BDL	401.38	BDL
1D	7254.1	BDL	9466.7	BDL	9553.2	BDL	63820	3789.2	776.6	5032.4	BDL	1021.62	BDL
2A	2005.8	BDL	2542.6	55.56	2590.2	BDL	60967	383.0	161.2	1515.2	BDL	315.58	BDL
2B	2082.8	BDL	1968.5	50.72	3185.3	BDL	39790	378.7	135.5	1226.5	BDL	307.23	BDL
2C	1690.4	BDL	2063.7	39.24	2610.2	BDL	44841	341.4	162.3	1231.1	BDL	295.41	BDL
2D	1797.8	BDL	2076.2	39.44	2464.0	BDL	46877	483.7	182.9	1289.6	BDL	339.52	BDL
3A	448.7	BDL	758.5	33.51	2471.8	BDL	47423	707.6	100.5	508.3	BDL	159.13	BDL
3C	2336.4	BDL	1918.6	49.59	7510.7	BDL	50335	512.7	208.7	1294.1	BDL	312.92	BDL
3D	2308.1	BDL	2328.3	58.42	3675.1	BDL	50572	432.8	152.7	1867.0	BDL	311.11	BDL
4A	2456.0	BDL	2821.6	91.20	2175.2	147.19	24820	997.7	174.3	2575.8	273.30	418.18	95.53
4B	2322.1	BDL	2864.5	58.74	1894.3	BDL	9103	1366.5	141.3	2320.9	244.70	362.46	86.53
4C	2665.5	BDL	2801.0	97.09	2229.1	BDL	11801	1398.1	201.9	3003.4	289.81	413.59	131.07
4D	1345.2	BDL	1904.5	41.42	1424.5	BDL	6268	1817.0	133.3	2103.0	BDL	257.99	74.95
5A	1868.4	BDL	1796.1	45.56	3657.9	94.24	28651	1364.1	148.2	1568.1	178.45	307.89	46.22
5B	2263.5	BDL	2855.5	40.14	5316.5	BDL	27982	1707.3	196.3	1699.5	151.83	308.26	44.04
5C	1750.6	BDL	1470.6	38.26	4218.1	BDL	24233	552.3	184.7	1296.9	147.87	329.39	44.55
5D	1783.6	BDL	1897.0	48.78	4657.3	BDL	24483	732.5	181.5	1573.8	162.77	349.94	58.54
6A	1963.9	BDL	1755.7	57.67	2587.4	76.58	49028	423.9	131.8	1480.6	163.14	313.22	47.37
6B	1685.1	BDL	1565.5	43.57	2554.2	77.31	48916	343.1	127.0	1337.5	149.32	302.71	46.05
6C	1256.7	BDL	1299.5	45.71	1909.8	BDL	39925	390.4	148.3	1158.8	123.31	317.44	42.86
6D	1684.0	BDL	2105.9	55.78	2517.2	BDL	26478	509.8	162.4	1563.6	165.40	334.33	62.31
7A	1265.3	BDL	1008.6	43.78	6348.3	BDL	59626	455.7	164.7	1074.5	129.37	260.21	37.92
7B	1783.7	BDL	1787.7	65.56	3730.6	83.48	64247	403.6	144.1	1766.4	204.11	318.38	52.82
7C	1450.7	BDL	1185.5	49.82	7177.5	BDL	65741	371.1	174.3	1156.6	142.15	318.63	35.06
7D	1278.1	BDL	834.1	39.05	3934.0	BDL	58698	533.3	125.6	1037.0	115.12	226.40	35.20
8A	2564.8	BDL	2298.0	85.71	2437.9	181.58	12302	710.8	147.1	1998.9	262.48	437.12	69.43
8B	2853.3	BDL	2976.4	86.58	2393.9	BDL	8644	924.5	164.9	2852.6	301.61	419.68	97.67
8C	2027.5	BDL	1853.6	85.31	2138.9	BDL	5095	1318.5	151.7	2063.5	246.92	395.73	82.46
8D	2365.6	BDL	3028.0	86.81	2425.4	BDL	10745	1319.2	176.3	2738.6	296.83	444.74	100.17
15A	1778.6	BDL	3413.3	43.96	8534.1	BDL	4898	1323.8	169.3	1105.0	BDL	319.04	BDL
15B	1834.8	BDL	3441.4	42.33	7965.4	BDL	4733	1697.9	155.5	1108.1	BDL	318.02	BDL
26A	1340.5	BDL	1873.0	28.06	3744.0	BDL	3952	1006.1	85.9	780.7	BDL	245.47	BDL
26B	1271.2	BDL	1822.5	30.70	3940.2	BDL	3863	795.6	86.0	743.3	BDL	239.14	BDL
37A	1276.6	BDL	2840.7	29.95	9743.6	BDL	4375	671.1	116.0	785.1	BDL	220.51	BDL
37B	1278.8	BDL	2934.9	31.11	10142.2	BDL	4687	538.3	111.4	632.0	BDL	221.54	BDL
48A	3282.3	BDL	5307.8	99.29	2663.5	BDL	9231	5262.4	181.8	2486.8	BDL	427.23	BDL
48B	3176.8	BDL	5397.8	84.25	2459.1	BDL	4970	5190.6	196.7	2639.8	BDL	426.52	BDL

Sequential Extraction ICP-AES Results

All in ppm	Al	As	B	Ba	Be	Ca	Cd	Co	Cr	Cu	Fe	K	Mg
MDL	0.05	0.06	0.04	0.005	0.001	0.01	0.01	0.008	0.008	0.005	0.01	0.1	0.01
BL-1	BDL	BDL	BDL	BDL	BDL	BDL	BDL	BDL	BDL	BDL	0.05	EXC.	BDL
1A-1	0.582	BDL	0.058	0.014	BDL	20.20	BDL	BDL	BDL	0.006	4.93	EXC.	11.89
2B-1	0.385	BDL	0.046	0.016	BDL	18.92	BDL	BDL	BDL	BDL	3.91	EXC.	12.38
3A-1	0.201	BDL	BDL	0.005	BDL	23.81	BDL	BDL	BDL	0.007	2.79	EXC.	8.52
3C-1	0.473	BDL	BDL	0.019	BDL	28.08	BDL	BDL	BDL	0.013	4.26	EXC.	13.34
4A-1	0.678	BDL	BDL	0.008	BDL	7.60	BDL	BDL	BDL	BDL	5.04	EXC.	6.07
5A-1	0.624	BDL	0.045	0.018	BDL	19.96	BDL	BDL	BDL	0.006	5.08	EXC.	10.72
6B-1	0.269	BDL	0.052	0.019	BDL	19.94	BDL	BDL	BDL	BDL	2.54	EXC.	13.36
7A-1	0.401	BDL	BDL	0.010	BDL	27.23	BDL	BDL	BDL	0.008	4.96	EXC.	12.00
8B-1	0.603	BDL	BDL	0.021	BDL	5.98	BDL	BDL	BDL	BDL	3.79	EXC.	3.66
15-1	0.296	BDL	0.086	0.017	BDL	10.59	BDL	BDL	BDL	0.032	2.55	EXC.	4.45
26-1	0.289	BDL	0.095	0.023	BDL	11.95	BDL	BDL	BDL	0.009	2.06	EXC.	6.68
37-1	1.23	BDL	0.131	0.047	BDL	19.60	BDL	BDL	BDL	0.142	9.96	EXC.	12.07
48-1	0.663	BDL	BDL	0.029	BDL	8.52	BDL	BDL	BDL	0.007	4.79	EXC.	3.73
BL-2	BDL	BDL	BDL	BDL	BDL	BDL	BDL	BDL	BDL	BDL	BDL	EXC.	BDL
1A-2	0.020	BDL	BDL	0.052	BDL	15.32	BDL	BDL	BDL	BDL	0.267	EXC.	3.61
2B-2	0.020	BDL	BDL	0.100	BDL	14.38	BDL	BDL	BDL	BDL	0.538	EXC.	4.73
3A-2	0.020	BDL	BDL	0.011	BDL	7.07	BDL	BDL	BDL	BDL	0.265	EXC.	1.00
3C-2	0.020	BDL	BDL	0.086	BDL	17.26	BDL	BDL	BDL	BDL	0.556	EXC.	3.59
4A-2	0.020	BDL	BDL	0.050	BDL	6.62	BDL	BDL	BDL	BDL	0.450	EXC.	2.76
5A-2	0.020	BDL	BDL	0.084	BDL	15.20	BDL	BDL	BDL	BDL	0.394	EXC.	3.43
6B-2	0.020	BDL	BDL	0.139	BDL	17.48	BDL	BDL	BDL	BDL	0.562	EXC.	6.10
7A-2	0.020	BDL	BDL	0.029	BDL	11.26	BDL	BDL	BDL	BDL	0.502	EXC.	2.05
8B-2	0.062	BDL	BDL	0.142	BDL	5.97	BDL	BDL	BDL	BDL	0.585	EXC.	1.91
15-2	BDL	BDL	BDL	0.104	BDL	18.08	BDL	BDL	BDL	BDL	0.219	EXC.	2.83
26-2	BDL	BDL	BDL	0.158	BDL	17.80	BDL	BDL	BDL	BDL	0.275	EXC.	4.80
37-2	BDL	BDL	BDL	0.099	BDL	15.82	BDL	BDL	BDL	BDL	0.353	EXC.	3.61
48-2	BDL	BDL	BDL	0.154	BDL	5.76	BDL	BDL	BDL	BDL	0.396	EXC.	1.62
BL-3	0.130	BDL	BDL	BDL	BDL	BDL	BDL	BDL	BDL	BDL	0.099	EXC.	BDL
1A-3	0.081	BDL	BDL	BDL	BDL	0.045	BDL	BDL	BDL	BDL	0.150	EXC.	BDL
2B-3	0.161	BDL	BDL	BDL	BDL	0.034	BDL	BDL	BDL	BDL	0.507	EXC.	0.032
3A-3	0.104	BDL	BDL	BDL	BDL	0.018	BDL	BDL	BDL	BDL	0.301	EXC.	0.010
3C-3	0.115	BDL	BDL	BDL	BDL	0.036	BDL	BDL	BDL	BDL	0.364	EXC.	0.017
4A-3	0.176	BDL	BDL	BDL	BDL	0.037	BDL	BDL	BDL	BDL	0.556	EXC.	0.052
5A-3	0.076	BDL	BDL	BDL	BDL	BDL	BDL	BDL	BDL	BDL	0.204	EXC.	BDL
6B-3	0.117	BDL	BDL	BDL	BDL	BDL	BDL	BDL	BDL	BDL	0.384	EXC.	BDL
7A-3	0.061	BDL	BDL	BDL	BDL	BDL	BDL	BDL	BDL	BDL	0.168	EXC.	BDL
8B-3	0.146	BDL	BDL	BDL	BDL	0.017	BDL	BDL	BDL	BDL	0.497	EXC.	0.036
15-3	0.047	BDL	BDL	BDL	BDL	BDL	BDL	BDL	BDL	BDL	0.159	EXC.	BDL
26-3	0.140	BDL	BDL	BDL	BDL	0.037	BDL	BDL	BDL	BDL	0.477	EXC.	0.033
37-3	0.082	BDL	BDL	BDL	BDL	0.028	BDL	BDL	BDL	BDL	0.321	EXC.	BDL
48-3	0.201	BDL	BDL	BDL	BDL	0.023	BDL	BDL	BDL	BDL	0.637	EXC.	0.042

All in ppm	Mn	Mo	Na	Ni	P	Pb	S	Si	Sr	Ti	V	Zn	Zr
MDL	0.002	0.02	0.01	0.01	0.1	0.05	0.1	0.05	0.005	0.005	0.05	0.01	0.01
BL-1	BDL	BDL	BDL	BDL	BDL	BDL	BDL	BDL	BDL	BDL	BDL	0.023	BDL
1A-1	0.055	BDL	1.36	BDL	0.218	BDL	18.44	2.68	0.083	0.018	BDL	0.010	BDL
2B-1	0.061	BDL	1.71	BDL	0.298	BDL	21.51	2.94	0.072	0.009	BDL	BDL	BDL
3A-1	0.013	BDL	1.48	BDL	0.272	BDL	22.91	1.40	0.110	0.005	BDL	BDL	BDL
3C-1	0.068	BDL	1.58	BDL	0.496	BDL	27.43	2.42	0.103	0.014	BDL	BDL	BDL
4A-1	0.062	BDL	1.04	BDL	0.017	BDL	8.59	2.57	0.030	0.020	BDL	BDL	BDL
5A-1	0.068	BDL	1.64	BDL	0.229	BDL	17.80	2.70	0.074	0.017	BDL	BDL	BDL
6B-1	0.061	BDL	2.08	BDL	0.325	BDL	26.20	2.07	0.084	0.006	BDL	BDL	BDL
7A-1	0.039	BDL	1.54	BDL	0.319	BDL	27.28	1.58	0.114	0.012	BDL	BDL	BDL
8B-1	0.173	BDL	0.99	BDL	0.022	BDL	4.01	2.46	0.019	0.018	BDL	BDL	BDL
15-1	0.082	BDL	8.01	BDL	8.373	BDL	8.61	2.75	0.026	0.011	BDL	0.010	BDL
26-1	0.160	BDL	5.28	BDL	7.967	BDL	3.90	3.41	0.024	0.006	BDL	0.013	BDL
37-1	0.316	BDL	14.20	BDL	27.47	BDL	18.86	5.69	0.056	0.048	BDL	0.050	BDL
48-1	0.530	BDL	4.10	BDL	0.172	BDL	3.77	2.93	0.023	0.017	BDL	BDL	BDL
BL-2	BDL	BDL	0.312	BDL	BDL	BDL	BDL	BDL	BDL	BDL	BDL	BDL	BDL
1A-2	0.008	BDL	0.452	BDL	BDL	BDL	0.920	0.209	0.070	BDL	BDL	BDL	BDL
2B-2	0.025	BDL	0.563	BDL	BDL	BDL	0.830	0.425	0.068	BDL	BDL	BDL	BDL
3A-2	BDL	BDL	0.453	BDL	BDL	BDL	0.625	0.195	0.031	BDL	BDL	BDL	BDL
3C-2	0.012	BDL	0.614	BDL	0.129	BDL	0.936	0.305	0.082	BDL	BDL	BDL	BDL
4A-2	0.024	BDL	0.635	BDL	BDL	BDL	0.345	0.320	0.033	BDL	BDL	BDL	BDL
5A-2	0.011	BDL	0.629	BDL	BDL	BDL	0.827	0.316	0.066	BDL	BDL	BDL	BDL
6B-2	0.054	BDL	0.811	BDL	BDL	BDL	0.920	0.433	0.088	BDL	BDL	BDL	BDL
7A-2	0.005	BDL	0.663	BDL	0.101	BDL	1.130	0.199	0.055	BDL	BDL	BDL	BDL
8B-2	0.206	BDL	0.671	BDL	BDL	BDL	0.107	0.441	0.022	BDL	BDL	BDL	BDL
15-2	0.019	BDL	1.043	BDL	0.830	BDL	0.352	1.297	0.044	BDL	BDL	BDL	BDL
26-2	0.154	BDL	0.895	BDL	0.598	BDL	0.246	1.875	0.041	BDL	BDL	BDL	BDL
37-2	0.044	BDL	1.259	BDL	1.999	BDL	0.927	3.596	0.050	BDL	BDL	BDL	BDL
48-2	0.342	BDL	0.733	BDL	BDL	BDL	0.191	0.474	0.018	BDL	BDL	BDL	BDL
BL-3	BDL	BDL	2.34	BDL	BDL	BDL	0.307	1.83	BDL	BDL	BDL	BDL	BDL
1A-3	0.002	BDL	1.68	BDL	0.90	BDL	0.912	1.98	BDL	BDL	BDL	BDL	BDL
2B-3	0.005	BDL	1.48	BDL	0.38	BDL	0.756	3.73	BDL	BDL	BDL	BDL	BDL
3A-3	BDL	BDL	1.88	BDL	0.81	BDL	0.691	4.09	BDL	BDL	BDL	BDL	BDL
3C-3	0.004	BDL	1.50	BDL	2.57	BDL	1.078	3.38	BDL	0.005	BDL	BDL	BDL
4A-3	0.006	BDL	1.61	BDL	BDL	BDL	0.567	4.49	BDL	0.010	BDL	BDL	BDL
5A-3	BDL	BDL	1.49	BDL	0.91	BDL	0.837	4.20	BDL	BDL	BDL	BDL	BDL
6B-3	0.004	BDL	1.21	BDL	0.19	BDL	0.583	4.58	BDL	BDL	BDL	BDL	BDL
7A-3	BDL	BDL	1.41	BDL	1.39	BDL	0.662	3.88	BDL	BDL	BDL	BDL	BDL
8B-3	0.009	BDL	1.43	BDL	BDL	BDL	0.404	5.76	BDL	0.010	BDL	BDL	BDL
15-3	BDL	BDL	1.62	BDL	2.29	BDL	0.446	6.49	BDL	BDL	BDL	BDL	BDL
26-3	0.021	BDL	1.43	BDL	0.60	BDL	0.389	8.95	BDL	0.014	BDL	BDL	BDL
37-3	0.006	BDL	1.53	BDL	4.05	BDL	0.595	7.43	BDL	BDL	BDL	BDL	BDL
48-3	0.009	BDL	1.40	BDL	BDL	BDL	0.502	8.15	BDL	0.009	BDL	BDL	BDL

All in ppm	Al	As	B	Ba	Be	Ca	Cd	Co	Cr	Cu	Fe	K	Mg
MDL	0.05	0.06	0.04	0.005	0.001	0.01	0.01	0.008	0.008	0.005	0.01	0.1	0.01
BL-4	BDL	BDL	BDL	BDL	BDL	BDL	BDL	BDL	BDL	BDL	0.019	7.66	BDL
1A-4	0.876	BDL	BDL	0.007	BDL	7.96	BDL	BDL	BDL	0.008	5.20	57.18	1.554
2B-4	1.000	BDL	BDL	0.009	BDL	4.54	BDL	BDL	BDL	0.007	6.29	71.38	1.553
3A-4	0.442	BDL	BDL	BDL	BDL	5.44	BDL	BDL	BDL	0.006	2.63	31.35	0.726
3C-4	0.758	BDL	BDL	0.015	BDL	17.02	BDL	BDL	BDL	0.013	6.13	69.85	1.666
4A-4	1.063	BDL	BDL	0.006	BDL	2.22	BDL	BDL	BDL	0.008	5.10	39.25	1.225
5A-4	0.968	BDL	BDL	0.011	BDL	7.04	BDL	BDL	BDL	0.011	6.42	47.95	1.420
6B-4	1.053	BDL	BDL	0.010	BDL	4.50	BDL	BDL	BDL	0.006	6.26	57.11	1.361
7A-4	0.533	BDL	BDL	BDL	BDL	9.00	BDL	BDL	BDL	0.006	3.38	59.51	0.969
8B-4	1.122	BDL	BDL	0.009	BDL	1.28	BDL	BDL	BDL	0.007	5.80	30.89	0.481
15-4	0.697	BDL	BDL	0.024	BDL	12.91	BDL	BDL	BDL	0.007	4.82	45.32	0.790
26-4	0.688	BDL	BDL	0.019	BDL	4.75	BDL	BDL	BDL	BDL	4.84	71.78	0.846
37-4	0.776	BDL	BDL	0.028	BDL	16.87	BDL	BDL	BDL	0.007	5.75	74.66	0.712
48-4	1.215	BDL	BDL	0.010	BDL	1.05	BDL	BDL	BDL	0.009	6.57	49.25	0.400
BL-5	BDL	BDL	BDL	BDL	BDL	0.01	BDL	BDL	BDL	BDL	BDL	0.234	BDL
1A-5	0.43	BDL	BDL	0.057	BDL	5.87	BDL	BDL	BDL	0.018	9.53	3.92	0.70
2B-5	0.67	BDL	BDL	0.074	BDL	1.35	BDL	BDL	BDL	0.015	10.61	5.38	0.69
3A-5	0.26	BDL	BDL	0.023	BDL	1.59	BDL	BDL	BDL	0.011	4.50	1.88	0.41
3C-5	0.97	BDL	BDL	0.132	BDL	12.57	BDL	BDL	BDL	0.032	16.25	6.51	0.91
4A-5	0.49	BDL	BDL	0.032	BDL	1.13	BDL	BDL	BDL	0.009	5.89	2.67	0.73
5A-5	0.65	BDL	BDL	0.082	BDL	2.02	BDL	BDL	BDL	0.017	9.66	3.74	0.55
6B-5	0.66	BDL	BDL	0.080	BDL	1.23	BDL	BDL	BDL	0.016	10.19	5.45	0.51
7A-5	0.39	BDL	BDL	0.052	BDL	3.73	BDL	BDL	BDL	0.015	8.03	3.81	0.53
8B-5	0.43	BDL	BDL	0.035	BDL	0.61	BDL	BDL	BDL	0.008	4.86	2.84	0.31
15-5	0.42	BDL	BDL	0.067	BDL	2.68	BDL	BDL	BDL	0.014	5.11	3.61	0.27
26-5	0.36	BDL	BDL	0.051	BDL	0.88	BDL	BDL	BDL	0.011	4.72	5.12	0.25
37-5	0.56	BDL	BDL	0.085	BDL	6.77	BDL	BDL	BDL	0.014	6.26	5.17	0.31
48-5	0.43	BDL	BDL	0.033	BDL	0.39	BDL	BDL	BDL	0.006	4.37	3.35	0.21
BL-6	BDL	BDL	BDL	BDL	BDL	BDL	BDL	BDL	BDL	BDL	BDL	0.057	BDL
1A-6	37.5	BDL	0.07	0.226	BDL	20.42	BDL	0.080	0.104	0.108	481.3	4.2	33.1
2B-6	47.8	BDL	0.08	0.266	BDL	19.61	BDL	0.079	0.121	0.105	573.2	6.8	36.8
3A-6	17.6	BDL	BDL	0.077	BDL	12.51	BDL	0.035	0.049	0.103	333.7	2.7	15.9
3C-6	61.1	BDL	0.09	0.322	BDL	26.96	BDL	0.094	0.154	0.167	645.5	7.5	48.5
4A-6	38.1	BDL	0.05	0.165	BDL	20.58	BDL	0.064	0.099	0.076	367.5	4.1	30.9
5A-6	49.7	BDL	0.07	0.252	BDL	16.21	BDL	0.080	0.122	0.106	512.7	5.3	34.0
6B-6	50.3	BDL	0.09	0.265	BDL	18.66	BDL	0.085	0.131	0.113	579.0	6.7	37.8
7A-6	33.4	BDL	0.05	0.181	BDL	13.56	BDL	0.056	0.092	0.105	539.6	3.9	26.6
8B-6	37.6	BDL	0.05	0.145	BDL	15.43	BDL	0.059	0.097	0.073	307.4	3.8	26.4
15-6	33.4	BDL	0.07	0.172	BDL	13.23	BDL	0.050	0.082	0.073	279.4	4.2	23.0
26-6	33.1	BDL	0.09	0.171	BDL	13.97	BDL	0.051	0.085	0.084	277.4	5.3	23.8
37-6	41.7	BDL	0.05	0.216	BDL	19.36	BDL	0.059	0.107	0.115	324.5	5.7	29.3
48-6	35.0	BDL	BDL	0.152	BDL	13.13	BDL	0.054	0.091	0.077	279.7	4.2	22.6

All in ppm	Mn	Mo	Na	Ni	P	Pb	S	Si	Sr	Ti	V	Zn	Zr
MDL	0.002	0.02	0.01	0.01	0.1	0.05	0.1	0.05	0.005	0.005	0.05	0.01	0.01
BL-4	BDL	BDL	EXC.	BDL	EXC.	BDL	BDL	BDL	BDL	BDL	BDL	BDL	BDL
1A-4	0.215	BDL	EXC.	BDL	EXC.	BDL	0.555	1.79	0.013	0.033	BDL	0.055	BDL
2B-4	0.316	BDL	EXC.	BDL	EXC.	BDL	0.476	2.19	0.008	0.033	BDL	0.050	BDL
3A-4	0.037	BDL	EXC.	BDL	EXC.	BDL	0.350	1.25	0.009	0.015	BDL	0.033	BDL
3C-4	0.416	BDL	EXC.	BDL	EXC.	BDL	0.571	1.73	0.029	0.038	BDL	0.056	BDL
4A-4	0.195	BDL	EXC.	BDL	EXC.	BDL	0.317	2.16	0.005	0.035	BDL	0.022	BDL
5A-4	0.311	BDL	EXC.	BDL	EXC.	BDL	0.530	1.94	0.012	0.039	BDL	0.041	BDL
6B-4	0.330	BDL	EXC.	BDL	EXC.	BDL	0.500	2.31	0.009	0.037	BDL	0.053	BDL
7A-4	0.127	BDL	EXC.	BDL	EXC.	BDL	0.433	1.12	0.014	0.019	BDL	0.027	BDL
8B-4	0.268	BDL	EXC.	BDL	EXC.	BDL	0.243	2.21	BDL	0.038	BDL	0.022	BDL
15-4	0.369	BDL	EXC.	BDL	EXC.	BDL	0.225	1.97	0.019	0.028	BDL	0.075	BDL
26-4	0.439	BDL	EXC.	BDL	EXC.	BDL	0.202	2.17	0.007	0.022	BDL	0.078	BDL
37-4	0.428	BDL	EXC.	BDL	EXC.	BDL	0.304	2.30	0.028	0.034	BDL	0.078	BDL
48-4	0.197	BDL	EXC.	BDL	EXC.	BDL	0.292	2.29	BDL	0.037	BDL	0.020	BDL
BL-5	BDL	BDL	EXC.	BDL	EXC.	BDL	1.33	BDL	BDL	BDL	BDL	BDL	BDL
1A-5	0.252	BDL	EXC.	BDL	EXC.	BDL	1.72	1.50	0.03	0.01	BDL	0.040	BDL
2B-5	0.288	BDL	EXC.	BDL	EXC.	BDL	1.59	2.25	0.01	0.01	BDL	0.035	BDL
3A-5	0.047	BDL	EXC.	BDL	EXC.	BDL	1.50	0.86	0.01	0.01	BDL	0.024	BDL
3C-5	0.535	BDL	EXC.	BDL	EXC.	BDL	1.70	2.88	0.06	0.03	BDL	0.056	BDL
4A-5	0.143	BDL	EXC.	BDL	EXC.	BDL	1.50	1.48	0.01	0.02	BDL	0.017	BDL
5A-5	0.275	BDL	EXC.	BDL	EXC.	BDL	1.65	1.97	0.02	0.01	BDL	0.031	BDL
6B-5	0.272	BDL	EXC.	BDL	EXC.	BDL	1.70	2.11	0.02	0.01	BDL	0.038	BDL
7A-5	0.189	BDL	EXC.	BDL	EXC.	BDL	1.62	1.19	0.03	0.01	BDL	0.030	BDL
8B-5	0.142	BDL	EXC.	BDL	EXC.	BDL	1.62	1.25	BDL	0.01	BDL	0.015	BDL
15-5	0.198	BDL	EXC.	BDL	EXC.	BDL	1.45	1.37	0.01	0.01	BDL	0.029	BDL
26-5	0.124	BDL	EXC.	BDL	EXC.	BDL	1.38	1.43	0.01	0.01	BDL	0.026	BDL
37-5	0.257	BDL	EXC.	BDL	EXC.	BDL	1.50	1.88	0.03	0.01	BDL	0.037	BDL
48-5	0.091	BDL	EXC.	BDL	EXC.	BDL	1.54	1.28	BDL	0.01	BDL	0.012	BDL
BL-6	BDL	BDL	EXC.	BDL	0.603	BDL	BDL	0.072	BDL	BDL	BDL	0.005	BDL
1A-6	3.84	BDL	EXC.	0.081	18.49	0.143	1.243	61.86	0.046	1.222	BDL	0.604	BDL
2B-6	4.64	BDL	EXC.	0.095	20.21	0.187	1.004	78.66	0.058	1.337	BDL	0.706	BDL
3A-6	1.10	BDL	EXC.	0.066	12.72	0.078	2.596	31.94	0.027	0.591	BDL	0.297	BDL
3C-6	5.94	BDL	EXC.	0.121	28.87	0.226	2.012	84.33	0.071	1.761	BDL	0.883	BDL
4A-6	3.14	BDL	EXC.	0.082	10.81	0.129	1.651	63.15	0.044	1.180	BDL	0.517	BDL
5A-6	4.27	BDL	EXC.	0.098	18.68	0.162	3.012	74.60	0.057	1.392	BDL	0.686	BDL
6B-6	4.57	BDL	EXC.	0.103	22.07	0.196	1.138	80.47	0.057	1.469	BDL	0.772	BDL
7A-6	2.80	BDL	EXC.	0.071	21.82	0.178	3.342	58.20	0.044	1.083	BDL	0.540	BDL
8B-6	2.54	BDL	EXC.	0.076	8.18	0.111	1.033	61.35	0.038	1.140	BDL	0.487	BDL
15-6	2.49	BDL	EXC.	0.064	8.36	0.102	0.383	59.04	0.036	0.980	BDL	0.480	BDL
26-6	2.22	BDL	EXC.	0.066	8.69	0.101	0.516	60.35	0.034	0.988	BDL	0.532	BDL
37-6	2.98	BDL	EXC.	0.081	10.98	0.113	1.662	69.33	0.046	1.230	BDL	0.587	BDL
48-6	2.05	BDL	EXC.	0.066	8.99	0.105	2.311	60.89	0.038	1.056	BDL	0.471	BDL

Carbon, Nitrogen, Sulphur Combustion Results

Sample	N%	C%	S%		Sample	N%	C%	S%
1A	0.190	3.330	0.831		6A	0.270	4.770	1.068
1B	0.220	3.880	0.656		6B	0.320	5.370	1.074
1C	0.140	2.560	0.335		6C	0.310	5.510	0.756
1D	0.040	0.840	0.134		6D	0.180	3.100	0.376
2A	0.200	3.700	1.105		7A	0.150	3.110	0.967
2B	0.260	4.850	0.826		7B	0.190	3.600	1.229
2C	0.310	5.810	0.997		7C	0.210	3.620	1.128
2D	0.250	4.550	0.759		7D	0.150	3.010	0.967
3A	0.120	2.330	0.865		8A	0.070	1.420	0.143
3B	0.160	2.730	1.253		8B	0.060	1.060	0.087
3C	0.200	3.660	0.946		8C	0.040	0.760	0.047
3D	0.240	4.080	1.208		8D	0.050	1.020	0.095
4A	0.060	1.350	0.266		15A	0.27	3.66	0.084
4B	0.070	1.160	0.108		15B	0.27	3.60	0.077
4C	0.040	0.820	0.082		26A	0.44	7.35	0.097
4D	0.040	0.800	0.080		26B	0.46	7.85	0.100
5A	0.140	2.570	0.531		37A	0.36	7.32	0.118
5B	0.120	2.060	0.348		37B	0.40	8.06	0.132
5C	0.190	3.390	0.403		48A	0.06	1.15	0.076
5D	0.150	2.610	0.317		48B	0.06	1.10	0.038

SEM Compositional Results

Note: Data is semi-quantitative and intended for comparative purposes only.

	Composition By %								
Sample - Site	Oxides								
	Si	Fe	S	Ca	Al	Mg	P	Na	K
1B-1	2.39	28.08	6.13				3.47		
1B-2		20.74	5.19				10.78		
1B-3		27.29	7.18				4.78		
1B-4	11.99	7.11	3.22	4.32	5.49	3.16	1.77	1.38	
1B-5	12.89	7.27	3.79	1.48	6.07	5.55	0.69		
1B-6	17.09	1.68	1.23		11.90	3.74		0.30	1.85
1B-7	17.98	3.41	2.44	1.16	6.32	1.97	0.29	0.47	3.82
1B-11	14.10	4.56	7.61	1.44	4.20	1.39			1.30
1B-12	1.43	3.89	1.03			1.49	23.09		
1B-13	0.56	6.88				1.18	23.49		
1B-14	14.31	11.24	5.77		3.02	1.03	0.54		
1B-15	2.54	6.54	5.45	11.42	0.53	2.97	7.82		
2C-1	28.29	0.67	1.19	0.38	2.15	0.87		0.56	0.22
2C-4	14.70	4.42	4.04	1.56	6.78	4.04	0.45		0.79
2C-5	30.08		1.37	0.32	1.05	0.51			
2C-6	15.36	2.13	3.41	0.67	8.62	4.29		0.85	2.19
2C-7	21.43	0.46	2.00		6.86	3.76			1.40
2C-8	3.46	1.57	16.28	2.79	1.19	5.28	0.63		
3A-10	3.84	14.09	12.30	2.26	0.88	2.18			
3A-11	14.21	8.42	6.79	1.98	2.27	1.86			
3A-12	1.39	8.85	12.67	7.08		4.55	1.20		
3A-13	2.03	7.07	13.62	6.47		3.14	1.65		
3A-14	1.29	6.02	11.94	12.59		2.49	1.76		
3A-15	1.34	8.62	15.97	3.89		2.44	0.63		
5D-2	16.89	5.21	0.40		9.13	6.18			1.42
5D-3	23.14	0.54			7.39				7.36
5D-4	22.97	0.57			7.60	0.56			6.56
5D-5	12.23	13.14	3.09	3.31	4.38		1.13		2.08
5D-8	17.13	1.38	0.47		14.64	1.16		0.74	2.63
5D-9	19.23	4.33	0.74	0.43	7.02	3.10		2.98	1.09
5D-10	22.76	2.15	1.58		5.68	2.43		1.38	

	Composition By %								
Sample - Site	Oxides								
	Si	Fe	S	Ca	Al	Mg	P	Na	K
6B-9		0.92	1.42	42.58		3.65			
6B-10	2.76	5.00	16.65	1.56		6.00			
6B-11	2.74	5.23	16.76	1.77		5.37			
6B-12	7.11	6.48	12.45	5.00		2.96			
6B-13		4.56	18.50	3.66			2.73		
6B-14	1.18	6.37	13.98	3.05		10.85			
6B-15			0.67	48.65					
6B-16	0.50	9.83	14.75	1.47		8.45			
6B-17	7.18	5.71	14.21	0.49	2.02	1.68	0.24		
6B-18	3.79	8.43	16.48	1.77		1.17			
6B-19	8.67	5.84	12.83	1.20	2.12	1.64			
7A-3	2.25	16.50	11.74	3.43		3.22			
7A-6	2.54	13.16	14.64	1.39		2.35			
7A-7	4.66	15.76	11.19	1.67		3.19			
7A-8	3.27	8.57	15.82	2.54		2.33			
7A-9	4.86	8.34	13.90	3.71		2.87			
7A-10	3.15	11.56	13.44	3.64		3.20			
7D-1	18.38		0.21	4.29	12.16			3.36	
7D-2	22.78	0.30		2.89	7.82			2.16	
7D-3	25.57			5.99	4.53				
7D-5	10.22	3.26	7.52	4.22	6.46	4.08			
8D-12	20.09	4.14	0.80	1.29	7.39	2.56		0.94	0.45
8D-13	24.74	2.15	0.33	0.78	4.84	2.04		0.99	0.65
8D-14	17.30	4.15	1.10	0.89	7.63	6.29			1.31
8D-15	18.81	9.97			5.19	1.61			
8D-17	18.06	4.83	1.04	2.59	7.07	2.60	0.57		1.27
8D-20	18.84			4.08	11.96			3.63	

SEM Images

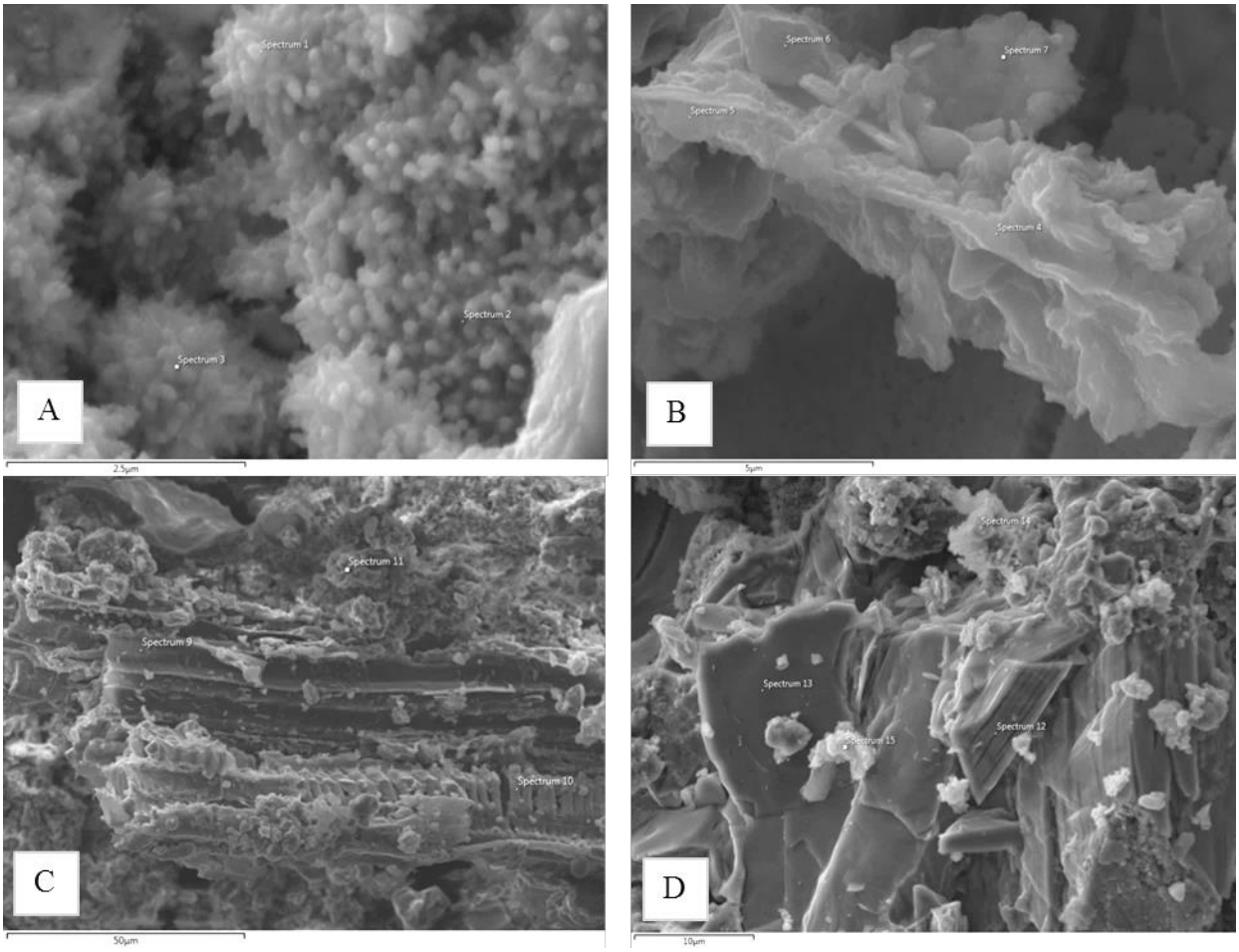

A: Sample 1B; sites 1-3. Iron oxide spheres.

B: Sample 1B; sites 4-7. Mineral crystal from creek sediment, probably biotite.

C: Sample 1B; sites 9-11. Organic matter surrounded by silicates.

D: Sample 1B; sites 12-15. Phosphate minerals surrounded by silicates.

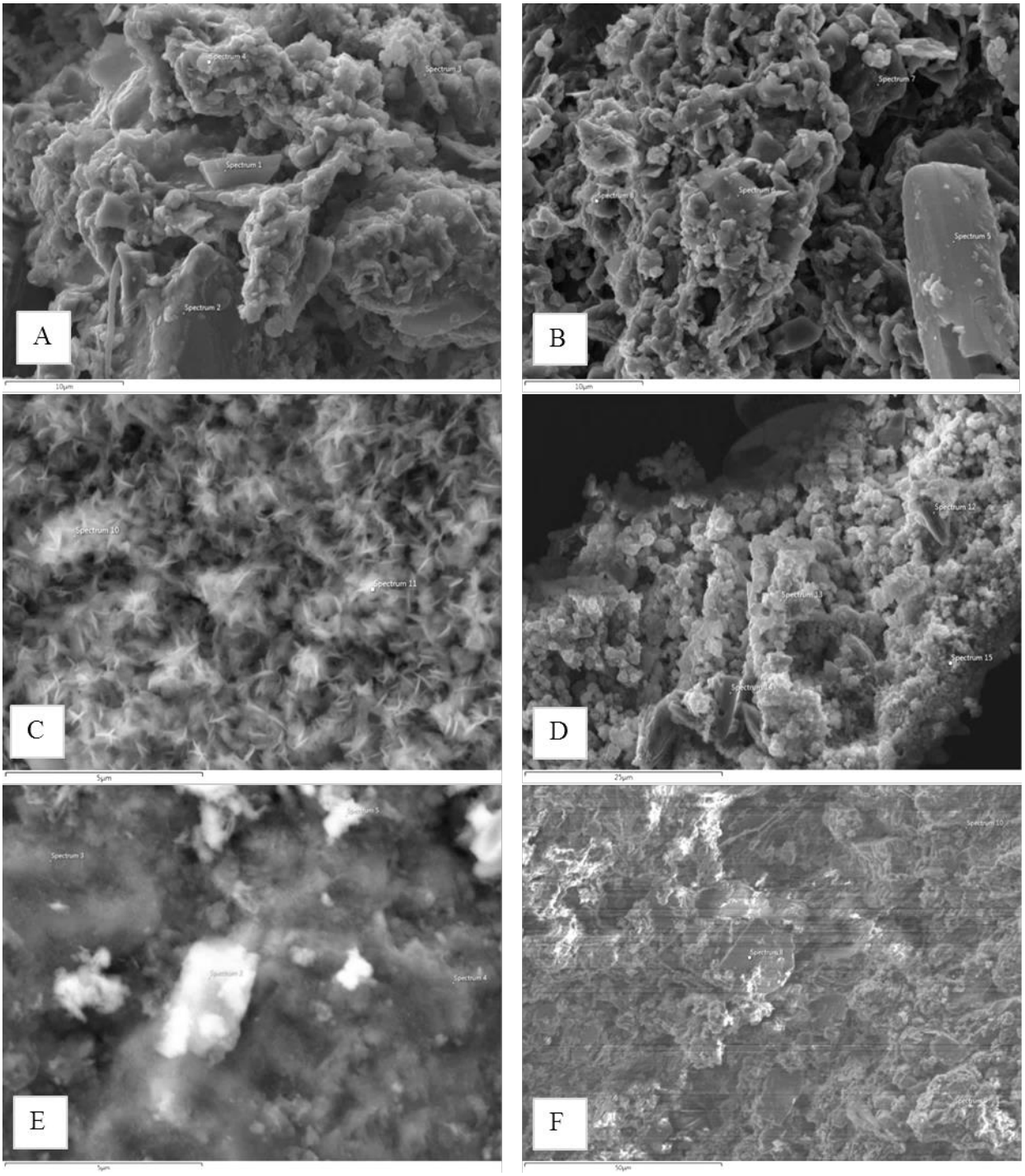

A: Sample 2C; sites 1-4, quartz and silicate grains of silica sand and creek sediment.

B: Sample 2C; sites 5-8, quartz and silicate grains of silica sand and creek sediment.

C: Sample 3A; sites 10-11, iron rich material on leaf compost.

D: Sample 3A; sites 12-15, iron and sulphur rich material.

E: Sample 5D; sites 2-5, silicate material.

F: Sample 5D; sites 9-10, aluminum-silicate minerals.

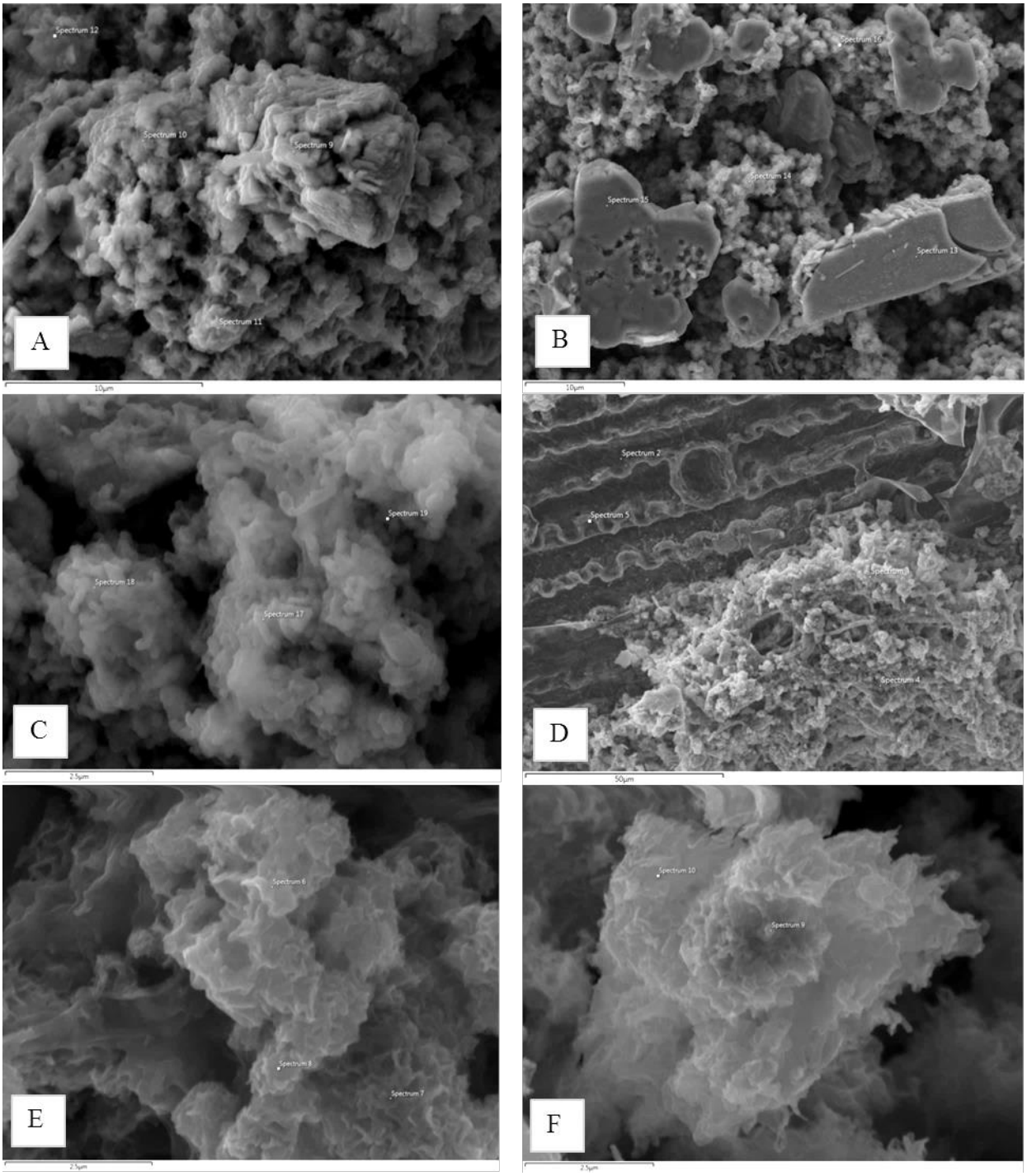

A: Sample 6B; sites 9-12, sulphur and silicate bearing materials.

B: Sample 6B; sites 13-16, sulphur and silicate bearing materials.

C: Sample 6B; sites 17-19, sulphur-rich precipitates.

D: Sample 7A; sites 2-5, organic matter in upper left, silicates in lower right.

E: Sample 7A; sites 6-8, sulphur-rich precipitates.

F: Sample 7A; sites 9-10, iron- and sulphur-rich precipitates.

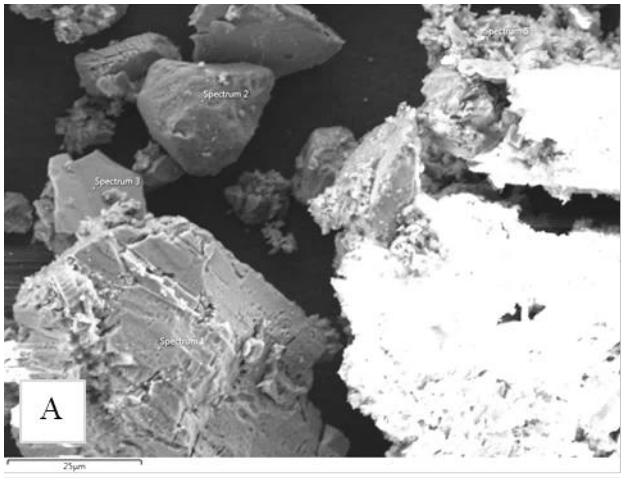

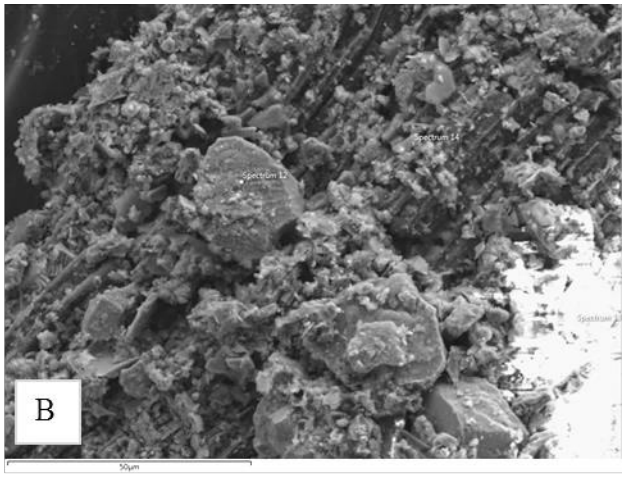

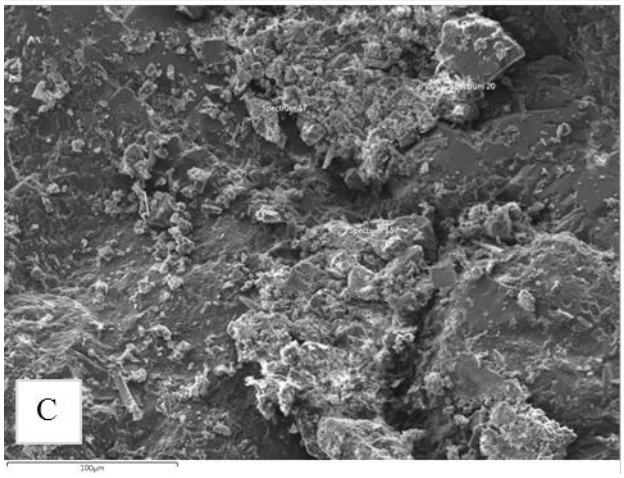

A: Sample 7D; sites 1-3, 5, quartz and aluminum silicates.

B: Sample 8B; sites 12-14, silicate materials.

C: Sample 8B; sites 15, 17, 20, silicate materials.

XRD Results

Samples 1A, 1B, 1C, 1D

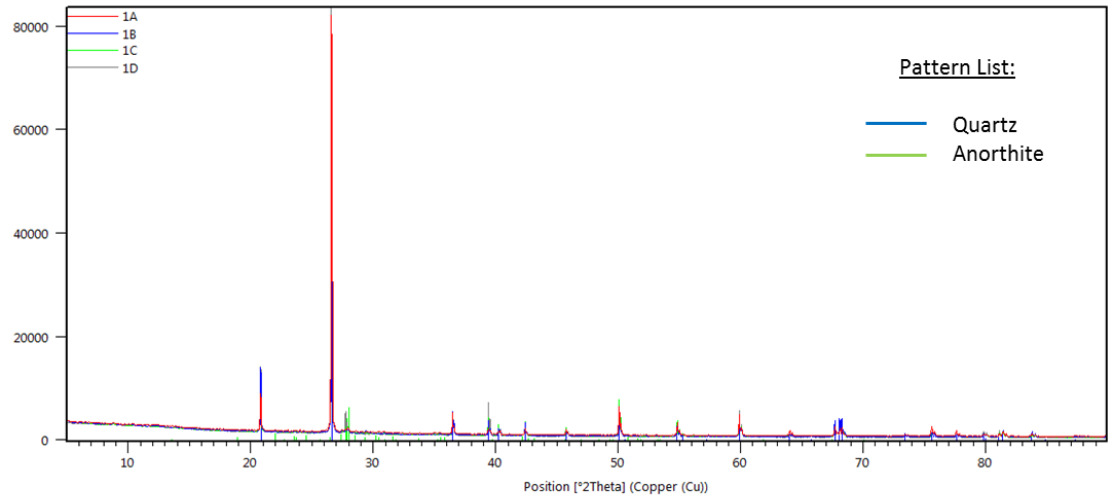

Samples 2A, 2B, 2C, 2D

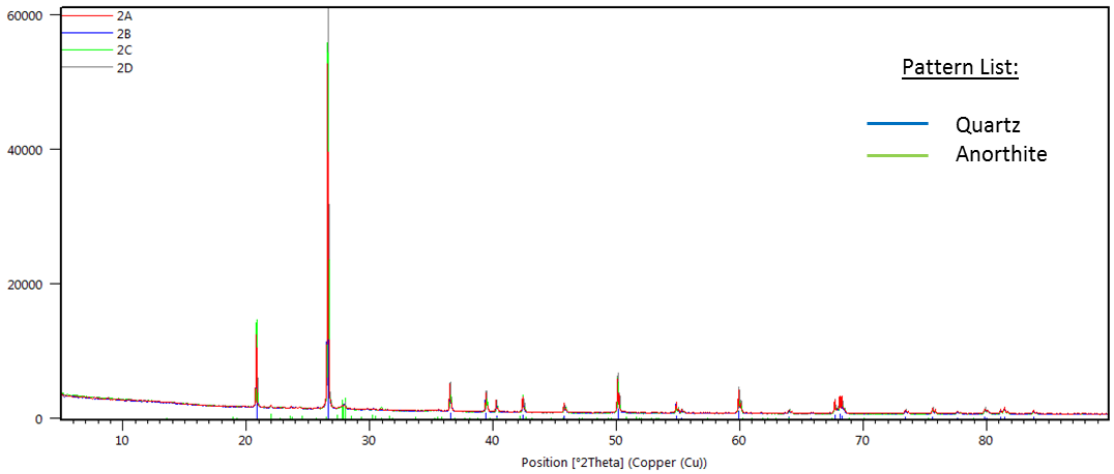

Samples 3A, 3B, 3C, 3D

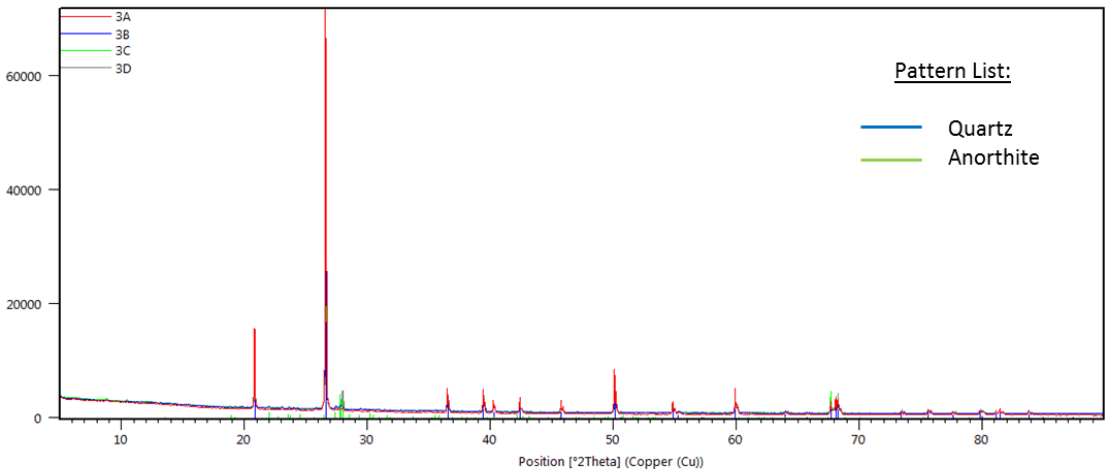

Samples 4A, 4B, 4C, 4D

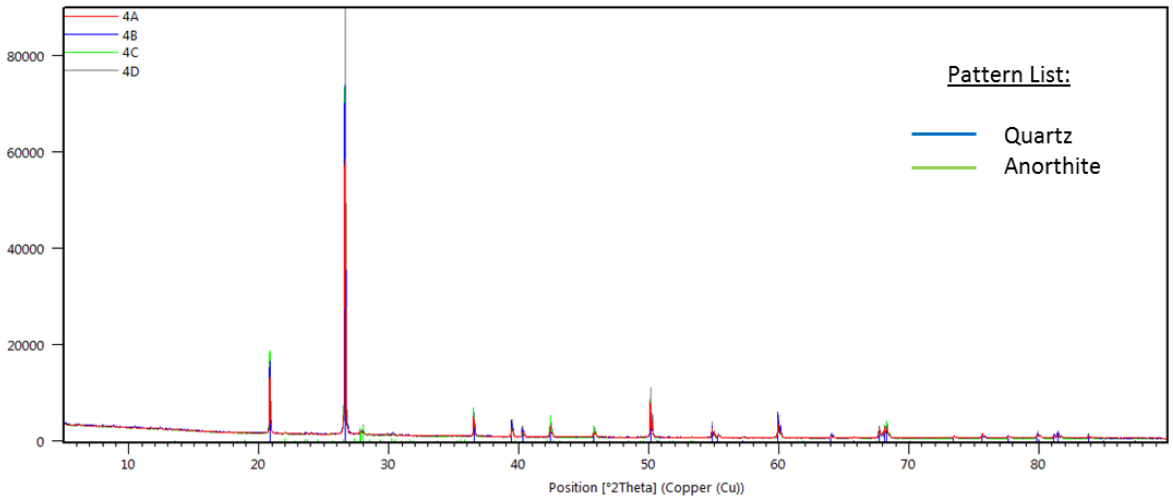

Samples 5A, 5B, 5C, 5D

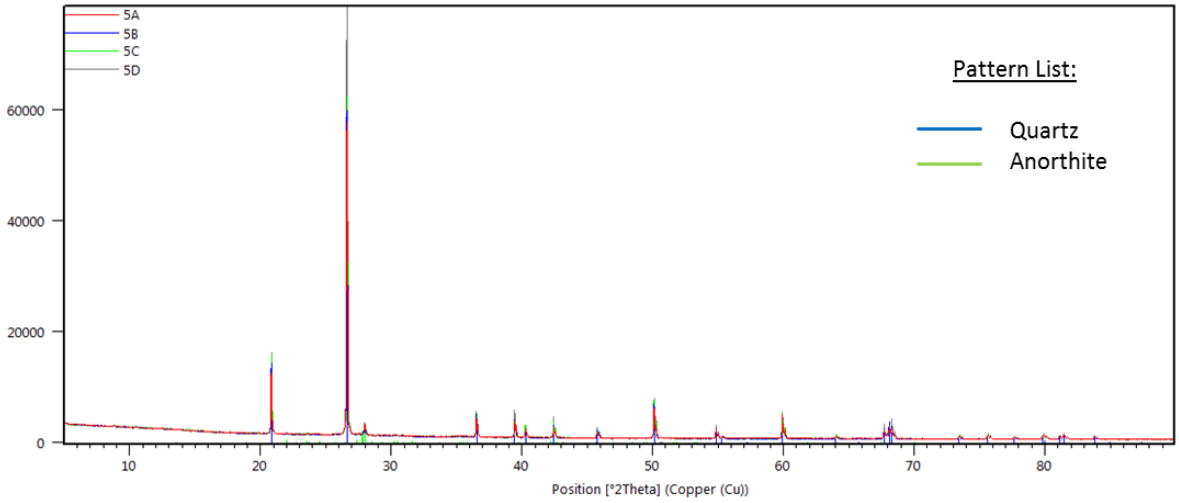

Samples 6A, 6B, 6C, 6D

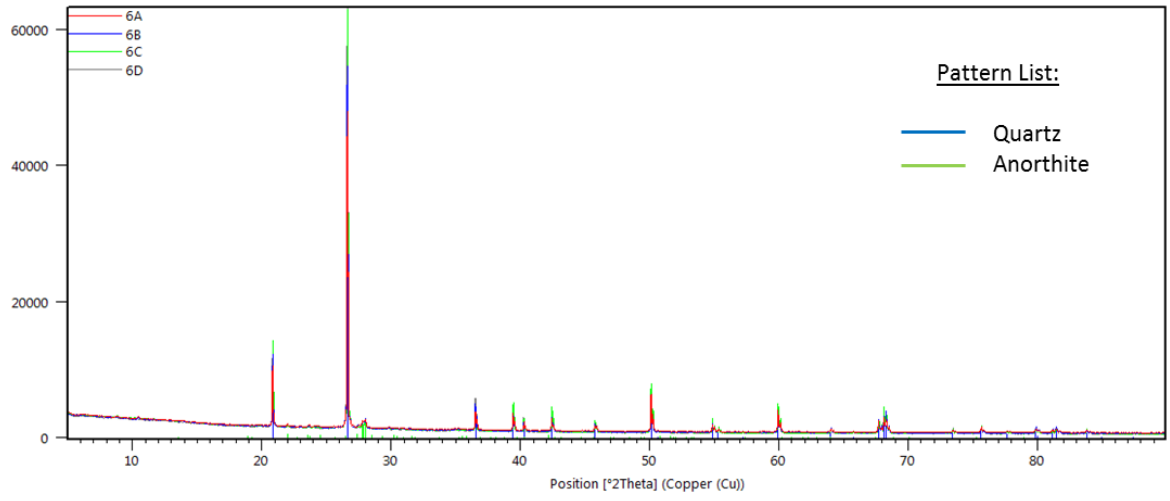

Samples 7A, 7B, 7C, 7D

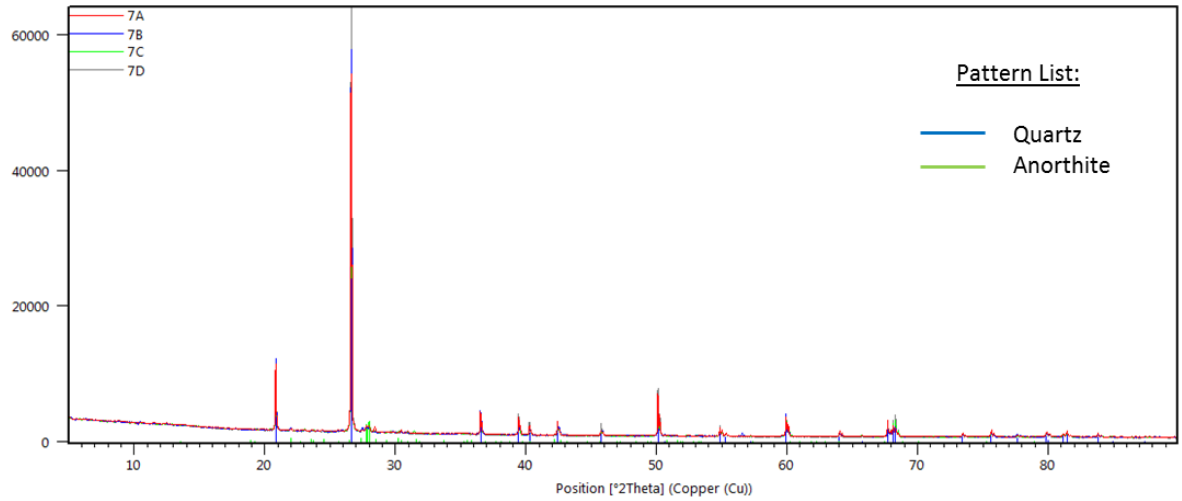

Samples 8A, 8B, 8C, 8D

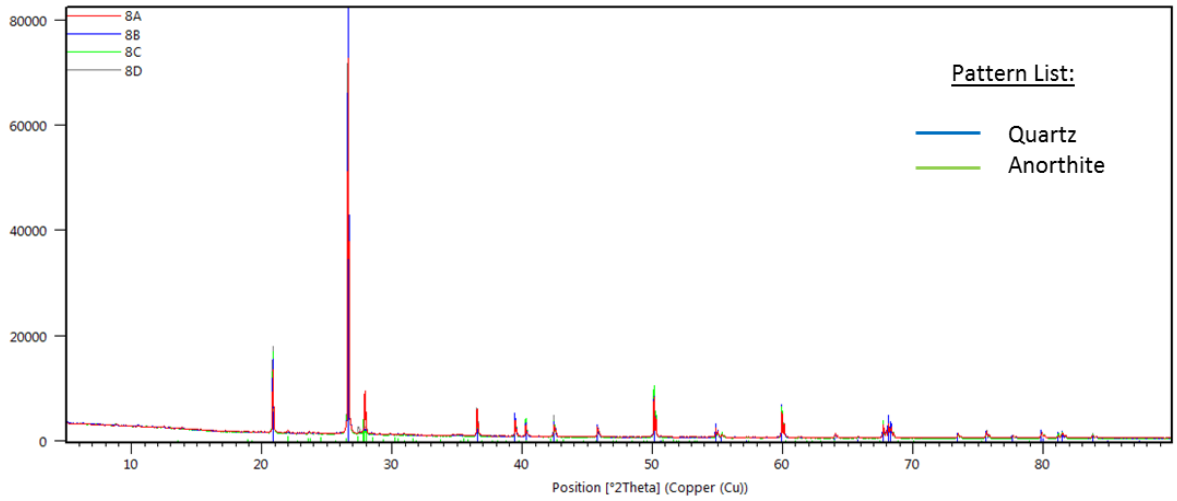

Creek Sediment Samples 1 - 3

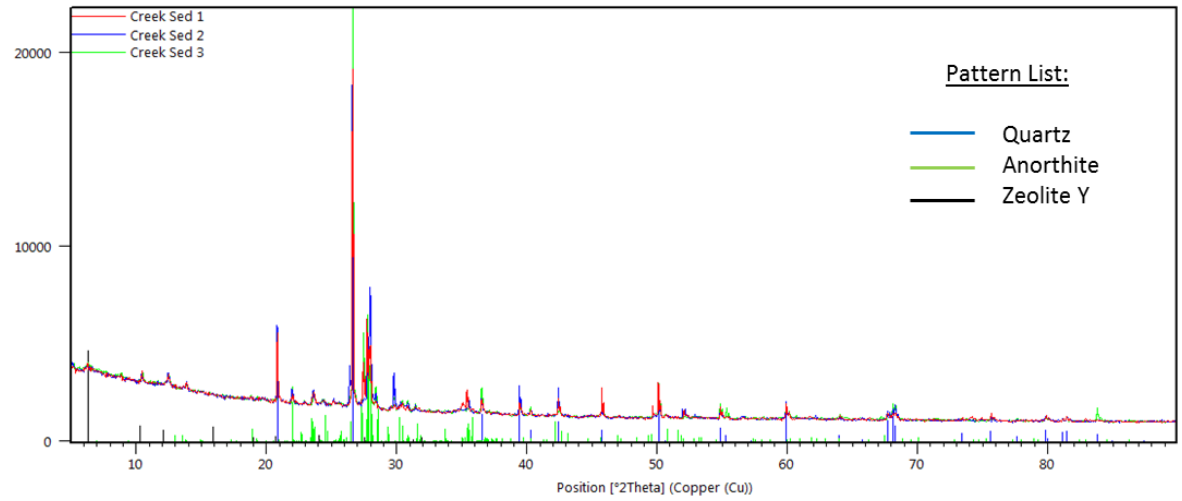

Saturation Index Calculated Values

Week 5			Week 10			Week 15	
Mineral	Value		Mineral	Value		Mineral	Value
Reactor 1							
Aragonite	3.18		Aragonite	3.34		Aragonite	3.56
Calcite	3.33		Calcite	3.49		Calcite	3.71
Dolomite	6.68		Dolomite	6.88		Dolomite	7.38
Goethite	8.81		Goethite	9.41		Goethite	8.98
Ferrihydrite	3.02		Ferrihydrite	3.62		Ferrihydrite	3.08
Hematite	19.62		Hematite	20.84		Hematite	19.97
Hydroxyapatite	11.49		Hydroxyapatite	13.46		Hydroxyapatite	13.59
Jarosite	4.51		Jarosite	6.46		Jarosite	3.63
Rhodochrosite	3.14		Rhodochrosite	3.06		Pyrite	-109.02
Pyrite	-98.82		Pyrite	-101.86		Mackinawite	-66.68
Mackinawite	-60.79		Mackinawite	-62.49		Gypsum	1.36
Gypsum	0.69		Gypsum	1.51		Vivianite	-2.85
Barite	3.27					Barite	3.5
Reactor 2							
Aragonite	3.16		Aragonite	3.92			
Calcite	3.3		Calcite	4.06			
Dolomite	6.71		Dolomite	8.16			
Goethite	9		Goethite	9.81		No	
Ferrihydrite	3.21		Ferrihydrite	4.02		Effluent	
Hematite	20.01		Hematite	21.63		Water	
Hydroxyapatite	8.47		Hydroxyapatite	14.47		Sample	
Jarosite	3.16		Jarosite	4.65			
Pyrite	-101.06		Pyrite	-114.8			
Mackinawite	-61.88		Mackinawite	-69.66			
Gypsum	-0.26		Gypsum	1.01			
Barite	2.14						
Reactor 3							
Calcite	3.04		Aragonite	3.9		Aragonite	3.9
Dolomite	6.63		Calcite	4.05		Calcite	4.05
Goethite	9.28		Dolomite	8.56		Dolomite	8.5
Ferrihydrite	3.49		Goethite	9.7		Goethite	9.32
Hematite	20.56		Ferrihydrite	3.91		Ferrihydrite	3.43
Hydroxyapatite	6.98		Hematite	21.41		Hematite	20.66
Jarosite	4.64		Hydroxyapatite	13.86		Hydroxyapatite	13.85
Pyrite	-102.71		Pyrite	-125.38		Jarosite	1.48
Mackinawite	-62.8		Mackinawite	-75.74		Pyrite	-124
Gypsum	-0.07		Gypsum	-0.18		Mackinawite	-75
Barite	2.22					Gypsum	0.4
						Barite	2.67
Reactor 4							
Dolomite	5.59		Aragonite	3.42		Aragonite	3.32
Goethite	8.82		Calcite	3.57		Calcite	3.46
Ferrihydrite	3.03		Dolomite	7.09		Dolomite	6.92
Hematite	19.63		Goethite	9.43		Goethite	9.21
Hydroxyapatite	7.29		Ferrihydrite	3.64		Ferrihydrite	3.32
Jarosite	4.99		Hematite	20.86		Hematite	20.44
Pyrite	-95.57		Hydroxyapatite	10.93		Hydroxyapatite	10.68
Mackinawite	-58.98		Jarosite	3.95		Jarosite	3.36
Gypsum	1.41		Rhodochrosite	3.01		Pyrite	-114.2
Barite	3.74		Pyrite	-114.13		Mackinawite	-69.57
			Mackinawite	-69.48		Gypsum	1.45
			Gypsum	1.53		Vivianite	-7.26
						Barite	3.73

Week 5			Week 10			Week 15	
Mineral	Value		Mineral	Value		Mineral	Value
Reactor 5							
Aragonite	3.23		Aragonite	3.65		Aragonite	3.8
Calcite	3.38		Calcite	3.8		Calcite	3.95
Dolomite	6.77		Dolomite	7.54		Dolomite	7.87
Goethite	9.06		Goethite	9.22		Goethite	8.73
Ferrihydrite	3.27		Ferrihydrite	3.42		Ferrihydrite	2.83
Hematite	20.12		Hematite	20.44		Hematite	19.48
Hydroxyapatite	12.36		Hydroxyapatite	14.37		Hydroxyapatite	14.12
Jarosite	5.37		Jarosite	4.76		Jarosite	2.28
Pyrite	-99.45		Pyrite	-108.54		Pyrite	-114.92
Mackinawite	-61.09		Mackinawite	-66.36		Mackinawite	-70.23
Gypsum	0.94		Gypsum	1.43		Gypsum	1.43
Barite	3.32					Barite	3.51
Reactor 6							
Aragonite	3.55		Aragonite	3.58			
Calcite	3.69		Calcite	3.72			
Dolomite	7.63		Dolomite	7.98		No	
Goethite	10.1		Goethite	9.42		Effluent	
Ferrihydrite	4.31		Ferrihydrite	3.63		Water	
Hematite	22.2		Hematite	20.83		Sample	
Hydroxyapatite	12		Hydroxyapatite	11.9			
Jarosite	5.51		Pyrite	-122.32			
Pyrite	-110.34		Mackinawite	-74.19			
Mackinawite	-66.84		Gypsum	0.54			
Gypsum	-0.07						
Barite	1.91						
Reactor 7							
Aragonite	3.13		Aragonite	3.51		Aragonite	3.58
Calcite	3.28		Calcite	3.66		Calcite	3.72
Dolomite	6.64		Dolomite	7.32		Dolomite	7.49
Goethite	8.33		Goethite	10.01		Goethite	9.64
Hemetite	18.66		Ferrihydrite	4.22		Ferrihydrite	3.74
Hydroxyapatite	5.98		Hematite	22.03		Hematite	21.29
Rhodochrosite	3.11		Hydroxyapatite	13.34		Hydroxyapatite	14.22
Pyrite	-97.55		Jarosite	6.85		Jarosite	5.5
Mackinawite	-60.2		Vivianite	3.77		Pyrite	-104.46
Gypsum	0.15		Pyrite	-102.34		Mackinawite	-63.68
Barite	2.45		Mackinawite	-62.34		Gypsum	0.82
			Gypsum	0.75		Vivianite	2.25
						Barite	3.2
Reactor 8							
Dolomite	3.86		Dolomite	5.03		Aragonite	2.63
Goethite	8.35		Ferrihydrite	3.84		Calcite	2.78
Hematite	18.7		Goethite	9.63		Dolomite	5.53
Hydroxyapatite	4.48		Hematite	21.26		Goethite	9.53
Jarosite	5.64		Hydroxyapatite	6.84		Ferrihydrite	3.63
Pyrite	-83.34		Jarosite	8.12		Hematite	21.07
Mackinawite	-52.1		Pyrite	-91.3		Hydroxyapatite	7.52
Gypsum	1.49		Mackinawite	-56.18		Jarosite	7.07
Barite	3.6		Gypsum	1.56		Pyrite	-96.14
						Mackinawite	-58.93
						Gypsum	1.45
						Vivianite	0.57
						Barite	3.64
Stock Water							
Aragonite	2.57					Aragonite	2.62
Calcite	2.72					Calcite	2.77
Dolomite	5.37					Dolomite	5.5
Ferrihydrite	2.89					Goethite	8.2
Goethite	8.68					Ferrihydrite	2.3
Hematite	19.36					Hematite	18.41
Hydroxyapatite	9.44					Hydroxyapatite	9.65
Jarosite	3.21					Jarosite	1.55
Pyrite	-105.46					Pyrite	-107.86
Mackinawite	-64.78					Mackinawite	-66.33
Gypsum	1.57					Gypsum	1.54
Barite	1.97					Vivianite	-7.44
						Barite	2.12